UNIVERSITY OF CENTRAL FLORIDA

DEPARTMENT OF ELECTRICAL AND COMPUTER ENGINEERING

SOLAR AUTONOMOUS BEACH BUGGY

Team E | Blue Team

SPONSORED BY:

Duke Energy

University of Central Florida

AUTHORED BY:

Caroline Kamm, Electrical Engineering

Patrick McBryde, Computer Engineering

Olesya Nakonechnaya, Computer Engineering

William Zhang, Computer Engineering

Advisors: Dr. Suryanarayana Challapalli

& Dr. Samuel Richie

Spring 2018

Date of Submission:

April 26, 2018

TABLE OF CONTENTS

LIST OF FIGURES

LIST OF TABLES

LIST OF ACRONYMS

AGPS	Assisted Global Positioning System
AWG	American Wiring Gauge
CAN	Controller Area Network
CCD	Charge-Coupled Device
CCS	Code Composer Studio
CECS	College of Engineering and Computer Science
CMOS	Complementary Metal Oxide Semiconductor
COM	Communications
DARPA	Defense Advanced Research Projects Agency
DCO	Digitally Controlled Oscillator
DGPS	Differential Global Positioning System
DOF	Degree of Freedom
DP	Double-Pole
ECU	Electrical Control Unit
ESR	Equivalent Series Resistance
GNSS	Global Navigational Satellite System
GPIO	General Purpose Input Output
GUI	Graphical User Interface
I2C	Inter-Integrated Circuit
IC	Integrated Circuit
IMU	Inertial Measurement Unit
LNA	Low-Noise Amplifier
LIDAR	Light Detection and Ranging
MCU	Microcontroller
MPP	Maximum Power Point
MPPT	Maximum Power Point Tracking
NC	Normally Closed or Not Connected
NHTSA	National Highway Traffic Safety Administration
NO	Normally Open
PCA	Planned Committed Actual
PCB	Printed Circuit Board
PPM	Passes per Minute
PWM	Pulse-Width Modulation
RC	Radio Control
RMS	Root-Mean-Square
RPM	Rotation per Minute
SAE	Society of Automotive Engineers
SLA	Sealed Lead Acid
SP	Single-Pole
SPST	Single-Pole Single-Throw
SPI	Serial Peripheral Interface
SRAM	Static Random-Access Memory

STC	Standard Test Conditions
TTFF	Time to First Fix
UART	Universal Asynchronous Receiver-Transmitter
UCF	University of Central Florida
USB	Universal Serial Bus
VCP	Virtual COM Port
WAAS	Wide Area Augmentation System

1 Executive Summary

Multidisciplinary students from the University of Central Florida participated in a new project called the Florida Solar Beach Buggy Challenge. This inaugural competition, sponsored by Duke Energy and the University of Central Florida, was created to stimulate interest in both autonomous vehicle design and solar-powered devices in a way that introduces both technologies to everyday life. The beach-going experience is integral to the Florida lifestyle, and by providing an advanced form of transportation in the beach environment, it becomes more accessible to more people. Moreover, this project is an excellent way to promote renewable energy and environmental awareness while addressing the safety concerns associated with beach vehicles through its autonomous collision avoidance system.

Several parameters were introduced in the competition guidelines to heighten the challenge such as payload, total distance, time limit, and of course the biggest constraint of all: budget. When creating and constructing this beach buggy, these constraints needed to be factored into the design process. Thus this project was an exercise in both technical skill and frugality in every element. The resulting innovations presented in the final design include an inventive frame design made out of wood, PVC, and aluminum, and a unique hand-made solar array module on an adjustable mount. These items lightened the entire weight of the buggy significantly, helping to diminish the number of required batteries to help power the vehicle. The mounting system for the solar arrays will allow the maximum amount of sunlight to reach the array at all times, further ensuring the optimum amount of power output.

In order for the buggy to fully possess the autonomous aspect, particular electronic devices were selected or designed that are capable of processing and collecting data. Some of these elements include microcontrollers, cameras, and proximity sensors. The designed microcontroller is extremely crucial to the performance of the beach buggy. It connects all of the sensors and controls, bridging the gap between the motors and sensors using the path finding algorithms incorporated by the computer science students.

Contributing to the vehicle's autonomous characteristic, various hardware and software details were carefully chosen to make sure that the buggy would perform its required tasks. Some of these components include cameras to visually gather information about the surrounding area and a computer-vision enabled processor to create 3D images.

This competition demanded creative design aspects, innovative, outside the box thinking, and master programming skills from each participating team. While this design only encompasses the electrical and computer engineering-related designs, the Blue Team has achieved an all-inclusive solution to this challenge that epitomizes the forward-thinking nature of this competition.

1.1 Initial Proposal – William

The University of Central of Florida announced the Florida Solar Beach Buggy Challenge to design a vehicle to the students within the College of Engineering and Computer Science (CECS). The departments from Electrical and Computer Engineering, Mechanical and Aerospace Engineering, and Computer Science engaged students in a fun and exciting interdisciplinary design challenge, while teaching students about the engineering design process and promoting interest and awareness of solar energy. Teams of students were selected to compete in this challenge. Dr. Samuel M. Richie represented the Department of Electrical and Computer Engineering. Dr. Kurt Stresau represented the Department of Mechanical and Aerospace Engineering. Dr. Mark Heinrich represented the Department of Computer Science. Dr. Suryanarayana Challapalli acted as the Program Manager and Adviser for this challenge.

The Florida Solar Beach Buggy Challenge engaged the University of Central Florida College of Engineering and Computer Science (CECS) students in a fun and exciting interdisciplinary design challenge. Throughout this challenge, students learned about the engineering design process and the value of working in a team environment. This challenge also promoted interest and awareness of solar energy as an important viable natural resource. A total of three teams of students were selected to compete in the first Florida Solar Beach Buggy Challenge. A basic requirement to participate in the challenge is that the teams must consist of interdisciplinary senior level students enrolled in a CECS senior design course.

The design objectives and constraints are listed in the initial proposal. The design objectives and constraints were as follows:
1. Autonomously traverse a 10–mile stretch of beach from Daytona to Ponce Inlet (and return) within 8-hour time span.
2. Capable of transporting one passenger (Max payload: 120 lbs.)
3. Top allowable speed –>3 mph
4. Run completely on solar energy
5. Do no harm to environment and beachgoers
6. Detect and avoid stationary and moving obstacles (e.g., rocks, docks, people, birds, turtles, etc.)
7. Budget: $2000 plus a $250 contingency fund from the Department of Electrical and Computer Engineering.

1.1.1 Project Motivation – William

The Accreditation Board for Engineering and Technology (ABET) requires students to demonstrate sufficient knowledge and skills that meet the respective program educational objectives. One of the student outcomes listed in the general criterion is "an ability to use the techniques, skills, and modern engineering tools necessary for engineering practice," [1]. The EEL 4919C and EEL 3915L - Senior Design - courses serve as capstone courses for students seeking the Bachelor of Science degree in either Electrical Engineering or Computer Engineering [2].

We believed designing a solar autonomous beach buggy vehicle would provide us with valuable experience as future engineers. Several technologies were involved in this project. This project helped serve as a platform for the students to showcase their knowledge and skills in their areas of interest. The Mechanical Engineering students focused on building the physical vehicle, the Electrical the Computer Engineering students focused on incorporating electrical power and control systems to the vehicle, and the Computer Science students developed the necessary software to make the vehicle autonomous.

1.1.2 Project Description – Patrick

The primary goal of this project is to promote interest and awareness of solar energy by creating a product that can solve a complicated problem without relying on traditional power means. To do this, Duke Energy is engaging senior students of the College of Engineering and Computer Science (CECS) to work across disciplines to design a completely autonomous beach buggy that will be powered by nothing more than the sun.

The Solar Beach Buggy Challenge is a new design competition that will allow students to explore expanding areas of technology including autonomous navigation, collision avoidance, electric vehicles, and solar energy. Not only is it an exciting platform for students to complete their engineering degrees, but it also brings awareness to environmentally-friendly alternatives to existing designs. This project will serve to enhance the beach-going experience and allow the team members to improve and practice their problem-solving skills in a challenging and practical application. At the same time, the hope is that the solar autonomous beach buggy will serve as a much-needed tool for anyone who wishes to enjoy the beach but may not be able to without assistance.

Safety and environmental awareness could address real problems for Daytona Beach and other beaches where driving is allowed and legal. In 2010, two children were struck and killed by vehicles driving legally along the on a beach: one on New Smyrna Beach [3], and one on Daytona Beach [3]. Concern since those incidents has grown and resulted in divisive legal debates. On top of that, environmental activists everywhere have expressed concern about preserving the wildlife and habitats around beaches, which are often disrupted by human presence. By designing a safe vehicle with no pollutants, this challenge protects the future of Florida beaches while allowing visitors to enjoy the beach driving tradition. It is for these reasons that one of Duke Energy's primary goals for this project is safety for both beachgoers and the environment.

The market for autonomous driverless cars is also expanding. For example, the California Department of Motor Vehicles recently began testing driverless cars on California roads [4]. Much like Florida, California has many beaches, and it is likely that as the legislation around these vehicles expands, people will begin looking to use them on a beach. While many of the same principles apply between driving on the beach and on normal roads, the increase in the amount of people directly on or crossing road areas increases significantly. As this happens the above safety concerns will become more and more relevant to the

public and as such specially design vehicles will start to be in greater demand. To be competitive in this upcoming market, this project aims to create a working prototype that is low cost in comparison to other similar devices. Since it will be attempting to compete in this market, Duke Energy requested that it be able to drive down the beach fully autonomously.

The idea of a completely solar-powered autonomous vehicle could be of interest to many prospective consumers. For example, a beach lifeguard could slowly patrol down the beach without having to do anything allowing for them to focus on watching the beach. This would make it and appealing product for beaches to purchase in an attempt to increase the effectiveness or serviceable areas of its lifeguards. Since this buggy will be completely solar powered and autonomous, the ecological footprint made by its presence is nearly zero which would bring the interest of people that are looking for a green way to travel along the beach.

Duke Energy has also requested that this beach buggy will be able to travel a large enough distance that it could be of use to the average beachgoer. Consequently, it needs to be strong enough to carry an average person that would need assistance moving on the beach or to transport the expected weight of what someone would need to carry on a beach outing. The main goal of these requirements is to have a useful, helpful vehicle for students to create so that they contribute something practical and not just educational. Additionally, this practicality extends to the technologies and research which the students will need to familiarize themselves with in their future careers, since they are relevant technologies in most current fields of all disciplines involved.

1.1.2.1 House of Quality

Incorporating the given requirements and the ones made to meet the budget, the House of Quality shown in Figure 1 covers all the engineering requirements, their acceptable range of values, marketing characteristics, and the level of positive or negative correlation between each of these properties. Arrows pointing upward signify positive correlation, while arrows pointing downward signify negative correlation. Double arrows are used for strong correlations. The positive and negative signs indicate the desired polarity of the characteristic.

The solar power requirement refers to the nominal expected solar power output under STC. The payload refers to the added weight to the buggy during the competition, which has been stated to be 120 lbs. For the sake of marketing appeal to more adults, some attempt to increase the acceptable payload was be given. Absolutely no collisions with any object, human, or animal were deemed acceptable, since this buggy must not pose any threat to the environment or living thing. A collision could also threaten the structural integrity of the buggy. A set distance of 20 miles was imposed in the competition rules, which the buggy must travel across at a maximum controlled speed of approximately 3 mph. The buggy's path must be determined autonomously. Its end destination must be fairly accurate with respect to its inputted destination. Since this buggy should be fully autonomous, the user controls must be limited to a simple "ON" or "GO" input, two

emergency stop inputs, and a GPS destination input. This final product must all be accomplished strictly under $2,000.00.

The battery storage requirement was necessary due to the uncertainty of the weather conditions. Sufficient battery storage must be included to account for a certain amount of cloud coverage. Therefore, the battery storage values in Watt-hours actually correspond to a maximum possible duration of operation without any solar input. 1920 Wh should provide approximately 3-4 hours of operation, while 4800 Wh should provide approximately 7 hours of operation. These thresholds were determined based on weight constraints, as determined by possible motor sizes, and estimated available surface area for the solar cells.

1.1.2.2 Weighted Rating Evaluation Method

Along with the House of Quality table, a Weighted Rating Evaluation Method Chart in Table 1 was also created to assist with any possible decision the team had to make. It became especially useful in scenarios where multiple alternatives exist and one alternative did not supersede the others by a significant amount. In this case, the ultimate decisions were between a buggy using multiple solar cells in a handmade solar array with a two- battery system and a buggy using one single solar panel with multiple batteries on a sturdier frame. The chart illustrated that the first design featuring multiple solar cells and a dual battery configuration was the better option of the two. Table 2 gives a brief description about the rating scale that was used.

Table 1. Weighted Rating Evaluation Method.

		Concept Alternatives			
		Solar Cells & 2 Batteries		Solar Panel & 4 Batteries	
Criteria	**Importance Rating**	**Rating**	**Weighted Rating**	**Rating**	**Weighted Rating**
Low Cost	40%	3	1.2	2	0.8
Lightweight	30%	3	0.9	1	0.3
High Efficiency	20%	3	0.6	2	0.4
Ease of Implementation	10%	2	0.2	3	0.3
Totals	100%		2.9		1.8

Table 2. Rating Description.

Rating	Value
Unsatisfactory	0
Poor	1
Adequate	2
Good	3
Very Good	4

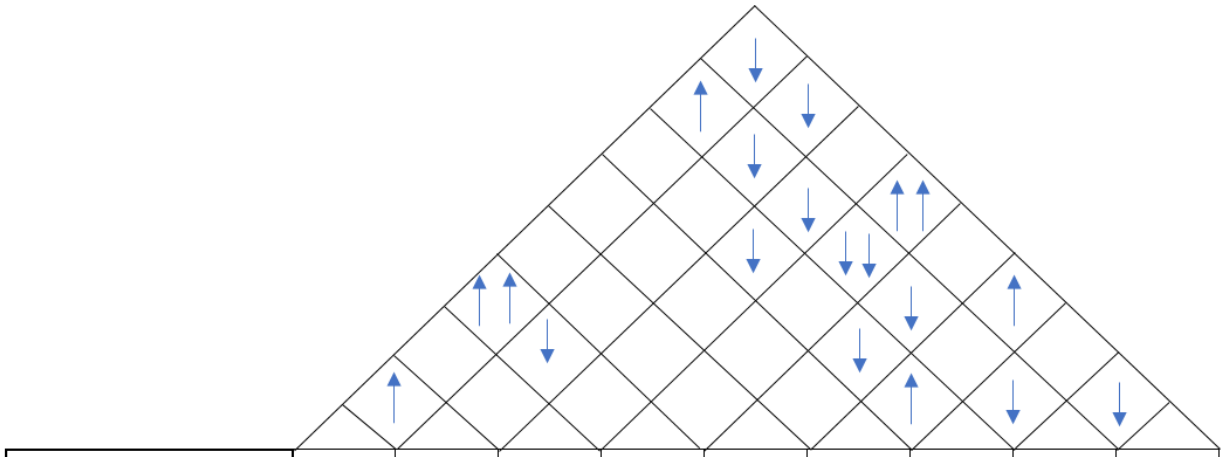

		+	+	+	+	+	+	-	-	+
		Solar Power	Payload	Collision avoidance	Distance	Navigation accuracy	Speed control	User Controls	Cost	Battery Storage
Durability	+		↑						↓	↑
Safety	+			↑↑			↑	↓	↓	
Efficiency	+	↑↑	↓		↑↑			↑	↑↑	↑
Intelligence	+			↑↑		↑	↑	↑↑	↓	
Cost	-	↑	↓	↓	↓	↓		↓	↑↑	↓
Weight	-	↑	↓↓		↑↑				↑	↓↓
Environmentally friendly	+	↑↑		↑↑					↓	↓
		500W STC – 1,100W STC	Payload > 120 lbs	Zero Collisions	Distance > 20 miles	Δ<100 ft with 95% precision	3 mph max +/- 0.5 mph	2 manual + 2 remote inputs	Final cost < $2000.00	1920 Wh – 4800 Wh

Figure 1. House of Quality.

1.1.2.3 Verification and Testing – Caroline

A summary of the requirements, range of acceptable values, and test protocols for verifying these values are included in Table 3 below. In order to verify the engineering requirements, test protocols were determined to physically measure the important quantities. Some of the requirements required repeated testing to statistically verify. Such requirements include collision avoidance and navigation accuracy, where only repeated tests using various test cases could determine the accuracy and precision of the system. Battery storage and solar power must be tested using electrical measurement tools. The remaining requirements are verifiable using basic measurement techniques and visual inspections.

Table 3. Requirements, Target Values, and Test Protocols.

Engineering Requirement	Acceptable Range of Values	Test Protocol
Solar Power	500W STC < Solar Input < 1,100W STC	Measure charge controller output using a digital multimeter during optimal testing conditions, namely midday during the summer.
Payload	Payload > 120 lbs	Verify structural integrity visually.
Collision Avoidance	Zero collisions	Run at least 15 unique test cases and repeat at least 5 times. Visually verify the response.
Distance	Distance > 20 miles	Measure using app-enabled odometer during a test run.
Navigation Accuracy	Delta from input destination < 100 feet with 95% precision.	Conduct test cases and measure delta from input destination using an odometer with enough frequency to verify 95% certainty.
Speed Control	3 mph maximum +/- 0.5 mph	Measure travel time with a stopwatch over a known distance at various motor controller settings.
User Controls	2 manual inputs and 2 digital inputs entered remotely	Visual inspection of the available inputs.
Cost	Final cost < $2000.00	Visual inspection of a final budget report verifiable by receipts.

Battery Storage	1920 Wh < Battery Storage < 4800 Wh	Discharge battery under load to 50% and measure cell voltage and integrated current using multimeter. Compare to data sheet.

1.1.3 Project Block Diagrams – Patrick

Below in Figure 2 is the interface diagram for the logic and sensor parts of the project, which shows how the electronics interfaced with both the mechanical portions and navigation portions of the project. Along with this it shows how the electrical and logic parts of the project communicated with each other internally. Included within the diagram are the data exchange protocols and data format that each part used to communicate with each other; if there was no such protocol then that part was directly connected to the correspond part.

Serial Peripheral Interface (SPI) was chosen to communicate with the Raspberry Pi's, which will be used as the main processors for path finding and image stitching of the stereo cameras. The reason that SPI was chosen for this interface was that it is the fastest and only full-duplex protocol that can easily be supported. Since it is highly undesirable to have a long delay between the Raspberry Pi and the motors, SPI is the ideal protocol for communication between the Raspberry Pi and the MCU.

On the other hand, the data transfer between the sensors, motors, and the main control unit will not have such high traffic nor need full-duplex communication. Thus, I2C was selected for its ease of implementation and synchronous nature, which was deemed necessary to avoid any timing problems. I2C has comparable speed to SPI when there is only one directional traffic for the majority of the communication. As will be shown later, I2C did not end up being used for the sensors as there were enough pins necessary for each sensor to be connected directly without having to share a bus.

The following Figure 3 shows the power system block diagram that depicts the flow of energy through the beach buggy. A custom solar array will be created that connects to the 24V battery array through a charge controller, which will protect the battery from being damaged by the solar array and limit any unnecessary discharge from the battery.

This battery array will connect to the electronics through a converter, or possibly multiple converters, that will step down the voltage and current to an acceptable level. It will also connect to the two motors that will be used for steering and driving through a dual channel motor controller. This motor controller will take the power from the battery array and combine it with the PWM control signal from the MCU to adjust the power delivered to the motor. Thus, the motor controller will retain control over both the speed and direction of the motor. Each of these block diagrams is color coded with which major discipline they belong to: blue for electrical and computer engineering, silver for mechanical engineering, and purple for computer science.

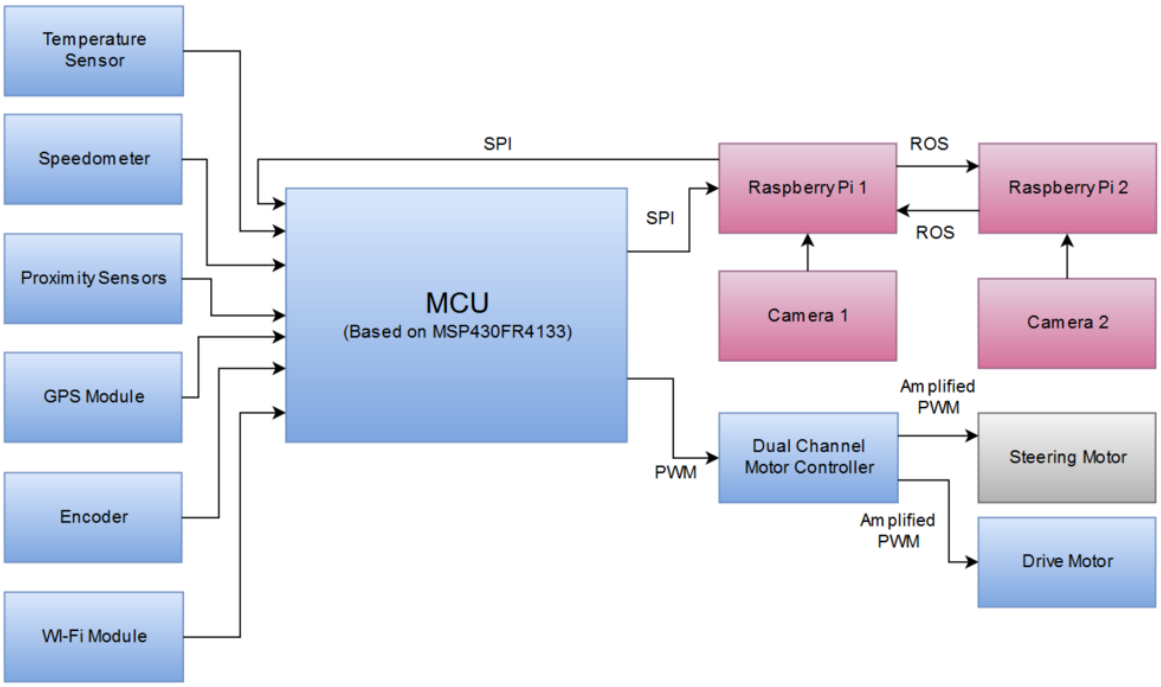

Figure 2. CpE Interface Block Diagram.

Figure 3. Power System Block Diagram.

The logic process flow that the buggy will use during operation is shown below in Figure 4. First the buggy will check the sensors to detect if an emergency stop is required, this should not be confused with a user inputted emergency stop that will take place unconditionally if the button is pressed. If this is the case it will immediately stop, flag the navigation system, then proceed to attempt to resolve the situation. If it does not detect an object it will send information to the navigation board and the set the motors for steering and driving to the appropriate values as it has received from the navigation board. Shown in blue is also the high-level decision making that the navigation system will take when calculating the values for the motors from its own readings and the data sent from the sensors.

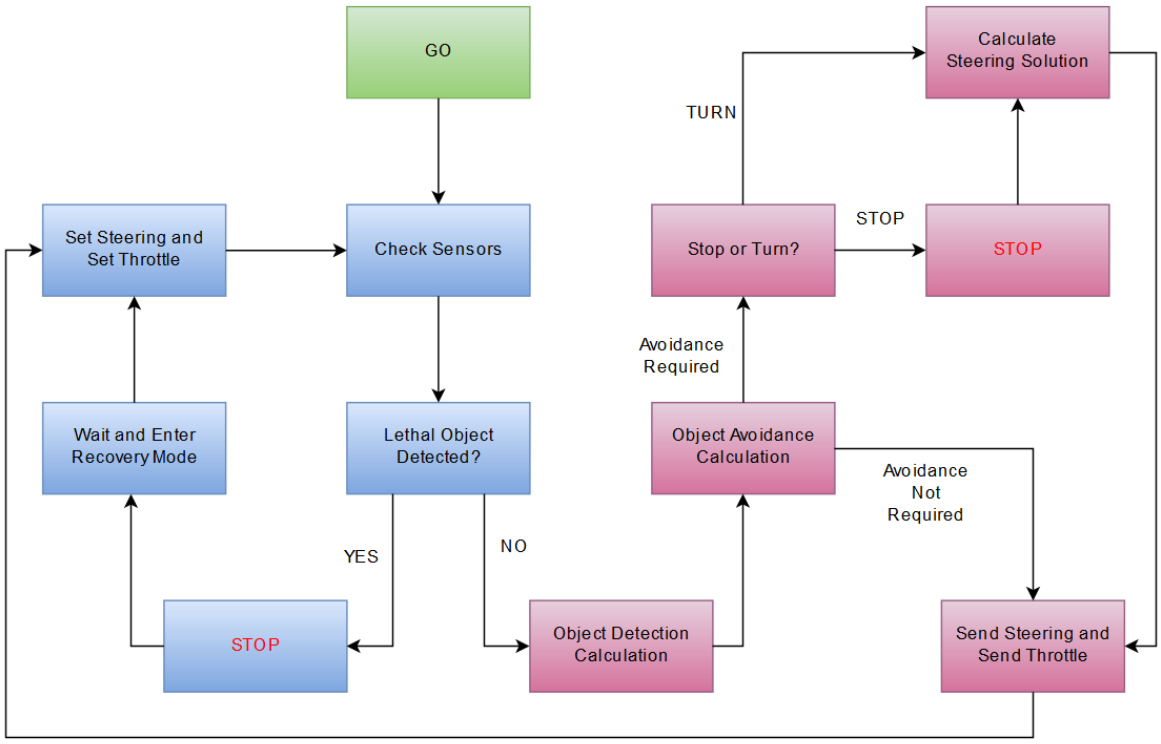

Figure 4. High Level Logic Block Diagram.

1.1.4 Broader Impacts

This project will hopefully inspire onlookers into learning more about robotics, engineering, and most importantly, renewable energy. The sun is a huge, largely untapped source of energy, and any onlookers to this project will hopefully be inspired to start thinking about solar power and its potential applications. Familiarity with something makes people more likely to give it a chance. Solar power is a currently widely misunderstood medium, and projects like this one can aid in spreading the word about it.

The most important contribution this project will provide to society at large is awareness of science and technology in the population. This project demonstrates what it takes to produce a working autonomous buggy; additionally, this document provides alternative options for creating something like this and weighs its costs and benefits. Hopefully, this project has produced a document that can prove to be a valuable resource for any future engineers seeking to build a similar project.

Finally, if this competition was deemed successful, it may pave the way for UCF to continue to hold it annually. In a competition like this, the real reward is the effort that all the competitors put in to improve upon the previous designs.

1.1.5 Realistic Design Constraints – Caroline

A variety of other factors are to be considered outside the listed competition rules and their associated design constraints. These constraints can be inferred from the context of the work environment including: economic, time, environmental, social, political, ethical, health and safety, manufacturability, and sustainability constraints. The following sections will explore each constraint topic and identify related specifications if applicable.

1.1.5.1 Economic and Time Constraints – Caroline

The biggest economic constraint on this project was the listed budget of $2,000. This budget must be split between product development and testing, but it does not incorporate maintenance due to the short intended lifespan of the vehicle. Since this project was not designed to be commercially available, factors such as payback to save the user money and profit from sales are not applicable.

The only time constraint was the two semesters to conduct design, production, and testing. The milestone discussion at the end of this document details exact dates for major accomplishments. The spring semester from January thru April is generally the timespan for design, while the fall semester from August thru November constitutes the construction and testing timeframe. All work must be completed by the day of the competition, which was determined to be November 18th.

1.1.5.2 Environmental, Social, and Political Constraints – Olesya

The solar powered beach buggy does have impacts on the environment. The buggy will not affect the environment in operation because it will stay clear from any obstacles and it will stay in the driving lane at all times. The buggy also does not run on fuel; therefore, it will not produce any CO_2 emissions that might be harmful to the environment. The only environmental constraint it will pose is the use of batteries. These batteries need to be disposed of properly or reused after the competition. The buggy will compete with other buggies in a friendly competition between teams that design and build their own buggy with the same requirements. The teams will be judged separately and scoring will be based on completion of the race, therefore the only social constraint will be to make sure the communication between the teams stays sparse to maintain the competition spirit. There is no political constraint for this project. The sponsor of this project created this idea as a "fun engineering" task to build a buggy and see what the students can accomplish with the budget and the use of solar power.

1.1.5.3 Ethical, Health, and Safety Constraints – Patrick

This project does not have any special ethical constraints. It has the common constraints of safeguarding users and bystanders against harm. Additionally, since this project is planned to be used on the beach, this project must take measure to make sure that how it traverses the beach autonomously does not disrupt the use of the beach by beachgoers or

the natural wildlife. This project should also take into account from where it is acquiring its parts to make sure the manufacturers of such parts are following ethical guidelines.

The main health and safety concerns of this project is the health and safety of the user and bystanders in the surrounding area. The health of the user is put at risk by this being an autonomous vehicle, as it could crash or drive in such a way to threaten the user. Additionally, as this is an electric solar powered vehicle it will be using potentially dangerous levels of electricity to power itself. These levels must be considered for the user's safety as this project cannot use dangerous energy levels without proper safeguards. The health of bystanders are also put at risk since this vehicle will be autonomous; running into or driving over a bystander could cause them harm. This project will have to take measures to ensure that the operation of this vehicle does not do any of these actions.

1.1.5.4 Manufacturability and Sustainability – William

The design of the buggy was custom made to fit the requirements of the Florida Solar Beach Buggy Challenge imposed by the College of Engineering and Computer Science. The buggy utilized commercial and raw products that enabled the vehicle to be powered by solar energy and to autonomously traverse the beach from Daytona to Ponce Inlet. To save on cost, this project utilized the labor of college students to get the vehicle under budget.

The design for this project was done by the mainly hands of college students. From the frame to the autonomous components, college students took it upon themselves to design a vehicle that was able to compete in the Florida Solar Beach Buggy Challenge. The chassis of the buggy was custom made by ordering raw materials that needed to be modified to fit the design specifications to meet the design requirements. The motors were selected to deliver the necessary torque to move and turn the buggy. The solar array needed to be assembled by the hands of college students. The electrical system needed to be connected by the hands of college students. Even the programming necessary to transform the buggy into a self-driving vehicle was made by two college students. College students from the College of Engineering and Computer Science at the University of Central Florida played a huge role in this project.

The buggy was designed with environmental friendliness and safety in mind. The buggy utilized natural resources that allowed the buggy to traverse the beach. The electrical system was fitted with two 12 volt batteries that were able to be charged by an array of solar cells. Solar energy provided the much needed energy for the buggy to complete the challenge in under eight hours. This natural resource provided an alternative mean in powering the buggy. However, the use of fossil fuel has been shown to produce pollution and harmful byproducts. The hope of this project is to bring awareness to the extraordinary capability that solar energy technology has improved since the last century.

With an initial investment of $2,000, this project was able to provide the user with alternative means to enjoy the beach-going experience. The buggy can be easily left

anywhere with a clear view of the sun to be able to charge the batteries from empty to full capacity. This is a small investment for anyone that is looking to enjoy the beach with assistance. The autonomous features of the buggy were able to give the users an unmatched experience that no other competitor is able to give.

1.2 Project Specifications and Requirements – Caroline

Seven major marketing characteristics for the design have been identified: vehicle durability, efficiency, intelligence, safety, low cost, low weight, and environmentally friendly. These reflect the original competition guidelines, which are summarized in the House of Quality in Figure 1 with their associated acceptable range of values. Realistic design constraints have also been imposed given the context of this project. The following sections expand upon these premises by imposing more specific requirements that are inferred outside of the stated competition requirements and are particular to this solar beach buggy design only. The Project Specifications and Requirements has been divided into three major sections: General Information and related assumptions, Power Requirements, and Electronics Requirements. By imposing these additional requirements, the components of the buggy were directly held against a related specification to determine whether it was capable of achieving the desired performance.

1.2.1 General Information – Caroline

Many of the specifications and requirements for this project are laid out in the project competition description. Other requirements are inferred from this given description and can be further developed in a longer list of specifications and constraints, such as the probable weather conditions and terrain assumptions. The sections below outline the stated parameters of the competition and expand on the related design constraints.

1) Cost: The vehicle has a strict budget, so efforts must be made to minimize overall costs. The total production cost, including cost of replacement, must be encompassed by this budget.

1.1 Total budget is $2,000 plus $250 for contingency/development.

1.2 Anything donated must be accounted for within the $2,250 total production budget.

2) Dimensions: The vehicle must retain lightweight characteristics in order to decrease the required power to propel the buggy. By reducing weight, the maximum potential distance increases while minimizing the cost of the power system.

2.1 To meet mechanical power estimates for a 500W DC brushed motor, the total weight of the assembled buggy without additional loads must be at maximum 430 lbs.

2.2 Height of the buggy must be minimized in order to keep the center of gravity low. However, sufficient headroom for the passenger must be provided.

2.3 The width of the buggy must not exceed the maximum vehicle width according to the Federal Size Regulations for Commercial Motor Vehicles, which dictates that the maximum width is 102 inches. Because this buggy is designed to

drive in a designated driving lane, designated by posts, the width must absolutely stay within this boundary.

2.4 The wheel dimensions must measure at least 18 inches in diameter and at least 4 inches wide in order to provide adequate traction and flotation.

2.5 The overall dimensions of the buggy must be small enough to be transported by a car trailer.

3) Weight Capacity: While traveling over beach terrain at a maximum allowable speed of 3 mph, the finished product must be capable of carrying one person plus any necessary equipment; therefore, the vehicle must retain structural integrity and be able to withstand any of these associated loads or stresses.

3.1 The Buggy must hold an additional 120 lbs. in the form of a passenger. Therefore, the buggy must hold a small seat and must be designed to withstand this load.

3.2 Since a passenger is expected to ride in the vehicle, a minimum of approximately 3 ft. must be given between the seat and any overhead structures. Some legroom must also be provided to accommodate an average-sized human.

4) Physical Characteristics: The buggy is exposed to several outdoor elements during operation, which requires its chosen material characteristics to withstand the expected environmental conditions from Daytona Beach to Ponce Inlet.

4.1 The buggy's performance cannot be altered by the introduction of trace amounts of water. Therefore, all electrical components must be properly protected from the environment. All materials must be able to withstand small amounts of water, sand, salt, and other common environmental elements.

4.2 The buggy must be able to withstand a maximum air temperature of 82 degrees Fahrenheit, which is the highest average historical temperature for Daytona Beach in November. This implies that the electronics may be subjected to even higher temperatures due to solar radiation. The buggy must be able to perform the task in the competition while meeting all requirements under such thermal constraints with the help of heat dissipation devices, i.e. heat sinks and fans.

4.3 The buggy is intended to be driven on hard, smooth surfaces, such as compact, wet sand that could be found on a beach. Softer surfaces, such as dry, loose sand or other compressible surfaces are not anticipated or accounted for during design.

5) Inputs: In order to make the vehicle more intelligent, fewer user controls must be implemented and must instead be replaced with autonomous systems. The vehicle must be intelligent enough to be able to automatically detect and avoid obstacles (human, animals, objects, etc.) by either turning or stopping. In addition to collision avoidance, it must navigate accurately using a GPS system. The power system inputs must be limited to the batteries and solar array, such that an optimally efficient system is implemented.

5.1 Energy input from solar cells must amount to at least 400W STC.

5.2 Energy input from batteries must compensate for any unmet power requirements. Two 12V batteries of at least 80 Ah and at most 200 Ah must be selected for this purpose.

5.3 Proximity sensors must be implemented in order to detect any obstacles not found from the camera system. Proximity sensor flags must be used to process urgent stops.

5.4 The camera system must be able to identify obstacles and change the buggy's path based on obstacle detection and pathfinding algorithms.

5.5 The GPS system must be able to accept destination coordinate information and trigger the pathfinding algorithm to handle this information.

6) Performance: The performance expectations are listed clearly in the competition description. Because the Solar Beach Buggy's performance is ultimately linked to the weather conditions through the solar power output, these performance parameters are only valid under predetermined weather conditions.

6.1 The buggy must traverse Daytona Beach for 20 miles. This includes travelling south 10 miles to Ponce Inlet, and from there returning 10 miles north back to the original starting position.

6.2 The buggy must achieve a maximum speed of 3 miles per hour.

6.3 The buggy must stop for any object accelerating towards its path of travel or any stationary object directly in its planned path of travel.

6.4 The buggy must only be expected to achieve this performance under a predetermined cloud coverage level.

7) Safety: Safety features must be provided for the person who is sitting inside the vehicle. Additionally, a safe environment must be maintained for other beachgoers and wildlife. The following safety provisions must be included for these purposes.

7.1 The buggy must have a seat belt for the passenger.

7.2 The buggy must be equipped with an on-board emergency stop button which immediately ceases power supply to the motors.

7.3 All on-board electrical components must be properly insulated and operate at safe voltages to prevent electric shock, arcing, fire, etc. in accordance with all applicable design standards.

7.4 Safety knowledge and training are necessary for designers and passengers of the beach buggy, which must include information on the above safety features.

1.2.1.1 Acceptable Weather Conditions – Caroline

This section will detail the weather conditions expected on the day on the competition, tolerances on the acceptable weather conditions, and a brief description of the maximum cloud coverage level that are considered acceptable for a full performance run. The weather conditions being considered are wind, sun position, and cloud coverage.

According to the Smyrna Beach Municipal Airport Statistics, the average wind speed for the month of November is 10.2 mph, while the average max wind speed is 13.9 mph [5]. A possible top wind speed for design and simulation purposes from this data could be 15

mph. However, these averages are spread across every day in November. A closer look at the statistics indicates that each days falls into a range of average wind speeds. The majority of the days in both November and December have average wind speeds between 10 mph and 15 mph, while the second most frequent interval was between 15-20 mph [6]. Table 4 summarizes this data.

Table 4. November Wind Speed Averages [6].

% Days	Avg. Wind Speed
14	< 10 mph
43	10-15 mph
29	15-20 mph
14	20-25 mph

Ideally, a day in the 10-15 mph range is representative of the competition day, but as a safety factor, the design and simulation were tested against a top wind speed of 20 mph in case the chosen competition day was in the 15-20 mph average range. Any higher observed wind speed on the day of the competition would have been deemed unacceptable weather conditions and was grounds for postponing the competition.

Sun position can be predicted accurately despite weather conditions. Even though it is invariant, sun position is an important function of power output from the solar panels and was used to calculate optimum panel tilt exactly. Sun position can be calculated exactly from latitude and day of the year. Many online models also exist for tracking sun position for a given day and time. The location of the competition was approximately at 29.2 degrees latitude and -81 degrees longitude. The altitude angle of the sun is estimated to be 35-40 degrees according to the Florida Solar Energy Center, so an approximate tilt for the solar panel is 90 degrees minus the altitude angle, or 50-55 degrees [7]. However, simulating a day in late November results in a per-hour altitude angle of the sun [8]. Table 5 outlines the estimated height of the sun throughout the day. Further solar calculations were performed to validate this information and ultimately calculate the solar output given a particular panel orientation.

Table 5. Simulated Sun Altitude Angles for Late November [8].

Time	Sun Zenith Angle	Panel Tilt Angle	Corresponding Events
7:00	0	90	Approx. Sunrise
8:00	11.5	78.5	
9:00	21.9	68.1	
10:00	30.7	59.3	
11:00	37	53	
12:30	39.7	50.3	Approx. Solar Noon
13:00	38.5	51.5	
14:00	33.4	56.6	
15:00	25.4	64.6	
16:00	15.5	74.5	
17:30	0	90	Approx. Sunset

Sun azimuth angles, which are a measure of the direction of the sun's rays from due north, can also be obtained from various online solar position simulators. Figure 5 contains approximate azimuth angles per-hour for late November. These azimuth angles were also verified with exact calculations and integrated into the final angle of incidence and hourly irradiation.

The last weather requirement is that the cloud coverage be low enough to produce reasonable output from the solar array. A partly cloudy sky might be acceptable if the cloud coverage takes up less than 20% of overhead airspace. Therefore, the solar array was sized approximately 20% more than the calculated array size. Good judgment needed to be used on the day of the competition to realistically assess the available daylight and whether or not it was sufficient to enable the buggy to meet the performance standards.

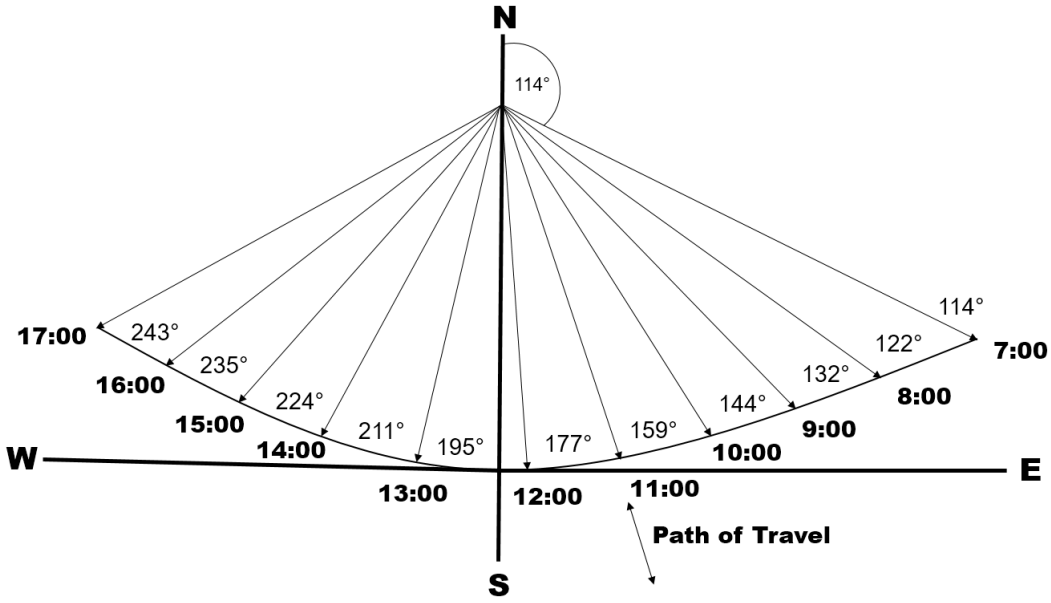

Figure 5. Simulated Sun Azimuth Angle for Late November.

1.2.1.2 Terrain Assumptions – Caroline

After inspecting the condition of the sand in the driving lane on Daytona Beach, the sand was identified as wet and compact. In the month of November particularly, due to lower temperatures and less solar radiation causing less evaporation, the sand was predicted to remain wet and compact. The sand was generally level with small irregularities that should be easily overcome by larger flotation tires, such as what was used on the beach buggy. The most important property of the surface is the rolling resistance, which is due to the constant deformation of both the tires and the sand under pressure. The rolling resistance is a complicated coefficient, also taking into account tire pressure, diameter, width, tire material, grain size, temperature, and tread. Therefore, the exact value cannot be found. One resource specifically lists car tires on solid sand as having a rolling resistance coefficient between 0.04 and 0.08 [9]. The calculations use 0.08 to derive a conservative value for required motor power. This means that the terrain was assumed to

be compact throughout the entire journey, but the buggy should have been able to endure small irregularities or patches of drier sand.

1.2.2 Power Requirements – Caroline

The following requirements pertain to all power components, including energy storage devices, energy generation devices, and high power connections.

1) Energy input from solar array must amount to at least 400W STC. The solar array was constructed out of individual solar cells, rather than pre-assembled solar panels.

2) A charge controller must be used to control the power flow from the solar array to the battery pack. This charge controller must have ample capacity for the installed solar panels and must offer some flexibility and/or customizability to expand or diminish the solar array size.

- 2.1 The charge controller must be intelligent enough to detect and pass low voltages and currents during periods of low light intensity.
- 2.2 The charge controller must be at least 90% efficient.
- 2.3 The charge controller must implement an MPPT algorithm.
- 2.4 The charge controller must be compatible with the voltage of the battery pack.

3) A battery pack must be installed equal to the motor size, which is 24V.

- 3.1 The listed amp-hours of the batteries must be between 80 Ah and 200 Ah.
- 3.2 The batteries must be capable of deep cycle discharge.

4) A dual channel motor controller must be used to dictate and monitor the power delivered to the motors by matching the power requirements of the motor, namely 24V with less than 30A.

- 4.1 The motor controller must communicate with the MCU via PWM.
- 4.2 The motor controller must be compatible with brushed DC motors.
- 4.3 The motor controller must monitor battery level for low voltage and over voltage.
- 4.4 The motor controller must provide both thermal and current limit protection.

5) All power distribution equipment must be sized for a larger capacity than the calculated power draw.

- 5.1 All wires must be correctly sized according to AWG recommendations.
- 5.2 A DC-DC converter must be used between the battery and the electronics equipment, and must be sized larger than the calculated power draw.
- 5.3 Protective circuitry components must be used whenever power connections are made, but may be included within the power components if appropriate, such as the charge controller and motor controller.

1.2.3 Electronics Requirements – Olesya

The solar powered beach buggy complies with the following requirements specifications to meet the design budget and constraints.

1) This project must include a PCB design and manufacture for at least one main microcontroller in the system. This design must be based off a MSP430 with any necessary alterations.

2) At least two proximity sensors must be included as a redundancy to the navigation system, which was the primary responsibility of the Computer Science Team.

3) Communication between the Computer Science Team and Electrical and Computer Engineering Team, including collision avoidance and navigation, must be conducted via SPI.

4) Each sensor must have its own set of GPIO pins with conversion circuits to connect to the controller.

5) Communication between the controller and the motor driver must be conducted via PWM.

6) Firmware must be written based on the data transfer protocols between the Computer Science Team and Electric and Computer Engineering Team.

7) Power must be provided by the battery to the controller via a DC-DC converter.

1.3 Design Standards and Codes – Patrick

This project will be following certain standards and codes for its design choices and construction. The goal of using these standards is to increase the reliability, safety, and overall efficiency of the final product. Many of these standards will also impact the manufactures that parts of the product will be created from, therefore these standards will also impact the location that parts are ordered from.

The quality of the printed circuit boards that will be ordered is a major concern for this project. As these circuit boards will be controlling the majority of the buggy if they were to fail there could be unforeseen problems. Below are related standards to the construction of printed circuit boards.

The IPC-SM-840D standard deals with the quality of solder mask on printed circuit boards. Making sure that the manufacturer of the custom printed circuit boards follows this standard will help to ensure that it works as intended [10].

The IPC-A-600 standard deals with determining the acceptability of printed circuit boards, specifically the training in doing so. This will also help to ensure the quality of the custom made printed circuit boards [11].

Among the devices that will be used in this project are servos which the UL 1004-6 standard helps to determine the suitability for such servos in normal use. Through the construction and testing of this project it will be necessary to verify electrical reading manually, the UL 61010-2-32 standard specifies precautions that need to be taken when taking these readings using hand-held devices [12][13].

Below is a list of relevant standards for the electrical components of the buggy from IEEE relating to sensors, software, and video technology.

The 2700-2014 – IEEE Standard for Sensor Performance Parameter Definitions is a common framework for sensor performance specification terminology, units, conditions and limits is provided. Specifically, the accelerometer, magnetometer, gyrometer/gyroscope, barometer/pressure sensors, hygrometer/humidity sensors, temperature sensors, ambient light sensors, and proximity sensors are discussed [14].

The 1044-2009 – IEEE Standard Classification for Software Anomalies provides a uniform approach to the classification of software anomalies, regardless of when they originate or when they are encountered within the project, product, or system lifecycle. Classification data can be used for a variety of purposes, including defect causal analysis, project management, and software process improvement (e.g., to reduce the likelihood of defect insertion and/or increase the likelihood of early defect detection) [15].

The 208-1995 – IEEE Standard on Video Techniques outlines methods for measuring the resolution of camera systems are described. The primary application is for users and manufacturers to quantify the limit where fine detail contained in the original image is no longer reproduced by the camera system. The techniques described may also be used for laboratory measurements and for proof-of-performance specifications for a camera [16].

The construction of the buggy has its own set of mechanical standards for working with metals. The below ASTM standards address the creation and use of steel and aluminum parts.

The ASTM B308 Standard Specification for Aluminum-Alloy 6061-T6 Standard Structural Profiles covers the structural profiles for 6061-T6 aluminum-alloy. It provides specifications for the tensile strength, yield strength, and elongation of the aluminum-alloys chemical composition after hot extrusion. This projects frame will have a large aluminum-alloy component, purchasing the aluminum-alloy from a company that uses this standard will help to improve this projects ability to rely on their statics for determining which pieces to use for its frame [17].

The ASTM A108 Standard Specification for Steel Bar, Carbon and Alloy, Cold-Finished deals with cold-finished carbon and alloy steel bars produced in straight length and coil to chemical compositions. The drive shaft of this project is planned to be constructed with carbon steel and it is important to the success of this project that it is able to select a shaft that will not fail. This standard allows this project to be able to have certain guarantees about the integrity of the shaft used [18].

The ASTM A36M Standard Specification for Carbon Structural Steel deals with carbon steel shapes, plates and bars of structural quality for use in riveted, bolted, or welded construction of bridges and buildings, and for general structural purposes. This project intends for many of the front mounting structure to be constructed using carbon steel. This standard provides this project with the ability to rely on the manufacture to provide it with suitable steel for this application [19].

The below IEC and IEEE standards apply to the on-board sealed lead-acid (SLA) batteries and contain information regarding the required performance and sizing of the batteries.

The IEC 60086-2, BS General Battery Standards addresses the requirements of batteries such as discharge test conditions and discharge performance. This standard will help this project in both selecting a vendor for its battery array, as a vendor using these standards would be more reliable in both dimensions and discharge statistics. But would also be beneficial to this project in testing and verifying these values after purchase of these batteries. As this project is a solar powered vehicle having a reliable battery array is paramount to its success [20].

The 1013 – IEEE Draft Recommended Practice for Sizing Lead-Acid Batteries for Stand-Alone Photovoltaic Systems deals with appropriately sizing a battery for a specific Photovoltaic system. As previously stated this project is dependent on its photovoltaic cells and batteries for operation thus this standard is highly beneficial for this project. Being able to size the battery to the solar array used in this project correctly both increases safety and efficiency but could also lead to a decrease in cost if it helps determine a smaller battery that would still meet this projects requirements [21].

Lastly, the NFPA 1192: Standard on Recreational Vehicles deals with fire and life safety criteria for recreational vehicles to provide protect from loss of life from fire and explosion. As this project will be dealing with high amounts of electricity, a fire is not something that can be ruled out. This standard will be helpful in guarding against such an event from occurring [22].

1.3.1 Design Impact – Patrick

All of these standards will have an impact of the final design of this project. The 2700-2014 – IEEE Standard for Sensor Performance Parameter Definitions will be important as this is an autonomous vehicle which relies heavily on its sensors to make smart and safe

decisions. Having a reliable way to ensure these sensors will operate as expected is a major concern. This standard will help to ensure the quality of the final product [14].

The 1044-2009 – IEEE Standard Classification for Software Anomalies will be beneficial to assist in the debugging process for creating the code for this product. As bugs in code is quite common it is beneficial to be able to easily classify and communicate between parties the reason for abnormal behavior within the code. This will help to reduce the amount of time is used during testing to identify the problem and increase the amount of time spent on solving the problem [15].

The IPC-SM-840D and The IPC-A-600 standards will impact the manufacturer that is chosen to create the printed circuit board for this project. This may add to the cost of ordering the printed circuit board but the reliability and safety that these standards provide is required in this project [10][11].

1.4 Patents and Intellectual Property

Since this team's design was the first of its kind, there were no patents or intellectual property to consider for the project.

1.5 Levels in Autonomous Driving – William

There are two prominent standards for classifying what autonomous driving means [23]. These standards are the J3016 of the international engineering and automotive industry association, Society of Automotive Engineers (SAE), and in Europe by the Federal Highway Research Institute. As of November 10, 2017, Rudolph and Voelzke writes that no car manufacturer has been able to achieve level 3 or higher in production. They also mentioned that several sensors are required for autonomous driving from Levels 1 to 5. These sensors can be categorized into 3 main groups: camera-, radar-, and LiDAR-based systems. In terms of autonomous driving, ultrasonic sensors are of minor importance [23].

The US Department of Transportation’s National Highway Traffic Safety Administration (NHTSA) defined five different levels of autonomous driving in 2013. The NHTSA updated their policy to reflect that they have officially adopted the levels of autonomy outlined in the SAE International’s J3016 document in October 2016. Bryant Walker Smith, professor at the University of South Carolina’s School of Law and School of Engineering and one of the top experts in the driverless cars world, explains that the levels of autonomy describe the system, not the vehicle. "A Level 5 automated driving system could be in a vehicle with or without a steering wheel," he further explains [24].

The levels of autonomous driving are described below in Table 6.

In order to achieve further levels of autonomous driving, vehicles must have cameras and radar systems. Based upon the standards set forth from J3016 and the Federal Highway Research Institute, we strove to achieve an autonomous driving level of 5.

Table 6. Five Different Levels of Autonomous Driving Defined by the US Department of Transportation's National Highway Traffic Safety Administration (NHTSA) [24].

Level 0	This is the most basic level of driving for the driving system. There is no autonomous features of the driving system. The human driver controls all aspect of the driving experience. The human driver controls the steering, brakes, throttle, and power.
Level 1	This next level described some driver-assistance features for the human driver. Some aspects of the driving experience can be done automatically by the system. However, the human driver is mostly in control of a majority of the driving experience.
Level 2	At this level of autonomous driving, the system has at least one driver assistance subsystem that controls some aspect of the driving experience. At least driver assistance system of "both steering and acceleration/ deceleration using information about the driving environment is automated." This can include cruise control and lane-centering. The human driver can be "disengaged from physically operating the vehicle by having his or her hands off the steering wheel AND foot off pedal at the same time," according to the SAE. However, the driver cannot be relaxed about the driving experience. He or she must always be ready to take control of the vehicle when the need arises.
Level 3	In Level 3 of the autonomous driving system, human drivers are still necessary. However, they not needed for a majority of the time. The vehicle should be able to take control of "safety-critical functions" of the driving experience, under certain traffic or environmental conditions. The human driver should be present and must be alert when intervention is needed. However, the human driver does not need to monitor the situation in the same way it does for previous autonomous levels.
Level 4	In this level, Level 4 vehicles are "designed to perform all safety-critical driving functions and monitor roadway conditions for an entire trip." There is still some limitations for the vehicle. The vehicle is limited to the "operational design domain (ODD)" of the system. This means that the vehicle is constrained by the driving scenario that the vehicle was designed to be driven in. The vehicle is unable to perform well in every driving scenario.
Level 5	In this level, the vehicle can be expected to perform equally to that of a human driver, in every driving scenario that a human driver is able to perform with success. The vehicle should be able to drive itself successfully in extreme environments and in harsh weather conditions.

2 Research

Researching the parts and functionalities of a vehicle is a critical step of the entire design. There are four major parts of the research: mechanical components, power components, electronics, and software. In this report, the power components and electronics research will be presented in the following sections. Also included is a brief overview of relevant existing technologies, and how information about those technologies could guide decision-making for this project.

2.1 Existing products – William

This project utilized preexisting technology from previous products to efficiently design the buggy. There are many products that encompass the desired aspects for the buggy. The physical frame design and drivetrain were modeled from previous "buggy" projects. The power system and electronics required to bring the buggy to life were modeled from previous senior design projects and other autonomous electrical vehicle products. The autonomous component of the buggy was implemented using a software approach.

In 2003, the Defense Advanced Research Projects Agency (DARPA) launched the Grand Challenge to initiate development in unmanned ground vehicle navigation [25]. The Challenge sought to develop an autonomous robot that is able to drive itself on off-road terrain. Stanford's robot "Stanley" was able to finish the course in 6 hours, 53 minutes, and 58 seconds. It was declared the first place winner of the DARPA Grand Challenge. We wanted to incorporate pieces of their software system into the design of the buggy. Stanley's software architecture served as a foundation for the buggy's software architecture.

A design for a low-cost autonomous vehicle control system was presented in paper [26]. The design included inexpensive microcontrollers, encoders, motor controllers, Light Detecting and Ranging (LIDAR), and camera. The researchers were able to transform a normal kids'-ride-on electric car to an autonomous vehicle research platform. They were able to determine a good performance system at a minimal cost through the use of commercially available components. Table 7 lists the items in the paper. As the design principles mentioned by the design philosophy of the Stanford Racing Team, autonomous navigation is a software problem. The vehicle's ability to be able to traverse the beach from Daytona to Ponce Inlet in 10 miles and back challenged the buggy's ability to detect and avoid obstacles and to efficiently utilize its limited power supply. The flowchart of Stanley's software system helped us understand which components ought to be needed for the vehicle to achieve autonomous control. The software consists of six main functional groups: Sensor interface, perception, control, vehicle interface, and user interface. Our vehicle mimicked a similar software system.

Table 7. List of Components from the Paper.

Item	Price (USD)
Camera Sensor	$45
Lidar Sensor	$135

ChipKIT Uno-32	$25
Arduino Uno	$20
Two encoders	$35
Other accessories	$20
Two Battery Controller Shields	$80
	Total: $360

2.2 Power Components – Caroline

This section contains information relating to relevant technologies, possible components, and general setup diagrams that were considered during the design of the power system. This includes the energy storage via the battery bank, energy generation via the solar cells, the charge controller to regulate the delivery of power from the solar cells to the batteries, the motor controller to regulate the flow of power from the batteries to the two motors, and the converters. Additional research will be presented for a battery generator, which could theoretically compensate for any missing power during vehicle operation. Lastly, extensive power calculations were performed to lay out the equations, assumed values, and possible solutions for the selection of the drive motor, electronics, solar array, and battery array.

2.2.1 Solar Cells – Caroline

During operation, solar energy was the only means of recharging the battery array. Therefore, optimizing the conversion from solar energy to stored electrical energy was crucial to a successful design. Both selection of the solar cells and the panel configuration needed to be researched to make a design decision. Although the solar cells did not realistically offer enough power to completely recharge the batteries during operation, the goal was to provide enough of a charge to extend the battery life to travel 20 miles.

Solar panels are essentially a grid of P-N junctions. Individual solar cells are arranged to generate a few Watts each, and each cell is doped on either side to be a P-type and N-type semiconductor. A circuit exists at the top of the N-type layer, which supplies energy as photons stimulate the exchange of electrons between the two semiconductor wafers. This exchange of electrons becomes the current flow. When multiple solar cells are strung together in parallel, the current is summed, and when the solar cells are wired in series, the voltage difference is summed. In this way, solar cells can be arranged to output a desired voltage and current [27].

2.2.1.1 Cell Types – Caroline

There are three general types of solar cells: single-crystal cells, polycrystalline cells, and thin film cells. Single-crystal cells, also called monocrystalline cells, have the highest efficiency in converting sunlight to electricity; however, this tends to have high production and retail costs. Lab efficiency is usually over 20% for these cells, which directly translates into higher space efficiency. Higher efficiency panels require less surface area to achieve the required amount of power output. Moreover, monocrystalline cells retain their higher efficiencies in low light conditions [28].

Polycrystalline cells are cheaper and less efficient with an average lab efficiency of 15%, but they do not perform as well in high temperatures. Therefore, they are less desirable than the monocrystalline cells. They can be distinguished physically from other cell types by their blue tint [29].

Thin film cells have the lowest cost while still having an average lab efficiency of around 13%, and they degrade faster than polycrystalline panels. Thin film cells also require a large amount of space compared to the other solar cell types, although they can be made flexible and heat-resistant [28]. In order to harvest the greatest amount of solar energy, monocrystalline cell panels were the best choice for this application, since the available surface area was limited.

2.2.1.2 Cell Optimization Techniques - Caroline

Several other factors, such as manufacturing quality, tilt, and fill factor can optimize or degrade the efficiency for each of these solar cell types. The tilt of the solar panel is often a primary concern during installation. In this particular challenge, the buggy travelled SSE for half of the journey, and then reversed direction to travel NNW. A typical winter irradiance profile in Orlando for a fixed winter tilt is shown in Figure 6, which implies that the usable daily irradiance close to the time of the competition occurs between 8:00 AM and 4:00 PM. However, this data also shows an average irradiance of around 400 W/m^2, or a total of 4000 Wh/m^2. This was a starting assumption of the available solar energy density for a late November competition day. Assuming that these are the hours of the competition, the recommended course of action was thus to mount the solar panel to face south, since the sun would lie to the south by the equator, albeit moving also from east to west. An automated solar tracker was not explored for this project due to financial restrictions. This data was supplied through Dr. Zhihua Qu's systems and controls lab at the University of Central Florida. However, more calculations were completed in the design to verify the exact hourly profile and angle of incidence for the proposed solar panel configuration.

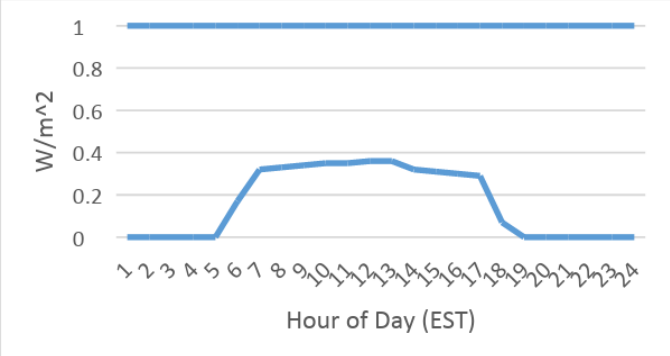

Figure 6. Solar Irradiance per Unit in December in Orlando.

Another way to optimize solar efficiency is to utilize as much surface area as is available, otherwise called the fill factor. For all available surface area on the buggy, a solar panel would theoretically be located above that space. During frame design, this relationship

was taken into account to create additional surface area whenever it was feasible. In this way, it was possible to consider using multiple solar panels as opposed to one, ideally mounted overhead.

Solar concentrators introduce one other way to maximize solar panel output. A simple lens or mirror can increase output if its size is on the same order of magnitude as the panel (or preferably larger), but this system also introduces additional heat. Panels have a maximum temperature that they can withstand, so this system would need to be closely monitored. Depending on how the buggy's frame was designed, some inexpensive form of solar concentrator, such as mirrors, could have been considered. However, irradiance was expected to be high in a beach environment due to combined effects of albedo and diffused solar irradiance, which means that the temperature of the panel was assumed to be high. Solar panels are notoriously less efficient at higher temperatures, so a solar concentrator was not given a design priority.

2.2.1.3 Solar Panel Options – Caroline

Three general options are available for this project. A solar panel could have been purchased with the exact desired power specifications. However, this was the most expensive option and was avoided. The second option was to utilize the solar panels made available by UCF's College of Electrical and Computer Engineering. Three solar panels models were available: the Suntech STP235 [30], the Heliosusa 6T [31], and the Sanyo HIP-190DA3 [32]. The Heliosusa 6T panel had the highest maximum power output at 250 Watts, followed by the Suntech STP235 at 235 Watts and the Sanyo HIP-190DA3 at 190 Watts. The manufacturer-listed efficiency for the Suntech panel is 14.4%. The efficiency of the Heliosusa is listed as 15.03%. The efficiency of the Sanyo panel is listed as 15.7%. While both the Heliosusa and Sanyo panels each weigh about 50 pounds, the Suntech panel is lighter at 40 pounds. Due to the importance of having a lightweight vehicle, the Suntech panel would have been the best match of these options for the beach buggy.

The third and best option, which was be pursued in the design, is constructing a solar array out of individual solar cells. This option is less expensive than buying a panel and much more lightweight than installing a manufactured panel. This option required soldering each cell together and creating a frame and base for mounting the cells. Monocrystalline cells were the optimal choice in order to maximize surface area efficiency. Cell selection, arrangement, and mounting techniques were explored further in the design.

2.2.2 Motor Controller – Caroline

Motor controllers are the connecting point for the microcontroller, the power supply, and the motor. More specifically, they feed into a motor driver which delivers power to the motor. The system receives directions from the microcontroller in regards to how much power should be allowed to flow into the motor, thus controlling speed and direction. Motor controllers are also important for ramping. Even if very low precision is used to

determine the speed level to minimize processing power, the motor should still ramp up slowly from stop to full speed. The reason for this is that allowing the full amount of current to suddenly flow to the motor might not only damage the motor, but it might also injure the driver from the sudden impulse. Thus, motor controllers fulfill an important role in the safe operation of motors.

For a brushed DC motor, a corresponding brushed DC motor controller was required. If a servo is used for a precision-based application, such as for the electric steering or sensor rotation, the servo would not require a motor controller, because it can communicate directly with the microcontroller [33].

Motor controllers work by translating different input voltages to different speeds. For example, in order to spin at 50% of the maximum speed, a DC motor would need to receive half of its rated operating voltage. Of course, DC motors work most efficiently close to their rated voltage, so the goal of the mechanical drivetrain design was simply to ramp up the voltage at a comfortable rate and then maintain full speed at 3 mph. In reality, this was difficult to accomplish. A constant voltage regulation of at least 70% of the rated motor voltage is generally recommended to achieve higher efficiencies. For a more sophisticated system, a feedback signal could have been used to check the difference between the command and the resulting motor speed. A feedback loop requires an encoder to measure the rotations of the motor over a given time and calculates rotational speed. Servos commonly have this feature. One of the great benefits of using a brushed motor is that there are many commercially-available options for compatible motor controllers and drivers [33].

2.2.2.1 PWM Signal – Caroline

Pulse width modulation (PWM) is one method of controlling the motor's speed. It requires turning on and off a constant voltage source at a specific rate in order to lower the perceived output voltage. The ratio between the high and low signals during one period is referred to as the duty cycle, or the percentage of the maximum supplied voltage.

$$\square_{\square\square\square} = \square \times \square_{\square\square}$$

In reality, these PWM signals are generated on the microcontroller at very low voltages and are transmitted to the motor driver circuit via the motor controller.

There are two ways to control PWM signals: sign magnitude PWM control, and locked anti-phase PWM control. Sign magnitude PWM essentially cycles between a positive and negative voltage, which is based upon a single bit direction input, and this controls the duty cycle. A negative signal means movement in the opposite direction, so theoretically any duty cycle from -100% to +100% is possible, and both motor directions are possible. Controlling a brushed DC motor with a sign magnitude PWM control signal requires one PWM control input, one directional control input, and the voltage source. Sign magnitude PWM requires more pins than locked anti-phase PWM control but offers twice the

precision control of the speed, which was not necessary for this application since the maximum acceptable vehicle speed was 3 mph ± 0.5 mph [33].

Locked anti-phase PWM control uses only a voltage source and a PWM control input. A duty cycle of 0% is full-speed reverse motion, 50% is stationary, and 100% is full-speed forward motion. Therefore, a full range of motion is possible with a single signal, but the precision is halved [33]. This could have been utilized in this project in order to limit the number of output pins on the MCU.

Communication methods also include serial (UART), RC, and I2C, which utilize bytes of data or radio signals to represent a similar concept of selecting speed intervals. However, these exact configurations often differ between manufacturers. All of these input signals represent valid ways of expressing motor control parameters [34].

2.2.2.2 Motor Driver – Caroline

The motor driver acts as the muscles of the motor controller and encompasses the actual power-controlling devices. Whereas the motor controller can only dictate how much power should pass from the batteries to the motor, the motor driver reconciles the PWM-generated signal and combines it with the actual input voltage of the power supply to output the final desired voltage to the motor.

For a brushed DC motor, such as the one being used in this project, the circuit that makes this power amplification possible is the H-bridge circuit. An H-bridge circuit is capable of amplifying the PWM signal using the power supply and also changing the direction that the motor spins by changing the direction of the current. H-bridge circuits are composed of four power MOSFETs. Motor direction is controlled by switching each pair of MOSFETs on and off.

H-bridges have two modes of stopping: free run mode and brake mode. In free run mode, the motor coasts to a stop due to friction. This mode is introduced by opening all four switches, thus isolating the motor from the power and allowing it to act as an inductor. This helps recover the remaining momentum in the motor. Meanwhile, brake mode equalizes the voltage on either side of the motor, thus causing the motor to discharge its built-up energy suddenly in a burst of heat. While effective, this mode causes motors to wear faster. On a final note, care must be taken to ensure that a short circuit is not induced when switching MOSFETs. This would cause overheating and ultimate failure of the H-bridge and other components [34].

Other desired features include surge protection and other safety measures that can be found in most packaged motor drivers. Generally, the greatest danger in using motor drivers is over-heating, so achieving a high-efficiency, low heat-generation motor driver was prioritized. Additional heat transfer methods, such as a heat sink and fan, are other critical components for a motor driver. Individually, the motor driver offers no feedback. An additional sensor, called an encoder, is necessary to solve this issue.

2.2.2.3 Encoder – Caroline

In order to construct a closed-loop control system, feedback must be taken from the output, namely the rotation of the motor, to the input, or the microcontroller. This is accomplished by installing an encoder. By using this measurement device, errors can be detected and corrected continuously to verify system status. Without encoder feedback, the actual output will remain unknown to the computer and could continue to deviate further from the desired output, making this component a necessity for any precise design [35].

Encoders are widely used as electro-mechanical devices capable of converting information from one form to another. Motor encoders in particular measure motion in terms of position, velocity, and direction by converting this motion to an electrical signal. For this project, a rotary encoder, which measures angular motion, was considered rather than a linear encoder, which only measures linear motion. Rotary encoders are generally mounted on the rear motor shaft and can either be incremental or absolute. Incremental encoders utilize pulse trains to determine relative angular position and speed when passed through a calibration algorithm. Absolute encoders measure absolute positions of the shaft directly by reading a binary code, referred to as gray code, along a disk as it rotates and allows the photodetector to receive light. Further, unlike incremental encoders, they retain position information after being powered off. A diagram of how this works is shown in Figure 7. Both types could have been integrated into this project according to their different purposes. For steering, where positions remains absolute and positions within a singular rotation must be closely controlled, an absolute encoder was more appropriate. Meanwhile, the important information at the drive motor was the speed and the direction of rotation, which aligns more closely with incremental encoder output [35].

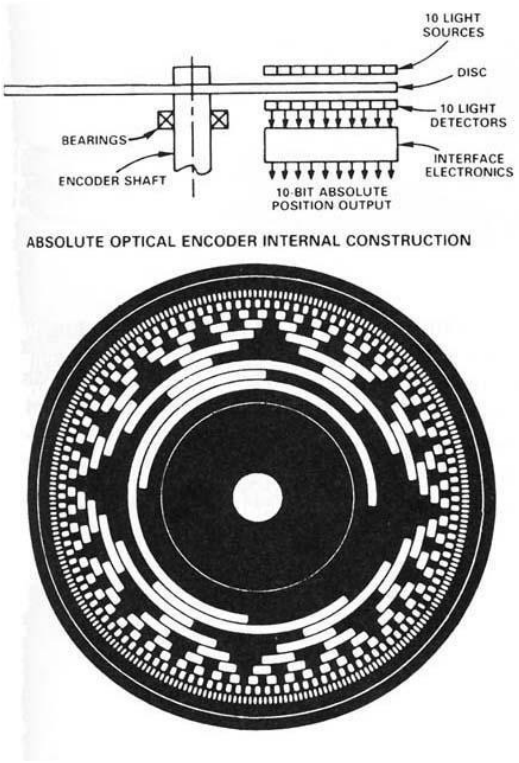

Figure 7. Absolute Optical Encoder Setup and 10-Bit Configuration Diagram. (Reprinted from public domain)

There are many different methods of performing these measurements, but the most commonly used and reliable methods are optical and magnetic encoders. Optical encoders use slits or reflective patterns on a disk, which is attached to the motor shaft, to pass light from a light emitting diode onto a photodiode as the disk rotates. However, this delicate system is susceptible to error through environmental contaminants and mechanical shock or vibration. This is not well suited to the motors onboard the buggy. Magnetic encoders, on the other hand, use Hall effect sensors to detect changes in the magnetic field as the motor shaft rotates, thus counting the number of rotations. This system tends to be more accurate, is not affected by dirt, and can better withstand mechanical impacts and vibrations. Magnetic encoders are the obvious choice for a drive motor in the beach environment [36].

The last classification is the quadrature encoder. This type of magnetic encoder uses two Hall effect sensors 90 degrees apart. These sensors are mounted next to a multi-pole permanent magnet which encircles the shaft. Each Hall effect sensor records a signal with a period corresponding to the time it takes to pass a positive and negative pole, but one signal will lag behind the other by 90 degrees. Depending on which sensor has the leading edge, the direction of the motor can be determined in addition to the rotational speed. This feature could be useful for verifying the direction of the drive motor, since the DC motor will be capable of reversing direction.

2.2.3 Charge Controller – Caroline

Charge controllers act as voltage and current regulators between the solar array and the batteries. Charge controllers are necessary to protect the battery from overcharging if the voltage of the solar array is greater than the floating voltage of the battery and can also closely match the charging voltages during the bulk and absorption charging stages. It is possible under certain conditions that the battery can discharge current back to the solar panel. Charge controllers have the additional feature of acting as a diode to prevent this situation. Moreover, the current is constantly changing as different amounts of irradiation are absorbed by the solar cells, but the batteries have a maximum current that is safe for charging, which can be regulated by the charge controller. Unfortunately, charge controllers also cut the efficiency of the power system by regulating excess power. In order to maximize the power delivered to the batteries during operation, efficiency should be optimized within the boundaries of the budget.

2.2.3.1 Maximum Power Point Tracking – Caroline

There are two kinds of charge controllers: Pulse Width Modulation (PWM) and Maximum Power Point Tracking (MPPT). PWM controllers are switches that connect and disconnect the solar panel from the battery to match the input voltage to the voltage of the battery. This is the same voltage regulation method that is used by the motor controller. MPPT controllers are able to transform incoming power at the Maximum Power Point to match the voltage of the battery plus load (DC to DC transformer), thus having a higher efficiency. However, MPPT controllers are more expensive. PWM would have been a good, inexpensive solution for this project because the cell temperature will be moderate, likely in the range of 45 to 75 degrees Celsius. At the same time, PWM charge controllers often lose 70% of the received solar energy or more, especially if the panel voltage is much higher than the battery voltage. MPPT controllers are a better choice for more extreme temperatures and for partial shading situations, both of which are disregarded in this application [37]. Still, the efficiency of MPPT controllers, which is often above 95%, is extremely appealing and better helps the beach buggy reach its performance targets.

Another option to purchasing a plug-and-play MPPT charge controller is to construct an MPPT charge controller using a commercially available MPPT integrated circuit design rather than purchasing one to lessen the impact on the budget while optimizing efficiency. Using this method, a specific MPP algorithm could have been chosen and executed. Two popular, low-cost algorithm implementations are Incremental Conductance and Perturb & Observe methods, which dynamically calculate the Maximum Power Point [38].

Perturb & Observe refers to the small incremental changes in voltages created by the charge controller and observing the power increase or decrease, which will indicate the slope of the MPP curve. The algorithm reaches equilibrium when the slope begins to change direction, although it is susceptible to steady-state error. An Incremental Conductance algorithm uses a similar method to sense the slope of the MPP, but instead

senses it by comparing the positive incremental conductance and negative instantaneous conductance. However, studies have shown that both methods achieve relatively similar efficiencies, while the Perturb & Observe algorithm retains a rather simple structure [39]. Any acquired MPPT IC's would likely utilize one of these two methods to calculate the Maximum Power Point (MPP). The Perturb & Observe algorithm was given preference for its simplicity.

2.2.3.2 Charge Controller Options – Caroline

Three primary options were considered based on the above research. If an MPPT charge controller could have been purchased with the budget, the Victron Energy SmartSolar Charge Controller MPPT 100 | 30 would have fit the estimated power requirements for the solar array, accepting a maximum nominal PV power input of 880W at 24V. It has a listed efficiency of 98% and self-consumes 10 mA. This device contains Bluetooth capability to monitor the generation and battery life using automatic battery voltage recognition. It also protects against over-heating [40]. However, the additional Bluetooth capability is not necessary for the design, and the cost is approximately $230.00.

The other option was to design and build a charge controller using the Texas Instruments TIDA-00120 Solar MPPT Charge Controller design. The design accepts a maximum of 20A at 12/24V from the solar array to a 12/24V battery array, but it could be redesigned to accept a maximum of 40A with a different MOSFET package. TI claims that the efficiency is above 97% at full load with a 24V solar array and 24V battery array. The rated voltage of the MOSFETs could also be upgraded to work with a 48V system. This design was also equipped with reverse battery protection, programmable alarms, and battery life detection using built-in battery charge profiles. It requires a minimal 10 mA of standby current. The algorithm it employs to calculate the MPP is the Perturb & Observe algorithm, which was preferred when compared to designing an Incremental Conductance algorithm [41]. The estimated cost to build was $150, making it significantly less expensive than the Victron controller. It was also more flexible if the power requirements needed to change, which could occur if either more solar cells could have been purchased or if less solar cells were installed.

The last option was to circumvent building a charge controller by configuring the solar array to exactly match the voltage of the batteries, and then connecting the panels to the batteries through a circuit breaker, a voltmeter, and an ammeter. A blocking diode would also have needed to be added for reverse current protection. While this system would have been half the cost of designing and building a custom charge controller, it had three main disadvantages. First, it is less autonomous, since the circuit breaker would have needed to be switched before and after each use of the buggy. Second, the batteries would not have been able to charge at optimal efficiency for every stage of charging. Since the voltage of the panel was fixed, either the batteries would have been charging at a slower rate, or the difference in panel and battery voltages would have been a direct power loss at least equal to the efficiency losses of the charge controller. Third, it had much less flexible parameters than the charge controller. For instance, if some of the cells broke during operation and the solar array voltage decreased in proportion to the damage, then

this would likely have caused the panel voltage to drop below the battery voltage. If so, none of the solar energy would have been received by the battery with no way to fix the issue. Another potential failure mode was an overcurrent situation. While the circuit breaker should have protected the battery if this occurred, that energy would also have been completely lost.

In order to gain design experience, protect against failure modes, and reduce the budget, the TIDA-00120 was used as a reference design for a custom-made MPPT charge controller and modified to optimize efficiency for this design's particular solar arrangement.

2.2.3.3 Efficiency

The TIDA-00120 Solar MPPT Charge Controller reference design is suitable for 12/24 V systems with up to 20 A. However, the design for the buggy must be created for solar panel inputs up to 48 V and an output current of up to 40 A. The batteries of the buggy were chosen to be 24 V and are capable of accepting up to 35 A. Therefore, these modified charge controller design specifications fit perfectly for this battery setup. As shown in Figure 8, an efficiency of 97% and above is reached in a 24V system based on the tests performed by Texas Instruments [41]. While upgrading the voltage capacity to 48 V would not have changed these efficiency estimates, upgrading the current capacity from 20 A to 40 A would certainly result in more losses. Therefore, design choices were made to enhance the efficiency of a larger capacity charge controller.

2.2.3.4 Battery Protection

Battery protection was the most important safety aspect of the buggy design since it was tied closely to the functionality of the final product. Failure to use a charge controller would have adversely affect the performance of the buggy. As described in the Solar MPPT Charge Controller design description, the Charge Controller was created with real world considerations which included reverse battery protection and programmable alarms [41].

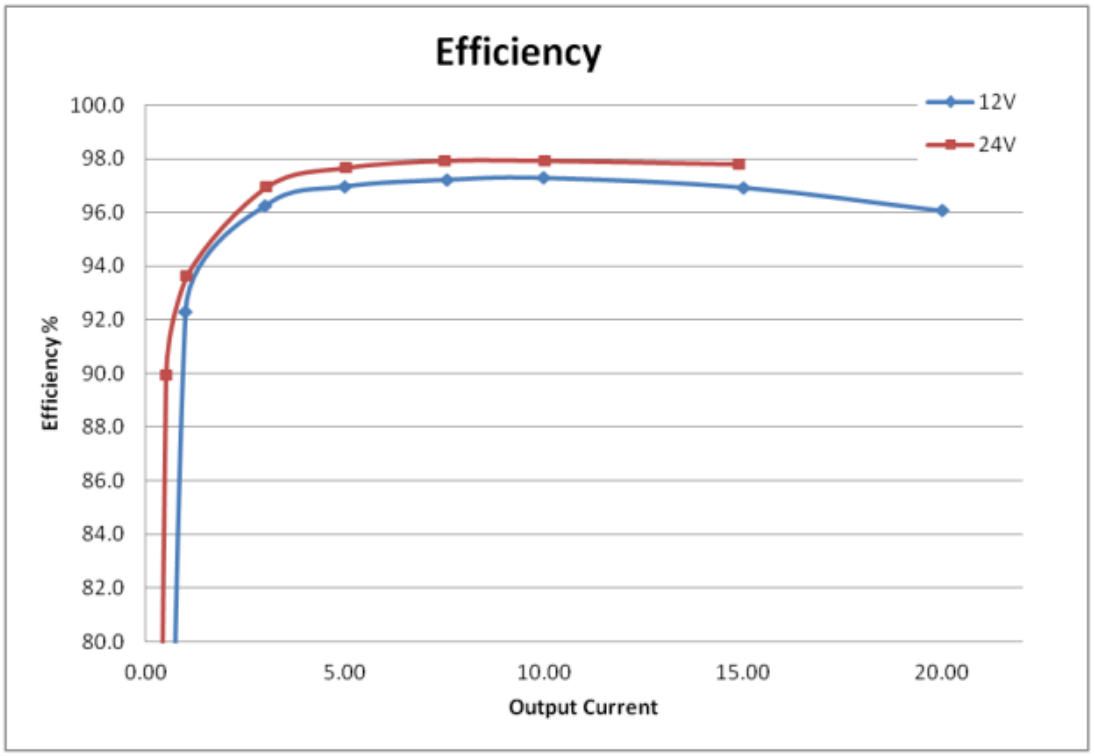

Figure 8. Efficiency% of 12V and 24V System [41].
(Reprinted with permission from Texas Instruments)

There are three major factors that would have caused battery failure: over-charging, over-discharging, and excess heating. To prevent over-charging, voltage and current regulation were used to protect the batteries from taking too much power, too rapidly. A microcontroller was used to monitor and control the charge functions. Over-discharging the batteries could have caused a short circuit and eventually turn off the system, which required a manual reset. To prevent over-discharge, the microcontroller was programed to monitor the battery voltage. “Off” and “On” threshold presets ere provided to turn on and off the output when the voltage drops and rises. Lastly, the microcontroller was also programmed to read the changes of a thermal resistor and disabled the input and output of the batteries until the temperature had returned to normal operating conditions.

2.2.4 Converters – Olesya

The Solar Powered Buggy’s battery will have an output voltage of 24 volts, which is too high for the smaller electronics (the microprocessors, sensors, and cameras), so the voltage will need to be stepped down to be able to provide power to these smaller electronics. Since the battery will be providing DC voltage, there will be no need to consider any AC to DC converters in the power calculation and design for the smaller electronics. Only DC to DC converters will be considered for this portion of the project.

The project will need to have a device that steps down the voltage, also known as bucking the voltage, and an additional voltage regulator if needed. Bucking the voltage can be done with a buck boost converter. Regulating the voltage is needed when the input

voltage to the electrical component requires a steady input, and that information can be found in the datasheet of the components used for the project. For example, stated on the datasheet [42], the raspberry pi requires a voltage of 5 volts with an allowable variation of plus or minus 5%, this means that the voltage should stay between 4.75 and 5.25 volts. In this case, the raspberry pi will need a steady voltage. Based on the datasheets, most of the smaller electronics considered for this project will need a steady input voltage.

A buck boost converter is a DC- DC component that is designed to either give an output voltage that is either greater than or less than the input voltage. Voltage regulators are typically used for two things. One, to regulate the voltage and changing the desired output as stated above, and two, to protect sensitive electronics that have integrated circuits against voltage spikes. The DC-DC converter modules are either designed with both components, a buck boost converter and voltage regulator, or just one of the two. Converted modules that step down the voltage to 12, 9, 6, or 3 volts are also typically designed to be accurate and have safeguarding against the voltage output that is going to be directly applied to the smaller electrical components.

In the case of the buggy, one option is a DC to DC converter module. Another option is a voltage regulator that is capable of an input voltage of 24 volts, and is designed with and output voltage with minimal fluctuation. The design should also consider the current flowing through the system to make sure that the current will be able to pass through the converter and power all the small electronics running at once, although this will not be a big concern with the variety of converters and the fact that the small electronics do not pull a significant amount of current.

The solar powered buggy will be powered by 1 full charge from a 24 volts battery array. Any infrared and ultrasonic sensors and rangefinders will take an input voltage of roughly 5 volts, and need a steady voltage to perform accurate scans. Depending on the voltage of any extra components added to the PCB, for example a GPS module [43], the PCB will need a steady voltage between 3 volts and 5 volts. As stated above, the raspberry pi will need a steady voltage of 5 volts. Therefore, a voltage regulator(s) will need to be include in the design.

If the printed circuit board design comes out to 5 volts, then one converter is needed. However, if the printed circuit board design comes out to 3 volts like the MSP430, then another converter will be needed to further step down the voltage from 5 volts to 3 volts to power the printed circuit board. In the case that the design needs two DC to DC converters, most of these converters can step down the voltage from 24 volts to 1 volt, so the same kind of converter can be used Raspberry Pi’s and the printed circuit board and later adjusted depending on their voltage requirements.

The 24 volts to 5 volts converter is a critical component because the converter will be providing power to sensitive electronics. The requirements for this component is efficiency and low-cost. While staying within the budget range, the efficiency should be as high as possible because the buggy will only run on one charge. The efficiency can be found by researching the step-down component of the module. For example, the

Dovewill Step Up and Down Module has a LTC3780 chip has 98% efficiency [44]. Some of the modules do not state which chip is used and therefore the efficiency is noted as not applicable.

Providing power to the raspberry pi also should be considered because the microprocessors requirements are different and more specific than smaller IOT processors. One way to provide power is through a micro USB 2.0 connection. The raspberry pi 3 (model 2) takes up to 2.5 amps at a steady 5 volts through the micro USB connection. Another way to provide power is through a GPIO pin. This route will not be taken because it introduces more risk to the system. The GPIO pins are not protected internally compared to the micro USB port on the board, which has a voltage regulator to make sure that only 5 volts are used. The wiring for this project and the length of the wire will need to be considered to sustain the minimum amps needed to run the raspberry pi(s).

Table 8 is the list of potential converter modules to use as the 5 volts and 3 volts converters in the buggy electronics that would be applicable to this project and meet the discussed requirements above.

Table 8. Converters Considered for the Solar Powered Beach Buggy.

Component	Sub-Components	Input voltage and current	Output voltage and current	Efficiency	Cost
DC to DC Voltage Regulator Step Down Up Power Supply Converter Module	LM2596 step down chip/ XL6009 step up chip/ Output voltage regulator	3.5V to 28V ---------- 1A (Maximum 3A)	1.25V to 26V ---------- 1A (Maximum 3A)	n/a	$9.95
KNACRO Waterproof Voltage Converter Regulator	n/a	10V to 30V ---------- n/a	5V ---------- 10A	Up to 96%	$10.60
Dovewill Automatic LTC3780 Voltage Regulators Step up/down Buck Converter DC	LTC3780 step down chip	5 V to 32 V ----------	2 V to 24 V ---------- .01 to 14 A	Up to 98%	$16.58

Yeeco DC 10A 150W Adjustable Buck Step Down Converter	n/a	7 V to 36V --- 	1.5 V to 35V --- 10 A	Up to 95%	$21.86
DZS Elec LM2596 Buck Voltage Converter	LM2596 step down chip	9 V to 36V --- n/a	5V --- 3A	Up to 92%	$9.99

2.2.5 Power Calculations – Caroline

In order to form an accurate estimate of the power requirements of the vehicle for the drive motor and other electronics, appropriate equations, assumptions, and physical analysis were conducted. The goal was to form a mathematical model which was revisited during the design to determine feasibility of the power system. This was necessary to ensure that the vehicle could endure the expected distance in the given amount of time. This model also guided battery and solar array purchasing decisions. The power calculations can be broken down into required motor power, electronics power consumption, and power provided by the solar array. The mathematical model will be presented, but the calculations will be reserved for the design. Final calculation results are located in Appendix C.

2.2.5.1 Motors – Caroline

The motor power calculations encompass the dynamic equations of the moving vehicle, weight estimates, the mechanical to electrical power efficiency conversion, and safety factor preferences for the final motor sizing. Generally, efficiency of conversion from electrical energy to mechanical energy is around 80%, although the exact number depends on the DC motor model. The weight of the vehicle is comprised of, in descending order of approximate magnitude, the batteries, the frame, the passenger, the tires, the motor, the electric steering system, and miscellaneous additions, such as electrical components. By summing these estimates, an approximate vehicle weight was obtained.

In general, the total force required to move a vehicle is the sum of the incline forces, rolling resistance force, drag force, and accelerative/inertial force. The drag force is going to be ignored, since the maximum vehicle speed is rather low at 3 mph. The incline forces are also ignored, since the beach is a generally level surface. The force due to rolling resistance and inertial forces will be approximately equal in magnitude. The force due to rolling resistance is expressed as:

$$F_{rr} = C * W * F_{rr}$$

The mass of the vehicle is m, the gravitation constant is *g*, and the coefficient of rolling resistance is C_{rr}, which was approximated in the Terrain Assumptions as 0.08.

The force due to acceleration demands can be quite complicated to calculate exactly, because both translational and rotational inertial forces for all rotating parts, including torque, must be combined. In order to sidestep this involved approach, an assumption will be made. First, the added force due to rotational forces will be combined into a single coefficient, referred to as the coefficient of accelerative resistance. This value must be less than twice the translational force, but obviously greater than one. A reasonable guess would be 1.5. If the coefficient is less or more than the real value, the vehicle will simply accelerate at a slower or faster rate. The desired acceleration is about 0.5 $\frac{□}{□^2}$, so that in under three seconds after a complete stop the vehicle will achieve its maximum speed. The equation for the accelerative force is expressed as:

$$□_□ = □ * □ * □_□$$

It should also be noted that this accelerative force is only required when increasing the speed of the vehicle. It was unknown how frequently the buggy would need to stop, so the motor must have been able to provide this much force in addition to the rolling resistance force at all times. This was done with the knowledge that the motor would be slightly oversized while traveling at constant speeds. The motor controller was extremely useful in ramping the motor down to 70-80% of full load for constant speeds. This extra power could also have been useful when compensating for more rolling resistance due to looser sand, if the terrain became muddy, or if the buggy stopped frequently and had to recover from the lost time.

Ultimately, motor selection was determined from the optimal combined cost of the motor and batteries without exceeding the power estimates. The final equations for the mechanical and electrical power demands are as follows:

$$□_{□□□□□□□□□□□} = (□_{□□} + □_□) * □$$

$$□_{□□□□□□□□□□□} = □_{□□□□□□□□□□□}/0.8$$

These equations determined both motor size and required power from the batteries to support full load conditions. While a 15% upsize in motor capacity was desired, it was not necessary since extra motor capacity negatively affected the budget.

2.2.5.2 Electronics – Caroline

Although the exact electronics used for the beach buggy were verified in the design, a short model consisting of the sums of the power draws from each component and a quick estimate of the total power draw can be presented. A table of the electronics and an expected range of power values is displayed in Table 9. During the design, the final power draw was calculated from summing the actual values particular to that component. Components such as the charge controller were assigned a wide range of estimated power draws due to the fact their power draw is a function of input power. The minimum and maximum estimates were determined from the minimum and maximum calculated solar generation multiplied by an efficiency loss of 0.04%.

Table 9. Estimated Electronic Component Power Draw.

Component	Estimated Power Draw (W)
PCB	3 – 7
Camera	1 - 2
Sensors (x2)	2 – 5
Converter	1 - 2
Motor Controller	1 - 3
Encoder	0.5 – 1.5
Processors (x2)	10 - 20
Charge Controller	5 - 30
Fan(s)	0 – 0.5
TOTAL	**23.5 – 71**

A separate estimate was also made for the steering motor. While the torque required of the motor was later measured when the buggy was assembled using a torque wrench on the steering shaft, an estimate was first given to complete the power calculations for selecting the solar and battery components. Torque is high at very low speeds approaching zero, so it was assumed that during operation, the steering system would not be turned on until the buggy had gained some momentum, maybe 1 or 2 seconds into its acceleration. A 12V motor at approximately 150W running for 20% of the total run time would result in 30W, which represents the approximate minimum power. A 12V motor at approximately 250W running for 30% of the total run time would result in 75W, which is an estimate of the maximum power. Thus, the total electronics power consumption was likely between 53.5 W and 146 W. While this power consumption is relatively insignificant compared to the power that was drawn by the drive motor, these estimations were especially important for determining required heat transfer from the electronics and ultimately determined the size and quantity of the necessary fans and heat sinks.

2.2.5.3 Solar Array – Caroline

There are two major steps involved in calculating the power output from the solar array: finding the angle of incidence and calculating the total irradiance. The first step involves using geometric relations between the sun and a tilted surface, which can be exactly calculated using the time of day, day of the year, and surface zenith and azimuth angles. Altitude angles express height, whereas azimuth angles describe direction relative to the horizontal plane, either north or south. The steps to calculate the angle of incidence are briefly explained below.

First, the declination angle is calculated, which is the angle between the sun and the equator. In the winter, this angle should be negative, and lies in the range of -23.34 and +23.45 degrees [45]:

$$\delta = 23.45 \sin\left(360 * \frac{n+284}{365}\right)$$

[degrees]

Next, the equation of time and consequent solar time calculation takes into account the deviation from clock time, which is divided roughly by 15 degrees longitude over the globe [46]:

$$E = 0.165\sin 2B - 0.126\cos B - 0.025\sin B \quad \text{[hr]}$$

Where B is equal to: $B = \frac{360(n-81)}{364}$ [degrees]

The solar time, which is specific to the actual location and deviates slightly from the standard time, is expressed below. All times must be expressed as decimal values [46]:

$$ST = CT + \left(\frac{1}{15}\right)(L_{std} - L_{loc}) + E - DT$$

[hr]

Where CT is the clock time, L_{std} is the degrees west of the standard meridian in the local time zone, L_{loc} is the longitude of the location in degrees west, E is the Equation of Time, and DT is the number of hours that are advance for Daylight Savings Time, if that is applicable. Otherwise, DT is zero.

Next, the solar hour angle is calculated. According to the standard meridian time zones, the hour angle should vary by 15 degrees every hour, with an hour angle of zero being solar noon. Negative values indicate morning times, while positive values indicate afternoon times [46]:

$$\omega = 15(ST - 12) \quad \text{[degrees]}$$

The two remaining variables for calculating the angle of incidence are the sun altitude angles and the sun azimuth angles. The sun altitude angle can be computed from [45]:

$$\alpha = [\cos\varphi \cos\delta \cos\omega + \sin\varphi \sin\delta] \quad \text{[degrees]}$$

Where latitude is φ.

The sun azimuth angle takes into account the sun altitude angle and is defined as the angle between the sun and due south on the horizontal plane [47]:

$$\gamma = \sin^{-1}\left[\frac{\cos\delta \sin\omega}{\cos(\alpha)}\right]$$

[degrees]

Lastly, the angle of incidence between the sun and a sloped plane is [47]:

$$\theta_i = (\cos\varphi \cos\delta \sin\beta \cos\gamma - \cos\varphi \sin\delta \cos\beta \cos\gamma + \cos\varphi \cos\delta \cos\beta \cos\omega + \sin\varphi \cos\delta \sin\beta \cos\gamma \cos\omega + \sin\varphi \sin\delta \sin\beta \sin\gamma \sin\omega)$$

[degrees]

Where the tilted surface has an azimuth angle of γ and a zenith angle of β. The sun altitude and azimuth angles are reserved for irradiation calculations and panel tracking.

The second half of the calculations are used to find the total hourly irradiation on the tilted surface. The first step is to find the sunset and sunset hour angle, which is found as [47]:

$$\omega_s = (-\cos\varphi \cos\delta \tan\delta)$$

[degrees]

The isolation intensity is calculated using the solar constant, but an adjustment must be made for Earth's elliptical orbit. This calculation represents the total insolation on a plane perpendicular to the sun [48]:

$$\square_0 = \square_{\square\square}[1 + 0.034 \square\square\square\ \square\square\square\ \left(2\square\frac{\square}{356.25}\right)]$$

[W/m^2]
Where I_{SC} is equal to 1367 W/m^2 and n is the numbered day of the year.

The extraterrestrial irradiation on a horizontal plane can be found using the following equation [48]:

$$\square_{0\square} = \frac{24}{\square}\square_0(\square\square\square\ \square\square\square\ \varphi\ cos\ \square\square\square\ \delta\ sin\ \square\square\square\ \omega_\square + \square_\square\ \square\square\square\ \square\square\square\ \varphi\ sin\ \square\square\square\ \delta) \quad [\text{Wh/m}^2]$$

The clearness index is a ratio of the total irradiation on a horizontal plane, including scattering and absorption effects, to the total extraterrestrial irradiation on a horizontal plane in that location. The clearness index can be found from collected weather data and was found from one source to be 0.54 in November for comparison [49]. Another source lists 0.499, but its data is not as current [50]. The clearness index can also be calculated using the expression [48]:

$$\square_\square = \frac{\square}{\square_{0\square}} \quad [\text{dimensionless}]$$

Where H is the monthly average daily irradiation on a horizontal plane and can be obtained also from weather data. One source lists it as 3.4 kWh/m^2/day for November [51].

The diffused radiation can be calculated from the monthly average daily irradiation and from the clearness index. It is obtained from [48]:

$$\square = \square(1.391 - 3.560\square_\square + 4.189\square_\square{}^2 - 2.137\square_\square{}^3) \quad [\text{Wh/m}^2]$$

When $\omega_\square < 81.4$ degrees.

The hourly radiation ratio can be used to find hourly values for the diffused radiation. The expression to convert to hourly values is [48]:

$$\square_\square = \frac{\square}{24}[0.409 + 0.5016\ \square\square\square\ \square\square\square\ \left(\omega_\square - \frac{\square}{3}\right) + (0.6609 + 0.4767\ \square\square\square\ \square\square\square\ (\square_\square - \frac{\square}{3})\ \square\square\square\ \square\square\square\ \omega)]\frac{cos\square\square\square\ \omega - \square\square\square\square\square\square\ \omega_\square}{sin\square\square\square\ \omega_\square - \square_\square\square\square\square\square\square\ \omega_\square}$$

[dimensionless]
Thus, the hourly total irradiation on an average day of the month of November is taken as [48]:

$$\dot{\square} = \square_\square\square \quad [\text{Wh/m}^2]$$

In the same way, the hourly diffused irradiation ratio is calculated as [48]:

$$\square_\square = \frac{\square}{24}\frac{\square\square\square\square\square\square\ \omega - \square\square\square\square\square\square\ \omega_\square}{sin\square\square\square\ \omega_\square - \square_\square\square\square\square\square\square\ \omega_\square}$$

[dimensionless]

This results in an hourly diffused irradiation on an average day in the month of November, expressed as [48]:

$$\dot{□} = □_{□}□ \quad [\text{Wh/m}^2]$$

The hourly beam radiation is the difference of the total irradiation and diffused radiation [48]:

$$\dot{□} = \dot{□} - \dot{□} \quad [\text{Wh/m}^2]$$

Finally, the hourly irradiation on a rotated and tilted plane can be calculated from [48]:

$$\dot{□}(□) = \dot{□}\frac{□□□□□□□\,\theta_{□}}{cos□□□\,\theta_{□}} + \dot{□}\left(\frac{1+□□□□□□□\,\beta}{2}\right) + \left(\frac{1-□□□□□□□\,\beta}{2}\right)□\dot{□}$$

[W/m^2]

Here, the angle of incidence is $□_{□}$, the sun zenith angle is $□_{□}$, the panel tilt is β with respect to the horizontal, and the reflectivity ρ is taken from a table of values. For sand, one source assigns a value of 0.15-0.45 [52]. Wet sand likely belongs in the lower part of this range. In the calculations, the reflectivity is assumed to be 0.3. These final hourly values roughly reflect the percentage per 1000 W/m^2 of the rated solar panel output.

2.2.5.4 Battery Array

To identify the appropriate battery array, a selection methodology had to be created. To do so, some parameters where defined to create applicable equations. The equations that calculate the capacity (Ah) of the system is as follows:

$$□ = \sum_{□=1}^{□} \frac{1.3*(□_{□□□□□□□□□□\,□□□□□□□,□} - □_{□□□□□□□□□□\,□□□□□□□□□□,□})}{□} \quad (1)$$

Where,

$$□_{□□□□□□□□□□\,□□□□□□□} = \sum_{□=1}^{□} \frac{□_{□□□□,□}}{\eta_{□□□□,□}} \quad (2)$$

$$□_{□□□□□□□□□□\,□□□□□□□□□□} = \sum_{□=1}^{□} □_{□□□□□□□□□□,□} * \eta_{□□□,□} \quad (3)$$

Firstly, looking at equation 3, *m* refers to the number of components feeding power to the battery, $□_{□□□□□□□□□□}$ stands for the total amount of power generated by the component and $\eta_{□□□}$is the efficiency the kind of battery absorbs the power. Then, regarding equation 2, *n* is the number of components receiving power from the power, $□_{□□□□}$ represents the power the component needs in Watts, and $\eta_{□□□□}$ evinces the efficiency of the component. This means the actual power being used after losses. Lastly, referencing equation 1, □ is the time the buggy is supposed to run for in hours, and *V* is the voltage of the battery bank. It is noteworthy that the final result is multiplied by 1.3 to account for deep cycles no lower than 20%, combined with a small safety factor of 10%. In turn, this also covers environmental factors and leakages that could affect final power output.

2.2.6 Circuit Protection Devices – William

A circuit protection device is used to keep an undesirably large current, voltage, or power surge out of a given part of an electrical circuit. To limit these potentially dangerous conditions, circuit protection devices must be used. Circuit protection devices are used to stop current flow or open the circuit. These devices are usually connected in series with the circuit it is protecting in order to stop current flow or open the circuit. Circuit protection accounts for direct shorts, excessive current, and excessive heat [53].

2.2.6.1 Types of Devices – William

A circuit protection device is able to protect the circuit by opening and interrupting current to the circuit. When something is wrong in the circuit, the opening of a protection device will be able to show that. This should be corrected before the current is restored. The protection device opens when a problem exists. The device should be able to isolate the faulty circuit from the other unaffected circuits. It should also respond in time to protect unaffected components in the faulty circuit. During normal circuit operation, the protection device should not open [53].

Fuses and circuit breakers are two types of circuit protection devices. As the simplest circuit protection device, fuses work by being deliberately made to melt when the current gets too excessive. Since the beginning of the use of electricity, these devices have been in operation. Fuses can be described as a bare wire between two connections. The wire was smaller than the conductor it was protecting. This allowed the wire to melt away faster before the conductor was harmed by the excessive current. Tubes or enclosures are developed to hold the melting metal. This enclosure has made possible the addition of filler material, helping to contain the arc that occurs when the melting element melts. For low power uses, the finer material may not be required. Glass tube can be used to contain the melting element. This gives the advantage of being able to see when a fuse is open [53].

Circuit breakers are a helpful tool to protect circuits from excessive current. The disadvantage of using a fuse is that when the melting element has melted, it must be replaced. However, using a circuit breaker can be used more than once. This solves the issue of replacing fuses. This is a safe, reliable, and tamper proof method to protecting circuits. It is also resettable, so it can be reused without replacing any parts. This device is called a circuit breaker because it breaks open the circuit [53].

2.2.7 Power Distribution – William

Distributing the energy from the batteries was a major concern for the team. We had to be confident that all loads to source sufficient power from the battery bank in order to remain operational. A great way to handle the routing of power circuits to the buggy's electrical system was through the use of power distribution blocks. There are two main types of power distribution blocks - bussed and independent. These are non-fused distribution blocks and used primarily for routing and connecting power or ground

circuits. A bussed power distribution block will take a single larger input cable and allow it to be spit out to smaller cables for branch circuits, or working as a ground buss, can bring in smaller ground cables to a single ground cable that can then be run back to the battery. Independent power distribution blocks consist of barrier terminal blocks or stud type junction blocks. With these products, the connections are “independent” from each other and are not connected together internally. This allows for multiple individual circuits to be routed to a single location where each circuit can each have multiple connections going to it [54].

Power distribution terminal blocks are an economical and convenient way of distributing an electrical circuit from a single input source, to several devices in the electrical system. This can reduce the total number of wires in the electrical system, saving time and money. The use of a distribution block can eliminate the need to wire each device in the control circuit back to the power source by using one large wire on the input side, and several smaller wires on the output side to the devices downstream. As engineering students, we strove to create systems with a clean and professional appearance [55].

2.2.8 Relays – William

Relays are a great option to open and close circuits. They do this either through electromechanically or electronically. Relays are switches that control one electrical circuit by opening and closing contacts in another circuit. When a relay contact is normally open (NO), there is an open contact when the relay is not energized. When a relay contact is normally closed (NC), there is a closed contact when the relay is not energized. The application of an electrical current will to the contacts will change the states of the relay contacts [56].

Relays are used to switch smaller currents in a control circuit. They are not used to control power consuming devices except for small motors and Solenoids that draw low amps. This does not mean that relays cannot "control" larger voltages and amperes. Relays can "control" larger voltages and amperes by having an amplifying effect because a small voltage applied to a relays coil can result in a large voltage being switched by the contacts [56].

Electrical abnormalities, including overcurrent, undercurrent, overloads and reverse currents are possible dangers that may occur to damage electrical equipment. Protective relays can prevent these types of equipment damage by detecting these electrical abnormalities. Relays are also widely used to switch starting coils, heating elements, pilot lights and audible alarms [56].

2.2.9 Wiring – William

Choosing the proper size and fit for the power system is important for both performance and safety reasons. If the wires are undersized, this will incur a significant voltage drop in the wires resulting in excess power lost. In addition to that, there is a risk that the wires may heat up to the point in which a fire may result [57].

We used the American Wire Gauge (AWG) standard for choosing the right wire size for the power system. In order to carry a higher current safely through the wires, the wires must have a comparably lower amount of resistance. This is shown by the lower gauge number. Table 10 shows the capacity of various wire gauge sizes and their typical amp rating [57].

Table 10. AWG Wire Scale.

Gauge Number	Category	Rated Amps
3/0	A	200
1/0	A	150
3	A/B	100
6	B	55
8	B	40
10	C	30
12	C/D	20
14	D	15

The category column for Table 10 recommends what gauge number should be used between the components in a solar PV system. Figure 9 shows the corresponding category for recommended gauge number under the AWG standard. A gauge of 10- 12 is recommended for wiring the Solar PV Panels to a combiner. The wiring between the combiner to the charge controller is recommend to be in the category B range. Category B range from gauge numbers between 3 and 8. The wiring between the charge controller and the battery bank is recommended to be in the category B range, as well. The wiring between the charge controller and the power distribution block is recommended to be in the category B. The wiring between the power distribution block and to the load is recommended to be in the category B or C, depending upon the components attached to the block.

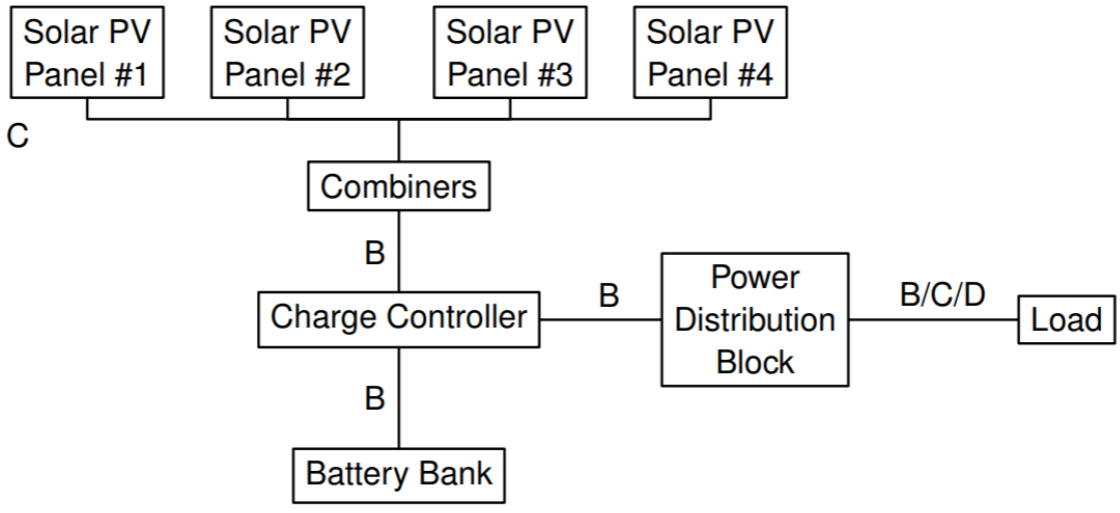

Figure 9. Recommended Corresponding AWG Category.

2.3 Electronics – Caroline

The electronic components consist of all data-processing and data-collecting components of the beach buggy. These include the microcontrollers, which were used as processors, the MCU built from a PCB, the proximity sensors, cameras, and all software development, both for collecting and transmitting the data and for manipulating the data to trigger commands. The general purpose of all electronic components is to enhance the autonomy of the vehicle. Navigation requires an intelligent pathfinding system with a GPS input and steering output, while obstacle detection requires significant sensor technology to find object distances, detect motor speed and position, and create a 3D spatial map. By effectively combining useful developed technologies and computers capable of processing that information, an autonomous vehicle is made possible. The following sections contain the research required to select or design each of those components.

2.3.1 Microcontrollers – Caroline

Although both the main MCU, which involved a PCB design, and the two Raspberry Pi's can be considered microcontrollers, they were ultimately used for different purposes. The MCU was modeled similarly to the MSP430 with necessary modifications to connect all of the sensors and controls, such as the proximity sensors, speedometer, encoder, motor controller, and charge controller. The two Raspberry Pi's were used mainly for image processing of the cameras, including pathfinding and GPS navigation. Proposed specifications, communication protocols, input and output types, and software options are reserved for the following sections.

2.3.1.1 PCB Design – Patrick

The main control unit's (MCU) primary function is to be the interface between the navigation boards, which will be doing the path finding algorithms and peripherals such as the motors and sensors. It will need to be able to interpret the signals from the sensors and other components so that it can send the relevant information to the navigation boards. The MCU will then have to be able to take the output from the navigation boards and translate those into the necessary signals to control the motor. For instance, the navigation board will decide that the driving motor needs to be running at 80% power. The navigation boards will send that data to the MCU using SPI communication. The MCU will read this and create the Pulse Width Modulation signal that translates to 80% power for the motor controller and send it to the motor driver.

Based on these requirements it was found that the Texas Instruments MSP430 family of LaunchPad boards have the necessary computing power within the price range to accomplish this task. However, there are certain features that are needed that are not supported by the MSP430. Texas Instruments has many boards that belong to the MSP430 family, so it would be necessary to select from among these. The standard board that would be the base design comes with an emulator that would be unnecessary in the

final design, as it is possible to use an emulator from another board by connecting them together. It is for these reason that a custom board based on the MSP430 would be the best option for this project.

During initial designs it was found that the numbers of General Purpose Input Output (GPIO) pins provided by the MSP-EXP430G2 would not be sufficient for this product as it has a small number of useable pins [58]. The design was then changed to be based off a board with a different processor that would provide an additional number of pins. The MSP430 FR4133 Development kit board was found to be the replacement [59]. Still being a MSP430 board, it has the benefits of being low power and supported by Texas Instruments, but provides additional GPIO pins that will be needed.

2.3.1.1.1 Composition – Patrick

To design the board schematic and board layout it was determined that the Autodesk software EAGLE would be the best option. Eagle was found to have a larger library when compared to other software such as PCB Artists from Advanced circuit. Along with EAGLE offers the software free to students for 3 years which makes it also one of the cheapest options for this project to use. The board schematic for the MSP430FR4133 is offered online at the Texas Instrument website which will be used as a starting point for the board design and layout. Each of the processors that will be considered will be compatible with the MSP4304133 design so it would be a matter or just changing the chip and not the entire design.

2.3.1.2 Software – Olesya

Common microcontrollers like Arduino, MSP430, Raspberry Pi, and the Beagle Bone can run on C Programming, C++, and Python. Once the PCB has been ordered and tested, the microcontroller will be loaded with code to interact with the peripherals. The PCB will process the information and relay that information to the navigation system running on the raspberry pi. The software will also include any processing of the feedback from the navigation system in case of an emergency stop via the user application. Software shall be written and uploaded on the PCB depending on which processor is selected in the PCB design. If the PCB design uses a TI processor found in the MSP430 family, then the software will be written in C and uploaded using ENERGIA or Code Composer Studio through the MSP430 development board. ENERGIA is an open source and easy to use IDE to interface with microcontrollers. Code Composer Studio (CCS) is an IDE strictly from TI. Both will work equally well.

If the PCB design uses a Broadcom BCM2835 SoC processor found in the Raspberry Pi A, B, and zero models, uploading the software will be more complicated. Since the processor is integrated with a lot of functionality, it is called a SoC, system on a chip, and therefore will need an Operating System. From there, a small sized operating like

Raspbian, or Ubuntu Core will need to be installed, and then code can be loaded and run. More information will be provided in the PCB design and testing sections.

2.3.1.2.1 MCU Software – Patrick

Texas Instruments MSP430 family of products all come with compatibility for developing and writing code with Code Composer Studio. Their boards come with an emulator that is designed to help streamline the process of writing and testing code when using their processors. Since the project will be using an MSP430 processor it was decided that CCS would be used to program and debug the Main Control Unit (MCU) microprocessor. The CCS IDE provides access to a multitude of libraries that will help in the writing and development of code for the microcontroller. Additionally, since CCS and the MSP430 line of products were design with each other in mind, CCS comes with built in support for optimizing and testing code for the MSP430.

2.3.2 Proximity Sensors and Range Finders – Olesya

The solar powered beach buggy will traverse the required 20-mile distance (10 miles to target and 10 miles back) autonomously. There are different levels of "autonomy" within the industry. Autonomy within the scope of this project is defined as the following.

There will be no input from the user to guide the buggy unless there is an emergency. The emergency stop is limited to a physical button and a button on the mobile application created for this project. The buggy will be using GPS to allow the user to select where the end location is. The guidance and navigation and the collision detection will be through computer vision. The processing for path finding cannot be offloaded.

This system will be able to move forward and detect any object coming its way and respond accordingly. The system should also be able to adjust its path if there are obstacles in the way. If there is a threat then the buggy will stop and go into recovery mode. There is also an emergency stop response that will be put in place for the user in case of an emergency and the buggy needs to come to an emergency stop. Any obstacles will be moved out of the way, and the buggy will begin recovery mode. This will all be implemented using a computer vision system that will process data from Raspberry Pi Camera Modules and sensors. The rest of the autonomous system of the beach buggy will be discussed in Software Sections.

2.3.2.1 Sensors – Olesya

Using range finding and proximity sensors is a low cost and simple solution when designing and building an autonomous vehicle. Proximity sensors will play a key role in the Solar Powered Beach Buggy Competition because they will provide critical input that the vision system might not be able to capture, such as the distances away from the objects. The sensors need to be accurate and the technology needs to match the specific range in which the buggy should stop. The sensors should be accurate because the limited battery will drain faster if the buggy stops from false positives. In the following

considerations of sensors, the important factors are weather, range, cost, and data output. The following research was done with the Buggy in mind. Some sensors were automatically ruled out based on the budget constraints.

The buggy's navigation will not function properly if the setbacks that these technologies might have is not considered. When selecting from the range finding sensors, there is a limitation to the ones that use light because it is unidirectional. Sensors that have emitters and receivers that can scatter the light to be able to provide a cone shaped coverage are typically found in depth sensor cameras and higher end technologies. Also, another consideration is the environment the buggy will be in. The beach will be windy with sunlight and sounds; and with this and any other interference from other electronics or machinery, some of the sensors might not to function properly.

2.3.2.1.1 RADAR – Olesya

Radio Detection and Ranging (RADAR) are commonly used in autonomous cars. There are two kinds of microwave designs for radar, Frequency-modulated Continuous-Wave (FMCW) radar and a most recent design within the industry, monolithic microwave integrated circuit (MMIC) radar. With the increase need of radar on automotive vehicles, there has been a lot of ideas and research to make radar smaller and cheaper.

A Continuous-Wave (CW) radar compared to FMCW radar has no way to mark time and calculate the distance, but when transmitting with frequency modulation, the change in frequency can be used to calculate the distance.

The difference in the frequency as shown in Figure 10 is proportional to the distance between the antenna and the object [60].

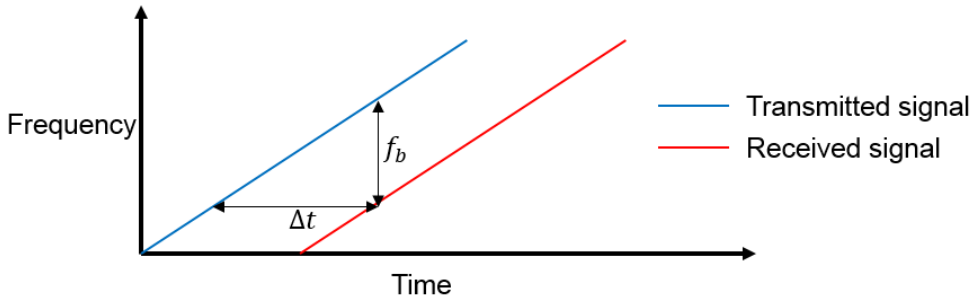

Figure 10. Radar Signals.

The benefit of using FMCW radar is that the target's distance can be measured while it is moving and the accuracy of this radar is very high. FMCW radar is also very simple in its design, giving more options for software implementation. There is a lot of industry-made FMCW radar. For example, Texas Instruments AWR1642 Single-Chip 76-to-81 GHz Automotive Radar Sensor is a FMCW radar sensor (from their Advanced Driver Assistance Systems product line) that can be modified to short, medium, and long ranges depending on its application [61].

Common designs for a MMIC radar are three transmission channels (TX) and four receive channel (RX) that are monolithically integrated. Current radar systems are either based on 24 GHz or 77 GHz, with higher accuracy, in terms of distance, when increasing the frequency. With higher frequency, the antennas are smaller and there is less interference. These radars fall into SRR (short range radar) and MRR/LRR (medium/long range radar) categories.

Although radar is commonly found in the industry they are not yet prevalent in the consumer market, and to get ahold of a good set for a low cost that can be integrated with the PCB design is not an option. Building the part is not within the project timeline or budget; therefore radar will not be included in the final design.

2.3.2.1.2 Infrared – Olesya

Infrared sensors use infrared light to detect objects by reflected light and triangulation. These sensors can be simple and cheap emitters and receivers or part of sophisticated IR cameras. Both IR sensors and cameras are commonly used for motion detection and depth imaging.

Rather than just identifying an object, common infrared sensors that calculate the distance have a position-sensible photo detector (PSD) and use the triangulation approach. These sensors are often called rangefinders and they have an emitter and the PSD. As shown below in Figure 11 [62] and as explained in [63], the current flows dependent on where the returning light beam falls. When changing the objects distance from the sensor, the beam changes where it falls on the PSD, and thus the current creates a voltage in a certain section of the PSD with the change in distance. The analog signal is translated to a digital output using an analog to digital converter. This signal is used to calculate the distance based on the percentage of the 'typical response curve,' a voltage output versus distance chart [63]. The infrared range finder has a non-linear output, so the distances increase linearly but the voltage output increases non-linearly. The distance can be calculated with an equation that is particular to every specific sensor's response curve.

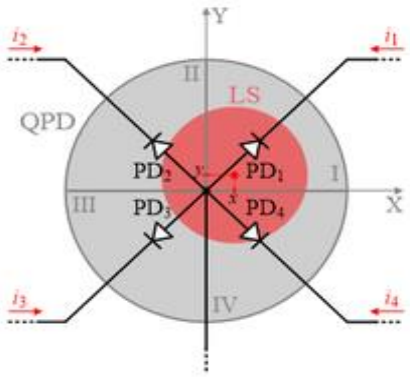

Figure 11. Position-Sensible Photo Detector Used in IR Range Finders.

Infrared sensors that use PSD technology are very useful because not only do they detect an object, but they also provide what distance the object is at versus a basic infrared transmitter and receiver sensor that only indicates that an object is within a specified range. This all depends on the brand and type. Using this sensor would be very useful because of this fact. Calculating distance would greatly improve the accuracy of the emergency stop and the navigation system.

The infrared range sensors have a few setbacks. Based off the data sheet, the detection area of the beam should typically be 20 to 35 degrees. Other research and projects such as [63] that have used this sensor do state the degree is much smaller, enough to make it difficult to detect chair legs. An additional concern is that the infrared sensors use light and the buggy will travel a path on the beach with typical Florida sunshine, so the buggy might have a problem because the light from the sun might interfere with the infrared sensors. However, after looking at applications using the sensors selected below, sunlight was not an issue. More basic infrared emitters and receivers are however affected by the sunlight. One last thing to consider about infrared range finders is that they do not support short to mid-range capabilities in one sensor. The short-range sensors max distance is too short for this application, and the mid and long-range sensors do not have the short-range distance detection for this application. This means it will be difficult to find an infrared sensor that will give the buggy a closer range of up to 3 or 4 inches and give the buggy a slightly longer range on the scale of 6 feet.

Infrared range finder sensors will be considered for the design because they are more accurate than ultrasonic due to the method and parameters used to calculate the distance. They provide accuracy of two to four centimeters and the degree of the beam comes out to be comparable to the ultrasonic sensors within the low-cost budget. A rough 15 degrees or less is still not enough coverage, so the sensors will need to be rotated by a servo to cover at least a 120-degree area with a rough range of 6 centimeters to 200 centimeters. Table 11 is the list of potential infrared sensors that would be applicable to this project and meet the discussed requirements above.

Table 11. Infrared Sensors and Rangefinders Considered for the Solar Powered Beach Buggy.

Component	**Price**	**Range**	**Output**	**Degree of beam**	**Supply voltage and current**
Sharp IR Sensor GP2Y0A60SZLF	$10.75	10 to 150 cm	Calculated Distance based on analog to digital converter output	< 15 degrees	4.5-5.5V 33-50mA
Sharp IR Sensor GP2Y0A710K0F	$24.95	100 to 500 cm	Calculated Distance based on analog to	< 15 degrees	4.5-5.5V 33-50mA

			digital converter output		
VL53L0X Time-of-Flight Distance	$9.95	3 to 200 cm	Calculated Distance based on analog to digital converter output	<15 degrees	2.6 – 5.5V 10- 40 mA

2.3.2.1.3 Ultrasonic – Olesya

Ultrasonic sensors emit sound at a high frequency and then calculate the time it takes for them to return. They are used to detect objects and measure distances. When comparing simple cheap sensors, ultrasonic sensors fall in the low-cost category along with infrared sensors for distance detection, and they have a longer distance range than the range found in infrared range finders.

These sensors calculate distance based on the time it takes for the sound waves to return, as seen with the SR-04 sensor graphic in Figure 12. Knowing the speed at which sound travels through normal atmospheric temperatures, the distance can be calculated by multiplying the time and speed, this is a very simple distance calculation [64]. However, this distance equation is not as accurate as the method to find the distance with infrared range finding sensors. The atmosphere that the buggy will navigate through, the noise from being attached to the buggy, the humidity depending on the day, and a lot of extra noise from the motors might throw off the measurements and cause the sensor to calculate the distance incorrectly.

However, some sensors like the HRLV-EZ0 have a pin to integrate a temperature sensor and protect against any disturbances in the signal. The last thing to consider is that putting the sensors together might cause interference between them. When designing the layout of the sensors, a precaution should be taken to make sure that minimal to no interference occurs from the surrounding noise or inaccurate measurements due to temperature.

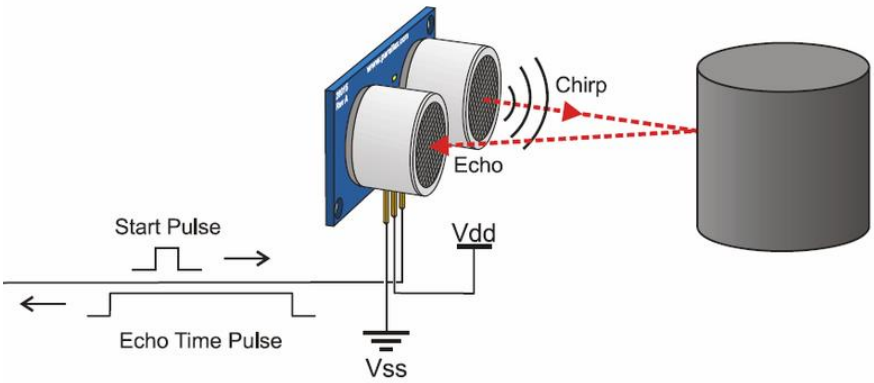

Figure 12. Ultrasonic Method Used in SR-04 to Detect Objects.

These sensors will be considered for the project because there are benefits in using these sensors over the infrared sensors. Using ultrasonic sensors allows the buggy to be in direct sunlight without introducing any potential problems, unlike the infrared sensors. Ultrasonic sensors also have a greater overall range than infrared sensors, which gives this project more possibilities when implementing the software. Additionally, the ultrasonic sensors are the lowest cost out of all sensors considered. The budget of sensors and any devices to rotate them is 60 dollars, and to have a coverage that is greater than 200 degrees around the front of buddy, the system will need at least four or five sensors. The second listed ultrasonic sensor will also be considered because it provides a greater range and it more accurate. However, this is a backup in case the SR04 ultrasonic sensor does not meet the requirements for this project. The budget is very limited, so if the SR04 preform as needed, the Maxbotix sensors will not be considered. Table 12 summarizes the sensors being considered.

2.3.2.1.4 Sonar – Olesya

Sonar sensors are very similar to ultrasonic sensors but are used for long range applications. These kinds of sensors were considered but are not applicable to the beach buggy project as back-up short range sensors.

2.3.2.1.5 LiDAR – Olesya

LiDAR is a major contender for autonomous systems in robotics. There are two kinds of LiDAR: MEMS using a rotating laser, and solid state, both of which focus on light. However, LiDAR is too expensive as a secondary system for object detection, but the idea of a rotating sensor will be added to the design.

Table 12. Ultrasonic Sensors and Rangefinders Considered for the Solar Powered Beach Buggy.

Component	Price	Range	Output	Degree of beam	Supply voltage and current
HC-SR04 Ultrasonic Distance Measuring Sensor Module	$3.80	2-500 cm	Calculated Distance based on analog signal	< 15 degrees	5V 15mA
HRLV-EZ0 Maxbotix Ultrasonic Rangefinder	$32.95	30- 500 cm	Calculated distance based on pulse width, analog voltage, and serial digital	< 40 degrees	2.5-5.5V 2.5-3.1mA

2.3.2.2 Stopping Distance – Olesya

The following uses the coefficient of friction for sand, found to be somewhere between 0.5 and 0.35, to calculate the stopping distance in meters [65]:

$$d = \frac{v^2}{2\mu g} \qquad \frac{1.34^2}{2 \times 0.5 \times 9.81} = 0.183 \quad , \quad \frac{1.34^2}{2 \times 0.35 \times 9.81} = 0.261$$

The buggy will take a maximum calculated distance of 0.261 meters to stop completely, or about 1 foot (30 cm). Therefore, the main factor for each sensor is the best range corresponding to each type of sensor. There needs to be enough time to processes any decision made by the vision system and enough time to be able to verify the data, depending on the sensor's accuracy.

Additionally, a consideration needs to be made regarding what the shortest range to detect an object should be, because the sensors offer different ranges depending on the technology used. Any processing done by the ECE system for verification and data conversion as well as the transmission to the CS system will be a delay. Therefore the detection of any object and the initiation of a stop or turn should begin at a minimum of one and a half feet from the buggy.

2.3.2.3 Redundancy – Olesya

Redundancy is defined as duplicate of critical components or functions of a system to increase the system's reliability. A redundant sensor system is valuable in case of a failed sensor. The sensors selected above as possible additions to the design do not have within them any redundancies to account for errors, because their designs are basic and low cost, so the redundancy will be implemented by software. Also, adding navigation software using computer vision will result in two different inputs for the same area to cross check the decisions the buggy makes.

Depending of the sensors that fit the requirements and budget, the analog output will be polled before making any decisions to make sure an accurate signal is sent to the navigation software. Redundant polling would eliminate any environmental causes from traversing 20 miles at one time as well as fix any discrepancies along the borders of the sensor ranges.

Failure rates and risk analysis of the smaller electronics are not within the requirements due to the fact that this project is being funded for a one-time race, rather than long term use.

2.3.2.4 Degree of Coverage – Olesya

The entire front of the buggy needs to be covered by the sensors because the navigation system will be using the sensor output data for decision making, if needed. Also, the

navigation system is comprised of two cameras looking forward, so in order to make sure the buggy will not turn into anything, the buggy must have sensors on the sides. After researching all the low-cost rangefinders and proximity sensors above, the areas that are captured by these sensors, based off a sensor's beam, are extremely narrow for this projects application.

Based on the datasheets, the Maxbotix Ultrasonic Rangefinder sensors have the largest capture area out of the ultrasonic sensors considered for this project of up to 35 to 40 degrees. Due to the buggy's environmental circumstances, only two kinds of infrared range finders were considered for this project and they both have a capture area of 15 degrees. Also worth noting, other projects using these sensors have seen a much smaller range than 15 degrees [63]. With a budget of 60 dollars for the sensor system, even if two Maxbotix sensors where selected, that would only provide the sensor system with an 80-degree range of distances, which does not meet the requirements. As stated above, the sensors should cover the entire front and sides of the buggy.

One option that provides a greater coverage is to align several of the lowest cost HC SR-04 sensors to the front and sides of the buggy. They are four dollars each, and cost less in a package of five. This would be possible but very impractical. Placing the sensors that close together can cause interference between sensors, and connecting an excessive amount of data pins to the MCU would be overkill. Additionally, the corners of the buggy would make it very difficult to place sensors, because only one or two of them would fit in a corner due to their size.

Another option would be to rotate the sensors. This is the common way that small robot projects implement proximity and range finding sensors. Shown in Figure 13, there is a greater amount of coverage from a small 95-degree rotation. Another benefit from this idea is that the pins to the PCB will be reduced. The buggy will need at least three rotating sensors to cover the front of the buggy. Side ones will be considered but are not as critical. The number of rotating sensors the buggy will have will depend on the budget. The way that the sensors will be designed and the exact rotation measurements and implementations are in the sensor design section of this document.

To be able to rotate the sensors, servos will be included in the budget. They are low cost, small, and are easy to implement. The Arduino micro servo found here [66] is cheap and requires a voltage of 3 to 6 volts which can easily be integrated with the other smaller electronics. The software implementation to rotate these sensors is simple and easily adjustable. Any other servo would be too complex and unnecessary for this application.

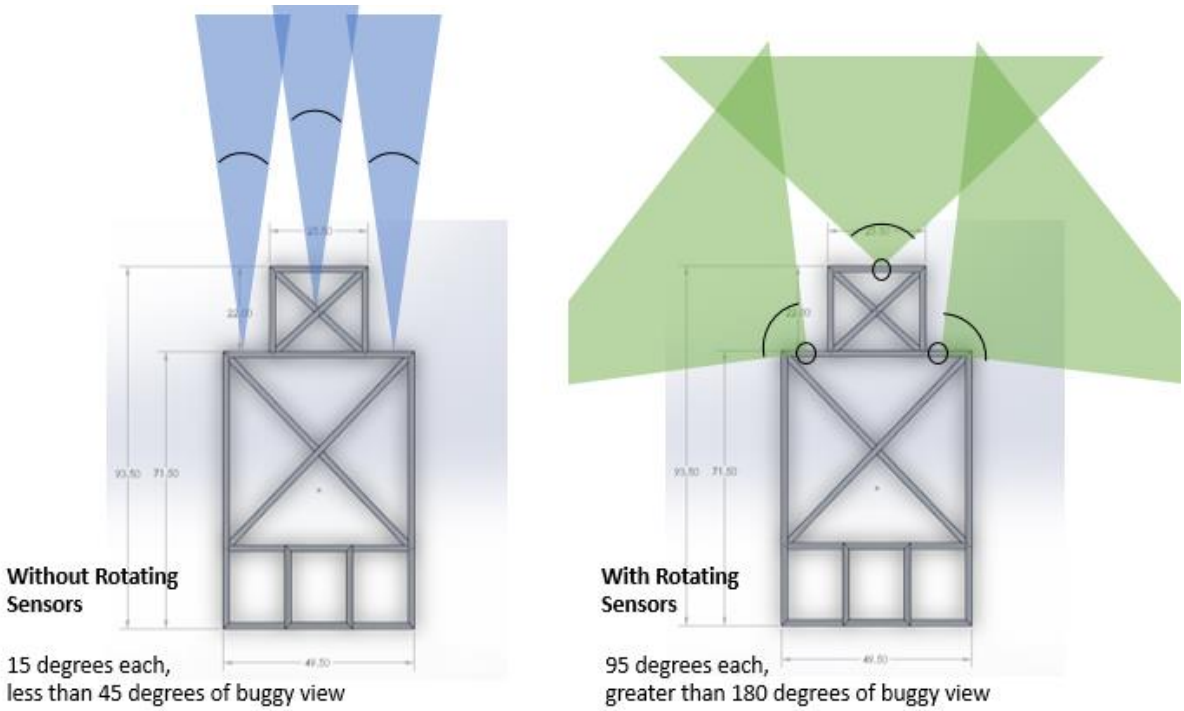

Figure 13. Comparison of the Sensor Area Coverage.

The type of sweep the sensors make can also impact the range of view. The way the sensors are laid out on the buggy's frame will be restricted by the frame materials and frame design. Typically for robotics applications if the sensors cannot see within a certain distance, the sensors are placed farther inwards to account for that and give the robot that ability to see up-close if needed.

The frame of the buggy will be another consideration for the sensor selection. The buggy's frame will not allow the sensors to be place inwards to account for a range that starts at about half a foot or more. This is because the frame is already holding a lot of weight and making any more holes or cuts to the support will cause potential failure in the frame that is supporting the solar panel. Therefore, the short range on the sensors need to be at least within a few inches to the sensor to be able to mount them directly on the frame

The sweep itself can be configured differently. The sensors can go outward to inwards, or vice versa. Also, as shown in Figure 14, the sensors can go in opposite directions. These sweeps produce different results. The one on the left gets the center and the sensors are able to overlap, thus double checking each other. The one on the right has a greater degree but the data would need to be verified with a second sweep to make sure the sensor are detecting an object in front of the buggy. The kind of sweep that these sensors will be programmed to do will be fully dependent on the remaining code storage and the number of pins on the MCU. If they all go the same direction, then one output from the MCU can be shared between all the rotating sensors. This will save both space for code and pins on the MCU. If the sensors do not go the same direction, there would have to be a pin set up for every rotating sensor and that would create more code and a large

percentage of the MCU pins used. The limitations will be considered for the PCB design choices and incorporated in the PCB schematic layout.

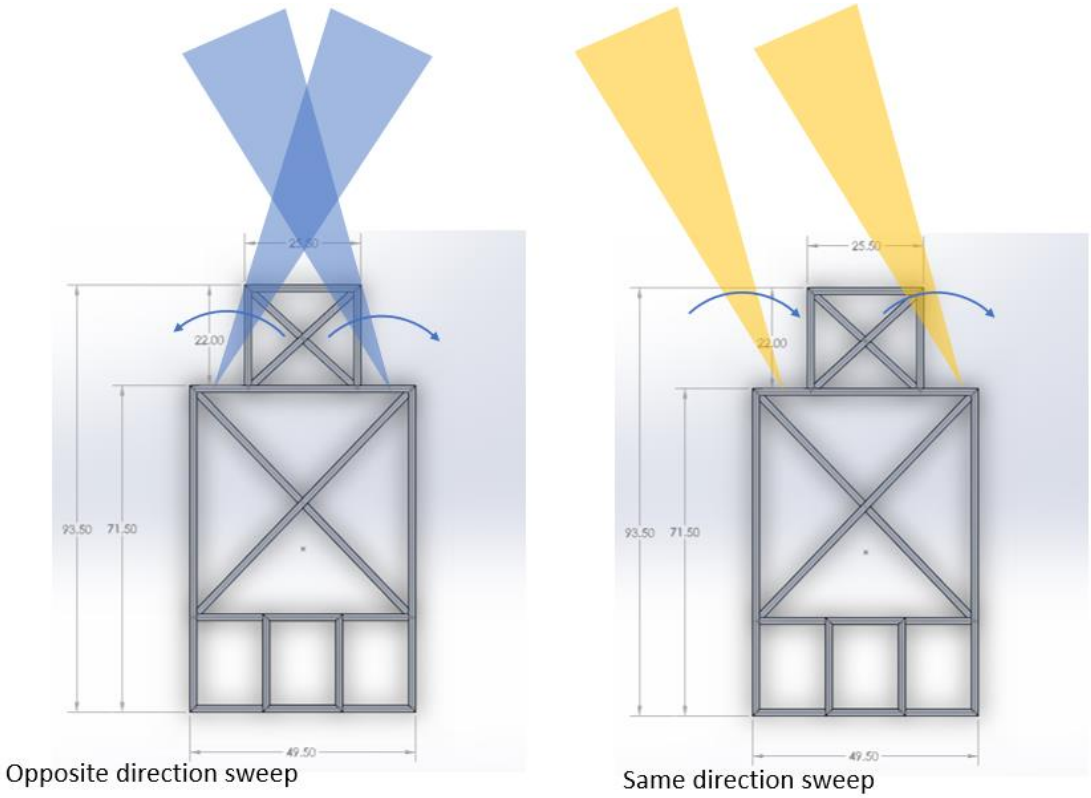

Figure 14. Sensor Sweeps that can Be Produced with Proposed Frame.

2.3.3 Cameras – William

Cameras are another form of technology that allow vehicles to "see" their surroundings. Humans use their eyes to visualize their surroundings, but vehicles require some sort of sensory device to visualize their surroundings in order to detect and avoid obstacles and other valuable property. For vehicles to have a complete 360 degree view of their surroundings, the vehicle can be outfitted with cameras at all angles. The images from the 2-D cameras are used to create a 3D mapping of the surroundings of the vehicle, allowing it to navigate itself within the environment [67].

2.3.3.1 How Digital Cameras Work – William

Digital cameras were the choice of cameras for the buggy to visualize its surroundings. Digital cameras use a piece of electronic equipment to capture incoming light rays and transform the energy into electrical signals. There are two existing technologies that is able to detect light. They are either the charge-coupled device (CCD) or a complementary metal oxide semiconductor (CMOS) image sensor. The image from a picture is composed of several millions of tiny colored dots or squares. They are called pixels. In a digital

camera, light from which the camera is pointing at zooms into the camera lens. The image sensor chip breaks up the incoming "picture" into millions of pixels. All this information is stored into memory as a number. The color and brightness of each pixel can be represented as a number [68].

The quality of a camera is determined by the amount of pixels the device is able to capture. Basic cameras have a small number of sensors that will allow for a few hundred thousand pixels to be captured (typically a grid of 640 x 480). Better quality cameras have as much as six millions of pixels (six megapixels). A higher megapixel camera will offer a photo with more pixels. The more dots on the photo, the higher resolution the picture is and better quality [69].

2.3.3.2 How an Image Sensor Converts a Picture into Digital Form – William

The CMOS chip captures light rays and turns them into digital signals all on the one chip. These chips offer very fast capture speed and are very inexpensive than their CCD counterparts. The process goes like: the incoming images is converted into an outgoing pattern of digital pixels. The chip measures how much light is arriving at each pixel. The amount of light is processed into a number that can be stored on a memory chip inside the camera. Therefore, a picture is simply a very long string of numbers to the digital camera [69].

2.3.3.3 How to Compare Webcams – William

Two key measurements that will indicate how well a webcam performs are resolution and frame rate. Although having a higher resolution size may make the camera quality higher, that will induce a bigger-sized file for the picture to be sent over a medium. Webcams deliberately capture a much lower resolution (more blurred, grainy, and "pixelated") images in order to have a smaller-sized file. Having a smaller-sized file means having the ability to transfer the picture of a medium much faster than for a larger-sized file. The frame rate (also called the refresh rate) measures the number of frames that a webcam is able to process per second. The frame rate can range from 24 frames per second to 60 frames per second. The lower end of the frame rate range still offer good capabilities for many usage, including for an autonomous beach buggy.

2.3.3.4 Advantage of Using Cameras in Autonomous Vehicles – William

The cameras on a Tesla’s vehicle are able to detect various objects during its drive [67]. Quinn writes that the camera’s ability to detect objects will allow cars to navigate in its environment without any response from the driver at all. One of the biggest advantages to using cameras is its price. Implementing cameras in autonomous vehicles may cost the consumer and manufacturer of the vehicle between a couple of hundred to a few thousand dollars. When using a technology like LIDAR, the system may increase by tens of thousands of dollars. Using cameras certainly has its advantages. But it also has its

disadvantages. The images from the cameras must be processed in order for the vehicle to make sense of what is happening in its surroundings. This requires more processing power than using a LIDAR-based system.

2.3.4 LIDAR – William

Light detection and ranging (LIDAR) enables a vehicle to observe the world with continuous 360 degrees of visibility and insanely accurate depth information. The vehicle would be able to sense its environment in all directions and be able to always know the precise distance (to an accuracy of plus or minus 2 centimeters) of objects in relation to itself. LIDAR works by continually emitting beams of laser light and measuring how long it takes for the light to return to the sensor. This technique enables a superior visualization of the vehicle's environment that is truly 3D rather than using a camera to build a 3D environment from 2D information. The exact measurement of any objects around the vehicle can be inferred up to around 60m, depending upon the quality of the sensor [70].

The reason for LIDAR's popularity with self-driving cars can be described through its ability to generate huge 3D maps. This allows the vehicle to navigate with extreme accuracy. LIDAR allows the vehicle to know ahead of time the boundaries of where it can and cannot be within the environment. LIDAR can detect whether there is a stop sign or traffic light 500 meters ahead of the vehicle on the road. This allows self-driving cars to progress much rapidly over the last 5 years [70].

Along with being able to generate an accurate map of its surroundings, LIDAR is able to detect and track objects with superior accuracy as well. As LIDAR technology evolved to reach higher-resolution and operate at longer ranges, LIDAR is able to detect and track obstacles for the vehicle to avoid collision and potential accidents. Modern LIDAR technology can differentiate between the kinds of objects within the vehicle's surroundings and even at what speed and which direction the object may be going in [70].

2.3.4.1 How LIDAR Works – William

LIDAR technology works by sending a laser pulse train and measures the time it takes to return to its source. The equation for measuring how far a returning light photon has traveled to and from an object is calculated by:

$$Distance = \frac{(Speed\,of\,Light * Time\,of\,Flight)}{2}$$

The laser instrument can send up to 150,000 pulses per second. The amount of time that each pulse to reflect back to the laser instrument is measured by a sensor on the instrument. Because the speed of light is a constant, the distance from the instrument can be calculated by measuring the time how long the pulse gets reflect back to the laser instrument. Repeating this process, the laser instrument is able to build up a complex map of the surface it is measuring. To aide to the data's integrity, a single Global Positing System (GPS) location can be added at each location of where the instrument is set up for ground-based Light Detection and Ranging [71].

2.3.4.2 Components of LIDAR Systems – William

There are four main components to most Light Detection and Ranging systems. These components include the laser, scanner and optic, photodetector and receiver electronics, and navigation and positioning systems/GPS. The lasers of a LIDAR-based system are categorized by their wavelength. Shorter pulses can help the LIDAR system attain better resolution, assuming that the receiver detector and electronics are able to sufficiently manage the increased data flow. The rate at which the images can be developed is affected by the speed that the image is scanned into the system. Different variety of scanning methods and types of optics can change the way LIDAR systems gather information. The backscattered signal gets read and recorded by the photodetector to the LIDAR system. Silicon avalanche photodiodes and photomultipliers are two types of photodetector technologies. In order for the vehicle to make sense of the LIDAR sensor, it is necessary to determine the absolute position and the orientation of the sensor to maintain useable data. Global Positioning Systems (GPS) and Inertial Measurement Unit (IMU) are two devices that provide the methods for translating sensor data into static points for use in a variety of systems. GPS provides accurate geographical information regarding the position of the sensor. The IMU records the accurate orientation of the sensor at that location [71].

2.3.5 Communication – Patrick

This project will have many different electronic parts interacting and communicating with each other, so it is necessary to have some form of communication protocol for this information transfer. Common protocols were researched for this project to determine their benefits and possible application to this project. These protocols were UART, I2C, and SPI.

2.3.5.1 UART – Patrick

For this project three protocols were considered. The first of these is the Universal Asynchronous Receiver Transmitter (UART). As the name states, UART is asynchronous. The main benefit of UART is its simplicity, to connect any two devices only two wires are needed. Along with this since there are a limited and small number of connections that will be using the buss at the end is not much of an issue. However, the fact that it is asynchronous outweighs the ease of implementation and use. Being an autonomous vehicle, it is necessary to have accurate and current data if the buggy is expected to have max efficiency and decision making. Additionally, UART requires extra bits to specify the end and beginning of data leading to 10 bits of time needed to transmit 8 bits of data. It is for this reason that UART was not chosen for communication [72].

2.3.5.2 I2C – Patrick

The second possible transfer protocol is the Inter-Integrated Circuit (I2C). I2C shares the same benefit of UART in only needing 2 wires while still supporting synchronization.

I2C is also the only protocol that support any number of master and slave units. It improves upon the UART excess data transfer by only needing 1 extra bit of transmission per 8 bits of data sent. As will be proven later, the main benefit that I2C has over SPI is that it only needs 2 wires per device but falls behind in terms of speed and full-duplex (sending and receiving at the same time) capabilities [73].

2.3.5.3 SPI – Patrick

The last protocol is Serial Peripheral Interface (SPI). SPI is synchronous like I2C, faster than I2C, and supports full-duplex unlike I2C. The major drawbacks of using SPI is that it only supports one master and the number of pins needed is much larger than I2C, which is a major concern in this project's design. Since this project is anticipating having between 6 and 10 devices talking to the microcontroller which all require multiple pins each, this will become an issue. Additionally, this project will only have one master, so this limitation does not really affect this project [74].

2.3.6 Communication between Devices – Olesya

There are several ways to troubleshoot the buggy during the construction, testing, and the competition. One option is to place LCD screen(s) on the PCB that will display the information coming in from several of the proximity sensors and voltage/current sensors. However, this approach is not effective and it is very difficult to apply when the buggy is moving. Another option is make a mobile application to display all this information.

For the second approach to work, the devices need to be able to connect to each other without a router and without internet. This network also need to meet the budget requirements, it needs to be wireless, draw a small number of amps, and be able to communicate within a mid-range distance.

The one option for an application is to create a Wireless Ad-Hoc Network (WANET). This kind of network allows the PCB to connect to the Apple or Android device without needing a router or access point to another network and can work wirelessly. To be able to apply this network to the buggy's electronics, the design would need a wireless antenna that is compatible with this kind of communication. This is not very common. However there is one brand that specializes in making this type of device for Arduino and other embedded electronics. The XBee module allows point-to-point, multipoint, and mesh networks. This module is a good consideration for the buggy's design because it runs low power mode and it's 3.3 volts is compatible with the PCB microprocessor all while allowing communication between devices. Some of the Bluetooth modules considered for this project run at 3 volts to 7 volts, at which they would need a specific configuration on the PCB. The PCB design can have a location on the chip to allow an interface to the Xbee so it can be programmable that will be based off the chips explorer breakout chip that give access to the serial pins [75]. The firmware will have to be installed using this connection, then the RX, TX, and RSSI will be used for communication once configured and programmed.

Another option is to add a Bluetooth module to the PCB board. Bluetooth would provide the same concept of a network of devices; however, Bluetooth is typically limited to a few devices. The Bluetooth module is lower in cost, which makes it also applicable for this project. The only concern is that the Bluetooth module that best fit the budget runs at a baud rate of 9600 bits per second, which is significantly less than the XBee module.

The following considerations in Table 13 will show a comparison of the two modules to be able to select the best fit approach for the solar powered beach buggy.

Table 13. Approaches to Create a Local Network to Communicate to the PCB.

Component	Price	Range	Running Voltage and Current	Data Rate	Type of communication
XBee 2mW Wire Antenna RF Module	$26.95	90 meters	3.3 V 50 mA	250,000 bps	UART PWM signal strength indicator
Bluetooth to serial port module HC05	$10.57	10 meters	3.3V to 5V 30 to 40 mA	38,400 bps	UART

2.3.7 Emergency Stop – Olesya

The start button and the emergency stop button will be the only inputs available to the user to control the buggy's movements, because the buggy will be autonomous. For the emergency stop button, a simple push button will be added to the buggy. This button will be connected to the wire that is providing power to the motor. To be able to stop the motor safely while keeping the electronics and the autonomous navigation system running, the electrical design will need to have the battery power the electronics continuously unlike the two motors. This power control system will be facilitated via the motor driver.

The most common way to implement the emergency stop would be to cut the power directly and implement a switch that would be connected to the push button as discussed in [76]. This design would be simple to implement and would be low cost. It would require cutting and striping the connection from the battery to the motor, and then solder the ends to the emergency cutout switch. In [76], the emergency stop was designed and built using heat shrink tubes. Using this approach for the buggy would be beneficial because the heat shrink tubes protect the wires from environmental hazards. The buggy will be traversing the beach, a humid environment that might also cause the buggy to get wet, so using safe wiring in the emergency stop would be a safe choice.

Another way to design the emergency stop is to add a relay to an emergency stop switch. Adding a relay will prevent any burnout. A relay would be feeding the power to the

buggy that will then be controlled by the emergency top switch button. This provides another layer of control but also costs more money.

This control for the emergency stop will be controlled by the ECE team. If the system uses a relay controlled by the signal from the PCB board, the application will have a button for an emergency stop that will go through the CS team. The physical button will also be routed through the PCB board too that will let the CS team know that the buggy is undergoing an emergency stop.

Another design to consider is implementing a regular stop button and an emergency stop button. All three buttons would reside on the vehicle, and the start and stop can be implemented on the application. Figure 15 shows the layout of implementing all three buttons on the two motors that the buggy will use. This is very high level and does not include protective circuitry, which will be discussed in its own section of this document.

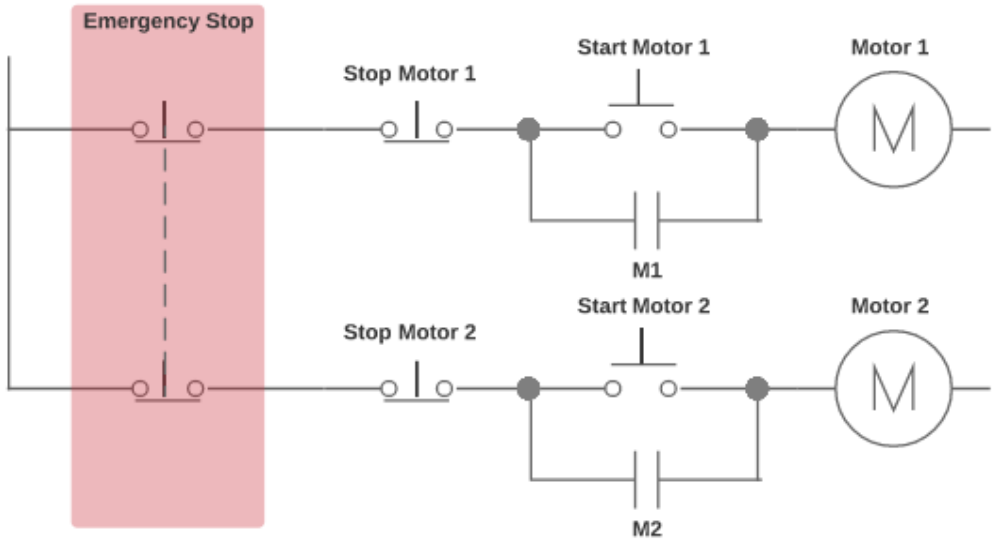

Figure 15. Start, Stop, and an Emergency Stop Implementation.

The budget for emergency stop is twelve dollars. There were no other options in the same price range and level of simplicity.

2.3.8 Global Positioning System – William

Most Global Positioning Systems are comprised of satellites and ground stations to compute position and time almost anywhere on earth. On average, there are at least twenty-four active satellites orbiting over twelve-thousand miles above earth. The satellites are spread apart so that there will always contain at most twelve satellites at any single location. The job of the twelve satellites is to transmit information back to earth over radio frequency (ranging from 1.1 to 1.5 GHz). A ground based receiver or GPS module can calculate its position and time using that information and some math hocus-pocus [77].

Attaching an antenna can improve the GPS receiver's ability to pick up a signal from the satellites. There are many antenna choices to choose from the market. Some of the most common ones include the ceramic patch antenna and helical antennas. The SMA antenna attachment allows the antenna to be mounted in a different location than on the main circuit.

GPS receivers send serial data at a specific bit rate. A common baud rate is 9600bps for 1Hz receivers. The time to first fix (TTTF) on the GPS module is affected by the number of channels it has. The more frequencies/channels the GPS module can check, the faster a fix will be found. After finding a lock, some modules will shut down the extra blocks of channels to save power. 12 or 14 channels should be fine for tracking, but it will take more time for the GPS module to find a lock [77].

The GPS chipset has the job of performing calculations and providing the analog circuitry for the antenna, to power control, to the user interface. The chipset is independent of the antenna type. It is possible to mix and match a wide variety of different antennas for GPS modules with specific antenna types. Ublox, SiRF, and SkyTraq are some common chipsets. They contain very powerful processors that allow for fast acquisitions times and high reliability. The difference between chipsets can be determine by power consumption, acquisition times, and accessibility of hardware [77].

GPS modules do not consume a lot of power. They do require energy to operate in order to calculate the data from the satellites and to obtain a lock. On average, most GPS modules require around 30mA at 3.3V to run while locking onto a satellite. Keeping the start-up time low can save power [77].

The math behind how GPS receivers to compute accurate position and time is through trilateration. This process uses multiple reference points. With GPS, there are four values that are needed for accurate position and time: latitude, longitude, elevation, and time. This is why having the GPS receiver able to view four satellites is important to its success [77].

2.3.8.1 How a GPS Receiver Calculates its Position and Time – William

Each satellite orbiting around earth sends data to a GPS receiver. This data contains a few different pieces of information for the GPS receiver to accurately calculate its position and time. One of the most important component of a GPS satellite is an extremely accurate atomic clock. The ability to timestamp when the satellite send its orbital position to the GPS receiver allows it to know the distance to the satellite that send that information. The GPS receiver can accurately calculate its position and time using at least four satellites. Having ground based stations that can communicate with the satellite network and GPS receivers can also improve the accuracy of receiver's ability to calculate its position on earth [77].

2.3.8.2 GPS Accuracy – William

There are many factors affecting the accuracy of GPS systems. These factors include signal to noise ratio (noisy reception), satellite position, weather and obstructions. If the GPS receiver is able to get a lock on four satellites, it is able to solve this problem. When the GPS receiver gets a lock on its first satellite, it can obtain the almanac information, which lets the GPS receiver quickly lock onto other satellites. The most accurate information the GPS receiver can attain occurs when it has a clear view of the sky away from any obstructions and is able to lock on more than four satellites. However, there are other ways to assist the GPS receiver if the weather and geography impedes on it [77].

Two external ways to improve the accuracy of the GPS receiver includes Assisted GPS (AGPS) and Differential GPS. AGPS uses wireless networks to help relay between the satellite and the receiver when the GPS signal is weak or not able to be picked up by the GPS receiver. AGPS can provide the receiver with the proper almanac data and the precise time. The ground base stations have higher computing power and better satellite signal to interpret the broken/fragmented information the receiver is receiving to provide a more accurate position reading to the receiver. This is mostly accomplished through the use of mounting GPS receivers on cellular towers. The GPS receiver is able to acquire a lock on the satellite much more quickly as well as receive more accurate information when it communicates with the GPS receivers on the cellular towers [77].

Differential GPS (DGPS) is similar to AGPS. Like AGPS, DGPS uses ground/fixed GPS stations to determine the location. However, DGPS finds the difference between both the satellite and the ground location reading. The ground based station broadcasts a signal, containing the error between the actual pseudorange and the measured pseudorange. This value is calculated by multiplying the speed of light by the time it takes the signal to travel from the satellite to the receiver. Wide Area Augmentation System (WAAS) is one form of DGPS. WAAS can be accurate to within 7.6 meters 95% of the time in terms of lateral and vertical accuracy. WAAS can even provide an accuracy of 1 meter lateral and 1.5 meter vertically [77].

2.3.8.3 Reading GPS Data – William

Most GPS modules have a serial port to connect to a microcontroller or computer. NMEA data is sent out of a serial transmit pin of the GPS module at a specific baud rate and update rate. The microcontroller can read the NMEA data by connecting the TX (transmit) pin of the GPS to the RX (receive) pin on the microcontroller. But to configure the GPS module, the RX pin of the GPS must be connected to the TX pin of the microcontroller [77].

2.3.9 Inertial Measurement Unit – William

The inertial measurement unit (IMU) is a combination of a gyroscopes and accelerometer. The IMU can provide two to six degrees of freedom (DOF). IMUs are used when the knowledge of the device’s exact position must be known. This piece of technology is a key component for autonomous operations in vehicles. It helps the system to monitor the dynamically changing movements of the vehicle [78].

When an autonomous driving system needs to continuously know the dynamics of the vehicle in terms of location, position on the road, direction, orientation, and velocity, IMUs are a great option to measure all these characteristics. The IMU provides a continuous stream of data related to the linear acceleration of the vehicle on three principal axes, together with the three sets of rotation parameters (pitch, roll and heading). When Global Navigation Satellite System (GNSS) data is not available in challenging GNSS environments, data from the IMU will be able to provide additional measurements related to distance traveled by the autonomous vehicle. This data will help correct for the most likely position of the vehicle within the environment. The IMU can provide data related to the velocity and the extent of acceleration towards obstructions that are sensed by the on-board imaging systems. The IMU can measure angular data between the direction in which the vehicle is pointing (heading) and where it is actually going (track) [79].

The ability to track how an automated driving system is moving through the environment allows for the autonomous vehicle to identify routes and obstructions, and provide the feedback required to the driving system to continually adjust its parameters to drive a route safely. To accomplish these demanding tasks, inertial measurement systems must provide real-time capability to continuously stream and measure orientations and positions to extremely fine accuracy and velocity measured to extremely fine accuracy. By having computer algorithms blend the inertial data with available raw GNSS information into a single uninterrupted stream of reliable and accurate navigation messages, the autonomous system should be able to receive the required information pertinent to position, orientations, direction and velocity. When the GNSS is unavailable or there are omissions in information received from imaging sensors, IMUs should still be provide the necessary continuous data stream to the autonomous driving system [79].

Let’s take a look at the components that make up the IMU: accelerometers and gyroscopes.

2.3.9.1 Accelerometer – William

Accelerometer measures how fast something is speeding up or slowing down. These devices can be used to sense both static (e.g. gravity) and dynamic (e.g. sudden starts/stops) acceleration. Accelerometers can be used for tilt-sensing and to sense motion [78].

When selecting an accelerometer, it is important to consider the following characteristics: range, interface, number of axes measured, power usage, and bonus features. The upper and lower limits of what an accelerometer is able to measure to known as its range. A low full-scale range means that the accelerometer is able to provide sensitive output information. This will allow the accelerometer to provide a more precise reading out of an accelerometer with a low-scale range. The accelerometer can either have an analog, pulse-width modulated (PWM), or digital interface. Accelerometers with an analog output will produce a voltage that is directly proportional to the sensed acceleration. This

interface is generally the easiest to work with because most microcontrollers have an analog-to-digital converter implemented. Accelerometers with a PWM interface will produce a square wave with a fixed frequency. Digital accelerometers usually feature a serial interface, either SPI or I2C. Digital accelerometers are more popular because these devices usually have more features and are less susceptible to noise than their analog counterparts. Accelerometers can sense up to three axes possible (x, y, and z). Accelerometers will usually have a required current consumption in the 100s of uA range. Some accelerometers will have additional features to help conserve energy when the accelerometer is no longer needed. Many more recently developed accelerometers have extra features to make them unique on the market. Additional features include, selectable measurement ranges, sleep control, 0-g detection, and tap sensing [78].

2.3.9.2 Gyroscopes – William

Gyroscopes measure angular velocity. They can measure how fast something is spinning about an axis. This piece of technology is not affected by gravity. Angular velocity is usually represented in units of rotations per minute (RPM), or degrees per second. The three axes of rotation are either referenced as x, y, and x, or roll, pitch, and yaw. It is only recent that gyroscopes are being used alongside accelerometers for applications like vehicle navigation [78].

When selecting a gyroscope, it is important to consider many factors, including range, interface, the number of axes measured, power usage, and bonus features. The maximum angular velocity that is expected to be measured should not exceed the maximum range of the gyroscope. To get the best possible sensitivity, the gyroscope's range should not be must greater than what's expected. A majority of the interfaces for gyroscopes will feature an analog output. There are a few that have a digital interface - either SPI or I2C. Inexpensive 3-axis gyroscopes have recently begun to appear on the market. Most gyroscopes are either 1- or 2-axis. It is important to know when selecting which of the three axes the gyroscopes will be measuring. Some two axis gyroscopes will measure pitch and roll, while others measure pitch and yaw. Most gyroscopes required a current consumption of somewhere in the 100s of uA range. When a gyroscope is no longer needed, some senses have a sleep functionality to conserve energy. Some additional features include a temperature output, which can be useful for compensating for drift [78].

2.3.10 Computing Platform Hardware – William

In order to process the various sources of information to determine the best possible decision for the autonomous vehicle to make, we must evaluate existing computation hardware implementation of existing autonomous vehicles on the market. Existing computing solutions targeted for autonomous driving include GPU-based solutions, DSP-based solutions, FPGA-based solutions, and ASIC-based solutions. A paper described the computing takes involved in autonomous driving and examined what the computing stack needs to accomplish to enable autonomous driving [80]. The most computation-intensive workloads was found to be convolution and feature extraction workloads in autonomous

driving scenarios [80]. Their experiments consisted of using an off-the-shelf ARM mobile SoC consisting of a four-core CPU, a GPU, and a DSP. They studied the performance and energy consumption of the workloads.

The most computation-intensive stage is the convolution layer in object recognition and object tracking tasks. Therefore, the researchers in the paper sought to implement a convolution layer to test the performance and energy consumption of the computing platforms. They found that the CPU platform was able to complete the convolution layer in about 8 ms, consuming 20 mJ. They found that the DSP platform was able to complete the convolution layer in about 5 ms, consuming 7.5 mJ. They found that the GPU platform was able to complete the convolution layer in about 2 ms, consuming only 4.5 mJ. They confirm that the GPU platform is the most efficient computing unit for convolution tasks, both in performance and in energy consumption [80].

They also tested the computing platforms in its ability process information during the feature extraction layer during the localization stage. Feature extraction generates feature points for the localization stage and is the most computation expensive task in the localization pipeline. They implemented feature extraction and measured the performance and energy consumption for each computing platform. They found that the CPU platform was able to complete the feature extraction task in about 20 ms, consuming 50 mJ. They found that the GPU platform was able to complete the feature extraction task in about 10 ms, consuming 22.5 mJ. They found that the DSP platform was able to complete the feature extraction task in only 4 ms, consuming 6 mJ. They confirm that the DSP is the most efficient computing unit for feature processing tasks, both in performance and in energy consumption [80].

The researchers also explored how well an ARM mobile SoC performs within an autonomous driving system. They found that the performance was "quite impressive" when the system was ran on the ARM mobile SoC. The localization pipeline was able to process 25 images per second. The deep learning pipeline was capable of performing 2 to 3 object recognition tasks per second. The SoC consumed 11 W on average when the full system was running. With the ARM mobile SoC system, the researchers were able to driving the vehicle at around 5 miles per hour without any loss of localization [80].

There were some limitations of the ARM mobile SoC within the autonomous driving system. The researchers confessed that the reason that why could deliver the performance on the ARM mobile SoC was because they fully utilized the heterogeneous computing resources of the system and used the best suited computing unit for each teach so as to achieve the best possible performance and energy efficiency. They were unable to fit all the tasks of an autonomous driving system using the ARM mobile SoC. They also expressed that they needed to upload raw sensor data and processed data to the cloud [80].

The achievements of the ARM mobile SoC system in the autonomous driving system shows that we are able to utilize low-quality processors to meet the requirements of the

autonomous beach buggy vehicle. However, some considerations should be taken into account for the computational-expensive tasks.

2.3.11 Controller Area Network (CAN) Bus – William

The Controller Area Network is used to allow communication between Electrical Control Units (ECUs) and sensors. CAN is a robust, low-cost message based protocol. Originally developed by Bosch, the CAN bus is essential to many applications, especially in the automotive industry. The CAN bus protocol allows ECUs to communicate with each other without complex dedicated wiring in between. Without as much wiring overhead, this allows for additional features to be added via software alone, e.g. electronic gearbox control. The primary purpose of the Controller Area Network is to allow any ECU to communicate with the entire system without causing an overload to the controller computer [81].

There are five critical advantages to using the CAN bus system. It is a low cost solution. ECUs can communicate via a single CAN interface, i.e. not direct analogue signal lines, reducing errors, weight, costs. CAN is centralized. The CAN bus system allows for central error diagnosis and configuration across all ECUs. CAN is robust. The system is robust towards failure of subsystems and electromagnetic interference, making it ideal for vehicles. CAN is efficient. CAN messages are prioritized via IDs so that the highest priority ID are non-interrupted. CAN is also Flexible. Each ECU contains a chip for receiving all transmitted messages, decide relevance and act accordingly. This chip allows for easy modification and inclusion of additional nodes [81].

3 Design

For the Blue Team's proposed solar-powered autonomous beach buggy to capture the unique mechanical elements, innovative electrical and computer supplements, and creative programming techniques, the ideas and efforts of every student involved were incorporated in this project. The following sections lay out the power system and electrical system designs for each type of component, as decided in the previous Research section. Due to the tight budget, only three of the components were custom-made: the solar array, the charge controller, and the microcontroller. The remaining items are commercially available, but offer the least cost for the most utility. Nonetheless, the goal of the following Design sections is to integrate these components into a unified system by explicitly stating each connection, subsystem, material, setting, and function.

3.1 Power System Design – Caroline

The power system for the vehicle includes the battery array, the solar array, the motor driver, the charge controller, the converters, and protective circuitry. The battery array involves both the specifications for the desired batteries as well as the proper gauge sizing for the wires between the batteries and the motor controller and converters. The solar array required knowledge of the solar cell specifications, panel layout, and wiring diagram. The motor driver design encompasses the board layout and applicable inputs

and outputs, along with the software implementation. The charge controller is the most complex design, requiring a complete schematic, PCB design, and software design with accompanying bill of materials. To organize the design, it will be broken down into major components. The converters only require specifications and connection diagrams. Lastly, the protective circuitry design will take a big-picture look at the power system and target connections that require current sensors, voltage sensors, relays, and thermal regulation to ensure that all of the components would operate safely for the duration of the competition.

3.1.1 Solar Array – Caroline

The final solar array consists of 180 solar cells purchased as a package of 300 solar cells, which was based on the best available price per cell. The size of the solar array was limited by the charging capacity of the batteries, which is approximately 0.2C or 24 amps. This limits the wattage of the solar array to 600 W max output during operation. Of the purchased cells, the unused cells were utilized for initial testing. In order to maximize output, the cells should be rated for at least 4 Watts each and sized no more than 156 mm by 156 mm. The approximate efficiency for such cells is around 18%. Generally, the only solar cell type that can match these specifications is monocrystalline. Each cell should produce at least 8 amps under STC. This means that four panels can be wired in parallel to achieve a maximum of around 32 amps or two sets of two panels can be wired in parallel to achieve a maximum of around 16 amps, both of which are compatible with a 40 amp charge controller; however, only the second option is compatible with the maximum battery charging capacity. Each cell should also be around 0.55 volts each ± 0.05 volts. At this voltage, between 40 and 48 cells can be wired in series to total of approximately 24 volts per panel. A summary of these specifications is detailed in Table 14. Data for the selected solar cell model, the Gintech Douro 3BB C3, is also included in Table 14 [82]. As evidenced by Table 14, the selected cells have very high specifications near the maximum to optimize generation.

Table 14. Acceptable Solar Cell Specifications and Gintech 3BB Cell Specifications.

Property	**Min.**	**Max.**	**M 3BB 4.44 Solar Cell**
Maximum Power (P_{max})	4.0 W	4.8 W	4.74 W
Voltage at MPP (V_{mpp})	0.5 V	0.55 V	0.544 V
Current at MPP (I_{mpp})	8.1 A	8.9 A	8.78 A
Open Circuit Voltage (V_{oc})	0.62 V	0.65 V	0.641 V
Short Circuit Current (I_{sc})	8.8 A	9.4 A	9.31 A
Cell Efficiency	17 %	20 %	19.4 %
Fill Factor (FF)	77 %	80 %	79.95 %

In order to minimize the temperature of the cells, a solar concentrator was not used. However, to enhance maneuverability of the solar array, four individual panels were constructed and mounted overhead. They significantly overhung the dimensions of the buggy, thus filling in surface area that was otherwise limited. These panels were manually adjustable with three degrees of freedom. In order to prevent shading of the back panels due to the front panels, the height of the panels were adjustable. The angle of

tilt for each panel was also adjustable from 0 to 180 degrees in order to absorb the greatest amount of sunlight. Further, the azimuth angle of the panels were adjustable between -90 and +90 degrees from the azimuth angle of the buggy.

In order to avoid overlapping or unnecessary heat transfer, each cell was separated by approximately 0.25 in. ± 0.05 in. In total 180 solar cells were used, divided among four panels, in a 7 x 7 grid minus four panels to provide room for mounting. The total area of a panel, including cell spacing, was 48 in. x 48 in. This gave a total surface area of 16 square feet per panel, or 64 square feet in total. A diagram with final spacing can be found in Figure 16.

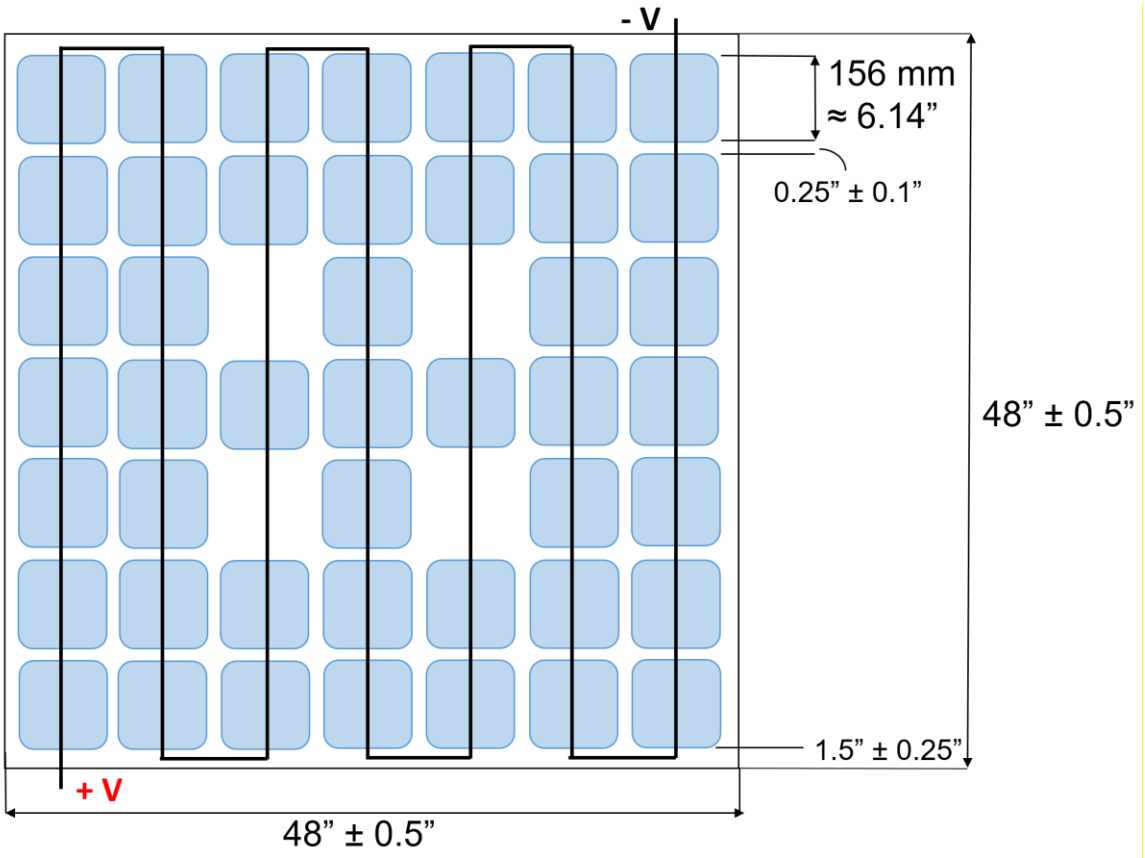

Figure 16. Solar Panel Wiring Diagram with Dimensions.

3.1.1.1 Wiring – Caroline

The wiring diagram of the solar array, shown in Figures 16 and 17, is a simple illustration of how to connect each of the solar cells to create a solar panel. Figure 18 shows how each panel connects to achieve the best possible voltage and current combination for the charge controller. The first step in connecting solar cells was to tab the cells. This involved connecting each cell using tab wire, a flux pen, and solder. Before attaching them to the mounting materials, several solar cells were tested and benchmarked against the specifications. In order to achieve the maximum possible solar generation, each solar

panel needed to produce the same current in series or voltage in parallel. If not, the output would have been significantly decreased by one faulty panel or cell.

Bypass diodes protect against uneven shading by allowing current to flow around high-resistance cells. They also protect against extreme damage such as severed wires and shattered cells. By allowing the current to flow around underperforming cells, only a section of cells become disconnected, and the consequences on power output are far less severe. For this design, 12 bypass diodes were used, or 3 per panel. In particular, a Schottky diode was used to reduce power consumption of the diode, as opposed to PN-junction silicon diodes with larger forward voltage drops. Active diodes were not chosen due to their higher cost [83]. The diode was rated for 15 A, which is almost double the current in each panel, and 45 volts, which is almost double the voltage of each panel. The selected model, AKOAK SHOMALVI2247, has a forward voltage drop of 0.55 V, as shown in the wiring diagram of Figure 17.

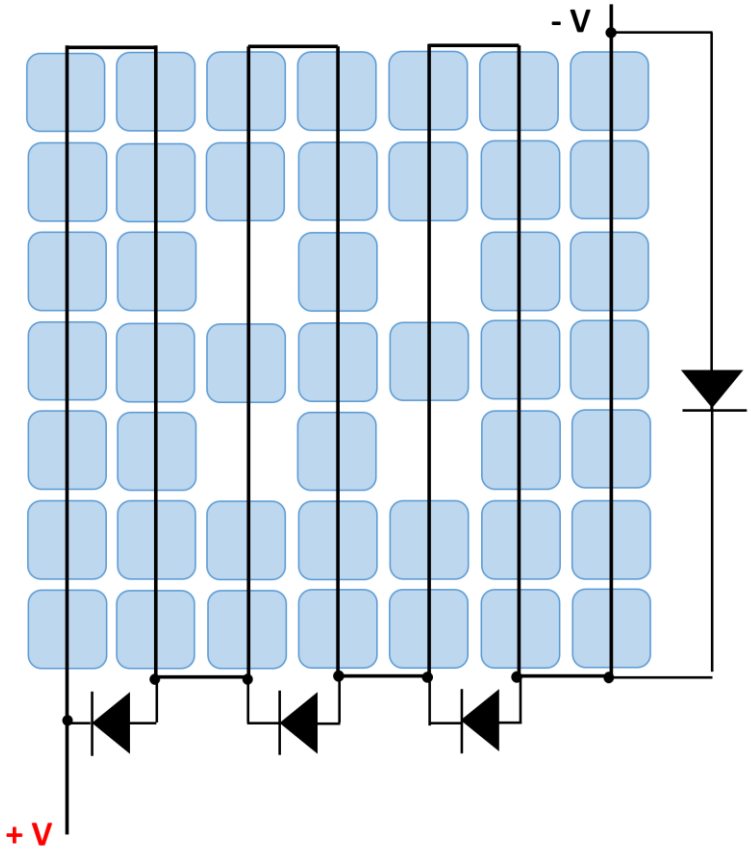

Figure 17. Bypass Diode Configuration per Panel.

In Figure 17, 45 cells at 0.544 volts each wired in series resulted in a panel voltage of 24.5 volts and a current of 8.9 amps. This resulted in a 218 W solar panel at STC. If two set of them are wired in series, and the these sets wired in parallel, as shown in Figure 18, the resulting array will have 51.8 volts and 16.8 amps for a total of 870 W STC. However, what is not shown in this diagram is the three busses on each model Douro 3BB 4.74 solar cell. Therefore, although the same arrangement was used to wire the cells,

three tabbing wires were required instead of the single tabbing wire as shown. At 870 W STC, this array delivered a maximum of 750 W to the batteries, assuming a 10% loss through the wires, charge controller, and battery charging inefficiency combined.

For a 20 amp system, a 10 AWG gauge wire is generally appropriate for a voltage drop of 2% if the length of the wire is no more than about 7 feet, which was the approximate required wire length from the assembled solar panels to the charge controller [84]. For each individual panel, 2mm tabbing wire was used to tab the cells. In order to wire each of the cells in series, the positive side of the cell was connected to the negative side of the next cell. Thus, the string of solar cells began on a positive cell side and ended on a negative cell side, as shown by the polarity indicator in Figures 16 - 18. At the top and bottom of the solar panel, where the rows on solar cells are joined to the next row, a 5mm bus wire was used to carry the current to the next row.

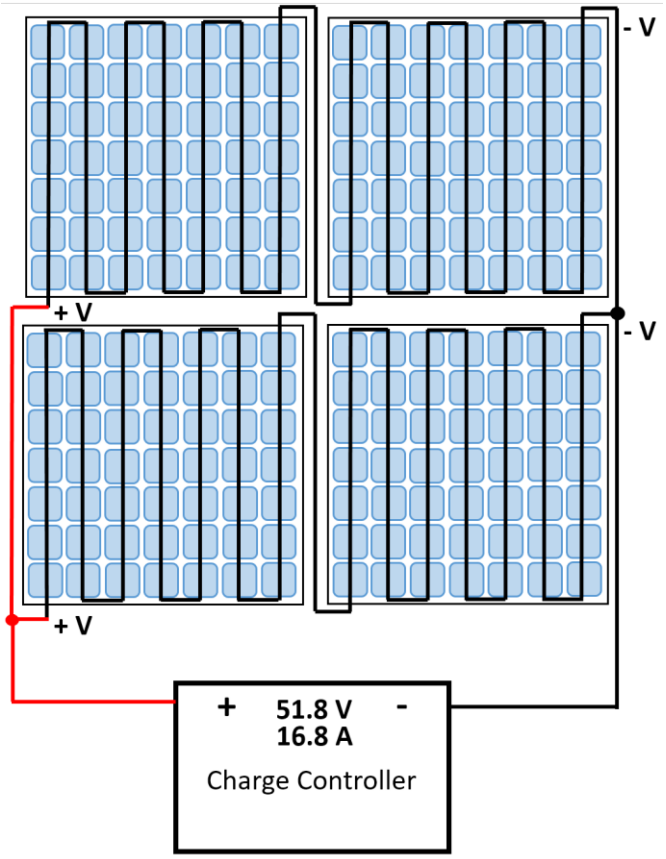

Figure 18. Solar Array Wiring Diagram.

3.1.1.2 Bill of Materials – Caroline

The complete bill of materials, including the solar cells, the materials required to wire the cells together and to the charge controller, and the bypass diodes, is shown in Table 15. In addition to the below bill of materials, a high-power soldering iron was needed for soldering the tabbing wire to the solar cells at a high temperature. This bill of materials also does not include smaller items such as holding tabs, solder paste, solder wire, and

electrical tape. It is likely that these additional items combined are no more than $5.00 in total, and they were eventually acquired for free through university resources.

Table 15. Bill of Materials for Solar Array.

Item	Approximate Cost
(200) Monocrystalline Solar Cells	$250.00
(500 ft.) Tabbing Wire 2mm	$25.00
(35 ft.) 10 AWG Wire	$14.00
(2) Rosin Flux Pen	$6.00
(30 ft.) Bus Wire 5mm	$9.00
(20) 45V 15A Schottky Diodes	$7.00
Total Cost	**$311.00**

3.1.2 Motor Driver – Caroline

The motor driver component was purchased commercially and included all necessary functions to control both the steering and drive motors. The selected model is the Cytron Technologies SmartDriveDuo-30 (MDDS30), a dual channel bi-directional brushed DC motor driver with a continuous 30 amp capacity. This motor driver accepts a battery voltage from a 7 to 35 volt sealed lead acid battery supply and motors from 7 to 35 volts, which encompasses the 12 volt steering motor and 24 volt drive motor. The motor driver is also capable of handling 80 amps of peak current for a few seconds upon start-up [85]. It retails for about $65.00, which is considered acceptable for the budget and is the cheapest known option for these specifications, besides designing and making one from scratch. Unfortunately, that could not be considered due to time constraints.

Although the MDDS30 is compatible with RC, Serial, and PWM communications, analog PWM was used to communicate between the microcontroller and the motor driver. The MOSFETs are switched at 18 kHz to reduce noise pollution. The MDDS30 is also equipped with additional features such as thermal protection, multiple input modes, battery over- and under-voltage indicators, and current limit protection. Manual push-buttons are included for quick manual testing to check functionality and for resetting the system. This became a very useful feature during prototype testing [85].

3.1.2.1 Board Layout – Caroline

Figure 19 below shows the setup and configuration for the MDDS30 in PWM input mode. The motors and battery supply are attached as shown. Since the maximum continuous current is 30 amps in under 10 feet of wiring, the wire gauge for both motors is 10 AWG. The batteries supply more current than just one motor will draw, so an 8 AWG is appropriate for the battery connections [84]. The arrows in Figure 19 to D5 and D7 represent grove 4-pin connectors, which were present on the microcontroller for P5.4-7. D5 is an analog connection for sending the PWM signals for each motor, whereas D7 is a digital connection for sending the binary direction of each motor in the case of sign-magnitude PWM. Sign-magnitude was determined to be the preferable PWM type due to its higher resolution of speed control. The switch diagram at the top of Figure 19 shows

an example switch selection to determine the input mode, single or mixed mode, exponential mode, and MCU mode. A white rectangle indicates the selected bit. The top bit is 1 and the bottom bit is 0 [85].

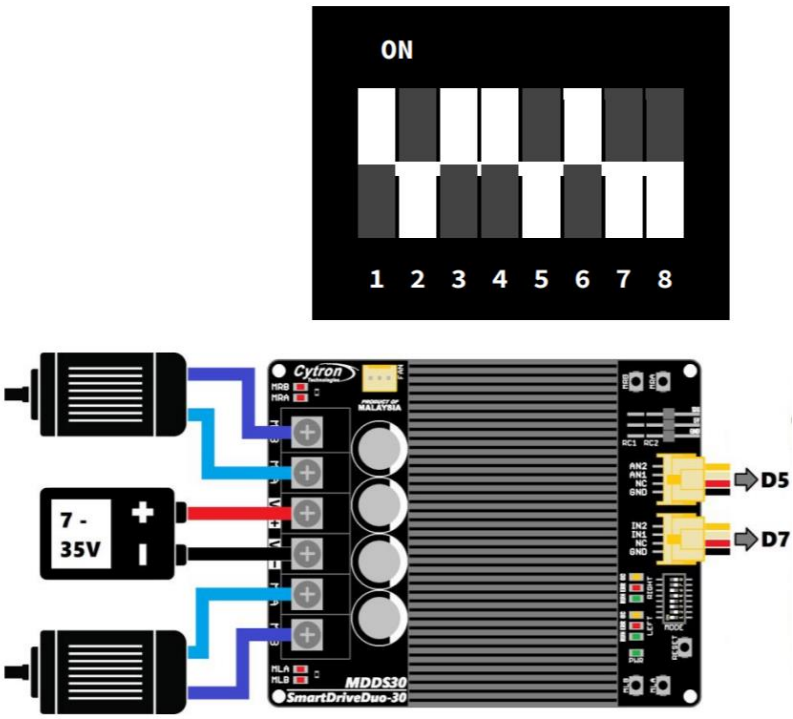

Figure 19. MDDS30 PWM Input Mode Diagram and Switch Settings [85].
(Reprinted with permission from Cytron Technologies)

Switches 1 and 2 are used to determine the input mode, which is selected in the diagram as 10. This selection is the PWM input mode. Switches 3 and 4 determine either single or mixed mode. Both motors will be active and independently controlled, which is selected by setting both SW3 and SW4 to 1, as shown. Switch 5 controls whether the speed should be linearly or exponentially set. Linear is more appropriate for lower speeds, so 0 is selected. Lastly, switch 6 chooses either locked anti-phase or sign-magnitude MCU modes. Sign-magnitude was chosen because it gives double the precision. This decision corresponds to an input of 1, as shown. Switches 7 and 8 determine the battery monitor type, which for this application is SLA. This corresponds to bits 1 and 0 for SW7 and SW8 respectively, unlike what is shown in Figure 19 [85]. A graphic of these decisions is included in Figure 20.

The middle of the board in the layout diagram is a heat sink, which is included due to the amount of heat that will be dissipated by the device. For this reason, a fan was located nearby to provide additional cooling. A fan connector is included on the board above the capacitors, but it was not used for mounting the fan [85].

Lastly, the list of safety features of the MDDS30 is extensive, which aligns with the overall objective for the buggy to be as safe as possible. The motor driver is protected from suddenly rotating upon startup by requiring an input “stop” signal. If the “stop”

signal is not given, the error LED on the board blinks twice to indicate an input error. An under-voltage warning is given when the error LED flashes three times. This indicates a low battery status but does not limit the operation of the motor driver. This proved useful for the passenger to know when to stop the buggy to allow it charge through the solar array. Over-voltage (over 35 V) can also be detected in the batteries. In this case the motor driver will not operate, and the error LED will blink 4 times. Over-temperature protection is provided via an onboard temperature sensor to monitor the temperature, which determines the maximum allowable current. The motor driver will automatically lower the duty cycle percentage depending on the temperature sensor reading in order to lower the current [85].

DIP Switch	1	2	3	4	5	6
RC	0	0	CHANNEL 00 - Mixed 01 - Independent Right 10 - Independent Left 11 - Independent Both		0 - Linear 1 - Exponential	0 - RC 1 - MCU
Analog	0	1				0 - Locked Anti-Phase 1 - Signed Magnitude
PWM	1	0				
Serial Simplified	1	1	0	BAUDRATE 000 - 1200 001 - 2400 010 - 4800 011 - 9600	100 - 19200 101 - 38400 110 - 57600 111 - 115200	
Serial Packetized	1	1	1	ADDRESS Start from 000 (Decimal: 0) to 111 (Decimal: 7)		

DIP Switch	7	8
RC	BATTERY MONITOR 00 - LiPo (Lithium Polymer) 01 - NiMH (Nickel-Metal Hydride) 10 - SLA (Sealed Lead Acid) 11 - Off	
Analog		
PWM		
Serial Simplified		
Serial Packetized		

Figure 20. Selected Motor Driver Settings.
(Reprinted with permission from Cytron Technologies)

However, one safety feature that is not equipped is polarity protection. If the wrong polarity of the batteries is installed, the motor driver will be permanently damaged. Further, the batteries should be connected to the motor driver at all times if the buggy is pushed during transportation. Manually spinning DC motors results in power generation, which would be delivered to the motor driver without a storage device. Increased power generation without an output simply raises the voltages, which would burn the components on the motor driver [85].

3.1.2.2 Software Implementation – Caroline

The block diagram in Figure 21 describes the software that were implemented for each motor. They are shown in parallel because they largely mirror each other, except for the difference in feedback loop data type. Command values were received from the Raspberry Pi modules, converted to the appropriate PWM signal, and sent to the motors. The PWM value for the steering motor was set as a low constant value to avoid sporadic steering movements. The absolute encoder's 10-bit binary code was then read after a short delay. When the new angle is compared to the commanded angle, the PWM signal can either continue or stop the motor.

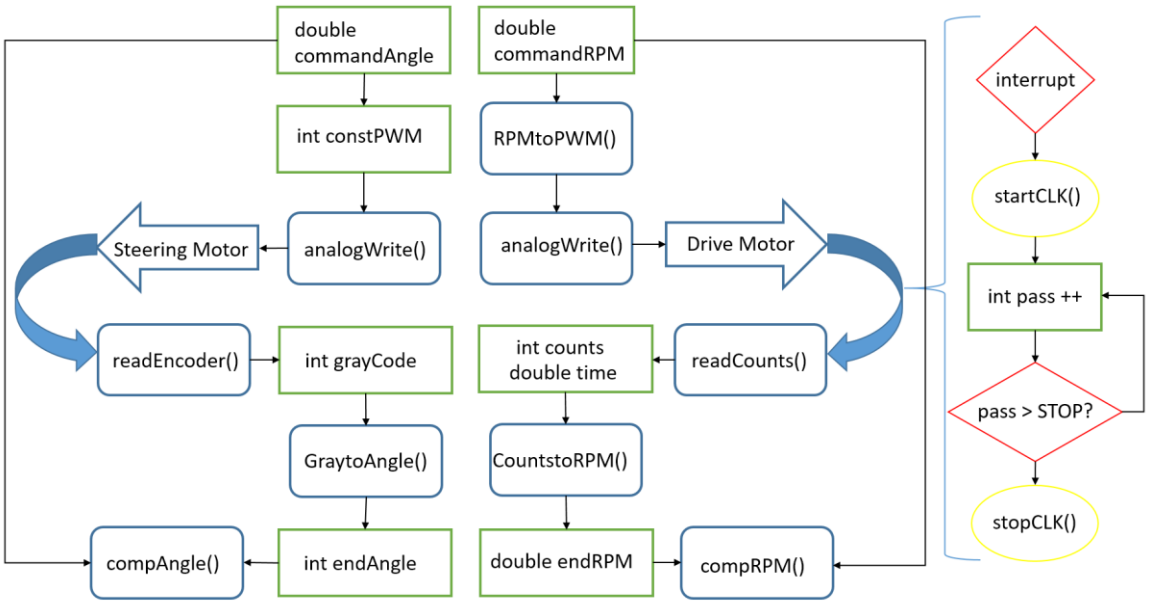

Figure 21. Motor Controller Software Block Diagram.

Likewise, when the commanded RPM value is converted to the PWM signal and sent to the drive motor, the speed is retrieved and converted from counts per time interval to RPM after a short delay. The best way to do this without unnecessarily extending this delay is by throwing interrupts in the background when the switch is triggered. That way, for every set number of passes, the clock begins and ends, and at the end of the interval, the number of passes and time duration are saved to their own variable. After converting these numbers to RPM, the measured value is compared to the original commanded RPM value. The PWM signal can then be adjusted as necessary to either slow down or speed up the drive motor incrementally.

3.1.3 Charge Controller

The charge controller is presented below as a modification to the original reference design by Texas Instruments, the TIDA-00120, which was originally a 20A MPPT solar controller designed for a solar panel input of 12/24V panels. This improved design is targeted for up to 48V systems and is capable of handling up to 40A, even though it is not

strictly necessary; this change offers improved heat dissipation abilities at no added cost. The charge controller is also designed for real world considerations, including programmable software that can raise alarms and output system statuses. The expected operating efficiency is above 97%, as per TI's test results, and efficiency was shown to improve with higher voltage systems [41]. The design objective is to obtain this high efficiency using the buggy's 48V solar array and 24V batteries at a maximum cost of $150.

3.1.3.1 Block Diagram

In Figure 22 the inputs and output of the charge controller are shown in a block diagram with the intermediation processes described in-between. Each of the blocks, including the current sensor, cut-off regulator, interleaved buck, photovoltaic full bridge driver, and microcontroller will be elaborated on further in the following sections along with comments on their associated circuits, which were modified to accommodate the new design specifications. The status and alarms block represents the software output, which will be described in a separate software section. Each of the labelled input and outputs can be found verbatim in the component schematics and traced between the components.

3.1.3.2 Bias Supply – Caroline

The bias supply for the charge controller is the portion that senses, regulates, and manages the power flowing to the controller and to the full bridge driver. It consists of three primary integrated circuits: the INA271 current sensor, the LM5019MR buck regulator, and the TLV70433DBV cut-off voltage regulator. The current sensor measures the current using a voltage drop typically across a shunt resistor, providing overcurrent protection and power monitoring. The main component, the interleaved buck, is a step-down DC-DC converter capable of accepting 100 V input and regulating down to a much lower voltage, depending on the external resistors. The cut-off regulator is included in order to output a steady voltage supply to the MSP430 and includes internal current sensors to tightly regulate the power. These devices allow the charge controller to be connected to the battery and a load continuously.

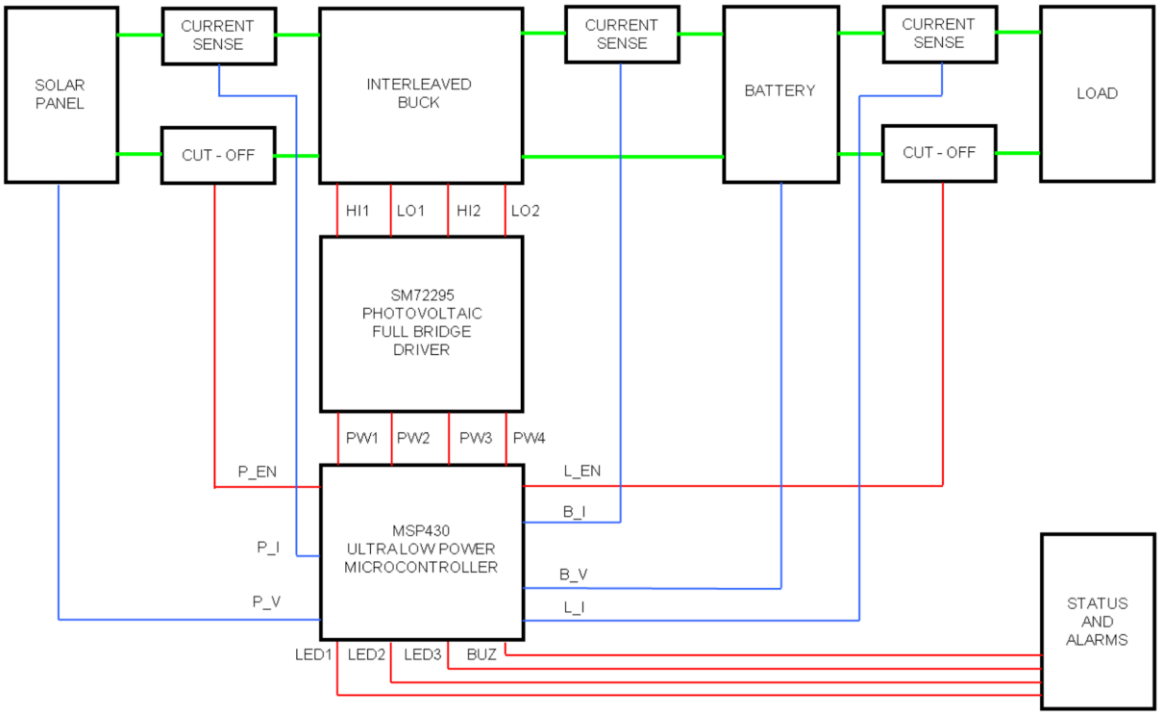

Figure 22. Solar Charge Controller Block Diagram [41].
(Reprinted with permission from Texas Instruments)

3.1.3.2.1 Current Sensor – Caroline

The component that can sense the current and protect the circuit from overcurrent situations is the INA271 current-shunt monitor. It accepts an input voltage from -16 V to 80 V and has a CMRR of 120 dB up to 130 kHz, meaning that its common-mode gain is almost completely removed compared to the differential gain. This results in a highly efficient noise rejection system that can sense voltage drops regardless of the value of the supply voltage. Naturally, it also has the ability to enable filtering. It operates from a voltage supply from 2.7 V to 18 V with 0.7 mA of current, so it consumes very little power. Like most of the components, the specified operation temperature is not to exceed 125 degrees Celsius [86]. The pins on this device are shown in Figure 23. The two inputs are connected by the shunt resistors and a power-supply bypass capacitor, since the power supply will be noisy or high-impedance. The power supply is on the V^+ pin.

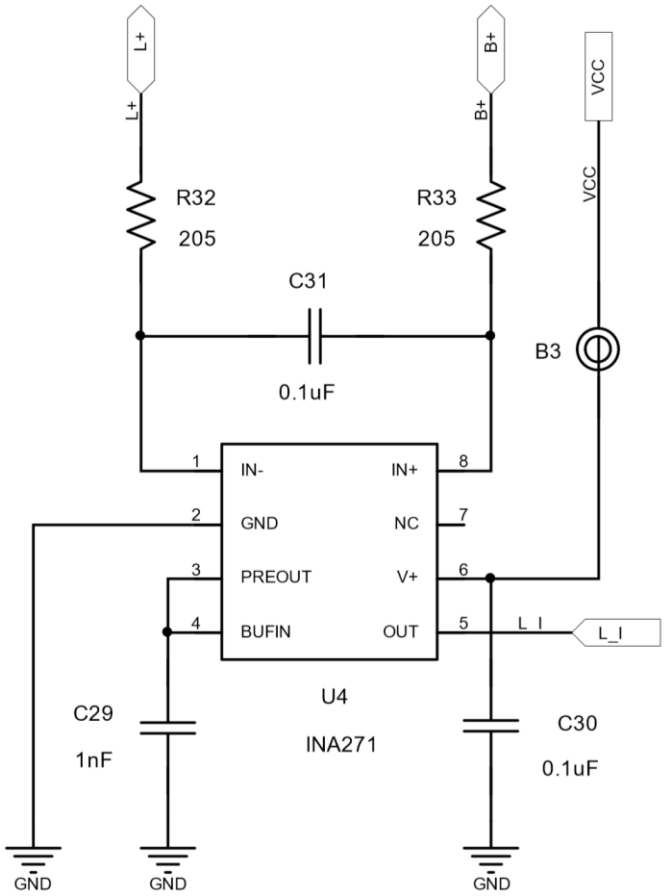

Figure 23. INA271 Current Sensor Schematic.

3.1.3.2.2 Interleaved Buck Converter – Caroline

Buck converters are higher voltage DC-DC converters that reduce the voltage while increasing the current. The interleaved buck, otherwise known as a multiphase buck converter, are highly efficient buck converters that operate with less losses at higher currents, as opposed to single-phase buck controllers [87]. The LM5019 is synchronous step-down regulator that is possible of very large step-down ratios, depending on the external resistors. It is capable of handling up to 100 V on the input at an operating current of merely 1.75 mA and supplying up to 100 mA on the output. Its features include short circuit protection, constant on-time control that does not need loop compensation, thermal shutdown, overcurrent protection, and bias supply under-voltage lockout. It manages to operate in a constant frequency despite input voltage changes. Again, the operation temperature should remain below 125 degrees Celsius, which was not threatened by the atmospheric conditions at the time of the competition [88]. The schematic for the interleaved buck is shown in Figure 24.

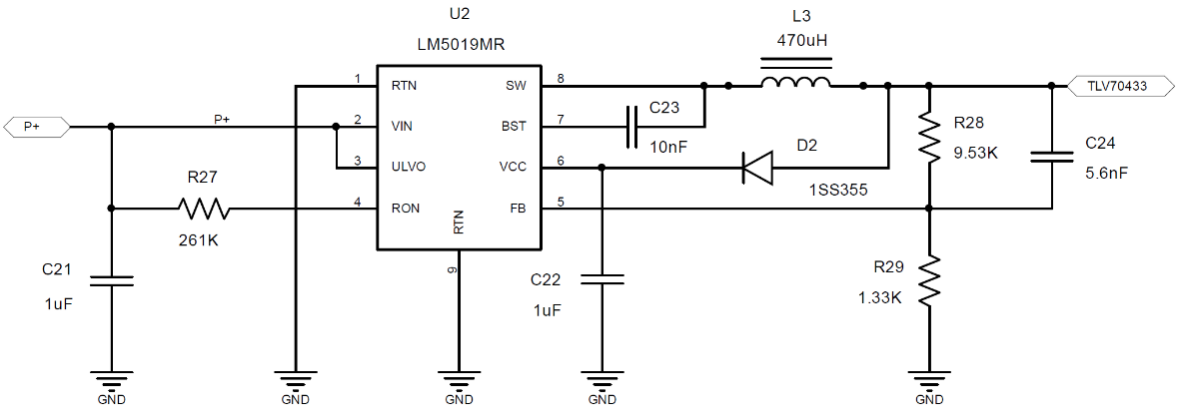

Figure 24. LM5019 Interleaved Buck Converter Schematic.

3.1.3.2.3 Voltage Cut-off Regulator – Caroline

After the interleaved buck regulates the higher voltage down to an acceptable voltage range, the TLV70433 low-dropout (LDO) regulator provides power management to the MSP340 microcontroller. These regulators have an ultralow quiescent current, thus minimizing internal power consumption and subsequent heat dissipation, do not produce switching noise, and have filtering capabilities. This lends itself well to a charge controller, since it is a power-sensitive application. It can operate over an input voltage range from 2.5 V to 24 V with a quiescent current of 3.2 μA, and similarly to the buck regulator can supply up to 100 mA on the output. The regulated output can be set to 1.2 V to 5 V with an accuracy of ± 2%. It has the same operating temperature threshold at 125 degrees Celsius. It is a simple device, essentially consisting of an internal current sensor, bandgap reference, operational amplifier, and voltage divider set by two resistors. In this design, its configuration in Figure 25 is almost identical to the typical application from the data sheet [89]. The output to pin J4.1 will be connected by a jumper to pin J4.2 to power the MSP430 during operation.

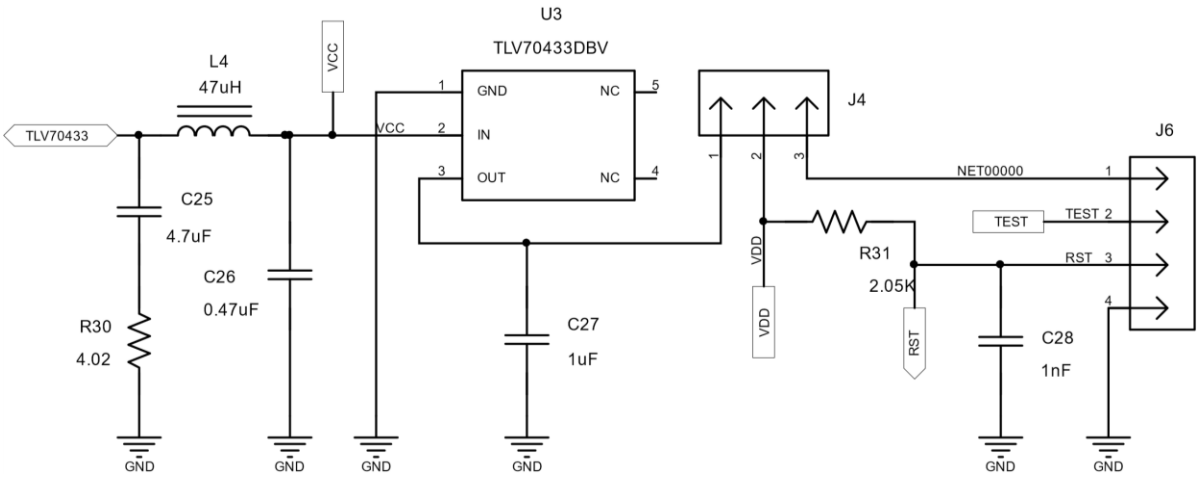

Figure 25. TLV70433 Voltage Cut-Off Regulator Schematic.

3.1.3.3 Microcontroller – Caroline

The microcontroller interfaces with all of the components to monitor statuses, direct commands, and process algorithms. The MSP430F5132 microcontroller was included in the TIDA-00120 design for this purpose and was kept in the design due to familiarity with this microcontroller. It boasts a low power consumption via five different low-power modes and by accepting a low supply voltage from 1.8 V to 3.6 V. The wake-up time from a sleep mode to active mode is less than 5 us, so its digitally controlled oscillator (DCO) is very responsive. It uses 16-bit architecture but supports 32-bit operations and includes two 16-bit timers. Its power management capabilities include supply voltage supervision so it can detect brownouts. Its serial communication interface allow for UART, synchronous SPI, and I2C for efficient communication. This particular model has 8 kB of flash and 1 kB of SRAM [90]. In short, it is an extremely flexible device with all of the features that would be necessary to hold all I/O's, compute algorithms, store data, and communicate with the other devices. The circuit diagram for this device is shown in Figure 26. The outputs on the far right go to LED's and output pins that can alert the user of errors.

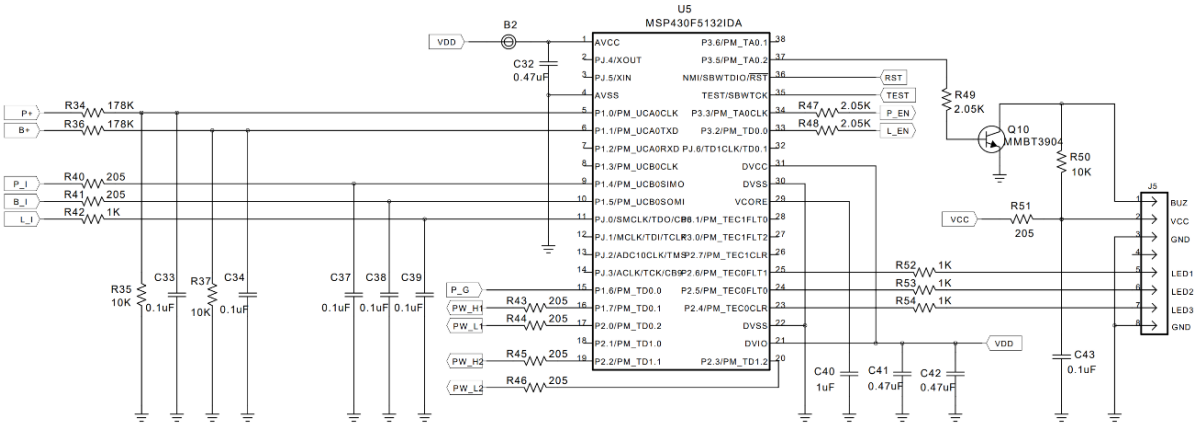

Figure 26. MSP430F5132 Microcontroller Schematic.

During the prototyping stage, Code Composer Studio (CCS) was used to program and configure the MPPT algorithm into this device using software provided by Texas Instruments. During testing, the code was then modified as necessary to accommodate the different input nominal voltage, which included setting various battery parameters.

3.1.3.4 Full Bridge Driver – Caroline

The full bridge driver uses four MOSFETs to pass current through a full bridge configuration, which makes up the actual power delivery function. The logic circuit provided by the microcontroller sends high frequency switching signals, which cause the gate drivers to drive power transistors. From the reverse side, the logic circuit is protected from the high-speed switching currents that degrade low-power digital control circuits [91]. This component thus continually takes instructions from the microcontroller, which continues to monitor the power flow, and delivers the incoming power through the interleaved buck and the current shunt monitor to the battery.

The SM72295 photovoltaic full bridge driver was created specifically for solar photovoltaic generation applications. Its gate drivers can provide 3 A of peak current to the MOSFETs, which is a large current capacity. Similarly to the interleaved buck, it includes two current-sensing transconductance amplifiers whose gains can be configured using external resistors. The amplifiers also filter out ripples in the current. In case of over-voltage, a comparator can be externally programmed to shut down the outputs. In case of under-voltage lockout where the power supply is too low, the Power Good indicator will shut down the gate drivers. It takes a power supply from -0.3 V to 14 V and relies on cumulatively around 4 mA in quiescent and operating currents, which is more power consumption than the other devices [92]. From this it can be concluded that the full bridge driver is the IC component that will cause the charge controller to require heat dissipation. The circuit diagram for the SM72295 is shown in Figure 27. The only downside to this IC is the pin spacing, which proved to be quite difficult to solder onto the PCB. After an assessment of available equipment and resources, it was decided to bring this IC, along with the four other IC's in this design, to Quality Manufacturing Services in Orlando, Florida for installation.

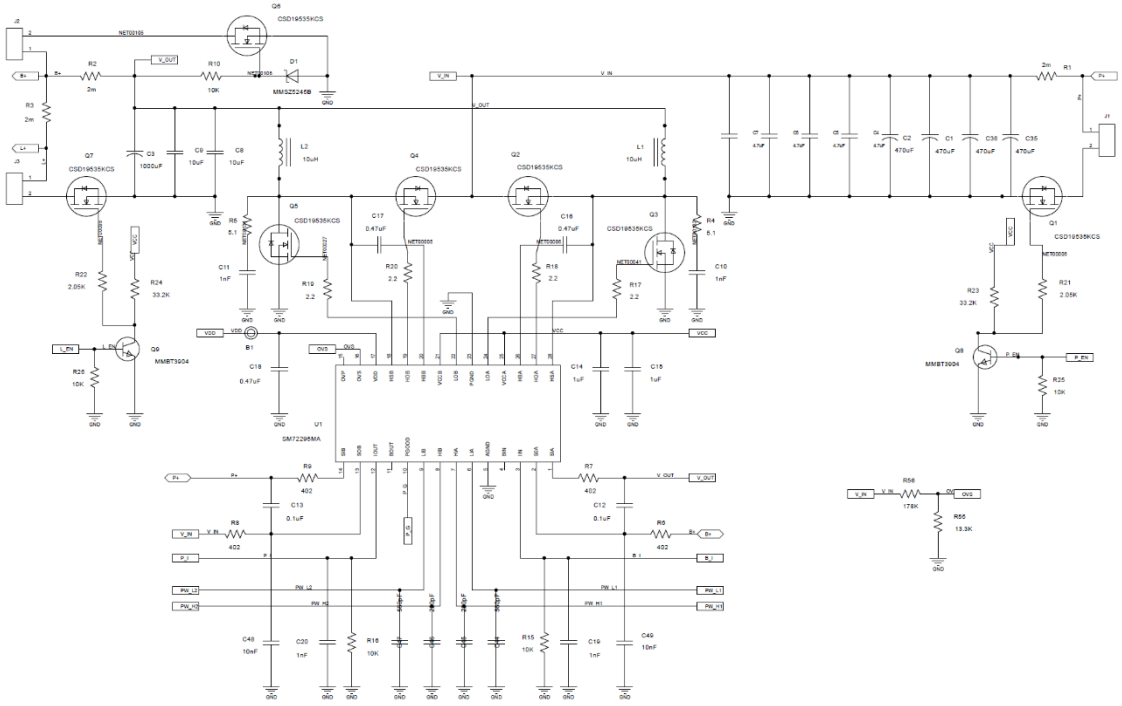

Figure 27. SM72295 Full Bridge Driver Circuit Diagram.

The circuit itself was derived from a few particular observations. First, the input capacitors to any MPPT charge controller have a notoriously high RMS current, or root-mean-square current. Adding subsequent capacitor modules results in a lower RMS current due to the increase in ESR, or effective series resistance. This is the primary contributor to the power dissipation within the MOSFET [93]. Figure 28 below shows the number of capacitor modules versus RMS current. It also shows the RMS current through the four driver MOSFETs for this specific design. For both 2 and 4 capacitor modules, a

small null occurs at a 50% voltage ratio, or a 24V battery with a 48V solar array. This indicates that this specific solar configuration could offer higher efficiency, heating the capacitors less and preventing a premature failure. As a whole, a 4-module capacitor array consumes about half the RMS current of a 2-module array. Therefore, the input capacitors were broken down into four 470 µF capacitors, model UHE1H471MPD [94]. This helped protect against efficiency losses due to small variations in voltage ratio caused by high temperatures or broken cells, which lower the MPP voltage. Further, adding two more capacitor modules at half the capacitance did not increase overall cost. Still, the capacitor temperatures were closely monitored during testing to confirm this design choice.

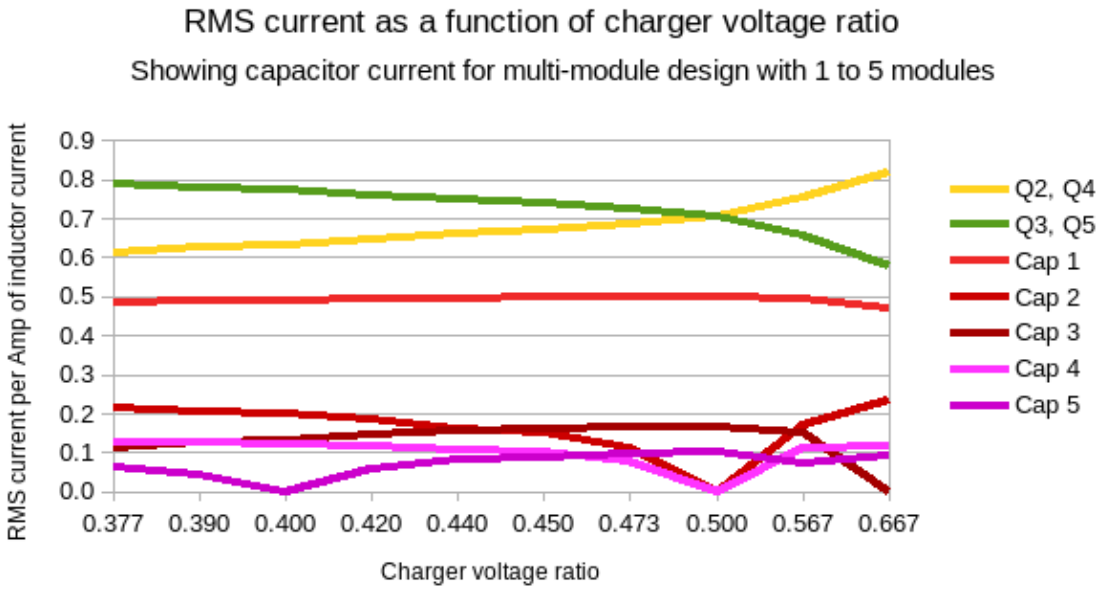

Figure 28. RMS Current vs Voltage Ratio and Capacitor Modules.

If the optimal array voltage is around 50V, then the MOSFETs should be rated to handle between 80 and 100V. Not only that, but a MOSFET had to be selected with a low gate-to-source on resistance and a high current rating. The selected MOSFET that was found to give the highest efficiency for a low cost was the CSD19535KCS. In addition to having these characteristics, it also had a high threshold voltage of 2.7 V, which means that turn on and turn off times are more symmetrical. This results in a significantly smaller loss in the transistor. Additionally, the MOSFETs in this design are driven from V_{cc} at 12V rather than V_{DD} at 3.3V, so there is no need for a low threshold voltage to accommodate a low logic level. A summary of the MOSFET specifications can be found in Table 16 [95].

A TO-220 package was chosen for the MOSFETs for increased heat dissipation, which allows more current to flow through them. Even though the current will remain below 20 A, this component will be able to operate more efficiently. The through-hole pin package is less expensive than an equivalent surface-mount, making this decision budget-friendly. However, ample room must be given both under and above the board for installation, since they will be located on both sides.

Table 16. CSD19535KCS MOSFET Specifications [95].

$T_A = 25^oC$		Value		Unit
V_{DS}	Drain-to-Source Voltage	100		V
Q_g	Gate Charge Total (10 V)	78		nC
Q_{gd}	Gate Charge Gate to Drain	13		nC
$R_{DS(on)}$	Drain-to-Source On Resistance	V_{GS} = 6 V	3.4	mΩ
		V_{GS} = 10 V	3.1	mΩ
$V_{GS(th)}$	Threshold Voltage	2.7		V
I_D	Continuous Drain Current (Package limited)	150		A
	Continuous Drain Current (Silicon limited), T_C = 25ºC	187		
	Continuous Drain Current (Silicon limited), T_C = 100ºC	133		
I_{DM}	Pulsed Drain Current	400		A
T_j, T_{stg}	Operating Junction and Storage Temperature range	-55 to 175		ºC

Additional MOSFETs Q1, Q6, and Q7 also serve an important purpose. Q1 is used to measure panel voltage and stop the battery from discharging when the panels are not illuminated. When the MSP430 turns Q1 on, it can measure the panel voltage; otherwise it only measures the battery voltage minus the voltage drop in Q8. The disadvantage is that this function will run continually, even at night if the charge controller is connected. Q6 is the component that will offer reverse battery protection. This transistor will only turn on if the battery polarity is correct. Lastly, Q7 is used by the MSP430 to measure the load voltage and protect against reverse load polarity. From the perspective of this design, the load terminal was not used during the competition. However, this load port could have served as a useful connection in the event that another component needed to be added to this design unexpectedly, such as an additional fan. If so, none of the other power components would need to be altered, which would have avoided extra costs. The voltage dividers for measuring both battery and solar panel voltages have a full scale range of a bit over 60 V, which is perfectly suited to a 50V solar array.

3.1.3.5 Software

The MPS430G2 LaunchPad shown in Figure 29 was used to program the charge controller. The configuration shown represents the connections needed for programming the device. RXD and TXD on the LaunchPad go to LED2 and LED3 located at J5 on the charge controller. The V_{cc} and ground pins on J5 should also be connected to the LaunchPad. Lastly, J4.2 and J4.3 should be connected using a jumper to provide power from the LaunchPad on J5, which is internally connected to J4 and J6 power pins. TI's GUI was used for controlling and monitoring the performance output of the charge controller during the programming stage and demo performances.

3.1.3.6 Board Assembly and Layout – Caroline

The PCB layout was designed using Altium. Once the base design from TI was uploaded, the modifications discussed above were translated to the board. This involved reshaping the polygon copper pours, adding through-holes for the TO-220 package MOSFETs and new capacitors, changing the parts, and adding new routed connections. The resulting board layout is displayed in Figure 30, which displays the top layer on the left and the bottom layer on the right. Its properties are contained in Figure 31.

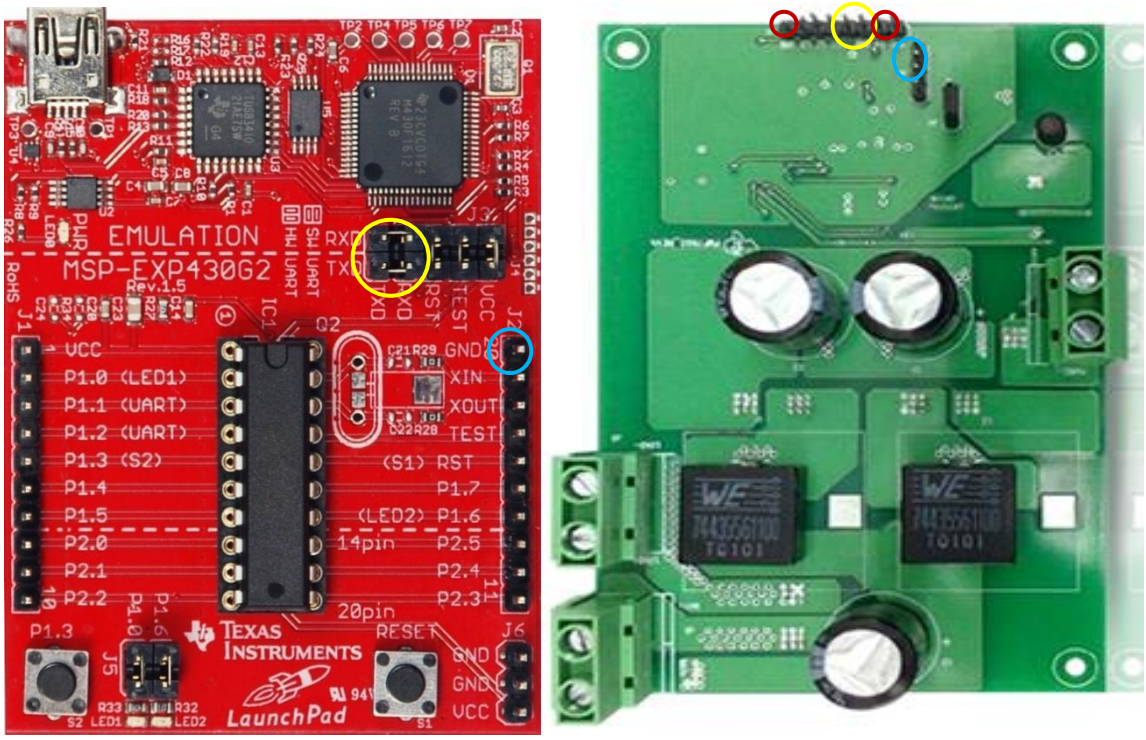

Figure 29. LaunchPad Connections for Programming.

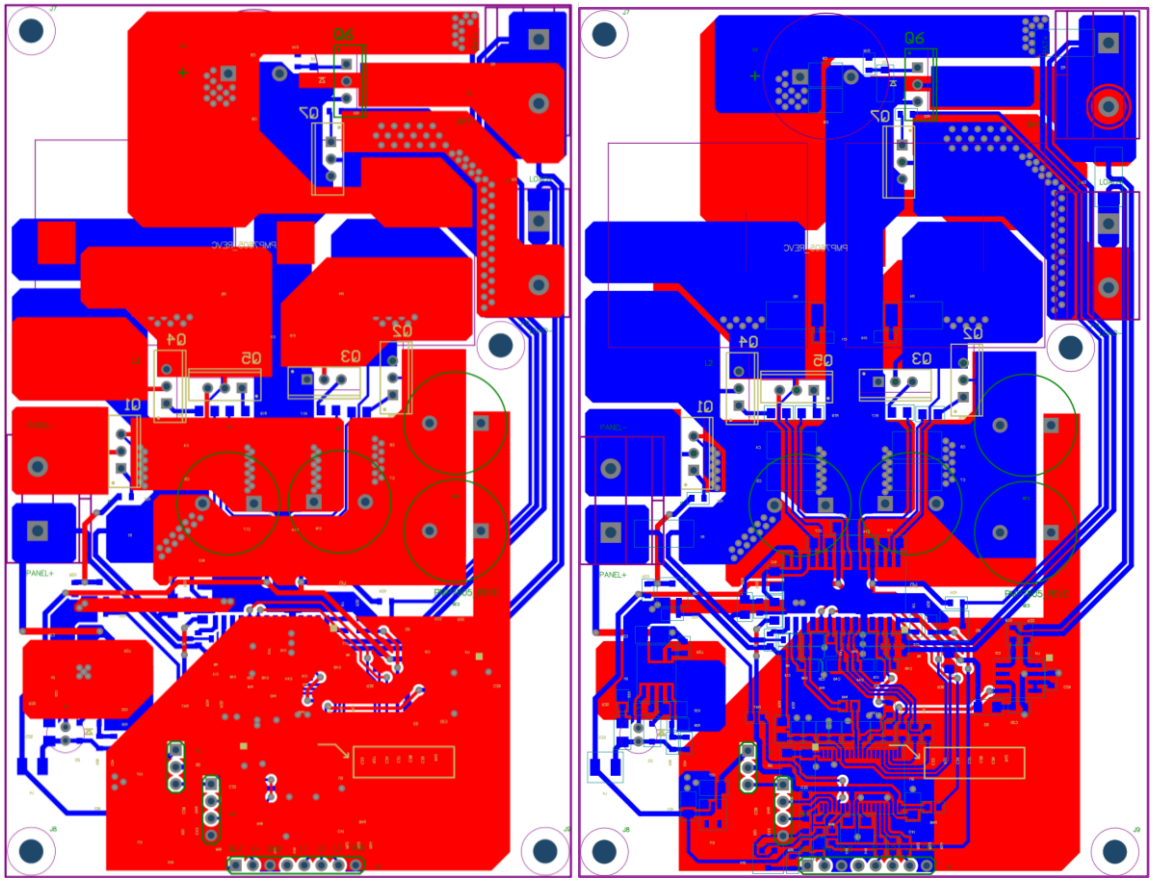

Figure 30. PCB Layout Top Layer and Bottom Layer.

FABRICATION CHART

FINISHED THICKNESS	SILKSCREEN	SOLDERMASK	FINISHED COPPER WEIGHT
☐ 0.031	■ LAYER 1	■ LAYER 1	☐ 1 OZ.
■ 0.062	■ LAYER 2	■ LAYER 2	■ 2 OZ.
☐ 0.093	☐ NONE	☐ NONE	☐ OTHER
☐ 0.125			

DESIGN	TRACE/GAP SPACING	LAYER COUNT
☐ SMD	☐ 0.010/0.010	☐ SINGLE SIDED
☐ THRU-HOLE	■ 0.008/0.007	■ 2 LAYER
■ MIX	☐ 0.006/0.006	☐ 4 LAYER
		☐ OTHER

Figure 31. Fabrication Chart Detail.

3.1.3.7 Input and Output Pins – Caroline

Table 17 lists the available inputs and outputs to the charge controller. Except for the panel and battery terminals, most of these are for programming purposes and were not used during operation. However, they were used during demo performances to monitor the alarms and output measurements.

Table 17. Inputs and Outputs to Charge Controller.

Junction	Pin	Purpose
1	1	Panel Positive Terminal
	2	Panel Negative Terminal
2	1	Battery Positive Terminal
	2	Battery Negative Terminal
3	1	Load Positive Terminal (NC)
	2	Load Negative Terminal (NC)
4	1	TLV70433 Output – Connect to J4.2 during operation; NC during programming
	2	V_{DD} – Connect to J4.1 during operation; connect to J4.3 during programming
	3	Connect to J4.2 during programming to provide power from LaunchPad on J6.1
5	1	To GUI during programming
	2	Input power (V_{cc}) connected internally from J4.2
	3	Ground (GND) – Short with J5.8
	4	NC
	5	SPI – Connection status for GUI connection (Output LED)
	6	SPI – Connect to Transmit (Tx) from LaunchPad for GUI connection (Output LED)
	7	SPI – Connect to Receive (Rx) from LaunchPad for GUI connection (Output LED)
	8	Ground (GND) – Short with J5.3
6	1	Input power (V_{cc}) from LaunchPad during programming
	2	Transmit (Tx) from LaunchPad during programming
	3	Receive (Rx) from LaunchPad during programming
	4	Ground (GND) from LaunchPad during programming

3.1.4 Smaller Electronics – Olesya

The buggy has small electronics that make up the computer vision system using Raspberry Pi's and Camera Modules, the printed circuit board, and the rotating proximity sensors and range finders. The following introduction will explain more about the smaller electronics' and the main reasons as to why these devices were chosen for the design.

The Raspberry Pi's have a lot of support in the hobbyist industry and within the past two to three years there has been computer vision prototyping using the Pi's. This is mainly because they are low cost, low power and extremely modular. A Raspberry Pi can run operating systems, games, and 3D graphics. They come with Cameras modules that can easily be plugged in and integrated for Computer Vision (CV) applications. The processors on the Pi's are also very competitive with all the other microcontrollers on the market today like the Arduino Nano and the Beagle Bone. The Pi's have a BCM2837 processor and the ARM CPU complex has a Quad Core Cortex A53 with dedicated 512 Kbyte L2 cache. This was necessary for the path finding algorithms that process pictures

and videos at frames per second, and for processing additional information from the proximity sensors and range finders. Splitting up the work with multicores and having a faster processor with dedicated cache increased the reliability of the buggy's navigation. For more details as to why Raspberry Pi's and Raspberry Camera Modules were selected for the Buggy's autonomous navigation hardware, please refer to the software section in the Buggy's design documentation.

A microcontroller design on a printed circuit board is a requirement for the project and an opportunity to minimize any unnecessary components on a pre- made board. The rest of the circuit board had additional pins for LEDs and the other periphrals including the encoder, speedometer, and GPS. For more details on the Printed Circuit Board design and layout please refer to the PCB section in the Buggy's documentation

The sensors provided the distance away from any obstacle entering the front view of the vehicle. The Computer Science team used that information based on the type of Computer Vision algorithms and neural networks they had implemented. The sensors were also included in the design for redundancy to the navigation system, and to decide if the vehicle should come to any stops. If the navigation system were to fail, the sensors should be able to aid basic obstacle avoidance. With the low-cost budget and the fact that the buggy also had a computer vision navigation system, the proximity sensors and the rangefinders used in this design are simple low- cost sensors and three out of five will be attached to mounts for rotation. For more details on the sensor design and layout, please refer to the sensor section in the Buggy's documentation.

3.1.4.1 Power Calculation – Olesya

When calculating the power requirements needed by the small electronics in the Solar Powered Beach Buggy, the amps that each component draws needed to be accounted for. Table 18 below lists all the components and their respective operating current. These calculations were based off Design A of the sensor system. Design A was final design for the first prototype because this design costs less, giving the PCB a slightly bigger budget. If the first design failed to meet the requirements, switching to Design B would not have required any changes to the power because both designs require roughly the same amount of power.

Altogether the amps needed for the smaller electronics was:

At 5 volts, the Raspberry Pi will draw 2A plus .4A with a camera module.
At 5 volts, the printed circuit board will draw at most 2A.
At 5 volts, the ultrasonic sensor will draw .015A.
At 5 volts, the infrared sensor will draw .050A.
At 5 volts, the servo will draw 1A.
At 5 volts, the temperature sensor will draw .0002A.

$$2*(2A+0.5A)+2A+4*0.015A+0.050A+3*1A+.0002A=9.1102A$$

This provided the information needed to select the best converter to power all the components. The safest choice was to use 24 volts to 5 volts 10 amps buck converter module. This is listed in Table 8 in the research section above.

3.1.4.2 Converters – Olesya

The converter will buck the voltage down to 5 volts. No other electronics were going to be connected to the buggy that needed any voltage higher than the 5 volts. It is noted that the servos can take above 5 volts, but the speed of the servos were not max speed, allowing the servos to also be connected to the converter output because supplying 5 volts to the servos will create a high enough speed to be able to rotate the sensors. The converter was selected based on the calculations for a max load with Design A of the sensor configuration. The only difference between the two designs is the addition of a temperature sensor with a 1:4 ratio of infrared/ultrasonic sensors in Design A compared to Design B with only a 3:2 ratio of infrared/ultrasonic sensors. Both designs still had 3 out of the 5 sensors rotating. The designs have a difference of ~ 0.1 amp, and because the max calculated amps used in the system at one time is 9 amps and the bus can support up to 10 amps, the calculations were the same for both designs.

Table 18. Smaller Electronic Chosen for the Solar Powered Beach Buggy.

Count	Component	Voltage	Operating Current	Microprocessor/ Peripheral	Pins
2	Raspberry Pi's	5 V +- 5%	2- 2.5 A maximum	Microprocessor	2 - 5V 2 - 3.3V 12 - GPIO 5 - GND
2	Camera Module	3.3 V	400 mA maximum	Peripheral	15-pin MIPI CSI
1	Printed Circuit Board	1.8V to 3 V	< 2A	Microprocessor	1 3v VCC 60 GPIO 1 GND
4	HC-SR04 Ultrasonic sensors	5V	15 mA	Peripheral	1 5v VCC 1 GND 1 TRIG 1 ECHO
1	VL53L0X Time-of-Flight Distance Sensor	2.6 to 5.5V	10mA to 50 mA	Peripheral	1 5v VCC 1 GND 1 SDA 1 SCL 1 GPIO
3	Tower Pro Micro	3V to 6V	750mA to	Peripheral	1 5v VCC

	Servo 9g SG90		1A		1 GND 1 PWM
1	Adafruit MCP9808 Precision I2C Temperature Sensor	2.7V to 5.5V	200 μA	Peripheral	1 5v VCC 1 GND 2 GPIO

The max current draw was 9 amps as calculated in the previous section. The simplest configuration was to buck the voltage to 5 volts from the battery and power all the components in series as shown below in Figure 32. After thorough calculations, the 10-amp, 50-watt converter by KNACRO was been selected. This DC-DC buck converter was a low-cost and had over-current protection, over-voltage protection, and short circuit protection. Other critical reasons this converter was selected was because it's waterproof, which suits the environment of the competition, and it has a efficiency of 96 percent, which is immensely beneficial due to the buggy having a very limited supply of energy.

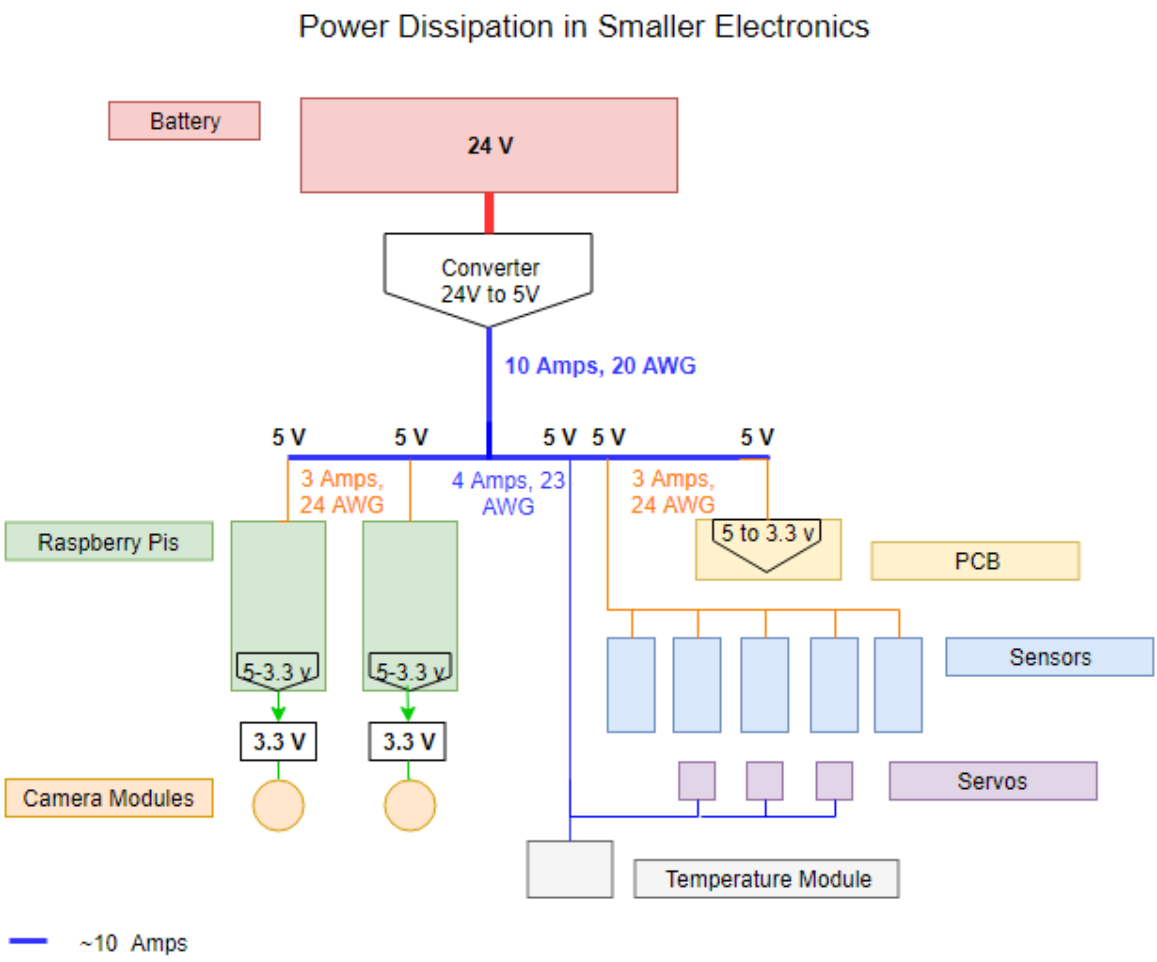

Figure 32. Power Configuration for Smaller Electronics in the Buggy.

Other converters shown in Figure 32 are within the electrical components themselves. The camera modules run at a lower voltage of 3.3 volts as shown in Figure 33 and were directly connected to the Raspberry Pi's with a Camera Serial Interface [96]. The Pi's have 5 volt to 3.3 volt voltage step-down regulators on the chip to retain exact logic-level voltages. The microcontroller also had a 3.3 voltage regulator to step down the voltage from 5 volts to 3 volts - 3.3 volts. This way, the design only needed one external converter and stayed within the 12 dollar budget allocated to converters. A more detailed description of the PCB step-down circuit is be described in the PCB design sections. Further information about additional protective circuitry such as fuses, voltage sensors, and current sensor not included in this converter are be discussed in the following sections to ensure the electrical safety of this vehicle.

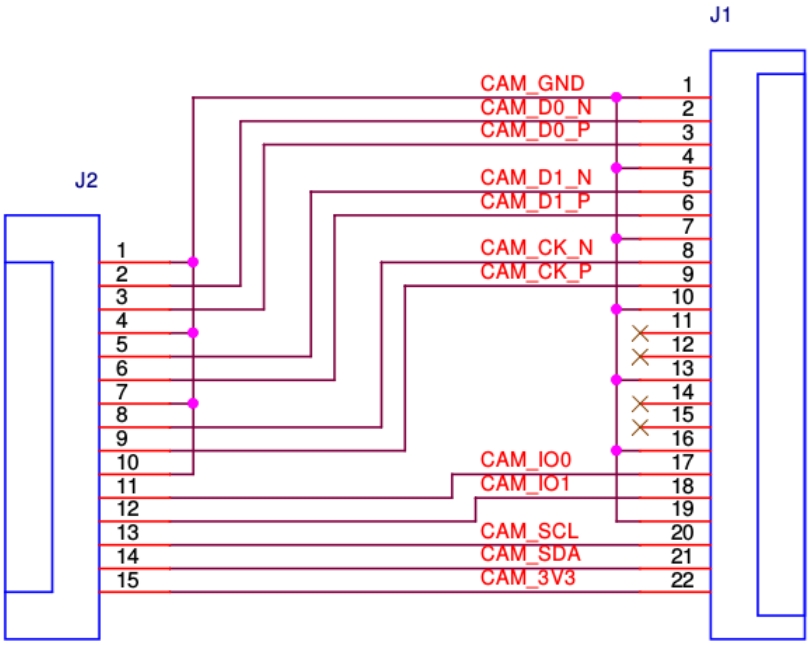

Figure 33. Camera Serial Interface Connection to the Raspberry Pi.

3.1.5 Protective Circuitry – Olesya

Circuit protection devices are used to limit the current or voltage in a circuit, which can potentially increase to an amount that might damage the components attached to that circuit. As stated in the power system design, the charge controller and the dual channel motor controller have protective circuitry integrated in the components. Extra precaution that was taken is discussed in the corresponding sections of the component's designs. Additionally, as discussed above, the KNACRO buck converter that supply's 5 volts to the microprocessors and sensors also has protective circuitry within the device. Further measures taken were to place sensors in critical areas that allowed the buggy to monitored for current flow and the voltage, particularly the electronics in the buggy while the buggy was operational.

3.1.5.1 Circuit Fuse Blocks – William

When connecting multiple systems to the battery, safety should be taken into account. The use of a circuit fuse block provides more access to the battery. There are several distribution blocks available on the market. Table 19 shows a list of fuse blocks that are able to meet the needs of the electrical system. Each model has specifications that are suitable to the design of the buggy. Because we would like to keep costs down, the fuse block from SuperDroid Robots was chosen. The team believes that the assembly of the fuse block will not hinder their ability in accomplishing the construction of the buggy. The fuse block's four available circuits will be enough to provide access to the various subsystems that need access to the battery.

Table 19. Fuse Distribution Blocks.

Model Name	Manufacturer	Number of available circuits	Assembled	Cost
6 Ganged	Del City	Six (6)	Yes	$17.84
ST Blade	Blue See Systems	Four (4)	Yes	$25.08
Fuse Block	SuperDroid Robots	Four (4)	No	$17.40

3.1.5.2 Fuses - William

For handling dc voltage ratings, fuses are generally rated to be maximum ratings and should not be exceeded. This means that the voltage rating of a fuse must be greater than the maximum voltage expected in the application. However, fuses are insensitive to voltage changes within their ratings so selecting the proper voltage rating is strictly a safety issue. Fuses can operate at any voltage below or equal to their rated voltage. Fuse current rating should be selected with a large enough current capability so that the fuse will not open under steady state conditions, yet will open during an abnormal (excessive) overload or short-circuit condition. This means that the fuses should be rated to be 150% to 200% above the maximum steady state input current at maximum load and minimum line input voltage [97].

Based upon the full load amps of the drive motor and steering motor, the electrical system must be able to handle over 30 Amps at any one moment. This leads for us to pick a 40A fuse that will be attached between the battery and motor controller.

Figure 34 shows the design of the power distribution block for the buggy electrical system. The power distribution block was used to allow access to the available power. The motor controller was attached to the power distribution block. The charge controller was attached to the power distribution block. The DC/DC converter was attached to the power distribution block. This leaves the power distribution block with one available circuit. The available circuit could have been used for additional future design changes.

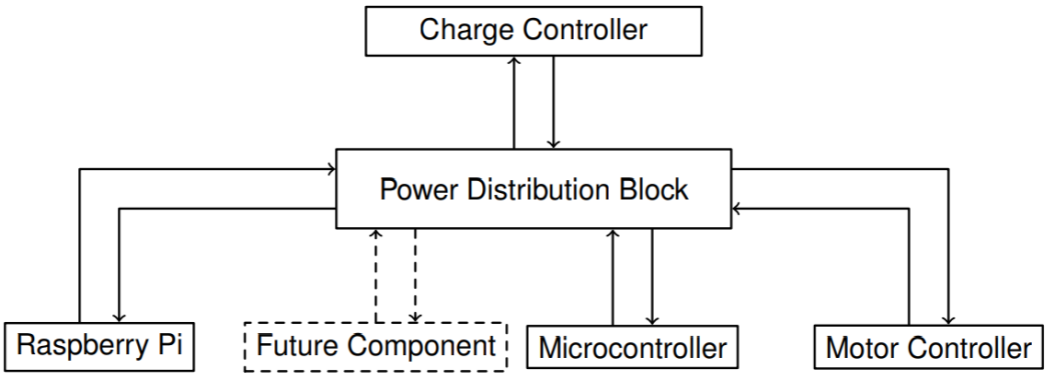

Figure 34. Power Distribution Block.

3.1.5.3 Fuse Protection in the Power System – William

One of the best ways to add protection to the power system is by using fuses. It is better for a cheaper component to break than a more expensive component. Therefore, the use of fuses is highly encouraged. As fuses protect the wiring from getting too hot, they are a choice greater in regards to safety. Clifton recommends three different locations that fuses should be installed within a solar system. The first is between the charger controller and battery bank. The second is between the charge controller and solar panels. The third location is not applicable to this project [98].

Figure 35 shows where the fuses were connected in order to guarantee protection to the solar system. We value safety as our highest concern. Therefore, we added an additional fuse between the charge controller and the power distribution block. This additional layer of safety helped ensure that the power system was protected at any given moment.

Some interesting decisions can be made for what fuses should be placed between the components. A 40A fuse should be sufficient between the solar array and charge controller. A 40A fuse should be sufficient between the charge controller and the power distribution block. A 40A fuse should be sufficient between the charge controller and the battery array.

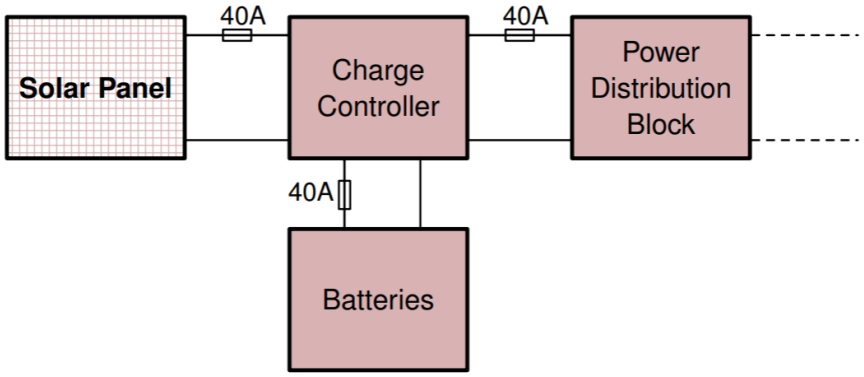

Figure 35. Possible Locations for Fuses.

3.1.5.4 Current Sensors – William

Another possible option was to utilize relays to further our endeavors to maximize safety. Relays are an excellent way to control the flow of current from a remote location. The microcontroller can be used to toggle the relay on and off. The relay can be attached between the power distribution block and the motor controller. This allows the microcontroller another way to control the motors. Figure 36 shows this design possible decision.

In the event that the motor controller is unable to take messages from the microcontroller, the microcontroller will be able to stop the motors by utilizing the relays to open the circuit. This will disconnect the power from the power distribution block to the motor controller. The motor will be without power. With a power supply, the motor controller will be unable to power the two motors. This extra layer of safety will allow us to have more than one way to stop the motor.

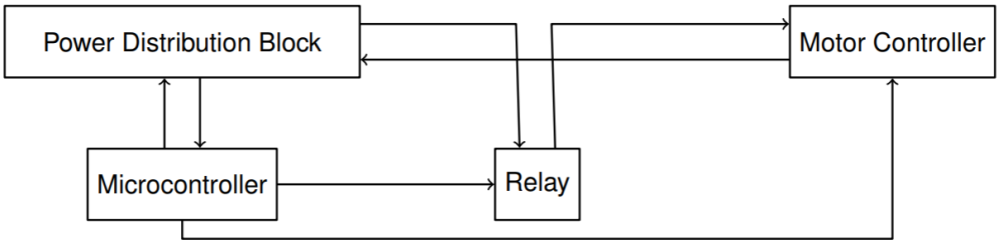

Figure 36. Possible Option for Relays.

The decision to include the relay as a medium between the power distribution block and the motor controller provides a layer of safety to the users of the buggy. If the motor controller is no longer able to take commands from the microcontroller, the microcontroller can easily remove the power to the motor controller. This simple solution is an effective safety feature.

3.1.5.5 Voltage Sensors – Olesya

Overvoltage suspension devices protected the circuitry from an increase of voltage. This can be caused by too much current, incorrect wiring, and insulation/isolation failures. The voltages were monitored using voltage sensors and a voltage divider circuit that was connected to the batteries as shown below in Figure 37.

The sensors were to be connected to a relay switch to but off power to the electrics. The voltage input to the motor will be monitored because any excessive current or voltage might damage the motors and or the power supply. Additionally, the electronics also had a voltage sensor on the main bus to track the voltage input to the sensitive integrated circuits shown below in Figure 37.

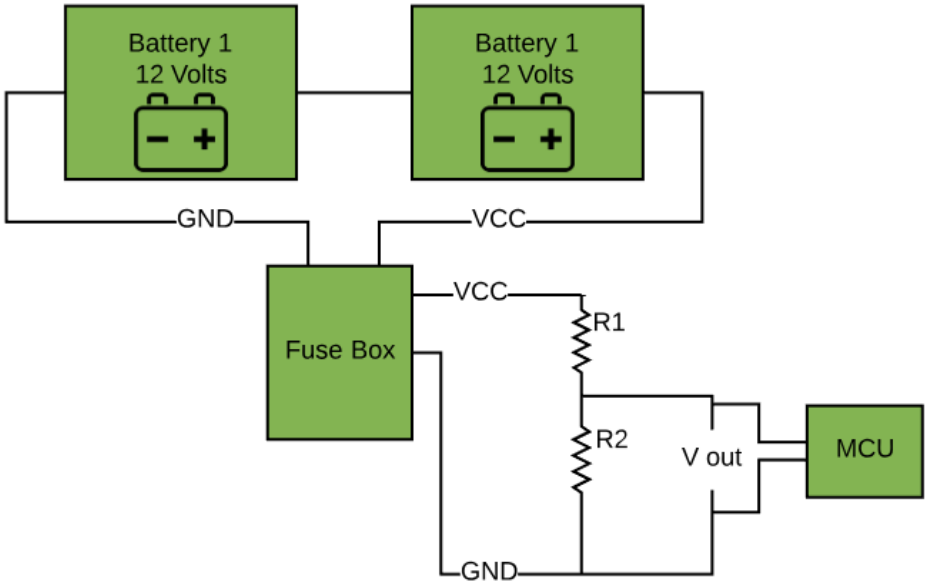

Figure 37. Data Acquisition circuit for battery usage and voltage monitoring.

Another reason voltage sensors and current sensors were considered was in the event that the budget could not cover designing and building a charge controller for this project. In the case where the budget is limited for the project, the protective circuitry was necessary. Best case scenario, was were able to purchase the charge controller with an allocation in the budget, the charge controller itself incorporated additional features to provide protection against any damages to the battery. If the charge controller would have been out of scope for the budget, Plan B would have been redundant circuitry with a resettable circuit breaker rated at 24 volts and 40 amps. To fully troubleshoot the electrical connection, sensors would have been placed before the circuit breaker to track the voltage and current coming into the battery just before the circuit breaker as shown in Figure 38.

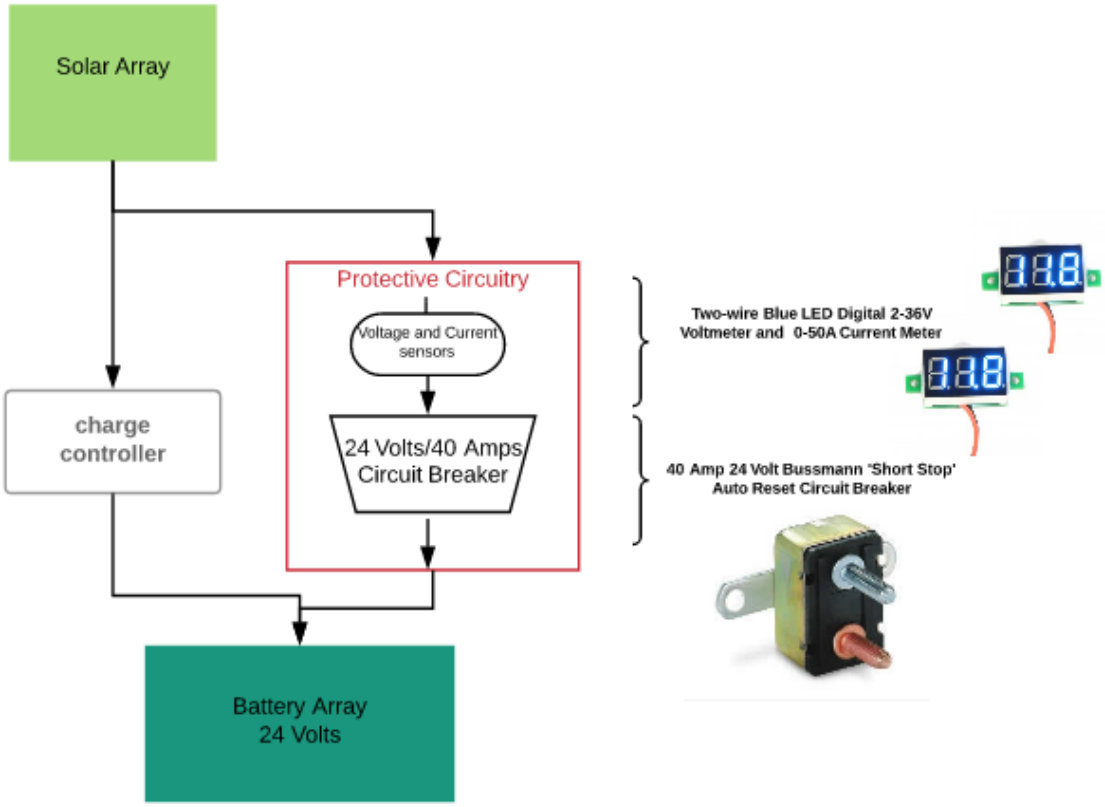

Figure 38. Protective Circuitry between the Buggy's Solar Array and Battery.

3.1.6 Power Verification – Caroline

Using all of the design choices, a final estimate of the hourly energy consumption and generation was computed. The generation was computed by multiplying the total number of solar cells, 180, by the rated wattage, 4.74 W, and multiplying by the hourly irradiance per 1000 W/m^2. Efficiency losses were estimated at 20% from the cell to the battery due to wiring, charge controller inefficiency, battery charging inefficiencies, and elevated temperatures. An extra 20% was deducted for the stated acceptable cloud coverage. Since the drive motor wattage is 500 W, and the listed efficiency is 78%, the calculated required electrical power to operate the motor at full rated load is 641 W. However, this

is assuming that the drive motor is running at full load, which is unlikely. A more accurate assumption of the motor performance is around 80% of full load.

Electrical consumption numbers were calculated as follows: the mean expected electrical energy was equal to the summed medians of the estimated component consumption from Table 9 minus the charge controller consumption. This value is equal to about 30 W. Then, the steering motor power consumption was calculated at 20% of the total run time, or 20% of 250 W, which is equal to 50 W. This gives a constant summed energy consumption by the electronics of 80 W. The energy consumption of the charge controller was set equal to the solar generation multiplied by 4%, which is the efficiency loss stated in the Texas Instruments design documentation. This is the amount of lost energy in the conversion process, and was added to the electronics energy consumption. Finally, for each hour the motor and electronics power consumption were deducted by the remaining watt-hours of the battery plus the added generation for that hour.

Since the competition is 8 hours long, and the most ideal time to compete is between 8 and 4 PM, then the final remaining watt-hours in the battery is calculated at 16:00 in Table 20. A 120 Ah actual capacity was selected to give an initial battery power of 2880 Wh. Then, the final remaining power left in the battery is 27% with respect to the actual capacity and 22% with respect to the rated capacity. Assuming one hour could be spent at rest in order to regain energy via solar generation around noon, this estimate is even higher. Likely, the actual performance would have resulted in a remaining battery storage between these two percentiles.

Table 20. Total Power Consumption per Hour.

Hour	Battery Power (Wh)	Irradiance (W/m^2)	Solar Generation (W)	Electronics Consumption (W)	Motor Consumption (W)
8:00	2880	154.76	86.19	86.16	512.8
9:00	2367.24	379.65	211.45	95.10	512.8
10:00	1970.78	632.89	352.49	105.18	512.8
11:00	1705.29	853.09	475.13	113.94	512.8
12:00	1553.69	961.65	535.60	118.26	512.8
13:00	1458.23	912.72	508.34	116.31	512.8
14:00	1337.46	729.40	406.24	109.02	512.8
15:00	1121.88	479.94	267.31	99.09	512.8
16:00	777.30	237.66	132.36	89.45	512.8

3.2 Electronics Design – Patrick

The electronics for this project will consist of the proximity sensors and the main control unit. The proximity sensors will be used to detect any objects that get to close to the vehicle and require and immediate stop. The main control will be a printed circuit board that controls and interfaces with the sensors and other peripherals such as the motor controller, charge controller, encoder, and speedometer. Additionally it will need to be

able to connect to and communicate with the navigation board to receive motor commands and send data.

3.2.1 Manual User Controls – Caroline

The manual controls for the buggy include two manual buttons or switches that are used to start and stop the vehicle. Each switch is a Single-Pole Single-Throw (SPST), which required a single input pin on the PCB plus ground and power terminals. A 10 kΩ resistor was used between V_{cc} at 3.3V and input pins P1.4 and P2.7, which were connected to the two switches in order to regulate the current. The buttons were colored appropriately: red for stop, and green for go. They were also be large enough to be seen from a distance, located conveniently in the vehicle, and given labels. The wiring diagram for both pushbuttons is included in Figure 39.

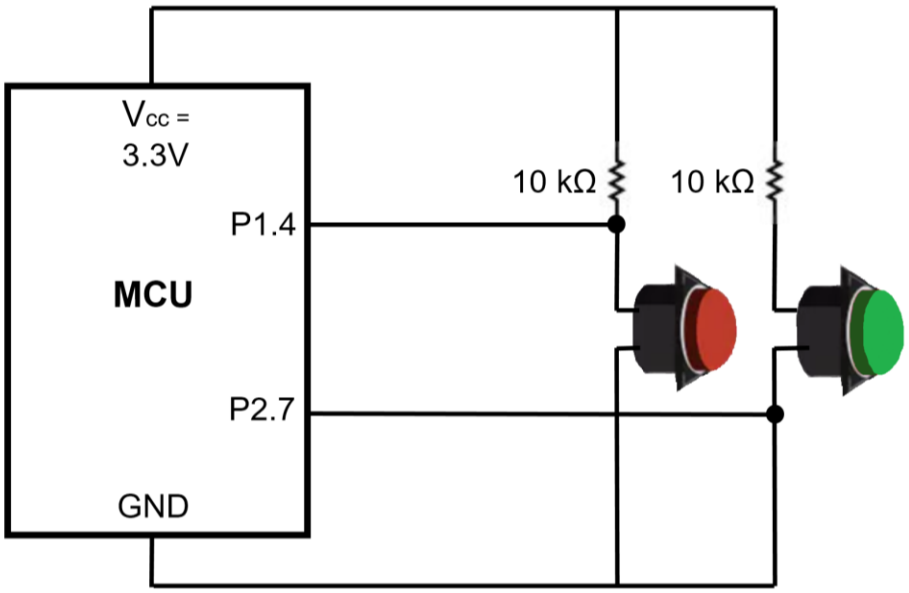

Figure 39. Manual Controls Wiring Diagram.

Upon pressing the green button, the motor driver is fed current as determined by the Raspberry Pi processors and delivered as a PWM signal from the MCU. The sensors and cameras then become active. The steering motor begins to accept commands via the motor controller, and all of the microcontrollers exit their sleep mode. The green button is then the only method of starting the buggy. This is to ensure the safety of the surrounding beachgoers and wildlife. If the buggy is started without a passenger, then it will possibly operate completely unsupervised. It could also be sent to a coordinate and stranded at a faraway location.

When the red button is pressed, the microcontroller first changes the output PWM signals to the motor driver to zero, thus stopping all power from flowing to both the drive and steering motors. This causes the buggy to coast to a stop within about one foot. The charge controller still continues to charge the batteries. The Raspberry Pi's then enter a

sleep mode. This sleep mode stops the Raspberry Pi's from processing the sensor or camera input and also stops powering the servos that rotate the proximity sensors.

The location of the manual button was designed to be accessible: both easy to see and to press quickly in case of an emergency by either the passenger or an observer. Figure 40 is a simulated image of the location of the manual emergency stop button and start buttons in red and green colors respectively. This image was prepared on SolidWorks and approximates the location of the pushbuttons relative to the rest of the frame. These buttons were labeled for clarity.

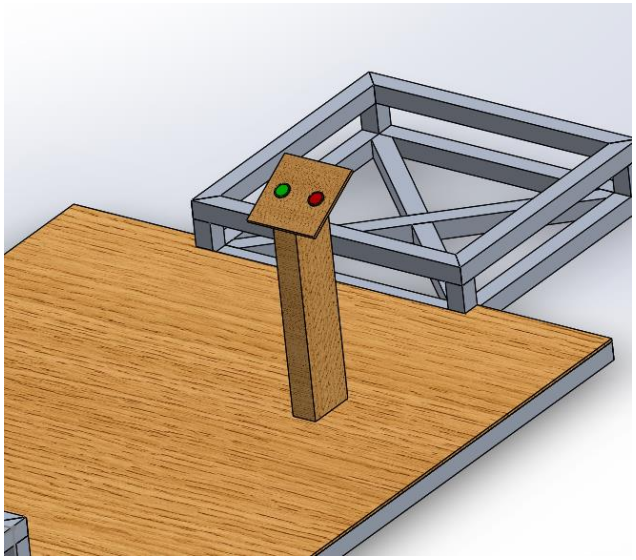

Figure 40. Manual STOP and GO Pushbutton User Interface.

3.2.2 Proximity Sensors – Olesya

Proximity sensors were critical to the Solar Powered Beach Buggy, and they provided data to assist and add redundancy to the guidance and navigation system as well as provide data needed for an emergency stop. The sensors were mounted on the Buggy and stayed at a consistent location. To get a full reading around the buggy the sensors were rotating via servos. They sent data to the PCB that processed the data and further relayed what is needed to the Raspberry Pi's.

Both microprocessors had peripherals. The Computer Science team decided to implement computer vision system using stereo camera module that was powered by the Raspberry Pi's. The Printed Circuit Board was not powering the proximity sensors and range finders or the servos, however the PCB was connected to the servos to send the correct PWM signal to rotate the sensors.

3.2.2.1 Sensors – Olesya

The sensors selected for this project were the VL53L0X Time-of-Flight Distance Sensor with a smaller range of 3 to 200 centimeters and the HC-SR04 Ultrasonic Distance

Measuring Sensor with a range of 2 to 500 centimeters. These sensors are shown below in Figure 41. The infrared VL53L0X and the Ultrasonic both measure distance from an object based on a specific formula dependent on the technology they are using.

These sensors are both under 10 dollars, so multiple sensors can be purchased along with servos while staying within the 60-dollar budget. Any other choices would have limited the number of sensors or the capability to purchase equipment to rotate them. There uncertainty with just how well the cheaper SR04 Ultrasonic sensors were going to work. Throughout all the applications using the SR04 ultrasonic sensors in the robot and Arduino community, the research shows that the sensors are not very reliable for accurate distance, and sometimes provides incorrect readings. There are many approaches to make the SR04 ultrasonic sensors more accurate. One approach was to re-solder the circuit to provide more voltage to the output pin. Another approach was to include a temperature sensor to account for the dependency in the distance calculation. With the environment considered, the latter approach was the best choice to design a more accurate sensor system. Therefore, there was two designs for the sensor system just in case the SR04 Ultrasonic sensors do not perform as needed for distance calculations and object detection. The two designs used these two sensors but different ratios to make up the total 5 sensors that were placed around the buggy.

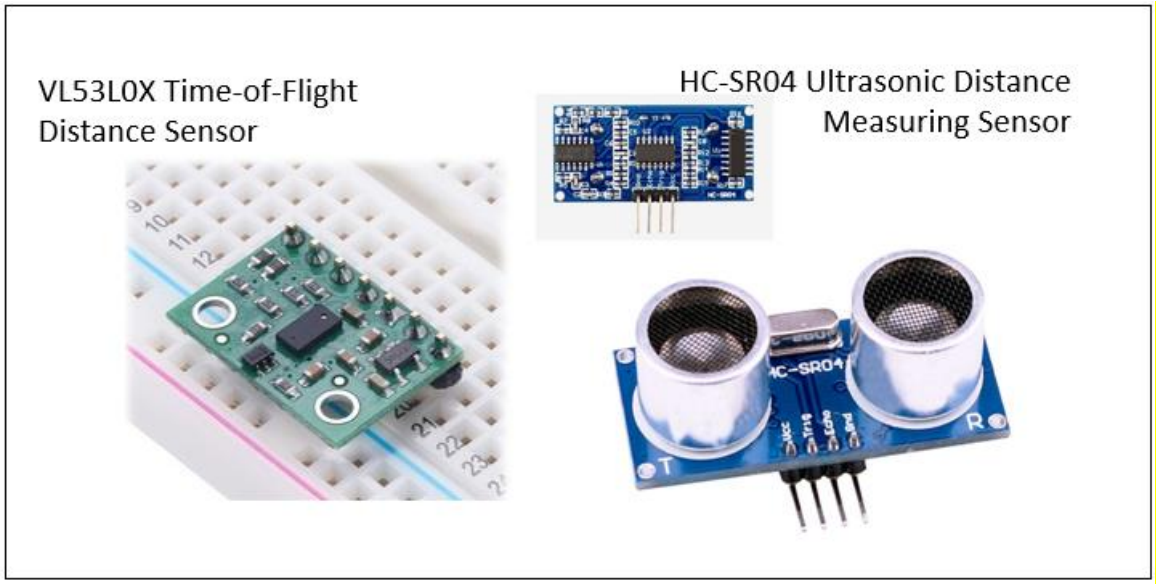

Figure 41. The Selected Sensors for the Solar Powered Beach Buggy.

The HC-SR04 Ultrasonic distance sensors emit sound waves at very high frequency, and based on the time it takes to get back, a basic distance formula can be used to measure the distance away from an object as follows:

$$distance_{object} = (\text{time for wave to come back} * \text{speed of the sound}) / 2$$

From this equation, the time is calculated by the code based on the time it takes for the sound released by the trig pin to hit the echo pin. For the constant in the about equation, (speed of sound) there needs to be two considerations. The first being, the speed of sound

which varies depending on the temperature and humidity The calculation for detecting an accurate distance that an object is from the buggy depends on the speed of sound, therefor the temperature and humidity needed to be accounted for to get accurate readings. Design A included a temperature sensor to provide accurate temperature values and the average humidity records for central Florida will provide accurate humidity values [o]. The buggy needed these values to be accurate when calculating the distance because the buggy will be running from the morning to the evening and the weather in Florida can drastically change. As a basis the speed of sound in dry air for 0 degrees Celsius is 331.3 meters per second [99]. From there, to calculate the speed of sound, the temperature (Tc) is multiplied by .606, which is the change in pressure per degree, and then added to the dry air at 0 Celsius get the correct value:

$$V(t) = v(0) + 0.61Tc \quad \text{m/s}$$
$$speed_{dry\ air} = 331.3 + 0.606 * Tc \quad \text{m/s}$$

However, there is still the need to account for the humidity. During the competition, the average humidity on the East coast in Central Florida at the end of November is between 30 to 40 percent [100]. The addition of humidity changes the value very slightly, but it will be important to keep the distance equation as accurate as possible to make up for any errors the sensors themselves might cause, especially since they were not fully protected by the outside environment. The final equation including H, the percentage of humidity, is the following:

$$speed_{humid\ air} = 331.3 + (0.606 * Tc) + (0.0124 * H) \quad \text{m/s}$$

This communication to the sensor was using the echo and trig pins on a serial/UART connection. The trig pin releases the sound wave and echo picks up the sound wave. This is manually done within the software, and the code was set based on an interrupt in the MSP430.

The infrared VL53L0X Time-of-Flight Distance Sensor, shown as part of the schematic in Figure 42, is also time based but uses infrared light instead of sound waves. The light that is emitted is reflected off an object and hits the receiver. This the VL53l0X the receiver is a Single Photon Avalanche Diodes (SPAD) array and detects the light coming back within the micro controller embedded in the chip, however exactly how this sensor calculated the distance is patented technology created by STMicroelectronics [101].

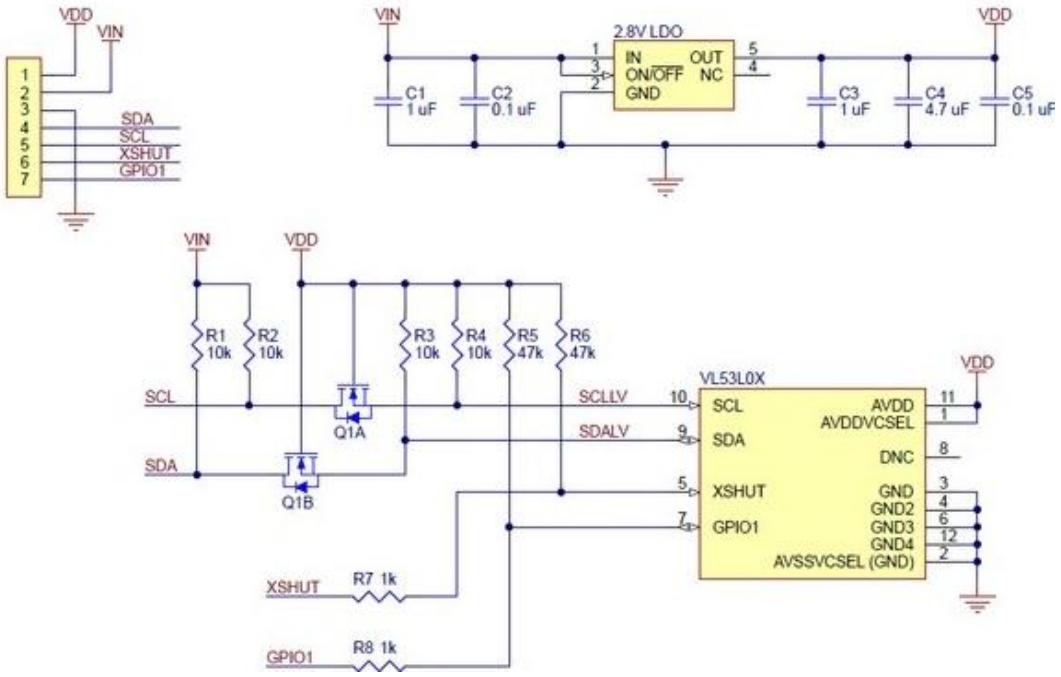

Figure 42. Schematic of the Pololu Chip Using the V153L0X ToF Sensor.

The VL53L0X ToF comes with an API to interface to get the distance that it is detecting. There is a simple to use Arduino library that interfaces with the sensor. This open source Arduino software was the basis of how the PCB will interface with the sensors API to get the distance and no calculations will need to be done. The communication will be done though and SDA and SCL pins with an I2C connection.

3.2.2.2 Layout Configuration – Olesya

There were two senor layout designs because the buggy was under a tight budget but still needed sensors to cover the full front of the frame while being accurate. Two designs where considered because the sensors fall under 10 dollars are not very reliable, therefore the first layout implemented is the lowest cost option and the second will be a backup option if the sensors did detect the objects within the range of 5 feet, and accurately detect them within 1.5 feet from the buggy. The two designs did not have a significant difference in power requirements, ~0.1 amps at most (swapping two infrared sensors for two ultrasonic sensors and a temperature sensor). Both sensors have the data pins run at 2.8 to 5 volts, so changing the sensors in the design would have been a simple swap.

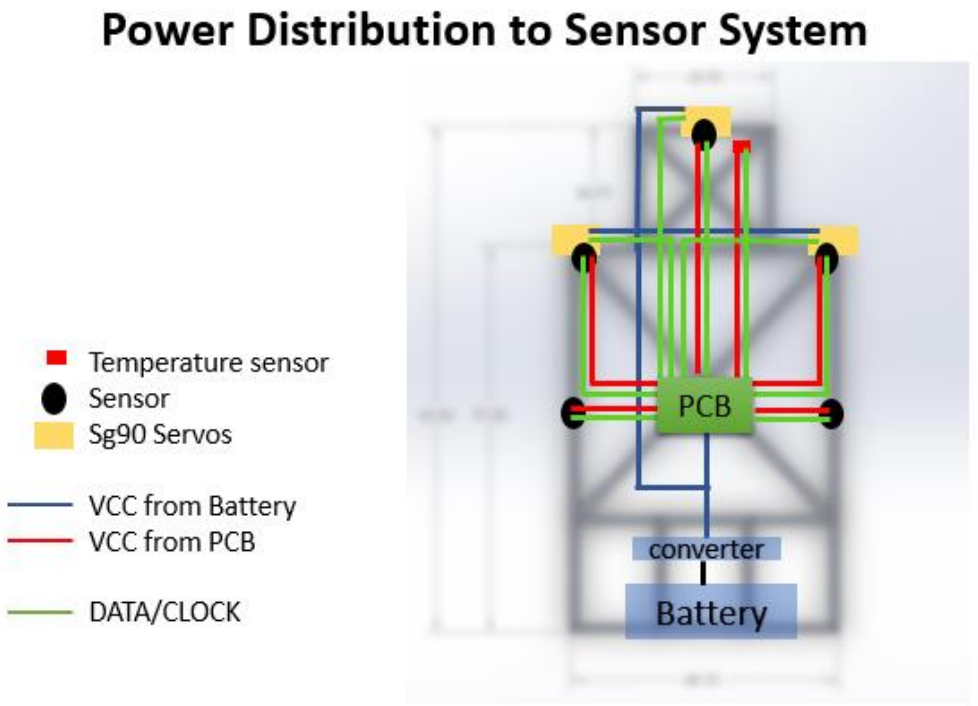

Figure 43. Wiring of the Sensors to the Printed Circuit Board or Buck Converter.

When designing the sensors and implementing the power and data pins with the PCB, there were several ways the system could be wired. The Printed Circuit Board however runs on 3 volts so there is a limit to how many components it can power. Since the sensors had 2 pins each not including the VCC of 5 volts and GND, it was more efficient to connect some components directly to the converter than to power all the sensors from the PCB. Looking at the final processor and layout decisions for the PCB, there was a pin that outputs 5 volts for peripherals. Therefore, the sensors can have all wires connected directly to the PCB. On the other hand, the servos require 5V or more, so it was best to put them on the main power line, as well as the fact that they pulled a lot more amps than the PCB and sensors. The servos were then connected to the 5V output coming from the converter and were controlled by one pin from the PCB. The temperature sensor was also be connected to the PCB for the VCC connection and the data pins. Note that the Raspberry Pi(s) are not shown in the diagram below but they were still within the Buggy's design. Figure 43 above shows the main connections between all the sensors and the PCB.

Design A: This design was the lowest cost design and had a incorporated temperature sensor to be able to calculate the distance more accurately. The total design consisted of the following components in Table 21 and come out to a total of $24.73.

Table 21. List of Components Used in Design A for the Sensor Layout.

Quantity	Part	Pins	Operating Voltage	Communication	Total Cost
4	HC SR-04 Ultrasonic	1 Trig, 5v 1 Echo, 5v	5 v	Serial /UART	$3.78

	Distance Sensor				
1	VL53L0X Time-of-Flight Distance Sensor	1 SDA I2C data pin, 2.8-5v 1 SCL, I2C clock pin, 2.8-5v 1 GPIO indicator, 2.8 v-5 v	5 v	I2C	$9.95
3	Tower Pro Micro Servo 9g SG90		5 v		$6.05
1	MCP9808 High Accuracy I2C Temperature Sensor	1 SDA I2C data pin, 2.8-5v 1 SCL, I2C clock pin, 2.8-5v	5v	I2C	$4.95
Total					**$24.73**

The following Figure 44 is a diagram of how the above list of components were attached to the buggy frame with the coverage from the rotating sensors. This diagram also includes the temperature sensor with the front most center sensor. This sensor was selected to be an infrared sensor because it is more accurate than the SR 04 sensors. This layout uses two SR 04 sensors on the side to detect if an object is a certain distance to the buggy before any turns are executed by the navigation system.

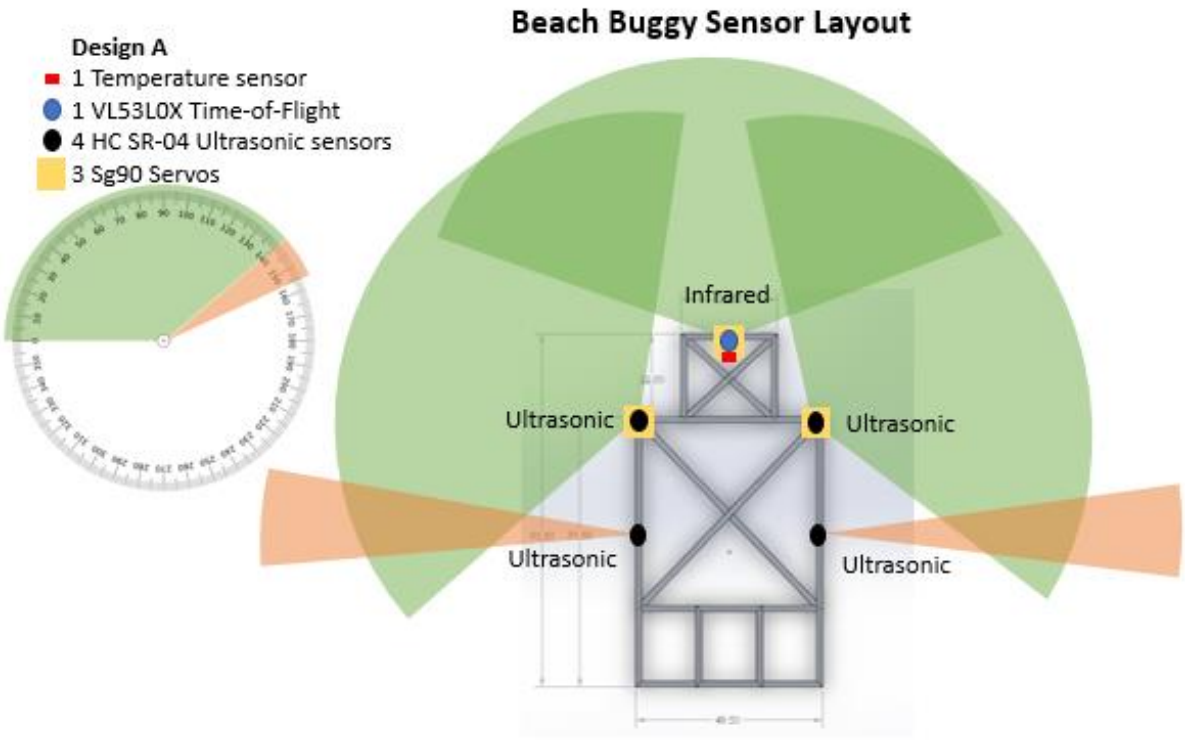

Figure 44. Sensor Layout Using HC SR04 Sensors and a Temperature Sensor.

Design B: This design was the backup design to the above design in case the SR-4 did not perform well in the beach environment. The following design will consist of the following components in Table 22.

Table 22. List of Components Used in Design B for the Sensor Layout.

Quantity	Part	Pins	Operating Voltage	Communication	Total Cost
2	HC SR-04 Ultrasonic Distance Sensor	1 Trig, 5v 1 Echo, 5v	5 v	Serial /UART	$1.29
3	VL53L0X Time-of-Flight Distance Sensor	1 SDA I2C data pin, 2.8-5v 1 SCL, I2C clock pin, 2.8-5v 1 GPIO indicator, 2.8 v-5 v	5 v	I2C	$29.85
3	Tower Pro SG Servos		5 v		$6.05
Total					**$37.19**

The following Figure 45 is a diagram of how the above list of components were attached to the buggy frame with the coverage from the rotating sensors. This diagram does not include the temperature sensors because the infrared sensors are more accurate than the SR 04. This layout uses two SR 04 sensors on the side to detect if an object is a certain distance from the buggy before any turns.

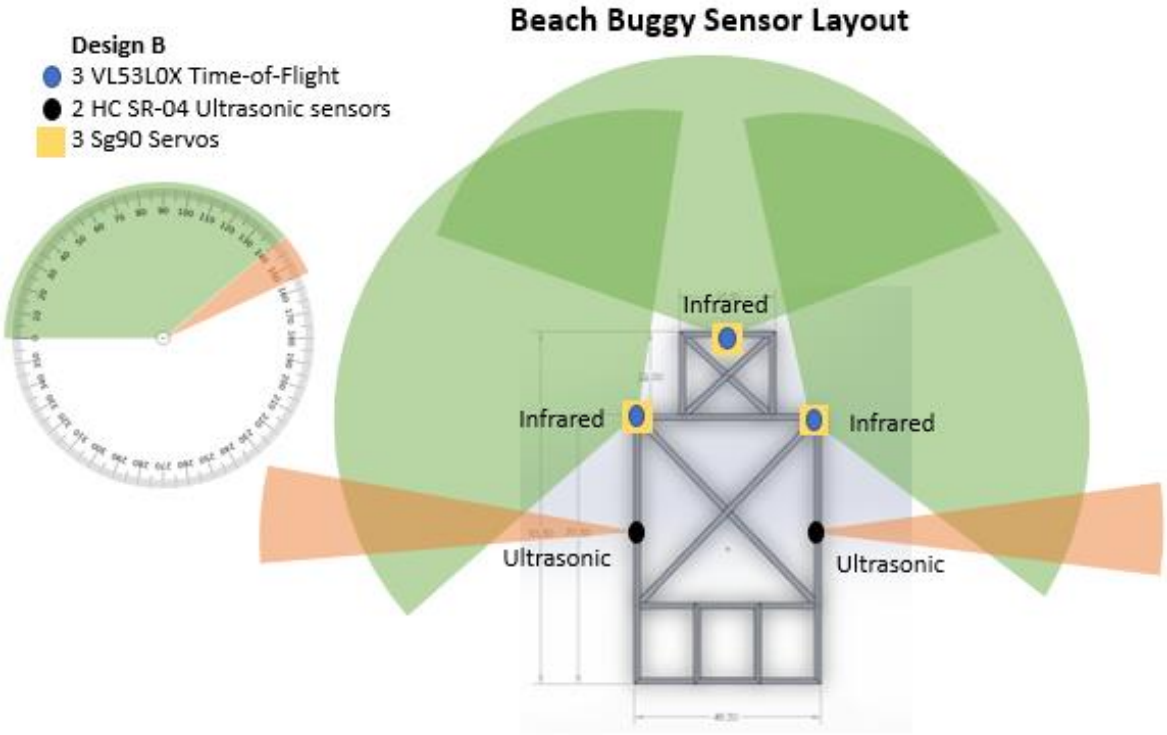

Figure 45. Sensor Layout Using VL53L0X Time-of-Flight Distance Sensor.

These sensors were mounted to the frame about one fourth of the way up the frame. They needed to stay in the lower part of the buggy because any obstacle on the beach has a greater chance of being identified there. For example, a beach ball, debris washed up on shore or even things like animals, humans, or signs/poles. Placing the sensors any further up the frame would have caused the navigation system to miss an obstacle in the way of the buggy. The temperature sensor was placed with the front most sensor to make sure that it's sensing the temperature of the surrounding area of the buggy, not within the buggy or near the motor. The side sensors were not rotating because of the budget and the purpose of just needing to be rear collision detection sensors. They were implemented on the sides to support any turns from the navigation system created by the CS team because their camera system had a front view only and did not capture the sides of the buggy. The information gathered from these sensors were sent separately.

Mounting the sensors at an angle to face downward was considered to create better chance of detecting objects within 6 feet of the buggy. However, with the rotations that the sensors were undergoing, and the frame constrains, it was not worth the effort to angle the sensors. The angle would then have thrown off the rotation and the data would

have been hard to normalize. The sensors stayed level with the ground and had their range cut off after 6 feet to 10 feet from the buggy.

3.2.2.3 Mounts – Olesya

In the layout, three of the sensors were rotating on servos as shown above in both Figure 44 and Figure 45, with 140-degree range of area scan each. This gave the sensors a good enough field of view, while at the same time staying within the servo limit of 180-degrees. Capturing any more data would have been be out of the scope for this project's needs and would have limited how fast a scan can be done. Another problem that was considered would be overlapping areas. At 140 degrees, the front left and front right sensors overlap the front most center sensor. The front sensor can be adjusted and lowered to a smaller angle in case stitching the data and configuring the sensors became too difficult once the design was implemented and tested. The exact rotation of the sensors was implemented in software as well as the size of the gear set attached to the servo. The input gear (attached to the servo) was smaller and the output gear (attached to the sensor) was bigger, providing the system with more control over the load attached the small servo. Figure 46 shows the mounts created for each sensor with the gear set. The sensors and servos were placed in this mount and drilled to the frame of the solar powered beach buggy.

The mounts were 3D printed for the solar powered beach buggy. This was because the way that the sensors were rotating were specific to the buggy, and which were to cover an angle of view specific to the buggy's frame. The options for 3D printing fell into the budget left over for the sensors. Depending on the access to printers, the materials varied. The two basic materials for 3D printing PLA and ABS. For the buggy's application, the plastic needed to be durable and strong. Therefore, the PLA filament was used to print the mounts.

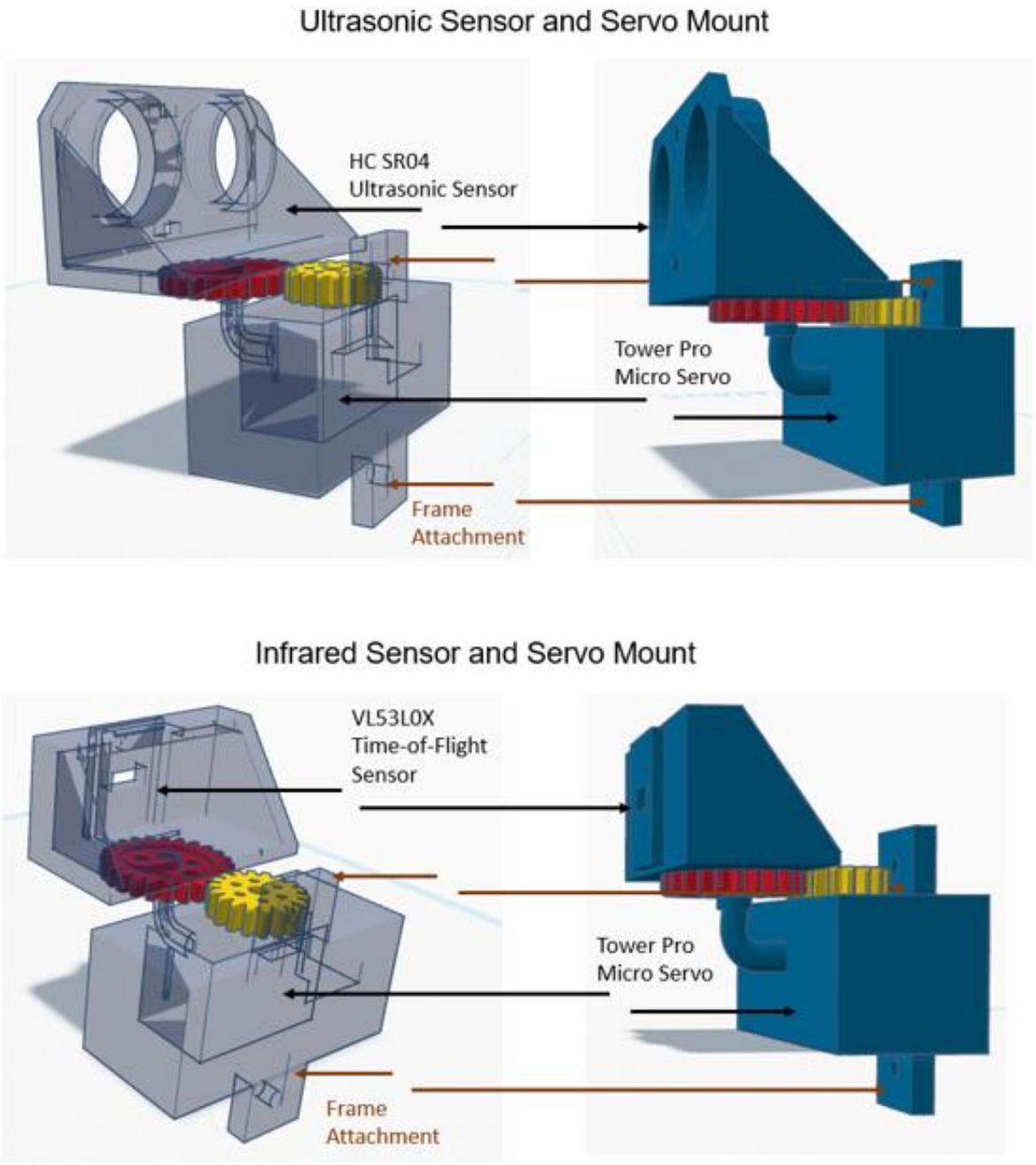

Figure 46. Sensor Mounts for Rotating Sensor Configuration.

3.2.3 PCB Layout – Patrick

The initial design of using the MSP430FR4133 processor and board was changed to be based off the MSP430FR5529. This was done as to solve program size concerns as the MSP4304133 has a much smaller memory than the MSP430FR5529. As the base of the main control unit there was the need for certain changes to integrate it with the other parts of the system. This section will discuss the need and method for accommodating those changes.

3.2.3.1 PCB Design Base – Patrick

The design base for the MSP430FR5529 board can be found on the Texas instruments website and will be used as the base design for this project. This design will be modified to better fit this project and its requirements.

The first major modification from the base schematic was the removal of the on-board emulator. The MSP430 line of microcontrollers come with an on-board emulator that is used to both program and debug the board. Since the final design is not going to include this emulator the base board that will be used for prototyping will be used to program and debug the MCU. The standard board come with jumper ports that are designed for connecting the emulator portion of the board to a separate board for programming purposes.
By doing this it is possible to streamline the actual MCU while still maintaining the benefit that the emulator provides. This helps to reduce the cost of the microcontroller without a loss in functionality. To use the emulator to program the microcontroller it was necessary to keep the jumper portion of the emulator, which will be the only thing that is present from that portion of the board.

3.2.3.2 Inputs/Outputs – Patrick

Based on the design of the buggy the Main Control Unit (MCU) will need to be able to handle a certain number of inputs and outputs to other parts of the complete system. The MCU will need to be able to communicate with the navigation board which will be done using the SPI communication protocol. It will need to be able to create signals to send to the motor controller which can be done in a combination of analog signals and digital signals using PWM. It will need to be able to get feedback from the motors and wheels in the form of an encoder on the front steering motor and a custom speedometer on the back wheel. The microcontroller will need to be able to process the information for the speedometer.

It will need to communicate with all of the sensors, which requires both sending signals to start reading and receiving the information that the sensor finds. The sensors that were chosen also require calculations to be done to determine the distance it is detecting. This will need to be done by the MCU before it is transmitted to the navigation board. The emergency stop and the start button will both be handled by the microcontroller, along with the servos that will be rotating the sensors. The required pins are summarized in Table 23 below.

Table 23. Necessary Inputs and Outputs.

1	Speedometer	16	Sensor 1.1
2	Encoder	17	Sensor 1.2
3	Encoder	18	Sensor 2.1
4	Encoder	19	Sensor 2.2

5	Servo 1	20	Sensor 3.1
6	Servo 2	21	Sensor 3.2
7	Servo 3	22	Sensor 4.1
8	Wi-Fi RX	23	Sensor 4.2
9	Wi-Fi TX	24	SPI 1
10	Emergency Stop	25	SPI 2
11	Start	26	SPI 3
12	Motor Controller(MC) 1.1	27	SPI 4
13	MC 1.2	28	GPS RX
14	MC 2.1	29	GPS TX
15	MC 2.2	30	

3.2.3.3 Design Decisions – Patrick

One of the main influences on the design decisions was which board to base the design off of and what processor that board would use. Since this project was using the MSP430 family of processors and boards these decisions were closely tied together. The first processor and board that was considered was the MSP430G2, which had the main issue of offering a limited number of pins that could be used. The number of pins required by this project exceeded the number that was offered by the MSP430G2, so options to reduce the needed pins were explored [58].

A possible solution is to use the I2C protocol to have multiple devices share a pin. To do this it would be required implement I2C hardware, either making custom hardware or adding a circuit to handle the heavy lifting. It was determined creating a custom version of the hardware was to time intensive for the time line of this project. The alternative was to use an I2C bus created by Texas Instruments and integrate it into the design of the MCU. This bus would handle all the hardware necessary to use the I2C protocol and allow for multiple devices on a single pin.

This would greatly reduce the number of pins needed but would require that the devices that are connected to it to be I2C compatible. The chosen I/O expander was the TCA6416A [102].

While this helped to decrease the number of pins necessary to implement the design, cutting the ten pins for the sensors down to three, this still did not reduce the number of pins required below the number of pins provided by the base MSP430G2 [58]. Another measure to reduce the number of pins required on the processor was to connect all the servo control wires onto a single pin. This would allow all the servos to share a pin and be controlled together. The down side to this approach was that it would be impossible to rotate each of the sensors individually. However, since there was no case in the design where this would be necessary, this limitation does not hinder the operation of the buggy, so this downside was deemed irrelevant. The benefit of this measure was instead of needing three separate pins, one for each servo control, only one pin would be needed.

Another component that required multiple pins was the motor controller. The dual channel motor controller that was being used has many different control settings that can be used, and which setting is used can change the number of pins it would require. The two modes that were considered is either completely analog or both analog and digital. The obvious benefit to using only analog was that it would require fewer numbers of pins. The benefit to using both is that it gives the ability for greater control and feedback from the motor controller.

Using only analog, it is only possible to know the speed that the motor is turning. Motor direction is based on the voltage above or below a certain threshold. If a slightly mismatched voltage signal is sent to the motor driver, this can lead to an extreme case where the buggy thinks that is moving forward when in fact it is moving backwards. It was for this reason that using both was worth the extra pins necessary. Additionally, the selected motor controller uses grove connections that use 4 pins. As two of these pins can be connected elsewhere, the NC and GND pins, Only the AN1, AN2, IN1 and IN2 will be connected to the board to limit the number of pins used.

With these improvements this left a required 22 GPIO pins for the design with only 16 being able to be supported by the base processor. This lead to the decision that a processor with a larger number of GPIO pins would be required. Because of the familiarity and support of using the MSP430 family line of products was desired it was decided to use another MSP430 processor that allowed for more pins.

There were two main processors under consideration: the MSP430G2533I and the MSP430FR5529. These two processors compare similarly in terms of price and features. As they are both part of the MSP430 family, they are low power and supported by both Texas Instruments emulators and Code Composer Studio IDE. Their main difference that this project is concerned about is the number of GPIO pins. The MSP430G2533I provides 24 GPIO pins while the MSP430FR5529 provides 60 GPIO pins [58] [59]. Since number of pins was the main concern, and the processors were similar in terms of price, it was determined that the MSP430FR5529 would be used for this project.

An additional modification that had to be made was the addition to the board of a Wi-Fi module for debugging and control purposes. This module would allow for a computer to be connected to the device during testing to do troubleshooting during operation. This module would also be able to send a stop command for safety when testing the prototype and during development. The module would not need to have a high data transfer rate since it would only be necessary to transfer log data of inputs and outputs.

With this addition it was found to be unnecessary to have an onboard LCD that would serve a similar function while increasing the cost of manufacturing. The cost of the PCB is closely tied to the size and LCD screens take up a lot of space. Additionally, since this would be only used for debugging it would be difficult to access during operation to take readings, along with outdoor operation making it difficult to read. For this reason, the LCD screen on the base schematic was removed, this combined with the removal of the board emulator greatly reduced the size of the processor and therefore the cost.

3.2.3.4 Sensor Interfacing – Patrick

The SR04 sensors that will be used as proximity sensors for the buggy were designed to be used with a 5V system. This poses a problem as the MSP430FR5529 operates at 3.3V which will not be sufficient to power or interface with the SR04 sensors. To be able to uses these sensors it will be necessary to step up the output signal of the MSP430FR5529 and to step down the input signal from the SR04. Additionally, the VCC signal of the MSP430FR5529 will not be able to power the sensors so a 5V signal must be provided.

For the VCC signal to the SR04 sensors it will be possible to make use of the 5V signal that is being used to power the MSP430FR133. As previously discussed it was needed for the MSP430FR5529 to be powered by a 5V signal so a step-down circuit was created. Since there is already a 5V signal available on the board it will be a simple matter of routing this signal to the VCC pins of the SR04 sensor. Likewise, the GND signal of the SR04 can be connected to the ground of the MSP430FR4113 as both the 3.3V signal and the 5V signals will share a ground.

For stepping down the ECHO signal of the SR04 for the MSP430 this can be accomplished by simply using a voltage divider circuit to scale the signal down to 3.3V that will be useable by the MSP430FR5529. Below in Figure 47 is the schematic of such circuit. In addition to adding the voltage divider an LED was added to help in debugging the system after construction. This LED will display and traffic along the line to help test if the sensor is sending any information back or if there is an issue with the processor or the code.

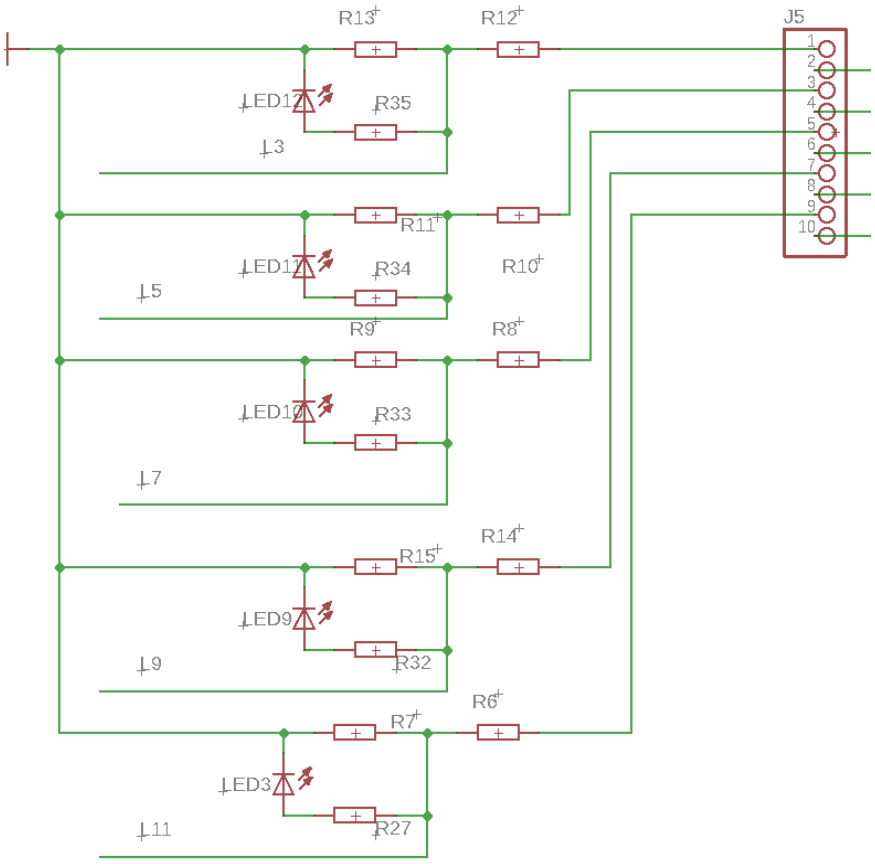

Figure 47. Interface between the MSP430 and SR04 ECHO.

For increasing the TRIG signal from the MSP430FR5529 to the SR04 it will be necessary to use a transistor circuit along with a 5V signal. As previously mentioned there was already a 5V signal available on the Main Control Unit which greatly simplifies the construction of this circuit. A transistor circuit was added that would which will allow the signal to be increased from 3.3V to 5V but would also invert the signal. Below in Figure 48 is a schematic for one such circuit, which can be seen has also had a LED added to allow for easy debugging of the system. As one of the major concerns was being able to trigger the SR04 sensor with the MSP430FR5529 this will help greatly to distinguish between a problem with the sensor and a problem with the board itself.

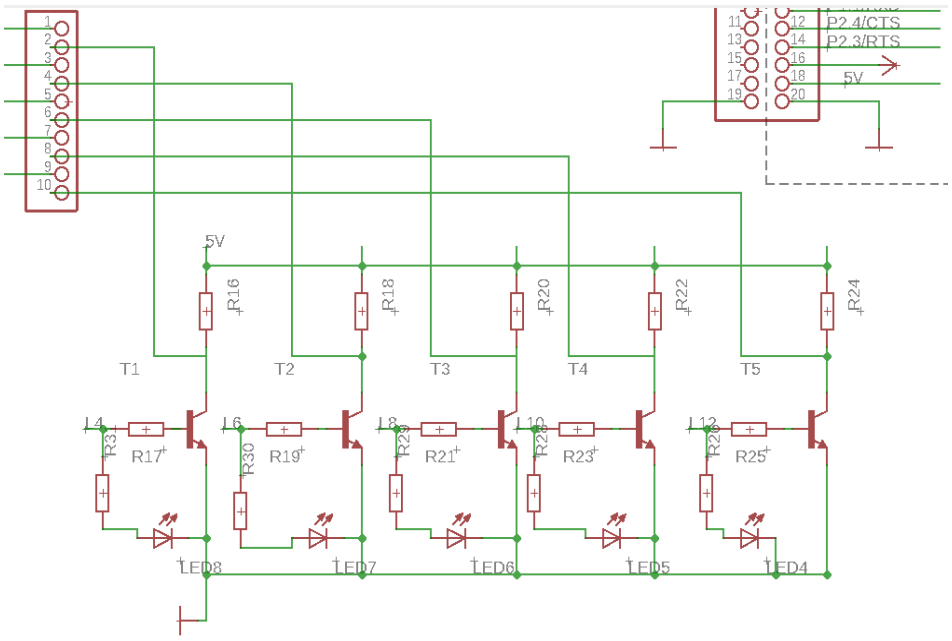

Figure 48. Interface between the MSP430 and SR04 TRIG.

Below in Figure 49 is the final board layout for the sensor interface, which shows the layout of both the ECHO, TRIG, and added LEDs for the connecting the main control unit to the sensors.

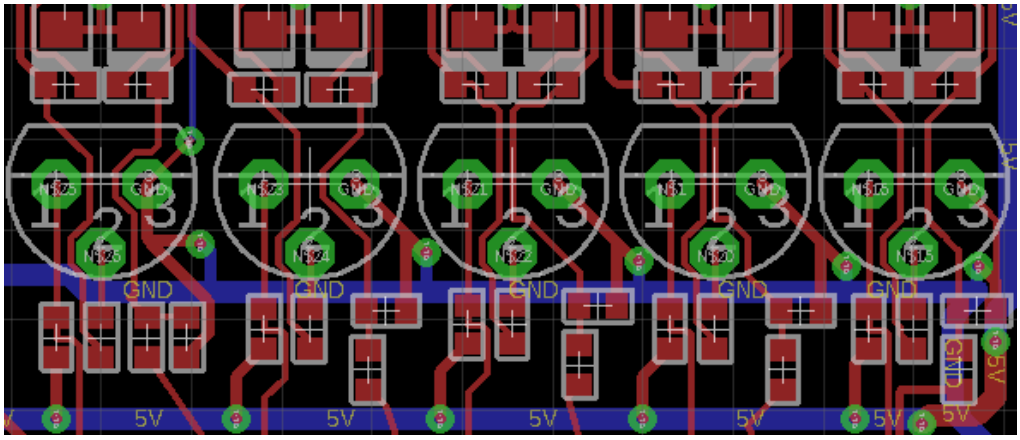

Figure 49. Sensor Interface Board Layout.

3.2.3.5 WI-FI Module – Patrick

Another needed addition to the main control unit was a Wi-Fi module for debugging purposes. This module would allow the MCU to expose data points to a connected computer for the programmer to be able to understand what is going on. The Wi-Fi module that was selected was the XBEE. This module requires a UART connection to receive and transfer data. The MSP430FR5529 provides UART ports that can be used to communicate with the XBEE and the built-in libraries can be used to manage these connections.

The XBEE also requires to be programmed before it can be used, this can be done by connecting it to a XBEE explorer that will provide a connection to a computer from programming. Another solution to this is adding the necessary connection to the main control unit which would allow for the XBEE to not require to be removed to be reprogrammed. To do this one of the XBEE explorer boards were used as a base to add to the main control unit.

The XBEE uses a 20-pin socket to connect to a, which will be added to the main control unit. Of these pins the UART connections on the XBEE (2, 3, 12, 16) will be connected to the UART pins of the MSP430FR5529 (P1.0, P1.1, P1.2, P1.3). The XBEE also requires a VCC and GND connection which will be connected to the MSP430FR5529 3.3V VCC pins. Along with this pin connections are exposed to allow for the XBEE to be connected to a computer and programmed. Below in Figure 50 is the board layout and in Figure 51 is the schematic for the XBEE after integration with the main control unit.

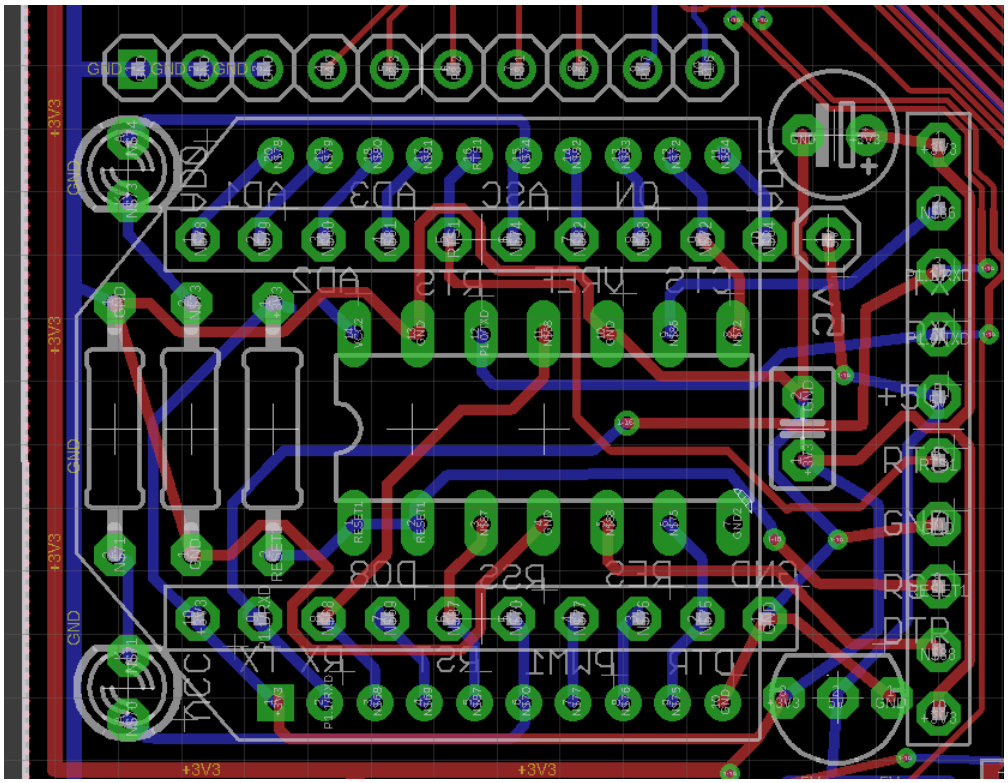

Figure 50. XBEE Explorer Board Layout after MCU Integration.

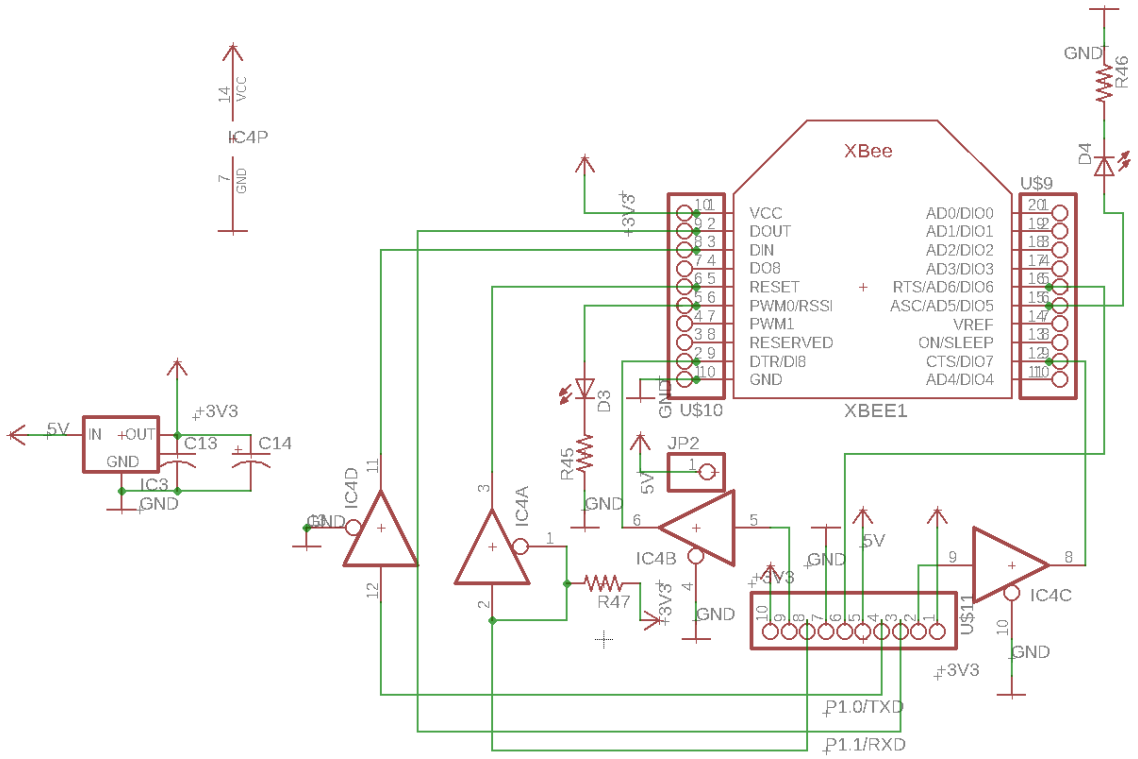

Figure 51. XBEE Explorer Schematic.

3.2.3.6 Motor Controller – Patrick

The connection to the motor controller requires both an analog signal and a pulse width modulation (PWM) signal for each motor. The analog is on a scale of 0V to 5V, while the PWM will accept between 1.3V and 5V. The PWM signal is controlled by its duty cycle such that the 3.3V output of the MSP430FR5529 will be sufficient for generating that. The analog is controlled by its output such that it will be necessary to step up the voltage to be able to have the full range of control offered by the motor controller. To do this a step-up circuit similar to the one crated for the sensors was used. The MSP430FR5529 does not provide any hardware support for creating a PWM signal so that this will have to be done using software. For this reason, any of the GPIO pins of the MSP430FR5529 will be useable for this connection. Below in Figure 52 is the board layout and in Figure 53 is the schematic for the motor controller interface.

3.2.3.7 Charge Controller – Patrick

The charge controller requires a single pin to be connected to be able to receive information from it. The charge controller sends a packet along this pin that contains information about the status of the charge controller. It will be necessary to implanted code to be able to unpack and read this information so that it can be sent to the Wi-Fi module when attempting to debug and test the system. This connection can be seen as part of the servo and encoder schematic listed in the below section.

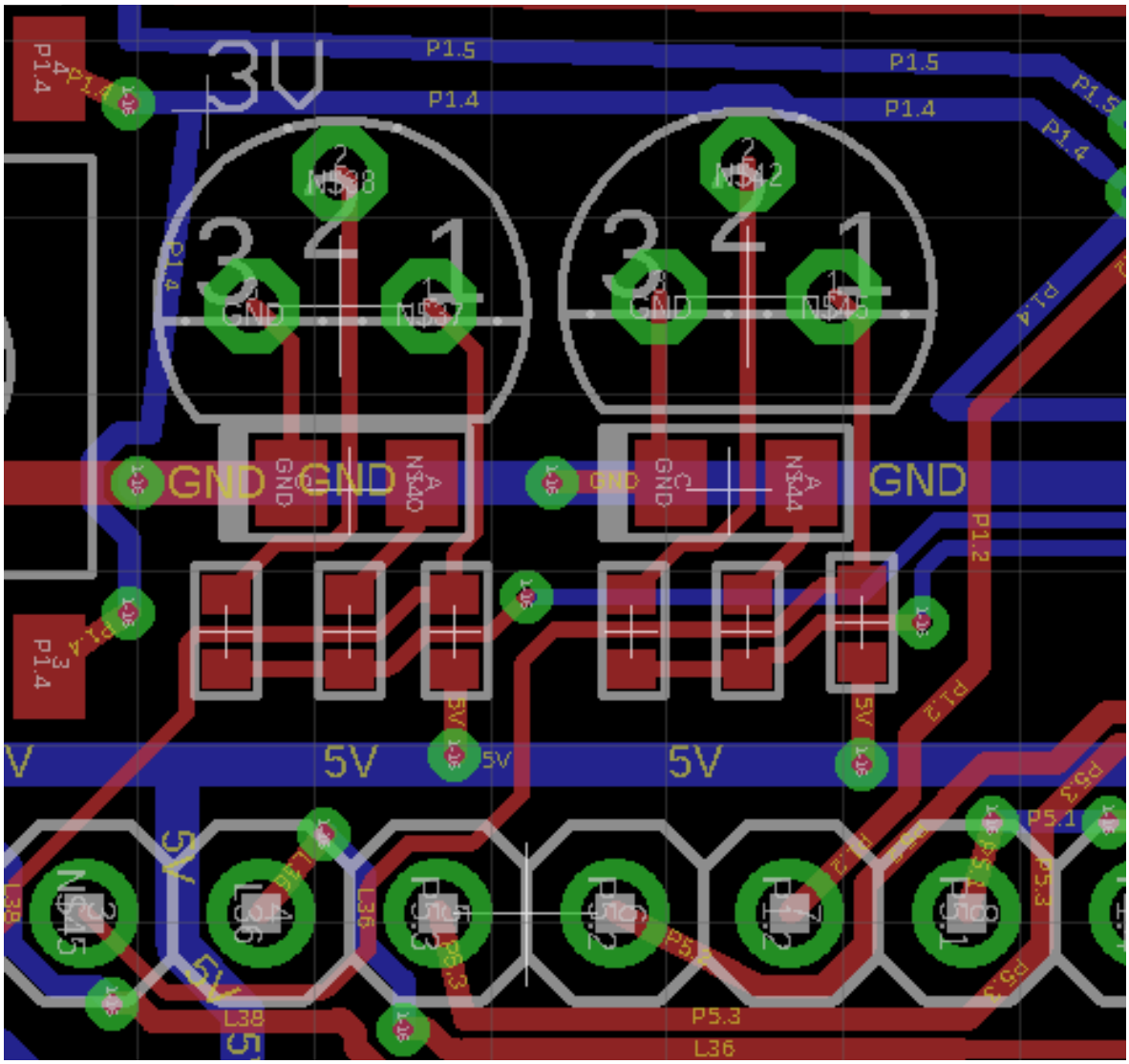

Figure 52. Motor Controller Step-Up Circuits Board Layout.

3.2.3.8 Servos, Encoder, and Speedometer – Patrick

The servos require a 5V control pin, along with a 5V VCC connection and GND connection. The VCC connection and GND connection will be handled outside of the main control unit so all that will be required for the MCU will be the control pin. To connect this control pin to the MSP430FR5529 the output of the MSP430FR5529 will need to be stepped up from 3.3V to 5V. This can be done once again with the same circuit used by the sensors that will step up and invert the signal from the MSP430. Since there is no requirement for the servos to ever be at a different position from one another it is possible for all of them to share one GPIO pin on the MSP430FR5529.

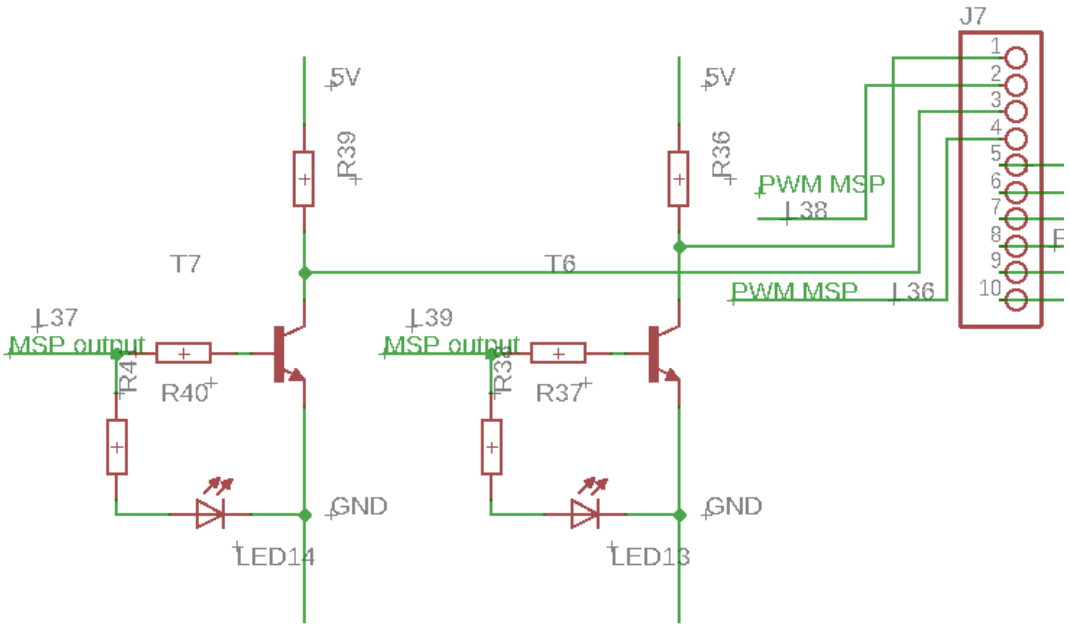

Figure 53. Motor Controller Step-Up Circuits Schematic.

The Avago AEAT-6010 encoder requires 5 pins for operation. It requires both a 5V VCC pin and a GND pin which can easily be supplied by the microcontroller. It has 2 control pins of CSn (chip select) and CLK (clock), with one output pin of DO (digital output). All of these are digital signals so that they can be controlled by the MSP430FR5529 GPIO pins. They all also operate on the range of 0-5V, so it will be necessary to add step up circuits to the CSn and CLK connections and a stepdown voltage to the DO. These will be identical circuits to the one previously used to the same end.

The speedometer is made by using a reed switch and magnets to calculate the speed form the rotation of the wheel. For this reason, it is possible to use almost any voltage for powering it, which will be the same voltage that is used to receive input from it. 3.3V was selected to power the reed switch so that it would be directly compatible with the MSP430FR5529, which will be used to calculate the speed. Thus, all that is required to connect the speedometer is a GPIO pin directly off of the processor. Below in Figure 55 is the schematic and in Figure 56 is the board layout for the connections to the servos, encoder, and speedometer.

3.2.3.9 Start and Emergency Stop – Patrick

The start button and emergency stop button will both be controlled through the MSP430FR5529. These will be simple switches that send a high signal when they are pressed. This will be all that is required so these buttons can hook directly into the MSP430FR5529. Additionally, buttons on the MCU will also be able to trigger these actions for easy testing and an additional backup system. Below in Figure 56 is the board layout for these buttons and connections. Within it can also be seen the LED's from the original board that were kept to be used for debugging purposes if needed.

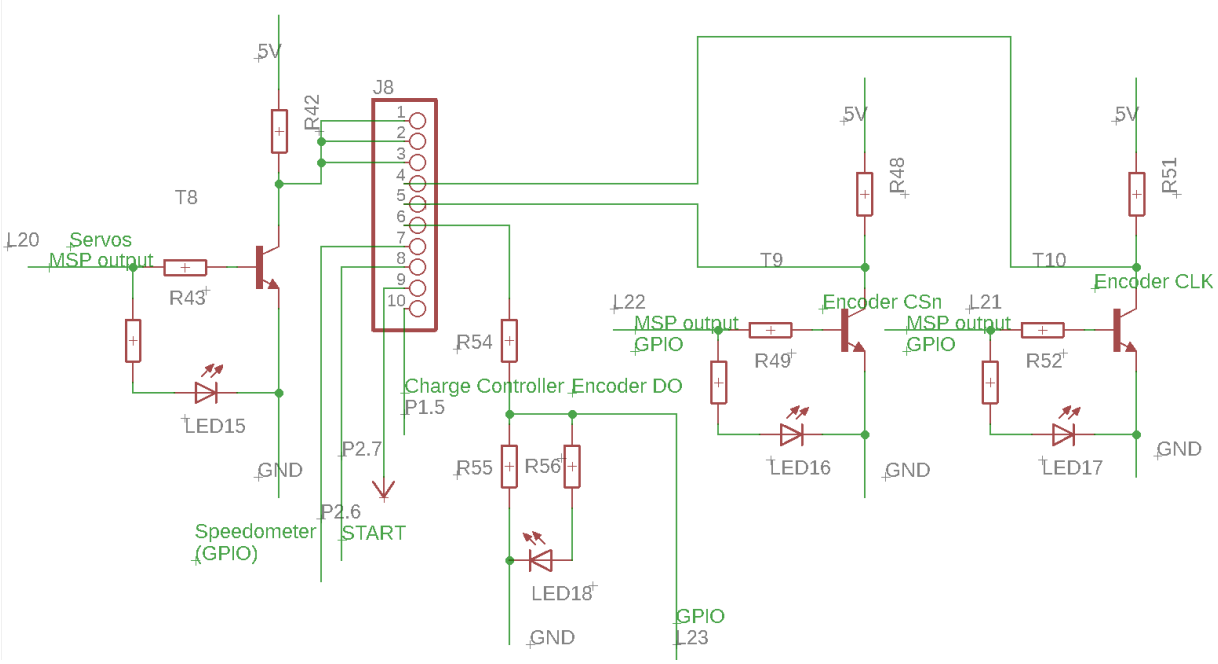

Figure 54. Sensor, Encoder, and Speedometer Interface Schematic.

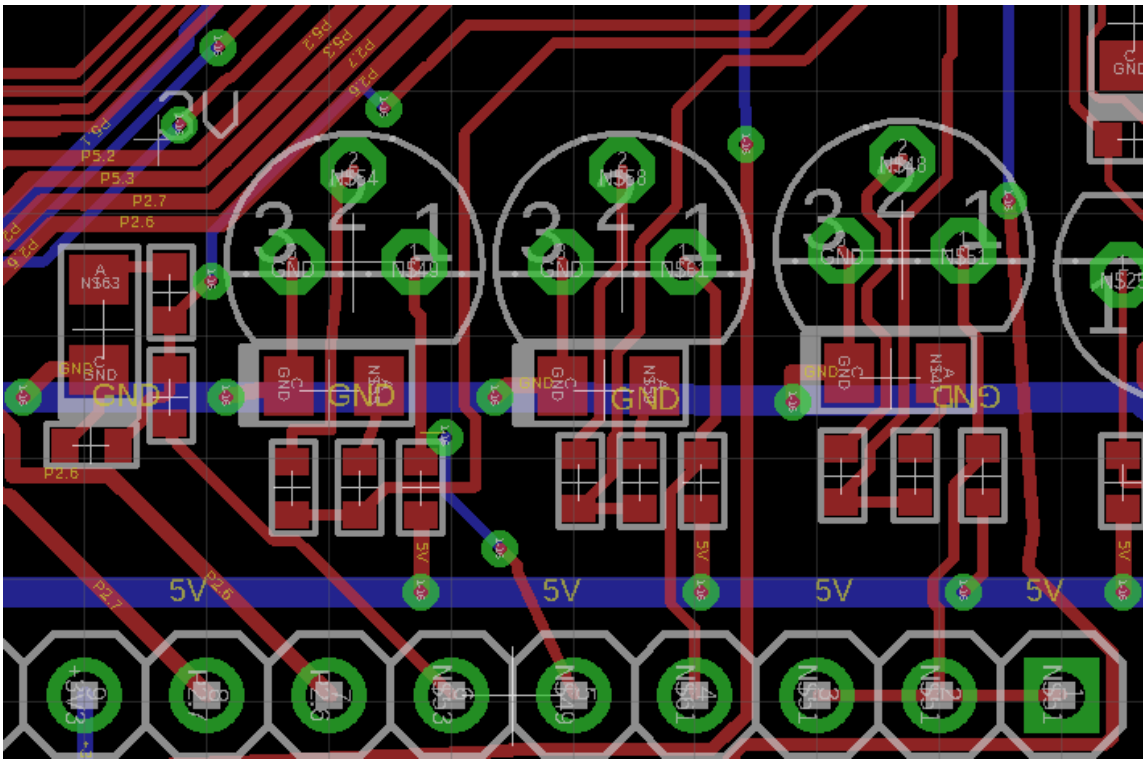

Figure 55. Sensor, Encoder, and Speedometer Interface Board Layout.

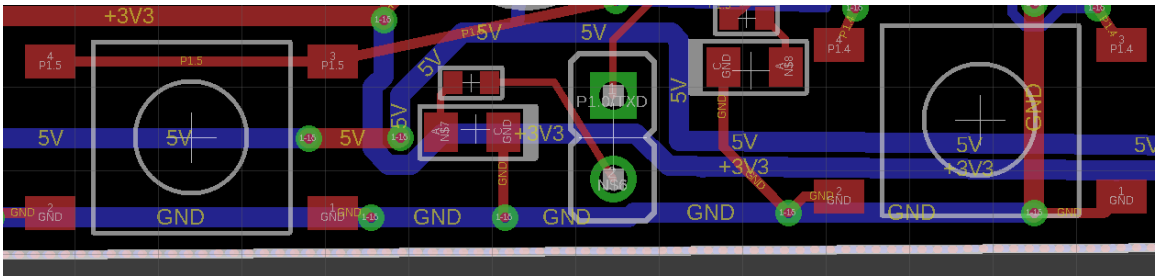

Figure 56. Start and Emergency Stop on Board Buttons Layout.

3.2.3.10 Communication with the Navigation boards – Patrick

To communicate with the Raspberry Pi's that will be doing the main navigation a SPI connection will be used. As previously stated, the MSP430FR5529 provides internal hardware support for SPI communication so to accomplish this all that much be done is providing an access point to connect these pins to the Raspberry PIs. The SPI protocol only allows for one master on each system, so it was decided that the MSP430FR5529 would be the master controller as it will be using SPI to connect to other parts while the Raspberry PIs will not. To do this SPI requires a slave select pin to determine when each slave can send or receive which need its own pin connection to the processor. This can be any of the GPIO pins on the MSP430FR5529. Below in Figure 57 is a schematic for these pin connections and in Table 24 is a chart of the pins required and their connection to the MSP430FR5529 processor. The final board layout can be seen in Figure 58 which shows the final design with all parts routed.

In Senior Design 2 the sensors were regulated to their own board for simplicity of implementation. Additionally the GPS removed and a GPS module was purchased due to last minute changes that had to be made.

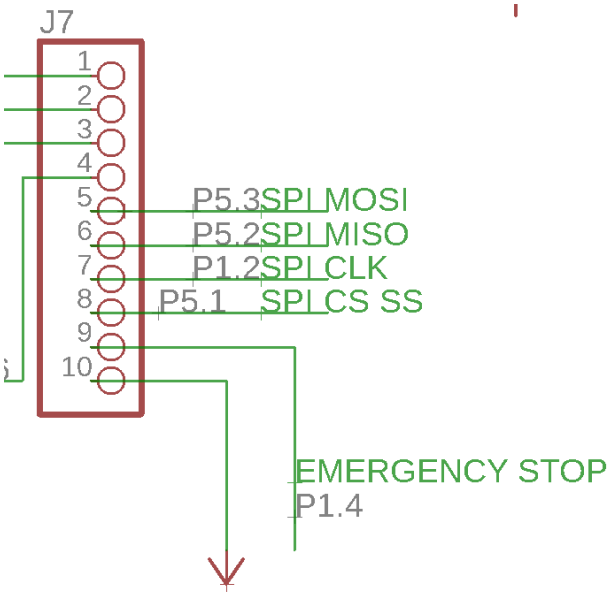

Figure 57. Raspberry Pi Pin Connections and Schematic.

Table 24. Pin Chart for PCB.

Planned		I/O
GPS RX	P7.1	
GPS TX	P7.2	
US Sensor 1 ECHO	P7.3	
US Sensor 1 TRIG	P7.4	
US Sensor 2 ECHO	P7.5	
US Sensor 2 TRIG	P7.6	
US Sensor 3 ECHO	P7.7	
US Sensor 3 TRIG	P3.0	
US Sensor 4 ECHO	P3.1	
US Sensor 4 TRIG	P3.2	
IR Sensor 1 ECHO	P3.3	
IR Sensor 1 TRIG	P3.4	
Motor 1 PWM	P5.7	
Motor 1 ANA	P5.6	
Motor 2 PWM	P5.5	
Motor 2 ANA	P5.4	
SPI MOSI	P5.3	
SPI MISO	P5.2	
SPI CLK	P1.2	
SPI CS SS	P5.1	
Emergency STOP	P1.4	
Emergency Stop PWR	VCC	
Start	P2.7	
Start PWR	VCC	
Servo Control	P6.4	
Speedometer	P2.6	
Charge Controller	P1.5	
Encoder DO	P6.7	
Encoder CSN	P6.6	
Encoder CLK	P6.5	
XBEE RX	P1.0	
XBEE TX	P1.1	

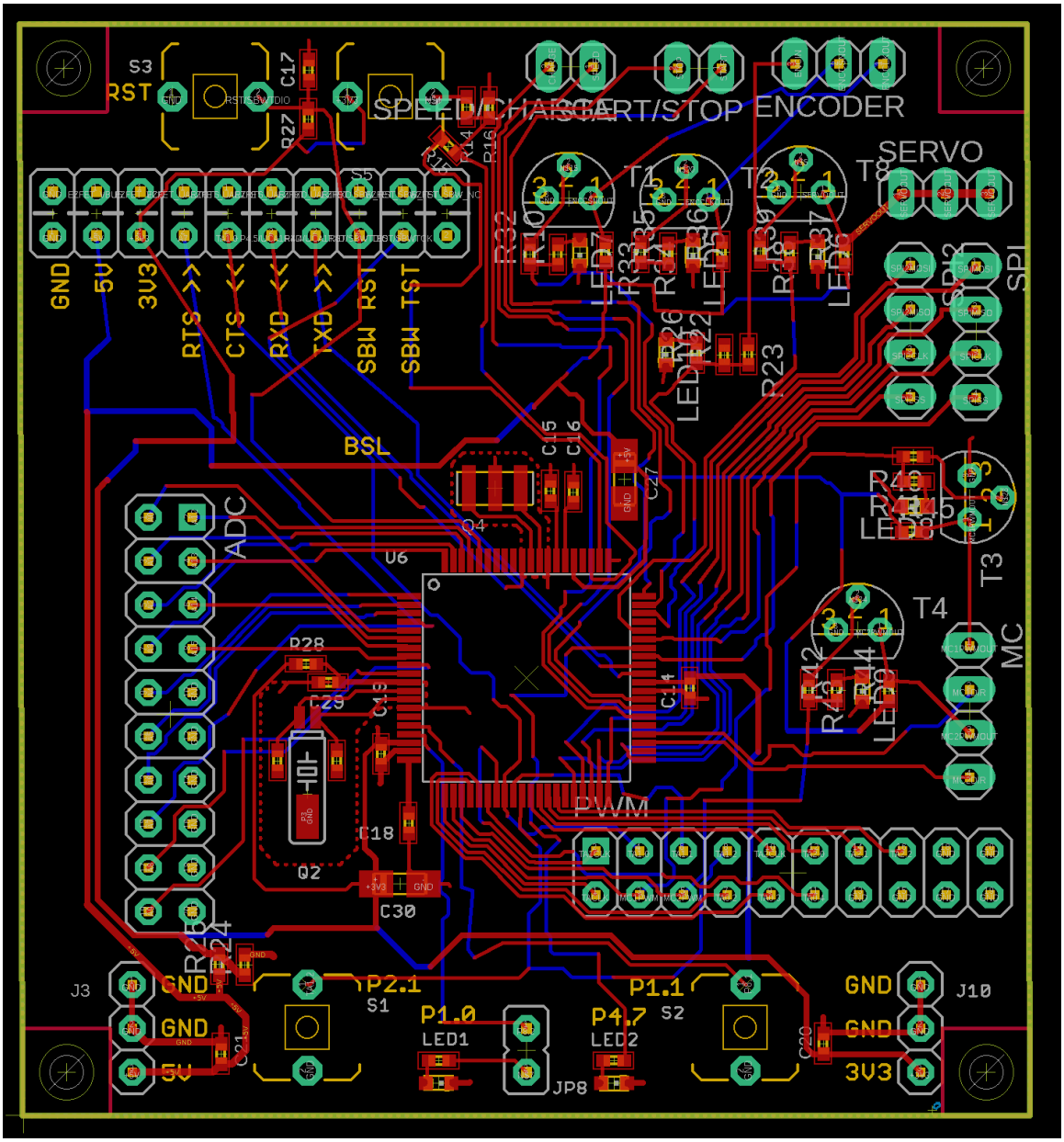

Figure 58. Final Board Layout.

3.2.4 PCB software – Olesya

PCB software can be written in C programming language for many reasons including particular processor, like the MSP430 series or the Arduino ATMega. Programming in C will also allow the team to use helpful open source libraries to interact to the sensors and servos that are written in C. The libraries allow the PCB software to interact with the sensors without re-inventing the wheel and allow the PCB software to interact with the Infrared sensor that has an API for its proprietary software.

Throughout building and testing, the software was written in Code Composer Studio using many of the features for debugging. This IDE included the property libraries for the

MSP 430 5529, and the code was configured to the specific microprocessor as shown in Figure 58, which was the first steps to program and test the PCB. Since the PCB did not have the eZ-FET on-board emulator, the code was uploaded using a MSP430 LaunchPad and jumped directly to the corresponding pins on the PCB board, that way there was a computer interface for debugging and programming. It was a simple step to connect the isolation jumper block connection to the microprocessor on the PCB instead of the processor on the LaunchPad. The IDE set up for the microprocessor that was used in the PCB, the MSP430 FR4133LP as shown in Figure 59 on the left. From there, libraries could be added and included into the code directly shown on the right.

Another factor in the PCB software was how much memory (FRAM) the processor had and how much code the PCB would store. The MSP430 FR4133LP has 16KB of non-volatile memory, of which 15KB was available to code memory [103] within FFFFh-FF80h and FFFFh-C400h memory addresses. On the other Hand, the MSP 430 FR5529 had 128KB available, which was within the scope of the project software requirements for the MCU.

Another key feature of Code Composer along with the chosen processor, the MSP 430 5529, was the option to use Texas Instrument's Real Time Operating System. Code Composer Studio's hardware support and extensive debugging tools that allowed tracking of flash memory that stores the main code, the 512 bytes of RAM, values of registers and expressions, etc. Additionally, Code Composer Studio supports TI Real Time Operating System that allowed for easy multitasking and memory configuration and control on a one core 16 bit processor. TI- RTOS provided features to create tasks that ran based on priority and easy configuration and set up for communication protocols such as Serial Peripheral Interface used to communication critical information to the navigation system (raspberry pi) and Universal Asynchronous Receiver-Transmitter used to receive data from the GPS module.

3.2.4.1 Architecture and Layout – Olesya

There were two main control systems: the Raspberry Pi's run by the CS team, and the ECE MCU. The Raspberry Pi was the master, and the MSP430 based PCB was the slave. Both systems were sensing the surrounding areas to make sure that the buggy is on the correct path and no obstacles are in the way. The CS team used computer vision and neural networks and the ECE team controlled the sensors. Both decided if the information coming in required any kind of action or stop. The CS team were able adjust the path and implemented a PID feedback loop, that took in the input from the encoder and speedometer sent from the ECE team.

When the buggy stopped, each system was notified, and each team had a recovery mode to be able to keep the buggy moving forward in the competition, as shown in Figure 60. Based from the stopping distance of approximately 1 foot, 1.5 feet was the selected distance that an object can come to the buggy and after that the buggy cuts power to the drive motor and preforms an autonomous stop. Each system validated the detection of an object and notified the other if a stop is about to happen, and this was done through a

packet sent between both systems that contained several flags and information about the systems. The steering and throttle was controlled by one unit to make ensure that there would be no problems with the buggy's movements. PWM control of the motors was implemented in the ECE system and the values at which the motors were to be set was implemented by the CS object detection algorithms.

The CS Team's navigation system was the only system to initiate turns. Before a turn is initiated, the non-rotating side sensors were to be checked before the turn by the system. This data was separate than the data coming in from the rotating sensors to simplify object detection.

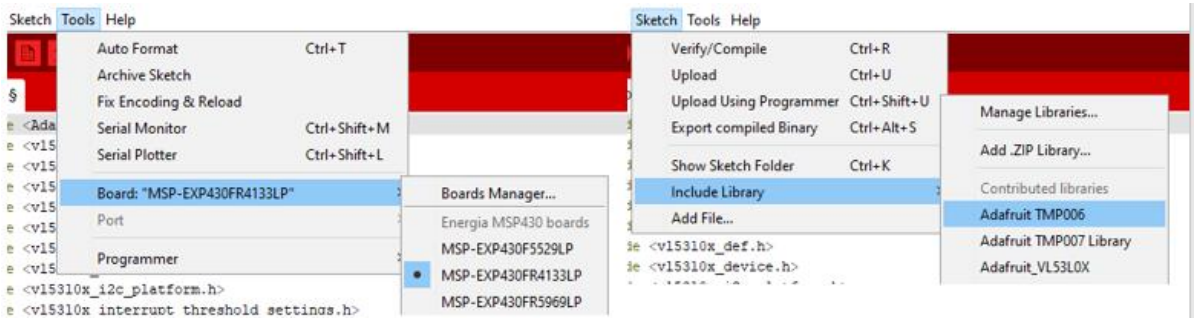

Figure 59. IDE That Will Be Used to Configure and Program the MSP430 FR4133LP.

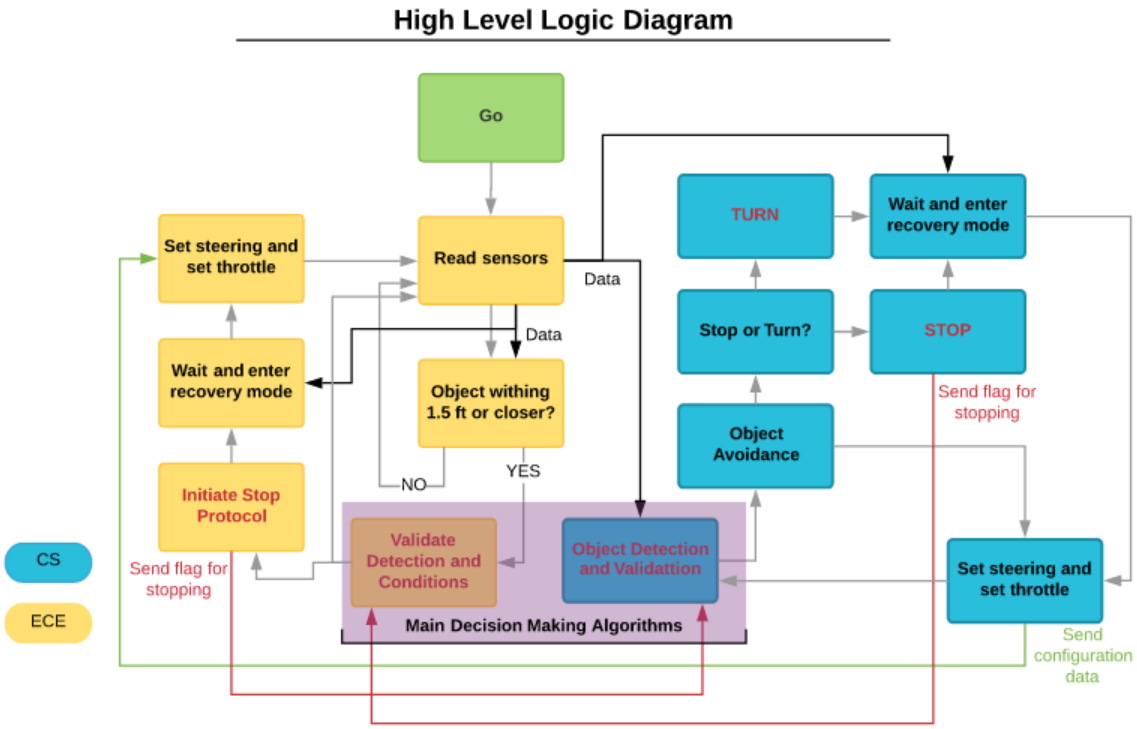

Figure 60. Overview of Logic Diagram Implemented for Solar Powered Beach Buggy.

3.2.4.2 Data Flow – Olesya

The PCB, was the main control unit and was connected to all the mechanical and electrical parts of the buggy. Figure 61 shows what the PCB controlled within the Solar Powered Beach Buggy. The PCB replayed the data and information to the CS team from the sensors and the GPS module, as well as taking in the information received by the navigation system written by the CS team to adjust the path. Any emergency stop was controlled by the PCB and the stop flag was sent to the raspberry pi so the navigation system was notified that the buggy had come to a stop. Any stops that the navigation system initiated, or a stop initiated by the sensors on the buggy would also be controlled by the PCB and the navigation system would also receive a stop flag to know that the buggy has come to a stop. The reset button was added as a physical button for debugging purposes.

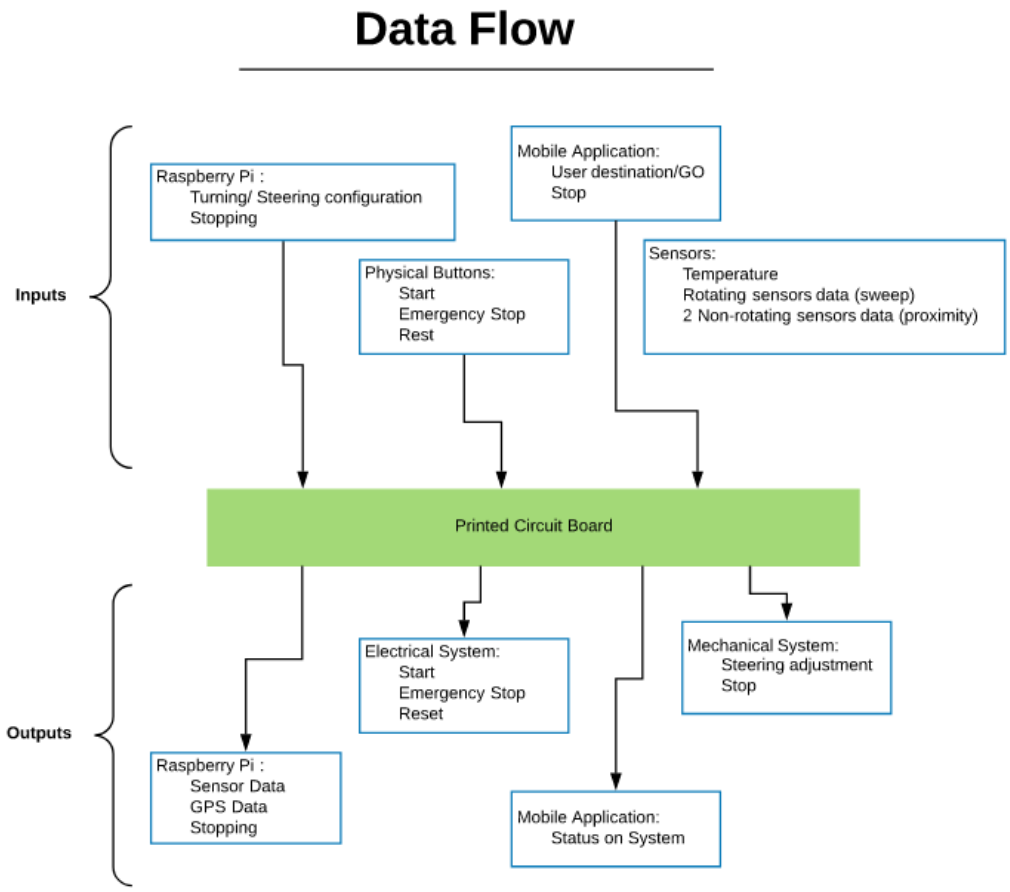

Figure 61. The Data That Will Be Processed by the ECE Team with the Printed Circuit Board.

One last decision was to have a mobile application where the user can enter in the destination and hit go which starts the navigation system. This is possible to implement on both the ECE system and the CS system. The PCB will have an Xbee antenna module to communicate to another device without the need of internet. This allows the user

interface to be implemented on the ECE side. With that design choice, a simple mobile application was created to gather all the information needed from the user. This was a simple GUI with the destination input and click of the go button. Once the PCB receives received the data, it would relay all the information to the navigation system. Then once the buggy has started, the application was used to track the status of the buggy's systems.

3.2.5 GPS Integration – William

Satellite receivers offer the vehicle an inexpensive means to autonomous navigation. The vehicle will take in coordinates from the user and deliver the user to his/her destination. Upon our findings of the available technology offering satellite services, navigational modules are an affordable option. These navigational modules are able to output absolute time, position, and velocity. The Global Navigational Satellite System's multiband enables convergence times in second and its multiple satellite constellations enhance availability. Since the vehicle is designed to traverse the beach from Daytona to Ponce Inlet, the navigational module's performance is contingent to a clear view of the sky.

3.2.5.1 GPS Module Options on the Market – William

There are quite a lot of navigational modules available on the market for consumer use. The U.S. government has allowed its satellites to be used for its citizens without any fee associated [104]. This has opened doors to many manufacturers to bring their line of products to the mass market. Because of the principal of being able to produce goods at a higher volume, the costs for the associated goods will also decrease. These navigational modules are a cost-effective solution to determine where an object is on the globe.

The market for navigational modules can include a very small antenna that can fit inside the module's small packaging. Table 25 shows what has been researched for navigational modules with ceramic patch antennas. The table shows a variety of potential navigational modules that have a built-in ceramic patch antenna. This allows for us to save on the cost of attaching an external antenna to the buggy. However, the downside is that the module must be facing upright to an open sky in order to optimally fix on to a signal from the satellites. There are GPS modules that are standalone. Some GPS modules are able to act as a self-contained receiver. However, the downside to this is that these GPS receiver modules must have an antenna to provide their service in order to communicate to the satellites. These standalone GPS modules allow us the ability to attach a wide variety of antennas. We are able to swap out a better antenna should the system become obsolete. Table 26 shows possible choices for navigational modules for the buggy to know its estimated location on the beach.

Table 25. Selected GPS Modules with a Built-In Ceramic Patch Antenna.

Part Number	Manufacturer	Price
A2235-H	Maestro Wireless Solutions	$20.90
GPS-13670	SparkFun Electronics	$39.95
PAM-7Q-0	u-blox America Inc.	$41.42

The market has a vast trove of antennas for us to choose from. Antennas come in a wide variety and sizes. There are passive and active antennas. Passive antennas do not have an amplification stage [105]. These antennas are tuned to the correct frequency. Active antennas have an integrated signal amplifier built right into the unit [105]. Antennas can have a Low Noise Amplifier (LNA) after the antenna and before the module to amplify the weak GPS satellite signals. Table 27 shows possible choices that may be compatible to navigational modules that require an external antenna.

Table 26. Selected GPS Modules Requiring an External Antenna.

Part Number	Manufacturer	Sufficient Documentation	Ease of Integration	Price
RXM-GPS-RM-B	Lix Technologies Inc.	Yes	No	$20.14
A2100-A	Maestro Wireless Solutions	No	No	$21.95
MAX-M8C-0-10	u-blox America Inc.	Yes	Yes	$23.50

Table 27. Selected External Active Antennas.

Part Number	Manufacturer	Recommended by Manufacturer	Price
APAMP-112	Abracon LLC	No	$11.22
960	Adafruit Industries LLC	No	$12.95
AA.161.301111	Taoglas Limited	Yes	$28.86

3.2.5.2 GPS Module Selection – William

Due to budget concerns, we should not select more than one navigational module. Having more navigational modules will allow for more layers of redundancy should a module fail. But this will increase the cost for the buggy. A decision must be made on choosing a single navigational module to communicate with the satellites.

The temptation to use a navigational module with a ceramic patch antenna will save on cost. However, the ceramic patch antenna limits where we must be able to place the module within the buggy. The use of the ceramic patch antenna makes the printed circuit board be placed upright in clear view of the sky. However, it may be more feasible for the printed circuit board to be placed against a vertical wall in order to save space for other components. Therefore, navigational modules with a built-in ceramic patch antenna will not be chosen.

We decide to use the flexibility of the standalone navigational modules. These modules allow us to place the antenna with greater flexibility than the modules with a ceramic patch antenna built-in. The RXM-GPS-RM-B module will not be used because it lack the ease of integration. We are college students. We are not experts in designing navigational systems. The more pins on the module, the more difficulty it is to work with the module. The A2100-A module was not selected because it lacked sufficient documentation and ease of integration. The hardware integration manual cannot be found on the

manufacturer's website. It was decided that the manufacturer has ceased to provide service to the module. The MAX-M8C-0-10 module was decided to be used for the navigational system. The module provided sufficient documentation that we college students love. This allows us to understand the details of the navigational module. We thank the manufacturer for this. The manufacturer has also included a hardware integration manual with the product. This manual will serve the college students well as they put the module onto the printed circuit board.

With the navigational module decided, we must now choose the right antenna for the module. The MAX-M8C-0-10 module is designed for usage with an active antenna, as stated by the manufacturer in the hardware integration manual. We love the fact that they expressed this requirement to us. Without knowing this, we college students would not have included an active antenna for the navigational system. The navigational module would not be able to function as desired. And we would no longer be able to compete in the challenge.

The manufacturer of MAX-M8C-0-10, u-blox, has also included recommended antennas for us college students to use as a guide in choosing antennas that will work with their module. Based upon their list of recommended antennas, the AA.161.301111 product was selected. It is manufactured by Taoglas. The antenna uses 10 mA at 3 V active. This may be an attractive feature for the power system.

3.2.5.3 Hardware Integration – William

The MAX-M8C-0-10 module has 24 pins for us to figure what they do and for us to configure the printed circuit board with. This will be a very fun experience for the college students. We are glad that the manufacturer includes a "Minimal design" section in the hardware integration manual. This will help us save time and energy on configuring the printed circuit board. This will limit us on what we need and not mess with the pins that are optional to the navigation system [106].

In the minimal design that u-blox has envisioned, Pins 1, 10, 12, and 15 will connect to ground, Pin 11 will connect to the antenna, Pins 6, 7, and 8 will connect to the voltage at the common collector, Pin 2 will connect to the microprocessor as the output, and Pin 3 will connect to the microprocessor as the input. Hopefully, the design on the printed circuit board matches what the minimal design is shown in the hardware integration manual. Hopefully, this design is suitable for the needs of the vehicle. Hopefully.

3.2.5.4 Pin Layout – William

The manufacturer has provided recommendations for the paste mask for its NEO-M8 series modules. This will be useful when we are undergoing the reflow soldering process to attach the module to the printed circuit board. u-blox suggests to use "No Clean" soldering paste. It is highly recommended. Therefore, we may need to spend a little more of our budget to use such high quality paste. "No Clean" soldering paste does not require cleaning after the soldering process has taken place. This will save us on time, but not on

money. We are college students. We should focus on trying to maximize time and money. But in reality, time can be more valuable than money.

u-blox has kindly provided drivers for their line of global navigational positioning system chips and modules. Because Microsoft has introduced a built-in platform for the support of sensor devices, u-blox is able to provide a standard way for u-blox to connect GNSS devices. The Windows Sensor and Location Platform offers developers a standardized way for u-blox to connect GNSS devices. We are able to use a standardized API and device driver interface to work with the sensor and sensor data. The u-blox Sensor Device Driver connects all u-blox GNSS receivers to the sensor and location API structure for Windows 7 onwards. The driver parses and converts u-blox GNSS messages into the standard sensor properties which can be accessed by the location and sensor APIs. This is a godsend to us college students. This do not want to spend time in build a usable data structure for this project. Thank you, u-blox.

We love that u-blox is able to provide us with drivers for their products. The integration of the u-blox MAX-8C module will be a zinch! The u-blox Universal Serial Bus (USB) Sensor Device Driver connects any u-blox global navigational satellite system (GNSS) positioning chops and modules to the Windows Sensor and Location Platform. The u-blox GNSS Sensor Device Driver conforms to Microsoft's Windows Driver Model. We are glad that their driver is able to conform to Microsoft's mode. This will save us valuable time as we get the vehicle to autonomous level.

u-blox furthers to support its customers by proving us a Virtual COM port (VCP) driver. This will connect or test u-blox GNSS positioning chips and modules with legacy Windows applications that can connect only to a COM port. This solution is intended to help us smoothly migrate their legacy location applications to the modern Windows Location and Sensor Platform.

u-blox is even more amazing! Their GNSS evaluation software (u-center) provides a powerful tool for evaluation, performance analysis and configuration of u-blox receivers. The u-center software is flexible for a wide range of its products. We hope this works for the MAX-8C module. If not, we should look into other navigational modules. Hopefully, MAX-8C is a good choice for our navigational system in terms of cost and time investment. Figure 62 shows what is expected from the software that u-blox has for the windows driver. We hope it will be an easy development process for us to get the board from production to competition-ready.

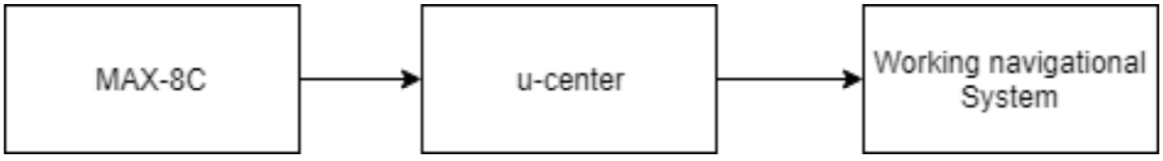

Figure 62. Software for MAX-8C.

3.2.5.5 Antenna and Antenna Supervision – William

The MAX-8C module are designed for usage with an active antenna. u-blox suggests that passive antennas can be used. They also note that an external LNA and SAW should be incorporated into the antenna design for best performance. However, since the MAX-8C module was designed for usage with an active antenna in mind, we should discuss how the active antenna should be implemented in this project.

3.2.5.5.1 Antenna Design with Active Antenna – William

Active antennas have an integrated low-noise amplifier integrated into them. Some active antennas require a power supply that will contribute to the total budget of the GNSS system power consumption. u-blox notes that amount is typically 5 to 20 mA. This is a small price to pay to have an improved antenna for the vehicle. u-blox notes that if the supply voltage of the MAX-8C receiver matches the supply voltage of the antenna, we should use the filtered supply voltage available at pin VCC_RF. The exact configuration is shown in the hardware integration manual. Figure 63 shows the antenna design so far.

The manufacturer notes that because the external voltage is fed into the most sensitive part of the receiver, the power supply should be free of noise. u-blox cautions that low frequency analog noise is less critical than digital noise of spurious frequencies with harmonics up to the GNSS frequency. u-blox has a module design with active antenna with external supply. So far, the select antenna does not say it needs an external power supply. However, in the event we change antenna decisions, we are freely able to purchase an active antenna with an external power supply.

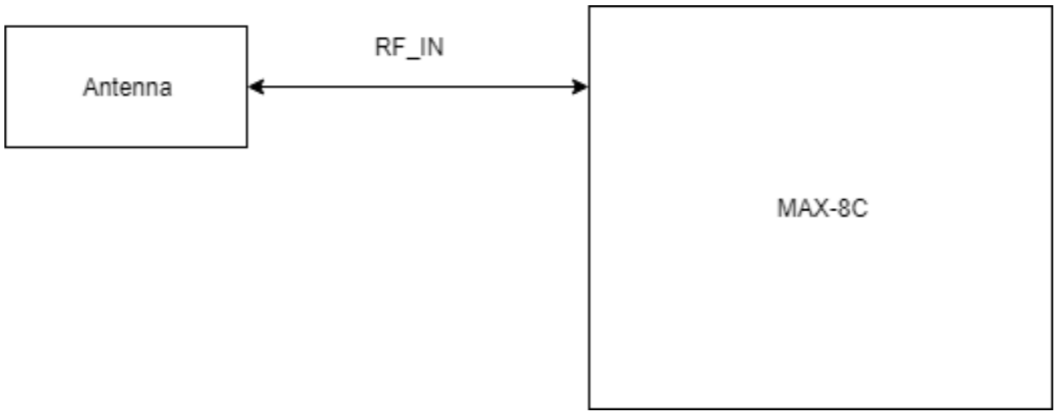

Figure 63. Navigational Module with Antenna.

3.2.5.6 Receiver Description – William

u-blox has provided us with a document that will describe the firmware features, specifications, and configuration for their M8 line of products. The Receiver Description provides an overview and conceptual details of the supported features. Within the same document, it also provides a section on Protocol Specification. This describes the NMEA

and RTCM protocols as well as the UBX protocol. This document will serve as a reference manual for us college engineering students.

In order to fully integrate the u-blox MAX-8C module into the printed circuit board, we must use the Receiver Description Including Protocol Specification document. The document describes the software aspect of the system features and configuration of u-blox receivers. The protocol version defines a set of messages that are applicable across various u-blox products. The MAX-8C module uses internal ROM. This module uses Protocol Version 17 and below.

The Receiver Description Including Protocol Specification document provides a list of possible lines in the boot screen of the navigational module and their meaning. This will be useful as we decipher the meaning of what the navigational module is trying to communicate to us.

3.2.6 Motor Feedback – Caroline

Two different methods of motor feedback were implemented to accommodate the two motors and tie into the electronics. One provides absolute directional feedback within a single rotation of the steering motor shaft, while another measures drive motor output speed. Each feedback loop was used to precisely adjust the PWM signals from the MCU through the motor driver to the motors, as described in the Software Implementation section of the motor driver design. The following sections lay out designs to accomplish these tasks using minimal cost solutions.

3.2.6.1 Speedometer – Caroline

There are two available ways to calculate the speed of the vehicle: use GPS coordinates to calculate speed, or use a mechanical sensor to detect RPM, which can be converted into linear speed. While using GPS coordinates to calculate speed is simple and does not require any additional components, it is not the most reliable. A mechanical sensor is necessary to confirm any speed calculated through GPS, although the GPS calculations can also be used for comparison to check against a mechanical failure. For the drive motor, there are two options to mechanically calculate speed. Either an encoder can be used on the shaft, or another sensor can be installed on the wheel, referred to here as a speedometer. However, since incremental encoders such as the HEDS-9000 are about $25, a speedometer was chosen to be the most budget-friendly option at a total cost of about $10.

Speedometers can operate using a number of different sensing techniques. One of the most common methods of counting rotations is with a magnetic switch and magnets mounted on the wheel. Each time the magnet passes the switch, the switch is triggered, and an MCU can count the rotation [107]. Multiple equally-spaced magnets can be used for further wheel position detection. Although this method gives much less precision than an encoder, the necessary precision for this application is low at around 1 count per 0.1 seconds.

Either a Hall effect sensor or a reed switch can be used to detect a magnetic field. Reed switches utilize the magnetic force to align two conductive wires that are kept in an air-tight enclosure. When the magnetic force is strong enough, the wires bend together and conduct. Reed switches are generally slightly cheaper and easier to use. It has less life cycles, but is also more reliable in every environment, and therefore fits the needs of the design [108]. Any number of magnets could be attached to the rim of one of the wheels. This design specifies 8 magnets due to the hub cap size. With a 21" wheel diameter, 8 equally spaced sensors at 3 mph will result in one sensor pass every 0.156 seconds, or 385 PPM.

If the reed switch is placed 1 inch away from the magnets, the calculated magnetic field strength will be 42.2 Gauss from the following equation [109]:

$$\square\square\square\square\square_{\square\square} \cong \square\square\left[\left(\frac{\square+\square}{\sqrt{\square^2+(\square+\square)^2}}\right)-\frac{\square}{\sqrt{\square^2+\square^2}}\right]$$

Online simulators are capable of giving more accurate results, since this above equation is a simplification of the original field equation for magnetic field strength along the normal axis to the flat cylinder face. However, the results are similar [110].

In this equation, Br for N35 magnetics is approximately 12 KGs, L = 6 mm, X = 25.4 mm, and R = 12 mm. This result is slightly more than the acceptable activation force range for the MDCG-4 reed switch. The specified force on the data sheet is 12 to 38 AT, or roughly 12 to 38 Gauss [111]. However, magnetic field strength dramatically decreases with even small distances away. It was critical to mount the reed switch close to the sensors to ensure that the switch could be triggered. Greater distances substantially increase cost of the magnets. This selection ensures that the switch can safely be placed 1 inch away from the wheel. Any equivalent magnet strength and geometry would also have worked from the above equation.

3.2.6.1.1 Circuit Diagram – Caroline

The schematic for the design is shown in Figure 64. This design shows the connection of the reed switch to the MCU on pin P2.6, the placement of the resistor to regulate current through the switch when it is closed, and the placement of the magnets along the tire. A front tire was used to mount the magnets due to hub accessibility.

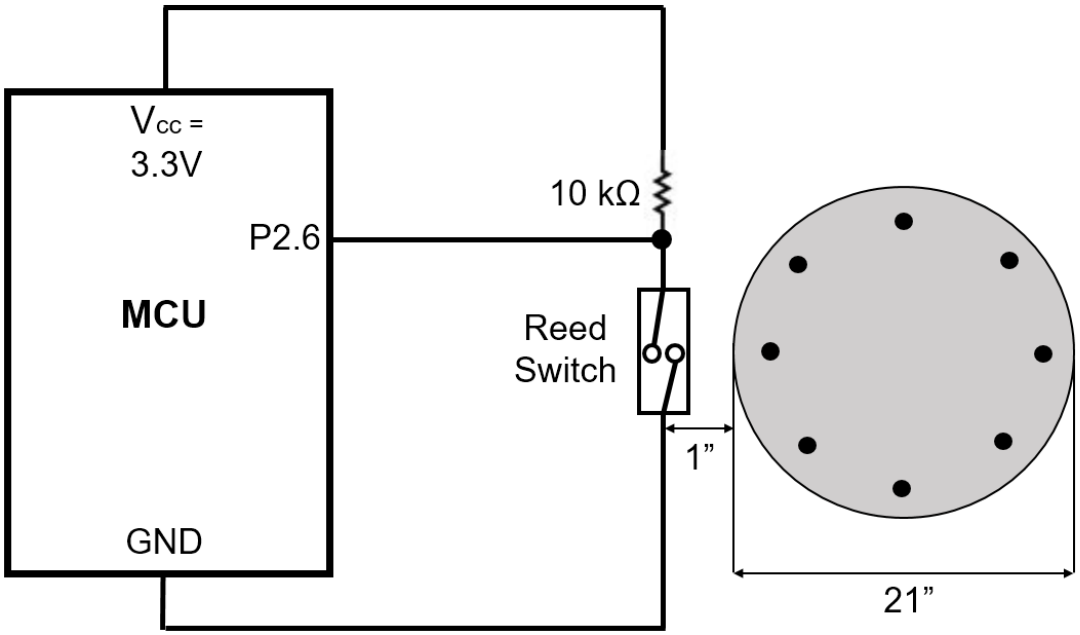

Figure 64. Reed Switch Speedometer Circuit Diagram.

3.2.6.1.2 BOM – Caroline

The Bill of Materials for this design is listed below in Table 28. The final cost was to be no more than $10.

Table 28. Bill of Materials for Speedometer.

Item	Approximate Cost
Magnetic Reed Switch MDCG-4	$1.32
10 kΩ Resistor	$0.05
Female header	$0.20
Male header	$0.20
(8) Neodymium Magnets N35 12mm x 6mm	$8.00
Total Cost	**$9.77**

3.2.6.2 Encoder – Caroline

Since the encoder for the steering motor must be very precise, an absolute encoder was utilized for feedback. Moreover, it was chosen to be magnetic to avoid any mechanical interference. The budget for the encoder was confined to about $25. From these criteria, a 10-bit absolute magnetic encoder was chosen, the Avago AEAT-6010, which costs $25.66. With 10-bit resolution, the encoder is able to detect position upon power-up within 0.35 degrees. The data will be provided to the MCU using serial bit stream, or SSI. It requires a 5V supply with a typical current of 16 mA, or 0.08W, thus not dissipating any substantial heat. It can operate in temperatures between -40 and 125 degrees Celsius,

which is well within operating conditions. It is manufactured for a 6 mm shaft diameter, which fits on the shaft on the steering motor. A diagram of the assembly is shown in Figure 65 [112].

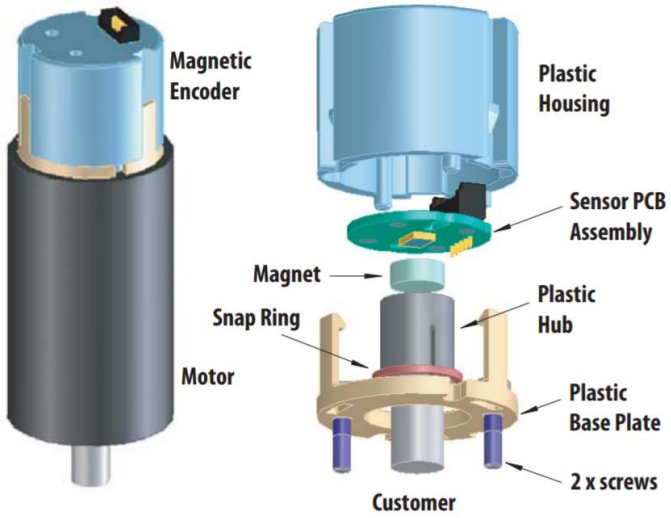

Figure 65. Avago AEAT-6010 Encoder Assembly Diagram [112].
(Reprinted from Avago Technologies, copyright expired)

The maximum linearity error is 2.4 degrees, which is substantial compared to the resolution but deemed acceptable for the application. The linearity error is zero at 0, 180, and 360 degrees, with maximum linearity error at 90 and 270 degrees. As long as zero linearity error is present at zero degrees, or when the wheels are pointing straight forward, this error does not negatively impact the buggy's steering accuracy.

The connection diagram for the encoder is shown in Figure 65. The Chip Select refers to the selection of the output serial data protocol to dictate communication timing. The input and output signals are transmitted using RS-422 standards. The exact MCU pin connections are also detailed in Figure 66.

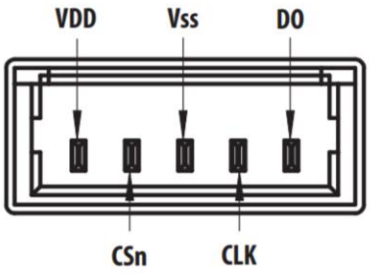

Pin	Symbol	Description	MCU Pin
1	VDD	5V Supply Voltage	Vcc
2	CSn	Chip Select	P6.6
3	VSS	Supply Ground	GND
4	CLK	Serial Clock - Input	P6.5
5	DO	Serial Data - Output.	P6.7

Figure 66. Avago AEAT-6010 Encoder Connection Diagram [112].
(Reprinted from Avago Technologies, copyright expired)

3.2.6.2.1 Software Controls – Caroline

Calculating the absolute direction of the steering motor from the encoder output is a simple task that can be described as follows. Three integer variables must be declared to store the chip select, the clock signal, and the digital output from the encoder. Another variable will also be declared to translate and store the digital output from the encoder. Then, the setup() function will declare which pins are inputs and outputs. It should also set the chip select and start the clock signal.

In a loop, the function readEncoder() will be used to repeatedly store the encoder data. This function will turn off the chip select and shift the 10-bit serial data output into a temporary variable by toggling the clock. Once all of the bits are stored, the chip select is again set, and the temporary variable is returned. A small delay should be incurred between each readEncoder() call, according to the sampling frequency of the encoder.

A plausible range of motion will be determined during prototype testing and will be incorporated into the software to ensure that the steering motor does not rotate the axis too far. A range of 120 degrees has been postulated for initial testing.

3.2.7 Future Design Considerations – William

This section is provided so that the initial design may be improved by the next generation of solar autonomous beach buggy engineers. We would like to see the vehicle better serve the beachgoer's experience. These items are able to provide for improved accuracy and reliability for the user. However, due to budget and time concerns, these items were not implemented in this design for the vehicle.

3.2.7.1 IMU – William

Inertia Measurement Units are a cheap and efficient means to gether a set of data without intervention from the system processor. The 6 DOR Gyro, Accelerometer IMU - MPU6050 [113] is capable of processing complex 9-axis Motion Fusion algorithms. The device is able to measure the motion and angle that the vehicle may be moving. This provides additional support for the navigational system.

3.2.7.2 Laser Distance Sensor – William

Laser rangefinders are an innovative solution to transforming the vehicle to perform self-driving tasks. There was a paper developed that states the researchers were able to build this sensor device in under $30 [114]. However, due to time concerns, we college students will not invest the time or energy in build a laser rangefinder for under $30. This would help keep costs down, but time is a more valued entity.

3.2.7.4 Graphics Processing Unit – William

Nvidia is making great advances to bring cars to be self-driving. One of their platforms is the NVIDIA DRIVE. It is the AI platform that is enabling a variety of vehicles to become automated and autonomous vehicles. However, due to the high cost of such platforms, it will not be considered.

3.2.7.5 CAN Bus – William

The Controller Area Network bus is able to cut down on the necessary wiring to sync up all the electrical components to a master device. But due to complexity of the system, it will not be invested for this design project.

4 Prototypes – Caroline

The following few sections outline small-scale prototyping plans for the solar array, PCB microcontroller, and other small electronics via a test bot. By taking incremental steps to develop the final products, progress was tracked without risking substantial money or time. These prototypes were used to confirm the design concept and obtain practice on using the associated components and manufacturing equipment.

4.1 Solar Cell Array Prototype – Caroline

Once the 300 solar cells had been purchased to make up the 180-cell solar array, there were several remaining solar cells to use as a prototype. Tabbing and mounting techniques were practiced on this material before assembling the final component. The mounting and tabbing were conducted the same way as specified for the solar array. As predicted, many solar cells broke during assembly. The remaining leftover cells were wired with tabbing wire to confirm the output voltage and current. The manufactured adjustable mounts were also attached to this prototype panel to better represent the final product.

4.2 PCB – Patrick

For prototyping and testing the PCB a pre-made board was used. The board that was used is the FR5529 LaunchPad Compared to the final board this one lacks the necessary step up and step down circuits which means using it with 5v peripherals may be inconsistent. The main goal of using this board was to test all the parts that will be connected to it. This board also has a smaller number of pins exposed. For this reason, while it was not be possible to connect every element to the test board it served its purpose of allowing parts to be tested for compatibility.

The sensors that were used were connected to make sure they were compatible. To do this they were connected and tested at different ranges, this also served to validate the ranges of the sensors. Additionally, the custom-made speedometer will require programming on the custom board. This was tested on the MSP430FR5529 LaunchPad to check that it was compatible and test the strain on the board.

To connect to the motor controller, it was necessary to generate a PWM signal in software with the micro controller. To test this the board was connected to an oscilloscope and the output checked against the desired one. This allowed the compatibility of the microcontroller and the motor controller to be tested even before it is possible to connect the two together. Likewise, this would have worked for proposed Bluetooth module but since this was removed from the final design this test was not conducted.

4.3 Test Bot – Olesya

In the building and testing stage of this project, there was three teams working on each part the buggy was fully assembled toward the ending of the second semester. This meant that the ECE team needed a frame to test on before the mechanical team can complete their project. The only solution to testing out the ECE team and CS team components was to place them on another, smaller chassis that was called the Test Bot. This test bot was purchased for the project as a platform for testing. The best and cheapest testing platform was a power wheels, and it was used at the beginning of the semester. With the test bot there was a way to test the sensors, the navigation system, and the electrical start and emergency stop buttons.

4.3.1 Sensors – Olesya

The sensor system was based off Design A from the Sensor design section. This incorporated the mounts made and the electrical diagrams created for powering these sensors. The Prototype followed the exact layout, and in the case that the sensors did not provide the system with accurate results needed by the navigation system, Design B would have been used.

The only thing would have changed was the price for the sensor system, the price would have increased with Design B because it used a higher ratio of the Infrared sensors that are more accurate that the Ultrasonic sensors. Mounts were created for both, and the distance calculations were possible for both as well. Voltage and current sensors might be a possibility to monitor the prototype depending on the budget, this was established after all the components are purchased.

To make sure that Design A would work, testing was done with the HC SR sensor to evaluate the accuracy. The following testing was first done with an Arduino for comparison, as shown in Figure 67, then transitioned to an MSP430 to test how the sensors preform. There were issues that arose with the voltage levels that the sensor's pins use. The TRIG and ECH pin need 5 volts, but the MSP430 runs at 3.3v. This was then incorporated into the PCB design to make sure the sensors can run properly and are not consistently running on the MSP430s voltage limit. The voltage divider shown below in Figure 68 was integrated on the PCB board. The voltage will be stepped down to 3.3 volts going into the PCB, then stepped back up to the sensor.

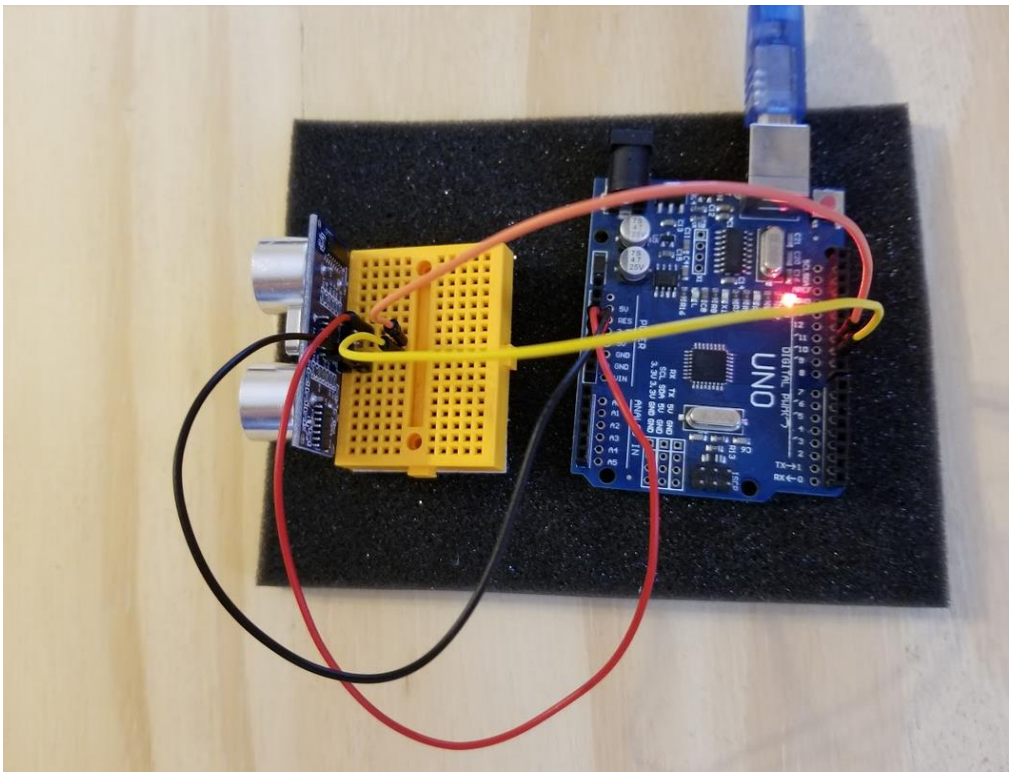

Figure 67. The SR-04 Ultrasonic Sensor Initial Testing with Arduino for Comparison.

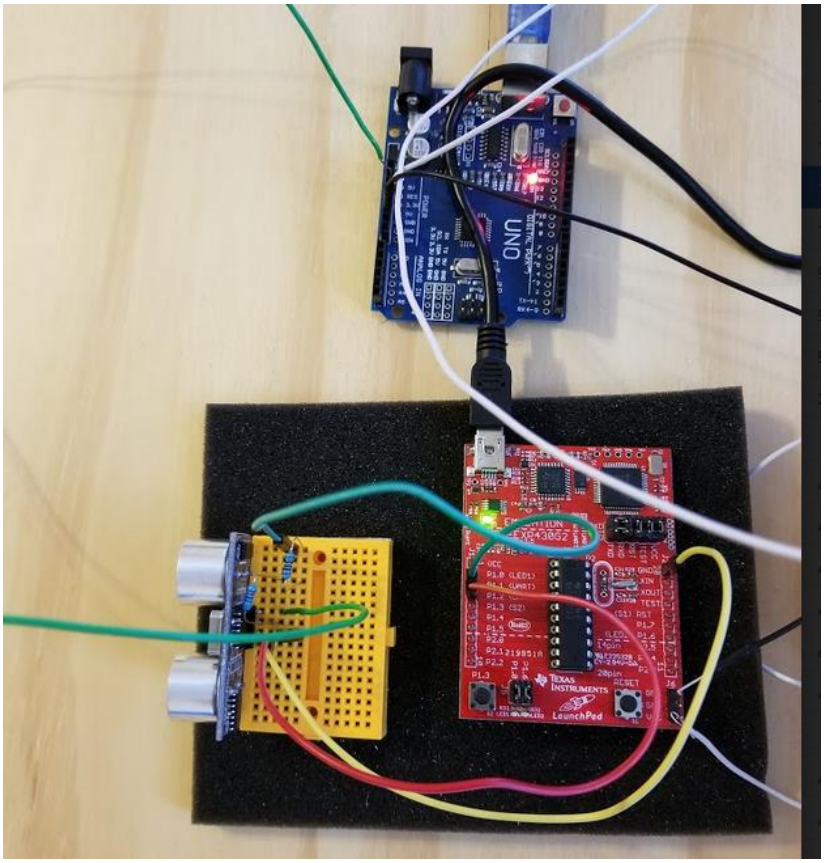

Figure 68. The SR-04 Ultrasonic Sensor Initial Testing with MSP430 for Compatibility.

The software used for testing was to test basic functionality. The results are below:

1. Does the sensor work?

Yes, the data coming back is valid/reasonable.

2. Is the sensor accurate in detect an object in the range specified in the code?

Yes, the led blinked within the threshold.

3. Is the sensor able to detect an object in the range specified accurately while rotating?

Yes, the led blinked within the threshold.

Testing for the infrared sensor was held Senior Design II. The same testing was done and the mounts were printed and configured to provide the proper speed that the sensor can handle while staying accurate.

4.3.2 GPS Testing – William

The navigational system was tested by having the navigational module report the location of itself to us. Since this occurred, we believe that the navigational system was working as intended. However if this is not the case, then the navigational system would have needed to be changed and/or altered.

5 Parts Acquisition – Caroline

After the smaller-scale prototypes had been built and tested with the available components, the design proceeded by ordering the remaining components. The ready-made components have been detailed throughout the design, including the manufacturer and estimated market price. Generally, these parts were purchased from reputable vendors at the lowest available market price and were integrated into the final prototype after proper testing procedures had been performed, which will be outlined in the next major section. The remaining task was then to acquire the components for the hand-made components, namely the charge controller and MCU. The following sections will explain the current plan for parts acquisition.

It is important to note that although the Bill of Materials for the MCU and charge controller are kept separate in this report, they were combined when ordering the components to minimize shipping costs.

5.1 Bill of Materials for MCU – Patrick

The bill of materials for the main control unit can be seen below in Table 29. It lists each part necessary for constructing the main control unit and corresponds each part in the schematic with its value, device, and package.

Table 29. Bill of Materials for MCU.

Item	Qty	Part	Value	Device	Package	Description	Price
1	5	C1, C2, C3, C8, C10	100n	C-EUC0402	C0402	CAPACITOR, European symbol	1.15
2	1	C4	1u	C-EUC0402	C0402	CAPACITOR, European symbol	0.23
3	2	C5, C6	12p	C-EUC0402	C0402	CAPACITOR, European symbol	0.28
4	1	C7	10u	C-EUC0603	C0603	CAPACITOR, European symbol	0.55
5	1	C11	1n	C-EUC0402	C0402	CAPACITOR, European symbol	0.43
6	1	C13		C-US025-025X050	C025-025X050	CAPACITOR, American symbol	0.24

7	1	C14		CPOL-USE2.5-5	E2,5-5	POLARIZED CAPACITOR, American symbol	0.62
8	2	D3, D4		LED3MM	LED3MM	LED	1.0
9	1	IC3		MC1700	TO92	VOLTAGE REGULATOR	0.45
10	1	IC4	74LS125N	74LS125N	DIL14	Quad bus BUFFER, 3-state	0.69
11	6	J1, J2, J5, J6, J7, J8		PINHEADER 1X10	PINHEAFER 1X10		0.3
12	1	J3	TEST_PIN2	PINHD-1X1	1X01	PIN HEADER	0.05
13	1	J101		PINHD-2X10	2X10	PIN HEADER	0.05
14	1	JP1		JUMPER_2.51MM	JUMPER-2.54		0.10
15	1	JP2		PINHD-1X1	1X01	PIN HEADER	0.10
16	11	LED1, LED4, LED5, LED6, LED7, LED8, LED13, LED14, LED15, LED16, LED17	Red	CHIP-LED	LED0805		2.255
17	7	LED2, LED3, LED9, LED10, LED11, LED12, LED18	Green	CHIP-LED	LED0805		1.435
18	1	MSP1	MSP430 FR4x	MSP430 G621IPM	LQFP64		3.01
19	1	R1	47k	R-EU_	R0402	RESISTOR, European symbol	0.24
20	27	R2, R6, R8, R10, R12, R14, R16, R17, R18, R19, R20, R21, R22, R23, R24, R25, R36, R37, R39, R40, R42, R43, R48, R49, R51, R52, R54	1k	R-EU_	R0402	RESISTOR, European symbol	0.648

21	7	R3, R7, R9, R11, R13, R15, R55	2K	R-EU_	R0402	RESISTOR, European symbol	2.0
22	18	R4, R5, R26, R27, R28, R29, R30, R31, R32, R33, R34, R35, R38, R41, R44, R50, R53, R56	470	R-EU_	R0402	RESISTOR, European symbol	0.936
23	2	R45, R46	200	R-US _0207/10	0207/10	RESISTOR, American symbol	1.72
24	1	R47	10K	R-US _0207/10	0207/10	RESISTOR, American symbol	0.49
25	3	S1, S2, S3	T062S	T062S	T062S		0.3
26	10	T1, T2, T3, T4, T5, T6, T7, T8, T9, T10	2N3904	2N3904	TO92	NPN TRANSISTOR	2.58
27	1	U$1	MAX-M8	MAX-M8	MAX-M8	u-blox MAX GNSS module	23.50
28	4	U$2, U$3, U$5, U$6	MOUNTHOLE_125MIL	MOUNTHOLE_125MIL	MOUNTHOLE_125MIL		
29	3	U$9, U$10, U$11	PINHD-1X10	PINHD-1X10	1X10-BIG		0.20
30	1	X1		SMACONNECTOR_EDGE	SMA_EDGELAUNCH	SMA Connector	2.5
31	1	XBEE1	XBEE	XBEE	XBEE		26.95
32	1	Y1	32.768kHz	MS3V-T1R	MS3V-T1R		1.31
							73.96

5.2 Bill of Materials for Charge Controller – Caroline

The bill of materials for the charge controller is listed in Table 30. Each part is assigned an item number, quantity, reference value that corresponds to the schematics, value, description, part number, and listed price from a vendor. These prices changed slightly as these two BOM's were combined and other vendors were incorporated or removed from the order list. The estimated cost of the components without the PCB was $88.14. This board and the MCU board were purchased together from PCBWay to reduce shipping costs. It was estimated that the cost to produce and ship the board will be $50.00, which fits in the allotted budget of $150.

Table 30. Charge Controller Bill of Materials.

Item	Qty	Reference	Value	Description	Part Number	Price
1	3	B1, B2, B3		Bead, Ferrite, 500mA	MU2029-301Y	0.3
2	5	C1, C2, C3, C35, C36	470uF	Capacitor, 50V, Low ESR, ±20%	UHE1H471MHD3	5.15
3	4	C4, C5, C6, C7	4.7uF	Capacitor, Ceramic Chip, 100V, X7S, ±10%	C4532X7S2-A475M-230KB	8.04
4	2	C8, C9	10uF	Capacitor, Ceramic, 50V, X7R, 20%	UMK325AB-7106MM-T	1.76
5	6	C10, C11, C19, C20, C28, C29	1nF	Capacitor, Ceramic, 50V, X7R, 5%	Std	4.02
6	10	C12, C13, C30, C31, C33, C34, C37, C38, C39, C43	0.1uF	Capacitor, Ceramic, 50V, X7R, 5%	Std	6.9
7	5	C14, C15, C22, C27, C40	1uF	Capacitor, Ceramic, 50V, X7R, 5%	Std	1.45
8	7	C16, C17, C18, C26, C32, C41, C42	0.47uF	Capacitor, Ceramic, 50V, X7R, 5%	Std	6.37
9	1	C21	1uF	Capacitor, Ceramic Chip, 100V, ±10%	HMK316B-7105KL-T	0.43
10	3	C23, C48, C49	10nF	Capacitor, Ceramic, 50V, X7R, 5%	Std	0.3
11	1	C24	5.6nF	Capacitor, Ceramic, 50V, X7R, 5%	Std	0.38
12	1	C25	4.7uF	Capacitor, Ceramic Chip, 50V, ±10%	UMK316AB-7475KL-T	0.45
13	2	C44, C47	560pF	Capacitor, Ceramic, 50V, NPO, 1%	Std	0.44
14	2	C45, C46	220pF	Capacitor,	Std	0.48

				Ceramic, 50V, NPO, 1%		
15	1	D1	MMSZ5245-B	Diode, Zener, 500mW, 15-V	MMSZ5245B-7-F	0.22
16	1	D2	1SS355	Diode, Switching, 90V, 225 mA Ifm, High speed	1SS355	0.2
17	3	J1, J2, J3	OSTT7020-150	Terminal Block, 2-pin, 32-A, 9.5mm	OSTT70-20150	
18	1	J4	S1012E-36-ND	Header, Male 3-pin, 100mil spacing, (36-pin strip)	S1012E-36-ND	1.41
19	1	J5	S1012E-36-ND	Header, Male 8-pin, 100mil spacing, (36-pin strip)	S1012E-36-ND	2.82
20	1	J6	S1012E-36-ND	Header, Male 4-pin, 100mil spacing, (36-pin strip)	S1012E-36-ND	4.23
21	2	L1, L2	10uH	Inductor, SMT Power, 20A, 1.5 milliohm	SER2915L-103KL	
22	1	L3	470uH	Inductor, Radial , ±10%	RLB0608-471KL	0.25
23	1	L4	47uH	Inductor, 110mA, 0.95ohm	CB2518T-470K	0.19
24	7	Q1, Q2, Q3, Q4, Q5, Q6, Q7	CSD19535-KCS	MOSFET, N-Chan, 100V, 150A, 3.1 milli-ohm	CSD19535KCS	20.30
25	3	Q8, Q9, Q10	MMBT3904	Bipolar, NPN, xx-V, yy-mA, zz-W	MMBT3904LT1	0.51
26	3	R1, R2, R3	2m	Resistor, 2 milliOhm, 3W, 1%	CSR2512C-0R002F1	2.07
27	2	R4, R5	5.1	Resistor, 5.1 Ohm, 1W, 5%	Std	0.38
28	4	R6, R7, R8, R9	402	Resistor, Chip, 1/16W, 1%	Std	0.8

29	8	R10, R15, R16, R25, R26, R35, R37, R50	10K	Resistor, Chip, 1/16W, 1%	Std	1.36
30	4	R17, R18, R19, R20	2.2	Resistor, Chip, 1/10W, 1%	Std	0.4
31	6	R21, R22, R31, R47, R48, R49	2.05K	Resistor, Chip, 1/16W, 1%	Std	1.2
32	2	R23, R24	33.2K	Resistor, Chip, 1/16W, 1%	Std	0.22
33	1	R27	261K	Resistor, Chip, 1/16W, 1%	Std	0.11
34	1	R28	9.53K	Resistor, Chip, 1/16W, 1%	Std	0.11
35	1	R29	1.33K	Resistor, Chip, 1/16W, 1%	Std	0.11
36	1	R30	4.02	Resistor, Chip, 1/16W, 1%	Std	
37	9	R32, R33, R40, R41, R43, R44, R45, R46, R51	205	Resistor, Chip, 1/16W, 1%	Std	
38	3	R34, R36, R56	178K	Resistor, Chip, 1/10W, 1%	Std	0.3
39	4	R42, R52, R53, R54	1K	Resistor, Chip, 1/16W, 1%	Std	0.8
40	1	R55	13.3K	Resistor, Chip, 1/16W, 1%	Std	0.2
41	1	U1	SM72295-MA	IC, Photovoltaic Full Bridge Driver	SM72295-MA	4.43
42	1	U2	LM5019MR	IC, 100 V, 100 mA Constant On-Time Synchronous Buck Regulator	LM5019MR	3.5
43	1	U3	TLV70433-DBV	IC, 24-V Input, 150 mA, Utralow IQ LDO Regulator	TLV70433DBV	0.83
44	1	U4	INA271	IC, Voltage Output, Unidirectional	INA271AID	2.89

				Current-Shunt Monitor		
45	1	U5	MSP430F-5132IDA	IC, Mixed Signal Microcontroller	MSP430F-5132IDA	2.68
						$89

5.3 PCB Vendor – Patrick

There are many options when it comes to purchasing a custom printed circuit board and there are many factors that go into pricing such a board. The most relevant pricing factors for purchasing a custom PCB board were found to be the number of layers of the board, and the size of the board. For ease of design printed circuit boards are created by layering sheets of copper on top of each other. This allows for the easy construction of connection of elements from different parts of the board. The more layers that a printed circuit board has the easier it is to place many components on different parts of the board. If the board is properly designed, it is possible to reduce the number of board layers needed. Because the board will be based on the MSP430 launch pad, which is a 2-layer board, and in terms of cost 2 layers boards are much cheaper to make. For this reason, all of the vendor pricings were created around the assumption that a 2 layer board would be ordered.

OSH Park prices their printed circuit boards based on the size with an average shipping time of 12 days after the order is placed. The short turnaround of under 2 weeks for getting the board back is beneficial due to the short timeline of this product. The pricing by size is will be helpful if the size is under a certain number of square inches, but also sends 3 boards. As other vendors offer a flat rate that could be cheaper if the board size exceeds a certain amount.

Advanced Circuits offer a flat rate of $33 per board and since it is USA based shipping will be not cost much more. A benefit of using Advanced Circuits is that they offer a free design tool that can check the design before manufacturing. As it has already been decided that this project will be using EAGLE as its board design tool this does not give any reason to use Advanced Circuits over another vendor. If the board size exceeds 20 square inches Advanced circuits would start to be a much cheaper option than OSH Park.

PCBway is a China based vendor that offers the cheapest board price of $5 for 5 boards. However, since it is international shipping is estimated to be around $23, so the actual price of acquiring the boards is $28. The ship time is expected to be 12 days which is comparable to the other vendors, but since it is international there is potential for shipping complications which must be considered.

ExpressPCB offers the pricing of 4 boards for $166, due to the cost constraints of this project it was not considered much further as a vendor since it was outside the budget. From this research it was concluded that OSH Park or PCBway would be best options, and in Senior Design 2 the final decision for which vendor that will be used was PCBway due to its price per number of boards.

6 Component Testing – Caroline

Each component went through rigorous testing to verify safety, datasheet specifications, and functionality. In doing so, the buggy was more likely to function correctly once fully assembled. The information retrieved from testing was also used to refine the efficiency estimations and performance modeling.

6.1 Solar Array Testing – Caroline

Three tests were conducted on the prototype solar cell array before constructing the final array. First, thermal stresses and wind loads were applied on the plywood base before assembly. The wood warped slightly, leading to a decision to use only one drop of glue per cells such that tensional stresses would not snap them apart. Then, the broken cells, mounted and unmounted, were tested by inspection to ensure that the final product would endure the competition.

The second test included calculating the expected hourly generation and measuring the output power with an ammeter and voltmeter. The results were compared to the calculations to estimate its precision, but because test conditions were never close to competition day conditions due to weather and limited space, this data was not analyzed further. A more accurate model could be generated if testing occurred in more acceptable conditions. The tilt of the solar panel during this test was configured by the mounting bracket in order to simulate the actual mounting condition.

The third test included comparing the measured output at STC to the power specifications given for the purchased solar cells. The results of this test were correlated with the results of the second test, as shown in Table 31. Unfavorable weather and orientation constraints caused data to only be recorded in minimal light conditions and partially cloudy conditions. The listed values are for the whole array. Ultimately, the purpose of these tests was to develop a realistic prediction model for solar generation and to ensure that the solar panels would endure the environmental conditions of the competition.

Table 31. Solar Array Testing Results

Parameter	Manufacturer Specification	Minimal Light Conditions	Partially Cloudy Conditions
Open Circuit Voltage (V_{oc})	57.69 V	44.1 V	51.0 V
Short Circuit Current (I_{sc})	18.62 A	0.8 A	8.9 A

During the construction of the final solar array, each row of cells was tested for defects before attaching it to the panel. This was done by attaching the tabbing wire and taking it outside for open circuit voltage and current testing to ensure the power output was reasonable given the weather conditions. The readings were simply scaled versions of the data given in Table 31. This test must be done when building a solar panel because a singular defected solar cell can significantly reduce panel output. After every cell had been tested, wired, and mounted, prototype tests two and three should be repeated to

again validate the prediction model. Once all of the data was collected, the array was mounted to the buggy for testing the charge controller.

6.2 Charge Controller Testing – Caroline

The charge controller was simulated using circuit simulator software, namely Multisim, before assembling the product. This verified that all smaller components are correctly sized, that there are no wiring misunderstandings, and that the expected output was obtained for a given power supply input. No abnormalities were found in the design, so the modified design presented previously immediately proceeded into manufacturing.

The charge controller was then assembled and tested using a DC power supply and an electronic load. In order for this product to be deemed acceptable, the efficiency must be at least 95% or preferably above 97%. Lab equipment limited the current that could be tested to 1.5 A, which is insufficient to measure full load efficiency, which increases with current and voltage. However, at 1.5 A, efficiency was measured at approximately 95%, which already passed efficiency expectations. Lab data is included in Table 32. A picture of the GUI output during this test is included in Figure 69.

Table 32. Charge Controller Lab Test Results

Panel Current (A)	Panel Voltage (V)	Battery Current (A)	Battery Voltage (V)	Efficiency (%)
1.1	44	1.8	25.5	95.0
1.2	44	1.97	25.5	95.2
1.3	44	2.16	25.5	96.3
1.4	44	2.32	25.5	96.0

The last phase of construction and testing involved connecting the charge controller to the assembled solar array and battery pack. Programming was accomplished via a LaunchPad module and a GUI provided by TI [41]. The overall input and output of the charge controller was measured for efficiency and maximum power output. However, these tests were performed under low light conditions and cloudy conditions, rendering them inaccurate models of the actual competition conditions. The heat was monitored at this time, but no significant amount of heat was generated to cause concern for full load operation, especially considering all components has an operating temperature up to 125 degrees Celsius.

Figure 69. Charge Controller Lab Test GUI Output.

6.3 Motor Driver Testing – Caroline

The motor driver test were conducted once the MCU testing and motor testing phases had been completed. For initial testing of the motor driver, a smaller brushed DC motor from the test bot was connected. The batteries were fully charged when beginning the test. The PWM signal was then slowly increased with a duty cycle from 0 to 100%. For each 10% interval, the voltage at the motor was measured to be exactly the percentage multiplied by 12V. It was found that the small test motor would not operate below 10-15%.

After the laboratory tests have been conducted, the system was tested with both the drive motor and the steering motor. It was found that the drive motor would not operate with a duty cycle less than 30%, and the steering motor would not operate with a duty cycle less than 20%. The motor driver never experience heating issues, although the lab tests were performed for only an hour. It was determined that the heat sink was successful at dissipating the heat from the motor driver.

6.4 Speedometer Testing – Caroline

The speedometer was easily tested by measuring the maximum distance required for the magnet to trigger the reed switch, which was approximately 1.5”. During installation, the switch was mounted within this maximum distance of the magnets on the tires, namely at approximately 1”. Once the buggy was assembled, a pre-determined distance was used to verify the number of counts and the calculated speed. The results did not deviate from the expected value.

6.5 Encoder Testing – Caroline

The encoder could only be tested after installing it on the extended back shaft of the steering motor. This includes wiring its 5 pins to the MCU. Once the software is completed, testing can begin by manually rotating the motor shaft to test the precision of the encoder and its functionality. At the conclusion of this test, the software outputs must be confirmed. A small gauge wire such as 24 AWG will be sufficient for connecting the power to the MCU.

When the steering motor is then attached to the front wheels, the buggy should be aligned with its wheels facing forward and execute a short run to determine an "origin" position for the encoder. This must be established before implementing autonomous steering operations. Otherwise, the steering will never output the driving direction as determined by the processors.

7 Administrative Content – Caroline

This project was kept on time and on budget using the following tools: milestones, which were imposed by both the Senior Design I course and by the team members, a Gantt chart, which was created at the beginning of the semester and regularly updated to reflect progress, and a budget. The budget was divided into two representations: the itemized budget and the Planned Committed Actuals (PCA) report. More information on the items included the budget, such as vendors, prices, and datasheets, was stored as product submittals.

7.1 Milestone Discussion – William

Below is the projected overview of the timeline this project is scheduled to undergo during the Spring 2018 and Fall 2018 academic schedules for the Team E (Blue Team). This document was created at the end of Senior Design I. The college students have experienced what working in a team environment is all about. The need to work together as well as to hold each other accountable for their work is a valuable experience for future engineering students. We all need to learn about managing the working dayto-day life of an engineer. This project has brought that experience to many of the members of this team.

The milestones listed below is an estimate showcasing the initial dates for the order of business for the college students. Some dates were pushes and pulled in order to account for the inexperience of some members. Some college students have still trying to better their time-management skills in order to push themselves as better engineers. This project has been a valuable stepping-stone for the college students.

Senior Design I:

Week of Jan 22	Decide on initial project idea
Week of Jan 29	Decide on roles and positions the team members would like to undertake

Week of Feb 12	Research sensors, microcontrollers, motors, and power systems.
Week of Feb 19	Design power supply setup and select nominal values
Week of Feb 26	Design beach buggy chassis and PCB layout
Week of March 12	Finish initial design of PCB and charge controller
Week of March 19	Design, simulate, and capture schematics
Week of March 26	Research and design autonomous algorithm
Week of April 23	Final report
Week of April 30	Continue modifying and improving algorithm

Senior Design II:

Week of August 13	Purchase hardware components
Week of August 20	Build chassis, connect motors
Week of August 27	Build PCB and other protective circuits
Week of Sept 3	Build protective casing and outer shell components
Week of Sept 10	Build power supply
Week of Sept 17	Interface components and test for proper connectivity
Week of Sept 24	Test sensors
Week of Oct 22	Test and modify algorithm
Week of Oct 29	Test the solar beach buggy
Week of Nov 19	Improve upon the original design
Week of Nov 26	Make sure the project meets expectations and is working as intended
Week of Dec 3	Improve and fix any problems or issues before presentation
Week of Dec 10	ECE Team members graduates from the University of Central Florida with his/her respective degree(s) in hand!

7.2 Gantt Chart – Caroline

The Gantt chart in Figure 70 was created at the beginning of the semester and was routinely updated and used to reevaluate the project's progress. Many of the original items became responsibility of the CS team, such as selecting and acquiring the cameras and Raspberry Pi microcontrollers. The figure is up-to-date at the time of this report submission.

7.3 Budget and Finance – Caroline

The budget and financing for this project is expressed separately. Table 33 contains the budget for each bulk system component. Further breakdowns of these item costs are contained in the respective design section.

The financing is contained in Table 34, which is a Planned Committed Actuals report detailing the current status of this project's financing. This table was used to continuously report the remaining funds, how the money has been allocated during purchasing, and as a record of when items have been received. All purchases were carefully evaluated by all teams before moving forward. The electric steering system redesign was the only

unexpected cost which exceeded the initial itemized budget by a significant amount and cause the team to utilize the $250 contingency fund.

SD2 Construction Schedule 8/24-8/31								
Task	24-Aug	25-Aug	26-Aug	27-Aug	28-Aug	29-Aug	30-Aug	31-Aug
Phase 1 Purchase Orders	Patrick							
Phase 2 Purchase Orders				Patrick				
Phase 3 Purchase Orders						Patrick		
Complete Construction Schedule	Caroline							
Set Adviser Meetings				Challapalli				
Set Group Work Meetings				Caroline				
Begin group construction activities								
Review ext. components						ECE		
Review ext. progress							ME	
Design sensor mounts			Olesya, Frank, Cong					
Continue building chassis/frame			Frank, Lanie, Erik, Caroline					
Obtain battery testing equipment			Arturo					
Assemble & test MCU prototype			Patrick, Olesya, Caroline					
SD2 Construction Schedule 9/1-9/8								
Task	1-Sep	2-Sep	3-Sep	4-Sep	5-Sep	6-Sep	7-Sep	8-Sep
Assemble steering mechanism					Erik, Caroline			
Obtain battery testing equipment	Arturo							
Assemble drive train					Frank, Lanie			
Test battery, motor controller, motor				Arturo, Caroline				
DELIVERABLE - Programmed motor controller		Caroline						
Test sensors with Arduino	William, Cong							
DELIVERABLE - Print sensor mounts	Frank							
Install sensor mounts					Frank, Olesya			
Assemble & test MCU prototype	Patrick, Olesya							
SD2 Construction Schedule 9/9-9/16								
Task	9-Sep	10-Sep	11-Sep	12-Sep	13-Sep	14-Sep	15-Sep	16-Sep
Receive Solar Cells								
Solar Panel Soldering							Caroline, Lanie, Cong	
Receive PCB's and components								
DELIVERABLE - Assembled MCU					Patrick, Olesya			
DELIVERABLE - Assembled charge controller					Caroline			
Install encoder	Caroline, Erik							
DELIVERABLE - Programmed encoder		Caroline, Patrick						
Assemble GPS	Olesya, William							
Program sensor output	William, Cong							
SD2 Construction Schedule 9/17-9/24								
Task	17-Sep	18-Sep	19-Sep	20-Sep	21-Sep	22-Sep	23-Sep	24-Sep
Solar Panel Soldering	Caroline, Lanie, Cong							
DELIVERABLE - Solar Panel Installation					Caroline, Lanie, Frank			
Complete chassis							ME	
Program charge controller							Caroline, Cong	
Test MCU	Patrick, Olesya							
Program GPS	William, Olesya							
DELIVERABLE - Emergency stop and go							William, Caroline	
Presentation Documents	Arturo, Erik							
SD2 Construction Schedule 9/25-9/30								
Task	25-Sep	26-Sep	27-Sep	28-Sep	29-Sep	30-Sep		
DELIVERABLE - Completed chassis	ME							
DELIVERABLE - Programmed charge controller	Caroline, Arturo, Cong							
DELIVERABLE - Integrated MCU	Patrick, Olesya, William							

SD2 Construction Schedule 11/1-11/8									
Task	1-Nov	2-Nov	3-Nov	4-Nov	5-Nov	6-Nov	7-Nov	8-Nov	
Mock Competition			ALL						
Contingency Time					ALL				
SD2 Construction Schedule 11/9-11/17									
Task	9-Nov	10-Nov	11-Nov	12-Nov	13-Nov	14-Nov	15-Nov	16-Nov	17-Nov
Prepare Final Presentation	ALL								
Practice Final Presentation					ALL				
COMPETITION									

Figure 70. ECE Gantt Chart.

Table 33. Itemized Budget.

ECE Purchases	
Item	Price
PCB	$50.00
GPS Package	$49.36
Camera Module	$51.12
Sensors	$60.00
Converter	$12.00
Solar Cells	$250.00
Tabbing Wire	$23
Other Solar Wiring	$24.00
Motor Controller	$65.00
Encoder	$25.00
On/off buttons	$5.00
Charge Controller	$100.00
Magnets	$7.37
SD Cards	$14.00
Total	**$735.85**
MAE Purchases	
Item	Price
Wheels/Tires	$20
Bearings	$40
Sprockets/ Chains/ Pulleys/ Belts	$200
Axles	$70
Electric Steering system	$70
Enclosures (for electrical components)	$20
Frame	$125.00
Motor (500 W)	$100.00
Batteries (24V)	$540.00
Total	**$1,185.00**
CS Purchases	
Item	Price
R Pi (x2)	$70
Total	**$1,991**

Table 34. Planned Committed Actuals Report.

Item	Planned	Committed	Actuals
GPS Package	$49.36	$34.75	$34.75
Camera Module	$51.12	$64.99	$64.99
Sensors	$60.00	$43.57	$43.57
Microcontroller	100.00	$124.89	$124.89
Converter	$12.00	$14.01	$14.01
Solar Cells and Panels	$250.00	$303.52	$303.52
Tabbing Wire	$23.00	$8.99	$8.99
Other Solar Wiring	$24.00	$32.19	$32.19
Motor Controller	$65.00	$65.00	$65.00
Encoder	$25.00	$25.91	$25.91
On/off buttons	$5.00	$4.00	$4.00
Charge Controller	$100.00	$123.97	$123.97
Magnets	$7.37	$11.98	$11.98
SD Cards	$14.00	$13.90	$13.90
Wheels/Tires	$20.00	$20.00	$20.00
Bearings	$40.00	$19.90	$19.90
Sprockets/ Chains/ Pulleys/ Belts	$100.00	$111.64	$111.64
Axles	$70.00	$71.25	$71.25
Electric Steering system	$70.00	$81.88	$81.88
Electric Steering system redesign	**$212.49**	**$212.49**	**$212.49**
Frame	$150.00	$148.35	$148.35
Motor (500 W)	$100.00	$$97.99	$$97.99
Batteries (24V)	$500.00	$445.98	$445.98
R Pi (x2)	$70.00	$73.48	$73.48
Miscellaneous	$50.00	$89.47	$89.47
Total	**$1,995.85**	**$2,244.10**	**$2,244.10**

7.4 Project Roles

Below are brief biographies on the roles of the ECE team members for this Solar Beach Buggy Challenge, including their degree expectations, technical roles, and project management roles.

7.4.1 William Zhang

William Zhang made great strides to work with his team to achieve the design specifications for the vehicle. William has taken upon himself to research the navigation

system for the vehicle to use. Several considerations from several resources were utilized for William to bring himself up to speed with current technology in navigational systems for autonomous vehicles. William loved how the United States government has open its satellite systems for public use. Other challenging areas that William was involved in were the designs of protecting the circuit from any potential risks. He led the choice to use a power distribution block to better organize the wiring of the electrical system. William research new ideas that may improve upon the initial design of the vehicle. These ideas may be implemented should the budget be increased.

William was also involved with several logistics in the organization of the team. William volunteered himself to take meeting minutes. This proved helpful when the team needed to reference items that were discussed beforehand. William provided suggestions and concerns for his teammates' calculations and work. William enjoyed reviewing his teammates' contributions.

7.4.2 Olesya Nakonechnaya

As a Computer Engineering Student, Olesya's tasks were throughout all areas of the buggy. Her main tasks in this project were to design the sensor system that were placed on the frame of the buggy as well as the software for the PCB. The sensor system included research, design, 3D modeling and gear research for the mounts, and interactions with the mechanical and computer science teams to make sure that the system she designed fit the requirements for all three teams. The sensors need to be tested and configured properly. She tested all sensors prior to Senior Design II to guarantee her designs met the requirements. She was also responsible for programming the software on the PCB including controlling the motors with PWM signals and implementing the GPS. She also participated in helping design the power system on the buggy and the protective circuitry of which her major task was setting up the electrical layout of the smaller electronics and choosing the correct converter(s). This included power calculations and interactions with the PCB design to make sure all the correct power and current requirements for each sensor and microcontroller is met. This included powering the PCB and the Raspberry pi's from the battery along with all peripherals.

7.4.3 Patrick McBryde

Patrick, who is majoring in Computer Engineering, took the lead on designing and integrating the MCU PCB with other parts of the project. It was his job to select a board and processor that the PCB would be designed off of, and then modify that board to fit the needs of this project. To do this he researched the communication protocols that would be used and common practices in designing a PCB. Patrick did the design work for the PCB in EAGLE and started with the MSP430FR5529 board, for which Texas Instruments provided the schematics. In addition to this Patrick took on the role of ordering and picking up all the parts for all three disciplines through the MAE department's accountant. He was in charge of filling out the necessary forms, resolving any issues, and picking up the parts once they were shipped to the MAE department.

7.4.4 Caroline Kamm

Caroline Kamm, who is majoring in both Mechanical Engineering and Electrical Engineering, assumed the role of project manager/liaison between disciplines. Her technical role included design of the charge controller PCB using Altium, design of the solar array, and mechatronic-related component selection, such as the electric motors, encoders, speedometer, and motor driver. She was also responsible for conducting power calculations to size the power and heat dissipation systems. As the project manager, her role was to keep all of the teams on schedule, within the budget, and in line with a detailed, comprehensive scope. Caroline also used PM documentation such as the Project Management Plan, Planned Committed Actuals report, budget, and submittals in order to manage the scope, schedule, and budget.

8 Conclusion & Recommendations

The main purpose of designing this solar powered beach buggy is to be environmentally friendly as well as promote interest in the solar field. Although this vehicle is designed on a smaller scale than a regular sized car or truck, the importance of this buggy being powered by solar energy could lead to possible future advancements to today's cars and trucks. Pollution would begin to become a thing of the past and solar energy would become the future.

Making the best decisions within the given restrictions of budget, time, knowledge, and other available resources is foundational to the engineering process. Within a given set of constraints, the best engineers make the best decisions. Clearly, no single drive system or piece of machinery is applicable to every situation. Knowledge and experience guide the best engineering decisions. This lesson will help these young engineers gain experience and knowledge by analyzing, calculating, drawing, and designing an autonomous solar vehicle.

Appendix A - Copyrights Permission

Texas Instruments

Hello Caroline,

Thank you for contacting Texas Instruments.

You have reached the Education Technology support division of Texas Instruments. You are authorized to print our designs in your education-related publications only.

If you have further questions or comments, please feel free to send me an email.

Kindest Regards,
Christina

Texas Instruments
Email: ti-cares@ti.com
General Information: (800) 842-2737
Technical Support: (972) 917-8324

Let me know how I'm doing. Fill out our customer survey at
https://na01.safelinks.protection.outlook.com/?url=https%3A%2F%2Feducation.ti.com%2Fus%2Fsupportsurvey&data=02%7C01%7Ccarolinekamm%40Knights.ucf.edu%7Cdf58f37fea9f4ca90f4e08d59e53b6fd%7C5b16e18278b3412c919668342689eeb7%7C0%7C0%7C636589004757314100&sdata=g5aaQXMLBUQSdxFd5J700i5vSGINJxMSUQ29ZR88bek%3D&reserved=0

---- Original Message ----
Hello,

My name is Caroline, and I am a student at the University of Central Florida completing my Electrical Engineering degree. For my senior project, my team is building a solar-powered vehicle, and we are planning on using your TIDA-00120 MPPT Controller design. Would you be able to grant us permission to use all the design/data sheet material for that design and those components (like the MSP430, SM72295, etc.) in our final report? It is for educational purposes only.

Thank you very much,
Caroline Kamm

Cytron Technologies

Hi Caroline Kamm,

Thanks for interested in Cytron's product.

Yes, you are able to do so. You can access all the information regarding SmartDriveDuo-30 from this link - https://www.cytron.io/p-mdds30. Thanks for your support! :)

Thanks and regards,

Idris Zainal Abidin
Cytron Technologies Sdn Bhd
1 Lorong Industri Impian 1
Taman Industri Impian
14000 Bukit Mertajam Penang
Tel: +604-548 0668
Fax: +604-548 0669
URL: www.cytron.com.my
Facebook: Cytron Technologies Sdn Bhd

On Thu, 5 Apr at 8:43 AM , Caroline Kamm <carolinekamm@knights.ucf.edu> wrote:
Hello,

My name is Caroline Kamm. I am a senior at the University of Central Florida and am pursuing a degree in electrical engineering. For my senior design project, I am building an autonomous solar-powered beach buggy, and I plan on using your SmartDriveDuo-30 to control the motors, although I have not purchased it yet. For my design report, I would like to request permission to use photos, connection diagrams, and other material. It is for educational purposes only. Would you be able to grant permission to use your material?

Thank you for your time!
Caroline Kamm

Appendix B – Bibliography

[1] ABET, "Criteria for accrediting engineering programs, 2016 –2017," 2017. [Online]. Available: http://www.abet.org/accreditation/accreditation-criteria/criteria-foraccrediting-engineering-programs-2016-2017/

[2] S. Richie, "Eel 4914c syllabus," 2017.

[3] New York Times. (2010) *A Challenge to Florida Beach-Driving Tradition*. [Online]. Available: https://www.nytimes.com/2010/09/10/us/10beaches.html [Accessed: 03-Mar-2018].

[4] State of California Department of Motor Vehicles. (2018) *Testing of Autonomous Vehicles with a Driver*. [Online]. Available: https://www.dmv.ca.gov/portal/dmv/detail/vr/ autonomous/testing. [Accessed: 03-Mar-2018].

[5] Wind.willyweather.com. (2018). *New Smyrna Beach Municipal Airport Wind Forecast*. [On-line]. Available at: https://wind.willyweather.com/fl/volusia-county/new-smyrna-beach-municipal-airport.html [Accessed 19 Mar. 2018].

[6] Iwindsurf.com. (2018). *Wind Information for Daytona Airport*. [On-line]. Available at: http://www.iwindsurf.com/windandwhere.iws?regionID=112&siteID=534&Isection=Wind+Yesterday [Accessed 19 Mar. 2018].

[7] R. McCluney. (1985, Mar.). "Sun Position in Florida." *Florida Solar Energy Center*. [On-line]. Vol. FSEC-DN-4-83, pp. 1-4. Available at: http://www.fsec.ucf.edu/en/publications/pdf/FSEC-DN-4-83.pdf [Accessed 19 Mar. 2018].

[8] Sunearthtools.com. (2018). *Solar Tool - Sun Position*. [On-line]. Available at: https://www.sunearthtools.com/dp/tools/pos_sun.php?lang=en [Accessed 19 Mar. 2018].

[9] Engineering ToolBox, (2008). *Rolling Resistance*. [On-line]. Available at: https://www.engineeringtoolbox.com/rolling-friction-resistance-d_1303.html [Accessed 23 Feb. 2018].

[10] IPC. (2018). Qualification and performance Specification of permanent Solder Mask. [On-line]. Available at: http://www.ipc.org/TOC/IPC-SM-840D.pdf [Accessed 17 Mar. 2018].

[11] IPC (2018). IPC-A-600 Acceptability of Printed Boards Training and Certification Program. [On-line]. Available at: http://www.ipc.org/ContentPage.aspx?pageid=IPC-A-600 [Accessed 19 Mar. 2018].

[12] UL. (2018). Standard for Servo and Stepper Motors [On-line]. Available at: https://standardscatalog.ul.com/standards/en/standard_1004-6_2 [Accessed 17 Mar. 2018].

[13] UL. (2018). Standard for Safety Requirements for Electrical Equipment for Measurement, Control and Laboratory Use - Part 2-032: Particular Requirements for Hand-Held and Hand-Manipulated Current Sensors for Electrical Test and Measurement [On-line]. Available at: https://standardscatalog.ul.com/standards/en/standard_61010-2-32_1 [Accessed 17 Mar. 2018].

[14] IEEE (2018). *IEE Std 2700-2014 – IEEE Standard for Sensor Performance Parameter Definitions*. [On-line]. Available: https://standards.ieee.org/findstds/standard/2700-2014.html [Accessed 17 Apr. 2018].

[15] IEEE (2018). *IEE Std 1044-2009 (revision of IEE Std 1044-1993) - IEEE Standard Classification for Software Anomalies*. [On-line]. Available at: https://standards.ieee.org/findstds/standard/1044-2009.html [Accessed 17 Apr. 2018].

[16] IEEE (2018). *IEE Std 1044-2009 (revision of IEE Std 1044-1993) - IEEE Standard on Video Techniques: Measurement of Resolution of Camera Systems* [On-line]. Available at: https://standards.ieee.org/findstds/standard/208-1995.html [Accessed 17 Apr. 2018].

[17] ASTM. (2010). *Standard Specification for Aluminum-Alloy 6061-T6 Standard Structural Profiles.* [On-line]. Available at: https://www.astm.org/Standards/B308.htm [Accessed 22 Apr. 2018].

[18] ASTM. (2013). *Standard Specification for Steel Bar, Carbon and Alloy, Cold-Finished.* [On-line]. Available at: https://www.astm.org/Standards/A108.htm [Accessed 22 Apr. 2018].

[19] ASTM. (2003). *Standard Specification for Carbon Structural Steel.* [On-line]. Available at: https://www.astm.org/DATABASE.CART/HISTORICAL/A36A36M-03.htm [Accessed 22 Apr. 2018].

[20] IEC. (2001). *Primary batteries – Part 2: Physical and electrical specifications.* [On-line]. Available at: http://image.sciencenet.cn/olddata/kexue.com.cn/bbs/upload/15791IEC60086-2_%7B10%5B1%5D%5B1%5D.1%7D(2001-10).pdf [Accessed 22 Apr. 2018].

[21] IEEE. (2018). 1013 – IEEE Draft Recommended Practice for Sizing Lead-Acid Batteries for Stand-Alone Photovoltaic (PV) Systems. [On-line]. Available at: https://standards.ieee.org/develop/project/1013.html [Accessed 22 Apr. 2018].

[22] NFPA. (2018). NFPA 1192 Standard on Recreational Vehicles. [On-line]. Available at: https://www.nfpa.org/codes-and-standards/all-codes-and-standards/list-of-codes-and-standards/detail?code=1192 [Accessed 22 Apr. 2018].

[23] G. Rudolph and U. Voelzke, “Three sensor types drive autonomous vehicles,” 2017. [Online]. Available: https://www.sensorsmag.com/components/threesensor-types-drive-autonomous-vehicles

[24] H. Reese, “Updated: Autonomous driving levels 0 to 5: Understanding the differences,” 2016. [Online]. Available: https://www.techrepublic.com/misc/autonomous-driving-levels-0-to-5-understanding-the-differences/

[25] S. Thrun, M. Montemerio, and H. Dahlkamp, “Stanley: The robot that won the darpa grand challenge.” pp. 661 – 692, 2006.

[26] L. Dang, N. Sriramoju, G. Tewolde, J. Kwon, and X. Zhang, “Designing a cost-effective autonomous vehicle control system kit (avcs kit),” pp. 1453–1458, Sept 2017.

[27] Union of Concerned Scientists, (2015). How Solar Panels Work. [On-line]. Available at: https://www.ucsusa.org/clean-energy/renewable-energy/how-solar-panels-work#.WnyfX6inFPY [Accessed 9 Feb. 2018].

[28] M. Dilthey. (2017). An In-Depth Look at the Different Types of Solar Panels. [On-line]. Available at: https://www.solarpowerauthority.com/depth-look-different-types-solar-panels/ [Accessed 9 Feb. 2018].

[29] M. Maehlum, (2018). Which Solar Panel Type is Best? Mono-, Polycrystalline or Thin Film? Energy Informative. [On-line]. Available at: http://energyinformative.org/best-solar-panel-monocrystalline-polycrystalline-thin-film/ [Accessed 20 Mar. 2018].

[30] STP235-20/Wd 235 Watt Polycrystalline Solar Module. (2012). [ebook] Suntech Power, pp. 1-2.

[31] Helios Solar Works 6T Series. (2011). [ebook] Milwaukee: Helios USA, LLC. Available at: http://pvpower.com/uploads/products/Helios_Solar_Works_6T_Series_Spec %20Sheet_2011.pdf [Accessed 24 Feb. 2018].

[32] Bifacial Photovoltaic Module HIT Double 190. (2010). [ebook] SANYO Energy (U.S.A.) Corp. Available at: http://www.panasonic.com/business/pesna/includes/pdf/eco-construction-solution/HIT_Double_190_Datasheet.pdf [Accessed 24 Feb. 2018].

[33] RobotShop Blog. (2018). How to Make a Robot - Lesson 5: Choosing a Motor Controller. [On-line]. Available at: https://www.robotshop.com/blog/en/how-to-make-a-robot-lesson-5-motor-controller-3695 [Accessed 5 Mar. 2018].

[34] Core Electronics. (2018). Motor Drivers vs. Motor Controllers - Tutorial. [On-line]. Available at: https://core-electronics.com.au/tutorials/motor-drivers-vs-motor-controllers.html [Accessed 5 Mar. 2018].

[35] Anaheimautomation.com. (2018). *Encoders: Optical and Magnetic, Incremental and Rotary*. [On-line]. Available at: http://www.anaheimautomation.com/manuals/ forms/encoder-guide.php#sthash.brlJUkNO.i9IyKzDp.dpbs [Accessed 20 Mar. 2018].

[36] R. Condit, (2018). *Brushed DC Motor Fundamentals*. Microchip Technology Inc., pp.5-6.

[37] Victron Energy, (2014). Which Solar Charge Controller: PWM or MPPT? [On-line]. Available at: https://www.victronenergy.com/upload/documents/White-paper-Which-solar-charge-controller-PWM-or-MPPT.pdf [Accessed 9 Feb. 2018].

[38] N. Barua, A. Dutta, S. Chakma, A. Das and S. S. Chowdhury, (2016). "Implementation of Cost-Effective MPPT Solar Photovoltaic System Based on the Comparison between Incremental Conductance and P&O Algorithm." 2016 IEEE International WIE Conference on Electrical and Computer Engineering (WIECON-ECE), Pune, 2016, pp. 143-146. Available at: http://ieeexplore.ieee.org/document/8009105/ [Accessed 9 Feb. 2018].

[39] J. Agresta and N. Mikolajczak, (2017). An MPPT Charge Controller for Solar Powered Portable Devices. [ebook] Worcester: Worcester Polytechnic Institute, pp.1-36. Available at: https://web.wpi.edu/Pubs/E-project/Available/E-project-042617-162303/unrestricted/Agresta_Mikolajczak_MQP_MPPT_Solar_Charger_1.pdf [Accessed 23 Mar. 2018].

[40] SmartSolar Charge Controllers MPPT 100/30 & 100/50. (2018). [ebook] De Paal: Victron Energy B.V. Available at: https://www.victronenergy.com/upload/documents/ Datasheet-SmartSolar-charge-controller-MPPT-100-30-&-100-50-EN.pdf [Accessed 10 Mar. 2018].

[41] Test Report of MPPT Charge Controller PMP 7605. (2013). 1st ed. [ebook] Dallas: Texas Instruments. Available at: http://www.ti.com/lit/ug/tidu219/tidu219.pdf [Accessed 6 Apr. 2018].

[42] Raspberry Pi, "Compute Module Datasheet." 6 Raspberry Pi (Trading) Ltd, 13-Oct-2016.

[43] "MSP430 Ultra-Low Power 16-Bit MCUs - TI | Mouser Europe", Mouser.com, 2018. [Online]. Available: https://www.mouser.com/new/Texas-Instruments/ti-msp430-mcus/?gclid=Cj0KCQjwzIzWBRDnARIsAAkc8hERRyng-4BYYrxgY_rJNhwa7zfWyu7BgCDnFC0Pp4s67mLLaZhSUu8aAuE2EALw_wcB. [Accessed: 04- Apr- 2018].

[44] "LTC3780 Datasheet and Product Info | Analog Devices", Analog.com, 2018. [Online]. Available at: http://www.analog.com/en/products/power-management/switching -regulators/buck-boost-regulators/external-power-switch-buck-boost/ltc3780.html# product-overview. [Accessed: 04- Apr- 2018].

[45] M. Kharseh. Solar Radiation Calculation. [On-line]. Available at: https://www.researchgate.net [Accessed 23 Mar. 2018].

[46] University of Minnesota. Appendix D: Solar Radiation. [On-line]. Available at: http://www.me.umn.edu/courses/me4131/LabManual/AppDSolarRadiation.pdf [Accessed 23 Mar. 2018].

[47] Itacanet.org. (2018). Part 3: Calculating Solar Angles. [On-line]. Available at: http://www.itacanet.org/the-sun-as-a-source-of-energy/part-3-calculating-solar-angles/ [Accessed 23 Mar. 2018].

[48] Itacanet.org. (2018). Part 4: Irradiation Calculations. [On-line]. Available at: http://www.itacanet.org/the-sun-as-a-source-of-energy/part-4-irradiation-calculations/ [Accessed 23 Mar. 2018].

[49] Anon, (n.d.). HOMER Pro 3.11. [On-line]. Available at: https://www.homerenergy .com/products/pro/docs/latest/solar_ghi_resource.html [Accessed 2018].

[50] C. Knapp, T. Stoffel, and S. Whitaker. (1980, Oct.). "Insolation Data Manual: Long-term Monthly Average of Solar Radiation, Temperature, Degree-days and Global KT for 248 National Weather Service Stations." Solar Energy Information Data Bank. [ebook] Golden: Solar Energy Research Institute, pp. 57-58.

[51] Rredc.nrel.gov. (2018). [On-line]. Available at: http://rredc.nrel.gov/solar/ old_data/nsrdb/1961-1990/redbook/sum2/12834.txt [Accessed 23 Mar. 2018].

[52] N. Gray, (2015). Facing Up to Global Warming: What is Going on and How You Can Make a Difference? (illustrated). [ebook] pp. 89.

[53] A. Bhatia, "Introduction to circuit protection devices," 2018. [Online]. Available at: https://pdhonline.com/courses/e245/Mod03-Chapter-2%20Circuit%20Protection%20 Devices.pdf

[54] WiringProducts.com, "Power distribution blocks," 2018. [Online]. Available at: http://www.wiringproducts.com/power-distribution-blocks

[55] A. Inc., "Power distribution terminal blocks," 2010. [Online]. Available at: https://library.e.abb.com/public/d990dda2cffe6ca8852577dc00674792/ 1SXU160108L0 201.pdf

[56] GALCO, "How relays work," 2017. [Online]. Available at: http://www.galco.com/ comp/prod/relay.htm

[57] W. N. Inc., "Choosing the right wire size," 2010. [Online]. Available at: https://www.windynation.com/jzv/inf/choosing-right-wire-size

[58] Texas Instruments. (2018). *MSP430 LaunchPad Value Line Development kit.* [On-line]. Available at: http://www.ti.com/tool/msp-exp430g2 [Accessed 7 Feb. 2018].

[59] Texas Instruments. (2018). *MSP430FR4133 LaunchPad Development Kit*. [Online]. Available at: http://www.ti.com/tool/MSP-EXP430FR4133 [Accessed 7 Feb. 2018].

[60] “Radar Basics", *Radartutorial.eu*, 2018. [Online]. Available at: http://www.radartutorial.eu/02.basics/Frequency%20Modulated%20Continuous%20Wave%20Radar.en.html. [Accessed: 04- Apr- 2018].

[61] *AWR1642 Single-Chip 77- and 79-GHz FMCW Radar Sensor*. Dallas: Texas Instruments, 2018, pp. 1-3.

[62] L. M. Manojlović, “AN-1173 Quadrant Photodiode Circuitry for High Precision Displacement Measurement,” *AN-1173 Quadrant Photodiode Circuitry for High Precision Displacement Measurement - Silego Technology*. [Online]. Available at: http://www.silego.com/products/582/312/Quadrant-Photodiode-Circuitry-for-High-Precision-Displacement-Measurement.html. [Accessed: 20-Apr-2018].

[63] "How to Build a Robot Tutorials - Society of Robots", *Societyofrobots.com*, 2018. [Online]. Available at: http://www.societyofrobots.com/sensors_sharpirrange.shtml. [Accessed: 04- Apr- 2018].

[64] *Ultrasonic Ranging Module HC - SR04*. www.indo - ware.com, 2018, pp. 1-4.

[65] "Coefficients Of Friction", *Roymech.co.uk*, 2018. [Online]. Available at: http://www.roymech.co.uk/Useful_Tables/Tribology/co_of_frict.htm. [Accessed: 04- Apr- 2018].

[66] Arduino, “Examples from libraries,” *Arduino - Sweep*, 2018. [Online]. Available at: https://www.arduino.cc/en/Tutorial/Sweep. [Accessed: 20-Apr-2018].

[67] J. Quinn, “Cameras: The eyes of autonomous vehicles,” 2017. [Online]. Available at: https://sites.tufts.edu/jquinn/2017/10/10/cameras-the-eyes-of-autonomousvehicles/

[68] C. Woodford, “Digital cameras,” 2017. [Online]. Available at: http://www.explainthatstuff.com/digitalcameras.html

[69] “Webcams,” 2017. [Online]. Available at: http://www.explainthatstuff.com/webcams.html

[70] O. Cameron, “An introduction to lidar: The key self-driving car sensor,” 2017. [Online]. Available at: https://news.voyage.auto/an-introduction-to-lidar-the-keyself-driving-car-sensor-a7e405590cff

[71] T. Agarwal, “All you know about lidar systems and applications,” 2017. [Online]. Available at: https://www.elprocus.com/lidar-light-detection-and-ranging-working

application/

[72] Sparkfun. (2018). *Serial Communication*. [On-line]. Available at: https://learn.sparkfun.com/tutorials/serial-communication/uarts [Accessed 5 Feb. 2018].

[73] Sparkfun. (2018). *I2C*. [On-line]. Available at: https://learn.sparkfun.com/tutorials/
i2c [Accessed 5 Feb. 2018].

[74] Sparkfun. (2018). *Serial Peripheral Interface (SPI).* [On-line]. Available at: https://learn.sparkfun.com/tutorials/serial-peripheral-interface-spi [Accessed 5 Feb. 2018].

[75] N. Seidle and J. Lindblom, "XBee-Explorer." Creative Commons, 03-Jun-2014.

[76] "Emergency Stop Button", Instructables.com, 2018. [Online]. Available at: http://www.instructables.com/id/Emergency-Stop-Button/. [Accessed: 04- Apr- 2018].

[77] a1ronzo, "The basics of gps," N.A. [Online]. Available at: https://learn.sparkfun.com/ tutorials/gps-basics

[78] Sparkfun, "Accelerometer, gyro and imu buying guide," 2018. [Online]. Available at: https://www.sparkfun.com/pages/accel_gyro_guide

[79] OxTS, "Why it is necessary to integrate an inertial measurement unit with imaging systems on an autonomous vehicle," 2016. [Online]. Available at: http://www.oxts.com/technical-notes/why-it-is-necessary-to-integrate-an-inertialmeasurement-unit-with-imaging-systems-on-an-autonomous-vehicle/

[80] S. Liu, J. Tang, Z. Zhang, and J. L. Gaudiot, "Computer architectures for autonomous driving," pp. 18–25, 2017.

[81] C. Electronics, "Can bus explained - a simple intro (2018)," 2018. [Online]. Available at: https://www.csselectronics.com/screen/page/simple-intro-to-can-bus/ language/en

[82] Gintech Douro Series. (2015, October). [ebook] Available at: http://www.gintechenergy.com/en/uploads/upload-documents/Data_Sheet-G156S3-3BB_C3_(M2)-2015_Oct-0F24-Draft_Verison.pdf [Accessed 10 August 2018].

[83] L. Goldbery, (2012). Active Bypass Diodes Improve Solar Panel Efficiency and Performance. [Online]. Available at: https://www.digikey.com/en/articles/techzone/2012/ dec/active-bypass-diodes-improve-solar-panel-efficiency-and-performance [Accessed 12 April 2018].

[84] Windynation.com. (2018). Choosing the Right Wire Size. [On-line]. Available at: https://www.windynation.com/jzv/inf/choosing-right-wire-size [Accessed 3 Apr. 2018].

[85] Cytron Technologies SmartDriveDuo-30 MDDS30. (2017). 1st ed. [ebook] Penang: Cytron Technologies, pp.1-18. Available at: https://www.robotshop.com/media/files/pdf/smartdriveduo-smart-dual-channel-30a-motor-driver-datasheet.pdf [Accessed 10 Mar. 2018].

[86] INA27x Voltage Output, Unidirectional Measurement Current-Shunt Monitor. (2018). 5th ed. [ebook] Dallas: Texas Instruments. Available at: http://www.ti.com/lit/ds/symlink/ina271.pdf [Accessed 6 Apr. 2018].

[87] D. Baba, (2012). Benefits of a multiphase buck converter. [ebook] Dallas: Texas Instruments. Available at: http://www.ti.com/lit/an/slyt449/slyt449.pdf [Accessed 6 Apr. 2018].

[88] LM5019 100-V, 100-mA Constant On-Time Synchronous Buck Regulator. (2017). 7th ed. [ebook] Dallas: Texas Instruments. Available at: http://www.ti.com/lit/ds/symlink/lm5019.pdf [Accessed 6 Apr. 2018].

[89] TLV704 24-V Input Voltage, 150-mA, Ultralow IQ Low-Dropout Regulators. (2015). 4th ed. [ebook] Dallas: Texas Instruments. Available at: http://www.ti.com/lit/ds/symlink/tlv704.pdf [Accessed 6 Apr. 2018].

[90] MSP430F51x2, MSP430F51x1 Mixed-Signal Microcontrollers. (2016). 16th ed. [ebook] Dallas: Texas Instruments. Available at: http://www.ti.com/lit/ds/symlink/msp430f5152.pdf [Accessed 6 Apr. 2018].

[91] S. Evanczuk, (2013). High-Efficiency Gate Drivers Play Key Role. [On-line]. Digikey.com. Available at: https://www.digikey.com/en/articles/techzone/2013/jul/high-efficiency-gate-drivers-play-key-role-in-solar-energy-harvesting [Accessed 6 Apr. 2018].

[92] SM72295 Photovoltaic Full Bridge Driver. (2013). 5th ed. [ebook] Dallas: Texas Instruments. Available at: http://www.ti.com/lit/ds/symlink/sm72295.pdf [Accessed 6 Apr. 2018].

[93] A. Raj, (2010). Calculating Efficiency: PMP-DCDC Controllers. [ebook] Dallas: Texas Instruments. Available at: http://www.ti.com/lit/an/slva390/slva390.pdf [Accessed 12 Apr. 2018].

[94] UHE Aluminum Electrolytic Capacitors. (2018). [ebook] Kyoto: Nichicon. Available at: http://nichicon-us.com/english/products/pdfs/e-uhe.pdf [Accessed 12 Apr. 2018].

[95] CSD19535KCS 100 V N-Channel NexFET™ Power MOSFET. (2014). 3rd ed. [ebook] Dallas: Texas Instruments. Available at: http://www.ti.com/lit/ds/symlink/csd

19535kcs.pdf [Accessed 12 Apr. 2018].

[96] *15 to 22 pin fpc connector adapter pinout? - Raspberry Pi Forums*. [Online]. Available at: https://www.raspberrypi.org/forums/viewtopic.php?t=156098. [Accessed: 20-Apr-2018].

[97] N. Sadiq, "Selecting fuses: Simple procedures to get the right overcurrent protection for dc-dc converters," 2010. [Online]. Available at: http://www.powerelectronics.com/passive-components/selecting-fuses-simple-proceduresget-right-overcurrent-protection-dc-dc-converte

[98] S. Clifton, "How to fuse your solar system," 2016. [Online]. Available at: https://www.renogy.com/blog/how-to-fuse-your-solar-system/

[99] ScienceDaily, "Speed of sound," *ScienceDaily*. [Online]. Available at: https://www.sciencedaily.com/terms/speed_of_sound.htm. [Accessed: 20-Apr-2018].

[100] "WeatherSpark.com," *Average Weather in November in Cocoa Beach, Florida, United States - Weather Spark*. [Online]. Available at: https://weatherspark.com/m/18784/11/Average-Weather-in-November-in-Cocoa-Beach-Florida-United-States. [Accessed: 20-Apr-2018].

[101] "VL53L0X ," *VL53L0X - World smallest Time-of-Flight (ToF) ranging sensor - STMicroelectronics*. [Online]. Available at: http://www.st.com/en/imaging-and-photonics-solutions/vl53l0x.html#sw-tools-scroll. [Accessed: 20-Apr-2018].

[102] Texas Instruments. (2018). *TCA6416A Low-Voltage 16-Bit I 2C and SMBus I/O Expander With Voltage Translation, Interrupt Output, Reset Input, and Configuration Registers.* [On-line]. Available at: http://www.ti.com/lit/ds/symlink/tca6416a.pdf [Accessed 5 Feb. 2018].

[103] Texas Instruments, "MSP430FR413x Mixed-Signal Microcontrollers." Texas Instruments Incorporated, Aug-2015.

[104] U. Government, "The global positioning system," 2017. [Online]. Available at: https://www.gps.gov/systems/gps/

[105] A. Milne, "Understanding the difference, and debunking the myths, between active and passive antennas," 2018. [Online]. Available at: https://www.rfvenue.com/blog/2014/12/15/active-v-passive-anntennas

[106] ublox, "Neo-8q / neo-m8 hardware integration manual," 2017. [Online]. Available at: https://www.u-blox.com/sites/default/files/NEO-8Q-NEO-M8-FW3_HardwareIntegrationManual_%28UBX-15029985%29_0.pdf

[107] A. Ghassaei, (2012). *Arduino Bike Speedometer*. [On-line]. Instructables.com. Available at: http://www.instructables.com/id/Arduino-Bike-Speedometer/ [Accessed 27 Mar. 2018].

[108] Standex Electronics. (2018). *Reed Sensors vs. Hall Effect Sensors*. [On-line]. Available at: https://standexelectronics.com/resources/technical-library/technical-papers/reed-sensors-vs-hall-effect-sensors/ [Accessed 27 Mar. 2018].

[109] Magnetsales.com. (2000). *Frequently Asked Questions*. [Online]. Available at: http://www.magnetsales.com/design/faqs_frames/faqs_2.htm [Accessed 27 Mar. 2018].

[110] Kjmagnetics.com. (2018). *K&J Magnetics - Magnetic Field Calculator*. [online] Available at: https://www.kjmagnetics.com/fieldcalculator.asp [Accessed 27 Mar. 2018].

[111] MDCG-4 15.3mm Sub-miniature Reed Switch. (2015). [ebook] Littelfuse, pp.1-2. Available at: http://www.littelfuse.com/~/media/electronics/datasheets/reed_switches/littelfuse_reed_switches_mdcg_4_datasheet.pdf.pdf [Accessed 27 Mar. 2018].

[112] AEAT-6010/6012 Magnetic Encoder 10 or 12 bit Angular Detection Device. (2011, Aug.). [ebook] Avago Technologies, pp. 1-6. Available at: https://www.broadcom.com/products/motion-control-encoders/magnetic-encoders/aeat-6010-a06 [Accessed 27 Mar. 2018].

[113] RobotShop, “6 dof gyro, accelerometer imu - mpu6050,” 2018. [Online]. Available at: https://www.robotshop.com/en/6-dof-gyro-accelerometer-imu-mpu6050.html

[114] K. Konolige, J. Augenbraun, N. Donaldson, C. Fiebig, and P. Shah, “A low-cost laser distance sensor,” pp. 3002–3008, May 2008.

Appendix C – Calculations

Hour	Battery Power	Irradiance (W/m^2)	Generation Overhead	Electronics Consumption	Motor Consumption
7	120 Ah x 24V	0	0	0	0
8	2880	154.7575846	86.19279385	86.15662813	512.8
9	2367.236166	379.6511912	211.4480977	95.10343555	512.8
10	1970.780828	632.8874843	352.4889628	105.1777831	512.8
11	1705.292008	853.0944905	475.1340476	113.9381463	512.8
12	1553.687909	961.6512208	535.5951094	118.2567935	512.8
13	1458.226225	912.7188141	508.3420293	116.3101449	512.8
14	1337.458109	729.3987038	406.2412339	109.017231	512.8
15	1121.882112	479.9442075	267.3066542	99.09333244	512.8
16	777.2954338	237.6580239	132.364492	89.45460657	512.8

Figure 70. Per Hour Power Calculations.

Hour	Theta Z	Theta A	Theta T/be	Theta Array	Declination	Beta(EofT)	E (of Time)	LST	Hour angle	Latitude	Sun Alt	Solar Azimuth	AOI
7	0	113.99	52	157	-21.18369	245.275	0.2007828	6.800783	-77.9883	29.2	-0.395496379	-65.787813	54.96775
8	11.55	121.97	52	120	-21.18369	245.275	0.2007828	7.800783	-62.9883	29.2	11.14982074	-57.853774	26.9189
9	22.03	131.71	52	130	-21.18369	245.275	0.2007828	8.800783	-47.9883	29.2	21.62071835	-48.1790529	16.45428
10	30.84	143.91	52	140	-21.18369	245.275	0.2007828	9.800783	-32.9883	29.2	30.42581183	-36.0687697	8.240078
11	37.12	159.05	52	160	-21.18369	245.275	0.2007828	10.80078	-17.9883	29.2	36.71663632	-21.0524895	1.531926
12	39.89	176.63	52	180	-21.18369	245.275	0.2007828	11.80078	-2.98826	29.2	39.53403677	-3.61352157	3.207633
13	38.58	194.67	52	190	-21.18369	245.275	0.2007828	12.80078	12.01174	29.2	38.30314489	14.31648056	3.407584
14	33.48	210.84	52	210	-21.18369	245.275	0.2007828	13.80078	27.01174	29.2	33.28841554	30.43816725	4.725001
15	25.48	224.08	52	220	-21.18369	245.275	0.2007828	14.80078	42.01174	29.2	25.37037479	43.6829524	13.00934
16	15.53	234.63	52	230	-21.18369	245.275	0.2007828	15.80078	57.01174	29.2	15.47802373	54.24616733	22.83177
17	4.31	243.16	52	260	-21.18369	245.275	0.2007828	16.80078	72.01174	29.2	4.30517446	62.79280337	37.17124

Daily Average	Isolation Intensity	Irradiation	H	Clearness	Diffused R	B	B(beta)	D(beta)	A(beta)	Monthly Average	omega(s)
	1404.730308	5968.600889	3400	0.569647739	1211.4134	2188.58661	4126.3316	978.617	196.0126	5300.961259	77.49101403

Hour	D average hourly	hourly irradiation	Total H/h	Diffused Ratio	Total D/h	Hourly Beam	Final Hourly Irradiation
8	1113.00463	0.042117105	143.1982	0.045527029	50.671794	92.5263637	154.75758
9	1113.00463	0.095229114	323.779	0.086721523	96.521457	227.257531	379.65119
10	1113.00463	0.147120093	500.2083	0.119181398	132.64945	367.558868	632.88748
11	1113.00463	0.186387767	633.7184	0.140694566	156.5937	477.124705	853.09449
12	1113.00463	0.20416854	694.173	0.149794939	166.72246	527.450575	961.65122
13	1113.00463	0.196399486	667.7583	0.145862343	162.34546	505.41279	912.71881
14	1113.00463	0.16485921	560.5213	0.129164778	143.761	416.760319	729.3987
15	1113.00463	0.116711925	396.8205	0.100840155	112.23556	284.584984	479.94421
16	1113.00463	0.062675512	213.0967	0.062818751	69.91756	143.17918	237.65802
						SUM (W)	5341.7617

Figure 71. Hourly Irradiance Profile Calculations.